In Situ Response Time Testing of Platinum Resistance Thermometers

EPRI

Keywords:
Nuclear
Sensor Response
Temperature Sensor

EPRI NP-834
Volume 1
Project 503-3
Final Report
July 1978

Prepared by
The University of Tennessee
Knoxville, Tennessee

ELECTRIC POWER RESEARCH INSTITUTE

In Situ Response Time Testing of Platinum Resistance Thermometers

NP-834, Volume 1
Research Project 503-3

Final Report, July 1978

Work Completed, January 1978

Prepared by

Nuclear Engineering Department
UNIVERSITY OF TENNESSEE
Knoxville, Tennessee

Principal Investigators
T. W. Kerlin
L. F. Miller
H. M. Hashemian
W. P. Poore

Prepared for

Electric Power Research Institute
3412 Hillview Avenue
Palo Alto, California 94304

EPRI Project Manager
David G. Cain
Nuclear Power Division

EPRI PERSPECTIVE

PROJECT DESCRIPTION

This final report, In-Situ Response Time Testing of Platinum Resistance Thermometers, brings to a close the second of a three part program to provide practical means for in-situ sensor time response measurement. A prior final report (EPRI NP-267) has been issued on the subject of pressure sensor response testing. An interim report on resistance temperature detector (RTD) testing (EPRI NP-459) is superseded by this document. The third and last project, exclusively concerned with the noise analysis approach to response time testing, has yet to be completed.

The response of RTD sensors is an important safety consideration where these instruments are used in reactor protection system applications. Current Nuclear Regulatory Commission (NRC) requirements specify that sensors be included in periodic safety system time response checks. The advantage of in-situ testing over sensor removal and test is not only a matter of convenience. Radiation exposure to personnel and possible damage to the sensor in the removal process are important considerations. More significant is the fact that laboratory tests cannot precisely duplicate the same conditions the RTD experiences in service. This may lead to greater uncertainty in the laboratory test results.

PROJECT OBJECTIVES

The project investigated three prospective methods for in-situ RTD response measurement: loop current step response; self-heating; and noise analysis. The intent was to assess the feasibility of each approach

within the context of NRC testing requirements, to validate techniques on the basis of laboratory test data, and to demonstrate techniques in commercial power plant applications.

CONCLUSIONS AND RECOMMENDATIONS

In-situ RTD response testing technology has been advanced to the point where it is believed that viable methods now exist for in-plant application. The project investigators provide suitable recommendations in the report as to the use of the alternative methods in meeting NRC requirements. The report should: provide sufficient detail to enable utilities to implement a suitable RTD dynamic test program; and provide a technical basis with which to justify the use of a particular method.

David G. Cain, Project Manager
Safety & Analysis Department
Nuclear Power Division

ABSTRACT

This report provides final results of Research Project 503-3, concerned with in-situ resistance temperature detector time response verification. The report covers the theoretical bases, laboratory experimentation, and in-plant testing of three prospective methods. Sensors employed in this project are representative of those employed in safety-related applications in the field.

Blank Page

PREFACE

This report documents research performed under contract with the Electric Power Research Institute. It is a revised and updated version of a previously issued interim progress report (EPRI Report NP-459). In order to make a complete, self contained report, this final report contains some portions that are identical with parts of the interim report. Also, portions of this report are taken from another report generated in this project. It was written by H. M. Hashemian and is titled, "In-Situ Response Time Testing of Platinum Resistance Thermometers in Nuclear Power Plants."

This report is in two parts. Volume 1 deals with thermometry fundamentals and testing methods that employ electrical heating of the sensor filament in a platinum resistance thermometer to obtain the test data needed to determine the sensor time constant or to detect changes in the time constant. Volume 2 deals with a method for estimating sensor time constants by analyzing the normal fluctuations in the sensor output (noise analysis).

Blank Page

ACKNOWLEDGEMENT

The help of a number of individuals and organizations is gratefully acknowledged.

R. L. Shepard and R. M. Carroll of Oak Ridge National Laboratory contributed significantly through their discussions and by arranging for equipment loans.

Florida Power and Light and Duke Power Company permitted testing in their nuclear power plants.

Combustion Engineering, Inc., Florida Power and Light Company, and Duke Power Company provided platinum resistance thermometers for laboratory testing.

Blank Page

TABLE OF CONTENTS

LIST OF FIGURES

LIST OF FIGURES (CONTINUED)

Blank Page

LIST OF TABLES

LIST OF TABLE (CONTINUED)

SUMMARY

Methods for in-situ response time testing of platinum resistance thermometers were developed, implemented and validated. These methods provide the technology needed to comply with the recommendations on sensor response time verification of temperature sensors outlined in U. S. Nuclear Regulatory Commission Regulatory Guide 1.118. The methods were validated by theoretical analysis, laboratory testing, and four in-plant tests on operating pressurized water reactors.

The methods are:

1. Loop current step response

   The temperature transient due to a step change in I^2R heating of the sensor filament is analyzed to determine the response that would have followed a fluid temperature change. The test can be implemented in a plant by connecting a test instrument at the point where the sensor leads are normally connected to their in-plant transmitter. The data analysis is best performed by a computer. Laboratory results show that the time constant estimates by this method are within 10 to 20 per cent of their true values.

2. Self heating

   The steady state temperature rise due to steady state I^2R heating of the sensor filament is used to detect changes in the sensor's overall heat transfer coeficient and consequently changes in its response time. The results are expressed in terms of the self heating index (ohms of resistance change/watt

of I^2R power). An increase in the self heating index indicates an increase in response time. The test can be implemented in a plant by connecting a test instrument at the point where the sensor leads are normally connected to their in-plant transmitter. The test data are analyzed by constructing a plot of resistance change versus I^2R power and measuring the slope. Limited information has been obtained on the sensitivity of the self-heating index to changes in time constant. This is needed to determine the change in self heating index required to indicate a given change in the time constant.

3. Noise analysis (Volume 2 of this report)

   Noise analysis uses the normal small fluctuations in sensor outputs to obtain information on sensor response characterstics. Basically, the idea is that fast sensors can track the actual fluid temperature changes better than a slower sensor. Methods have been developed for quantitative time constant estimation by noise analysis that apply when the statistical properties of the fluid temperature fluctuations are known. Unfortunately, it has been found that these assumptions are not routinely satisfied in an operating plant, making noise analysis unsuitable for quantitative response time measurement. However, noise analysis results are sensitive to changes in sensor characteristics, so noise analysis is useful for degradation monitoring.

It appears that the in-situ response time measurement problem for platinum resistance thermometers can best be handled by a test program that uses a combination of methods. This program would include degradation

testing (using the self-heating method and/or noise analysis method) on a more frequent schedule than quantitative response time testing (using the loop current step response method). Degradation tests only give qualitative information on changes in response characteristics from a reference condition, but they have the potential for greater simplicity and lower cost than quantitative response time measurements.

1.0 INTRODUCTION

1.1 Historical Background

The response time has been considered an important property of resistance temperature detectors (RTDs) since their early use for industrial temperature measurement. Classically, the response was measured prior to installation in the plant utilizing a measurement that involved plunging the sensor into flowing water. The time constant was usually defined as the time required to reach 63.2 per cent of the final response following a step change in fluid temperature.

The Nuclear Regulatory Commission added a new dimension to sensor response time measurement when it recommended that utilities operating nuclear power plants make in-situ time response measurements of sensors installed in the plant. This recommendation was promulgated in U. S. Nuclear Regulatory Guide 1.118.

1.2 Objectives of This Research

The research reported herein has the objective of developing a method for in-situ response time testing of platinum resistance thermometers of the type used in modern pressurized water reactors. The test is only required to show that the response time is less than a specified maximum allowable value; but, of course, actual determination of the response time is also acceptable. In addition, the testing method should have these characteristics:

1. Technical acceptability so as to receive Nuclear Regulatory Commission approval
2. Minimal cost for special equipment
3. Minimal complexity.

1.3 Approaches for In-Situ Testing

Several methods are plausible for in-situ testing of resistance temperature detectors (RTDs). The two broad categories are: (1) fluid temperature perturbations external to the RTD, and (2) internal perturbations of the RTD by ohmic heating in the sensing wire. Applicable methods related to fluid temperature perturbations involve:

1. analysis of the fluctuations in the sensor output during normal operation (noise analysis)
   a. using time series analysis
   b. using frequency domain analysis
   c. using correlation function analysis[1]
2. analysis of induced temperature fluctuations
   a. using control rod motions to cause power changes and concomitant temperature changes
   b. using steam valve or feedwater valve perturbations to induce primary fluid temperature changes
   c. using special local devices near the sensor such as fluid injection ports or small electrical heating elements.

Those related to internal perturbations include the analysis of:

1. a transient sensor output induced by above-normal current that causes ohmic heating of the sensor filament (usually called a loop current step response test)[2-4]
2. the steady state measurement of temperature rise vs. ohmic heating level in the sensor filament (usually called a self heating test).

In this report, the methods considered are:

1. the loop current step response (LCSR) test

2. the self-heating test
3. noise analysis (using time series analysis) - reported in Part B under separate cover.

These methods are used since they require no system modification and can be accomplished with a modest investment for test equipment. Induced fluid temperature perturbations are omitted because: (a) transients induced with control rods, steam valves or feedwater valves involve test complexity that is probably unnecessary for sensor response measurement (though these methods may be useful for measuring lags due to by-pass lines used for some sensor installations), and (b) special in-pipe hardware would involve an expensive plant modification that is unwarranted. Furthermore, testing by a remove-and-test procedure or a simple periodic replacement is ruled out because these methods ignore the important effects of the environment in the pipe where the measurement is to be made.

The loop current step response (LCSR) test exploits the fact that heat transfer resistances and heat capacities are independent of the direction of heat flow. Thus, the same heat transfer characteristics that control the transient response following a change in ohmic heating in the sensor also control the transient response following a change in fluid temperature change. Of course, the transients are not the same for both perturbations. For a fluid temperature change, the heat must diffuse through the assembly to the sensing wire. For an ohmic heating change, the heat is generated exactly at the point of measurement, then it diffuses through the sensor assembly to the fluid.

Since the response to a fluid temperature change is desired and the response to a change in ohmic heating is feasible in an installed RTD, there is a need to transform the ohmic heating transient into the transient

that would occur if the fluid temperature changes. This has been done for the case of a step change in ohmic heating and is referred to as the loop current step response transformation.[4,5] The transformation may be performed analytically for RTDs that meet two conditions necessary in the theoretical development (predominately one-dimensional heat transfer and negligible heat capacity between the filament and the center of the sensor).*

The physical basis for the self-heating test is that the temperature rise in a system with a given internal heat generation rate is inversely proportional to the overall heat transfer coefficient. Thus, the slope of the curve of temperature rise versus heat generation rate due to ohmic heating in the sensor element (the self-heating curve) is inversely proportional to the heat transfer coefficient. A change in the slope of the self-heating curve indicates a change in the heat transfer resistance. The slope of the self-heating curve is called the self-heating index and is usually expressed in ohms/watt. A change in effective heat capacity of the RTD system would change the response time, but would not change the self-heating index. However, only a change in the heat transfer resistance is considered plausible so an in-plant measurement of the self-heating index would provide an indication of changes in sensor response time.

Noise analysis is a well established diagnostic procedure. It may be used to identify the sensor dynamics so that an impulse response can

---

*In the interim report (EPRI Report NP-459) this condition was stated in a more restrictive way. The condition was previously stated as a centrally located sensing wire. The new statement of the condition is more precise and has application for at least one practical sensor design.

be obtained. Knowing the impulse response, one can readily determine the step response. Consequently, the time constant associated with a plunge test can be identified. Details relating to the application of noise analysis for this research are given in Volume 2 of this report.

2.0 RESISTANCE THERMOMETRY

2.1 Material Requirements

Resistance thermometry exploits the temperature dependence of metals to monitor temperature. Desirable properties of materials for resistance thermometry are:

1. large temperature coefficient of resistance
2. linear curve of temperature vs. resistance
3. chemical inertness
4. ductility
5. mechanical strength.

Platinum is an excellent material to provide these characteristics, and most industrial resistance thermometers use platinum wire as the sensing element.

2.2 RTD Characteristics

A typical RTD consists of a fine platinum wire mounted inside a metal sheath (usually stainless steel). It is important that the filament (the platinum wire) be insulated from the metal sheath. Two construction methods of mounting the filament are worth mentioning: 1) winding the filament on an electrically insulating support inside the sheath, then backfilling with magnesium oxide or cement, and 2) coating the inside of the sheath with a cement, then attaching the filament to the coating material.

Each of the construction methods has advantages. If a support structure is used to mount the filament, stress effects on sensor performance can be minimized; however, the back-fill material needed for electrical insulation has significant thermal resistance. If the filament

is very close to the sheath, as is the case for the second construction method mentioned above, the time response of the sensor is faster than when the filament is mounted on a separate support. The fast time response is desired for some applications.

RTDs may be designed for direct immersion into a fluid stream (wet-type) or for installation into a well in the stream (well-type). To improve the heat transmission in well-type sensors, a thermal bonding material is often used in the gap between the sheath and the well.

The sensors found in pressurized water reactors manufactured by different vendors are quite different. Table 2.1 gives specifications on some of the commonly-used sensors. Figures 2.1 through 2.4 show some of these sensors and X-rays to reveal their internal characteristics.

The resistance element is connected to lead wires that connect to appropriate instrumentation. Sensors may be constructed with the lead wire configurations shown in Figure 2.5. The multiple lead and dummy wire configurations are used in measurement systems to compensate for lead wire resistance to obtain accurate temperature measurements. RTDs are made with single sensing elements per sheath and with dual elements that allow two independent measurements with the same sensor.

The temperature coefficient of resistance of pure annealed platinum wire is 0.003925 $\frac{\text{ohms}}{\text{ohm}}$/°C (0.002181 $\frac{\text{ohms}}{\text{ohm}}$/°F). By selecting the wire length and diameter, one can obtain various values of absolute resistance at any temperature. Standard sensors have 100 ohms at 0°C or 200 ohms at 0°C. Temperature coefficients depend on platinum purity, and commercial sensors usually have slightly smaller temperature coefficients than pure platinum. A pure platinum 100 ohm sensor would have a temperature coefficient of 0.3925 ohms/°C (.2181 ohms/°F), and a pure platinum 200 ohm

TABLE 2.1

SPECIFICATIONS OF THE RTDS USED IN THIS WORK

Sensor Manufacturer	Model Number	Plants Where Used	Wet Type Or Well Type	Sensor Sheath O.D.	Well O.D.	Number of Sensing Elements Per RTD	2 Wire 3 Wire or 4 Wire	Dummy Wire?	Resistance at 0°F $R_o(\Omega)$
REC*	177-GY	B&W**	wet	.335"	NA	2	4	no	100
REC	177HW	B&W**	well	.290"	.410"	2	4	no	100
REC	104-AFC	C.E.	well	.125	.281"	1	2	yes	200
REC	176-KF	Westinghouse	wet	.375"	NA	1	4	no	200
REC	104ADA	C.E.***	well	.125"	.25	1	2	yes	200
REC	104VC	C.E.	well	.125"	.25	1	2	yes	200
Sostman	8606	Westinghouse	wet	.25"	NA	1	4	no	200

*Rosemount Engineering Company.

**Babcock and Wilcox Co.

***Combustion Engineering Inc.

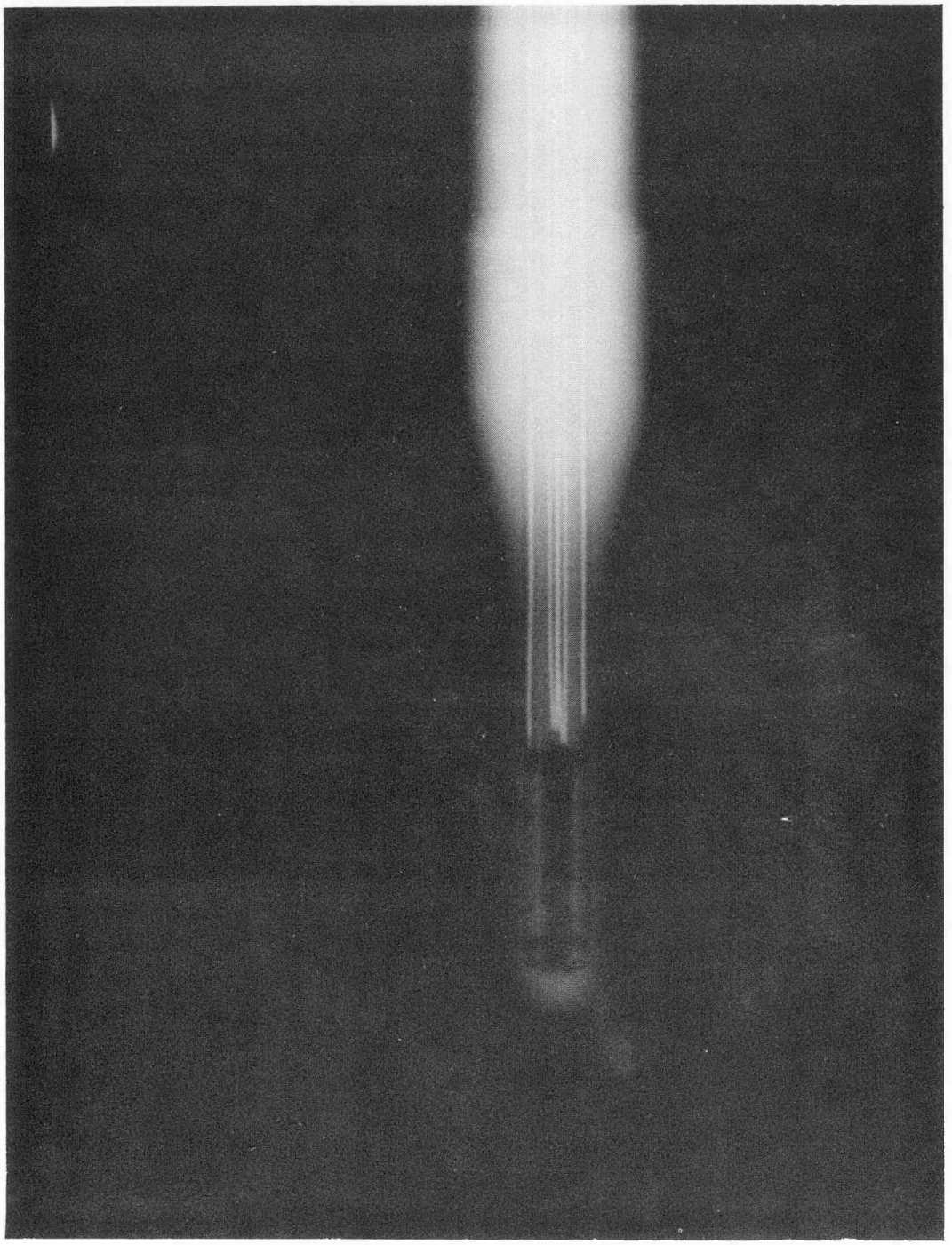

Figure 2.1a X-Ray of the Rosemount 177GY Sensor

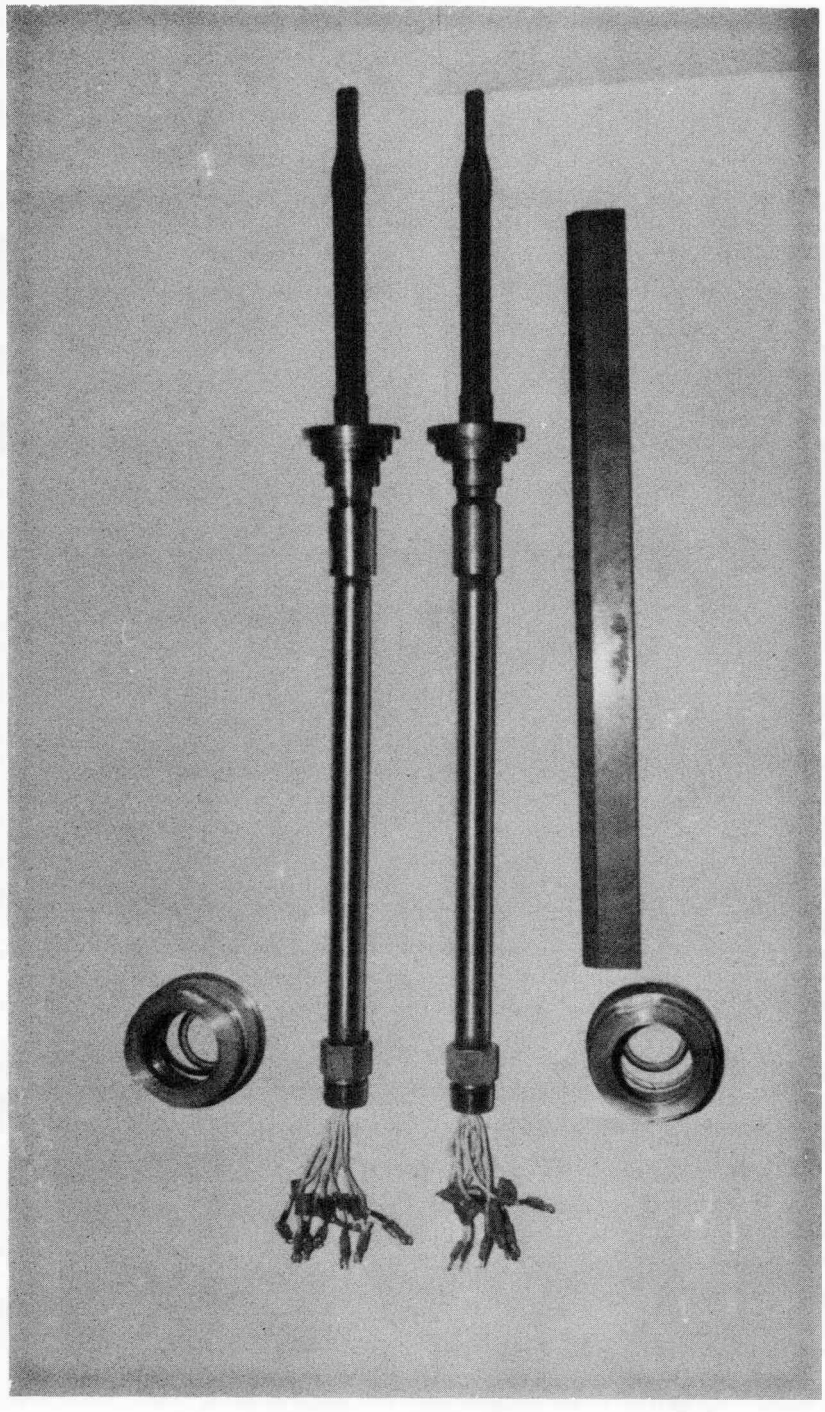

Figure 2.1b Picture of the Rosemount 177GY Sensor.

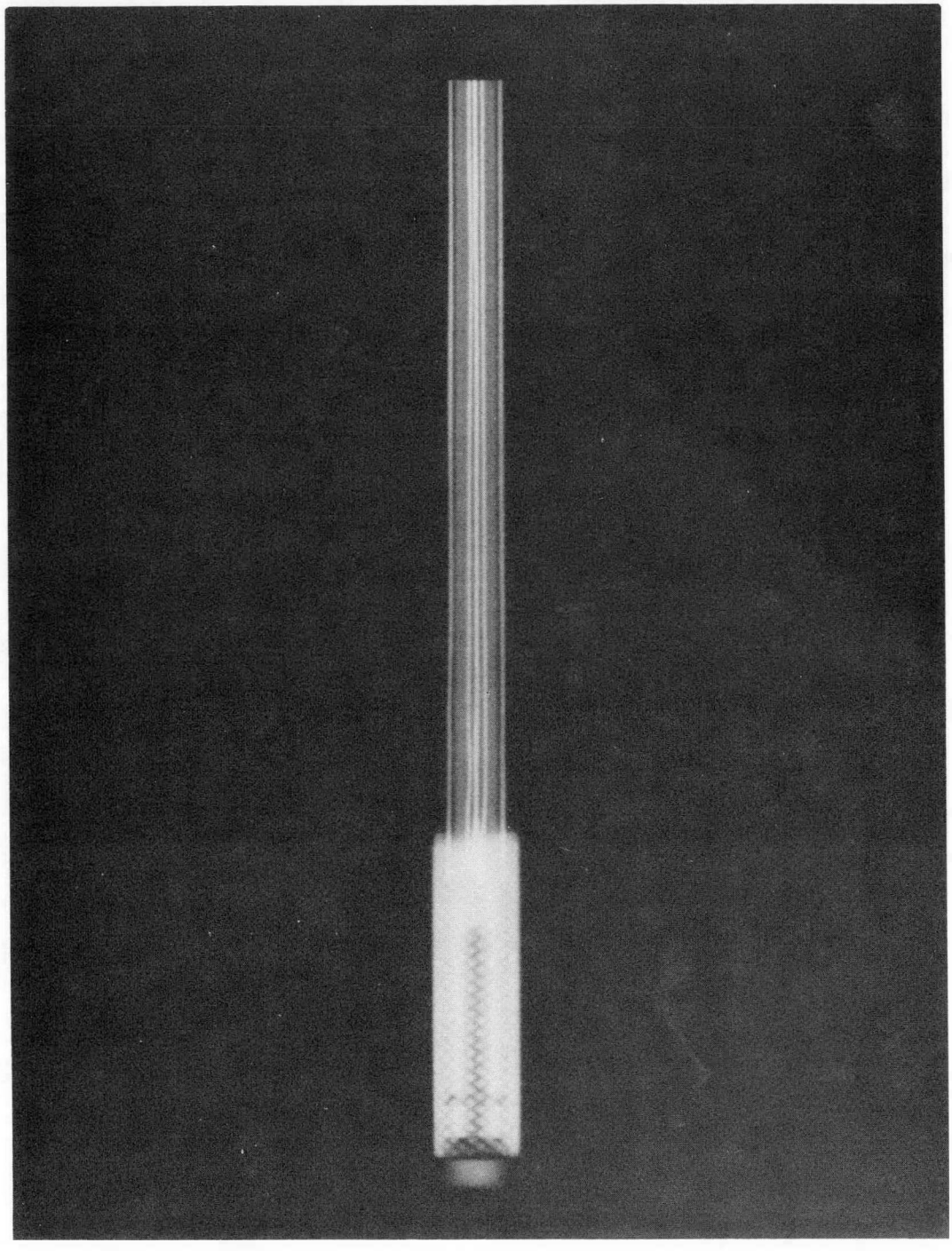

Figure 2.2a X-Ray of the Rosemount 177-HW Sensor.

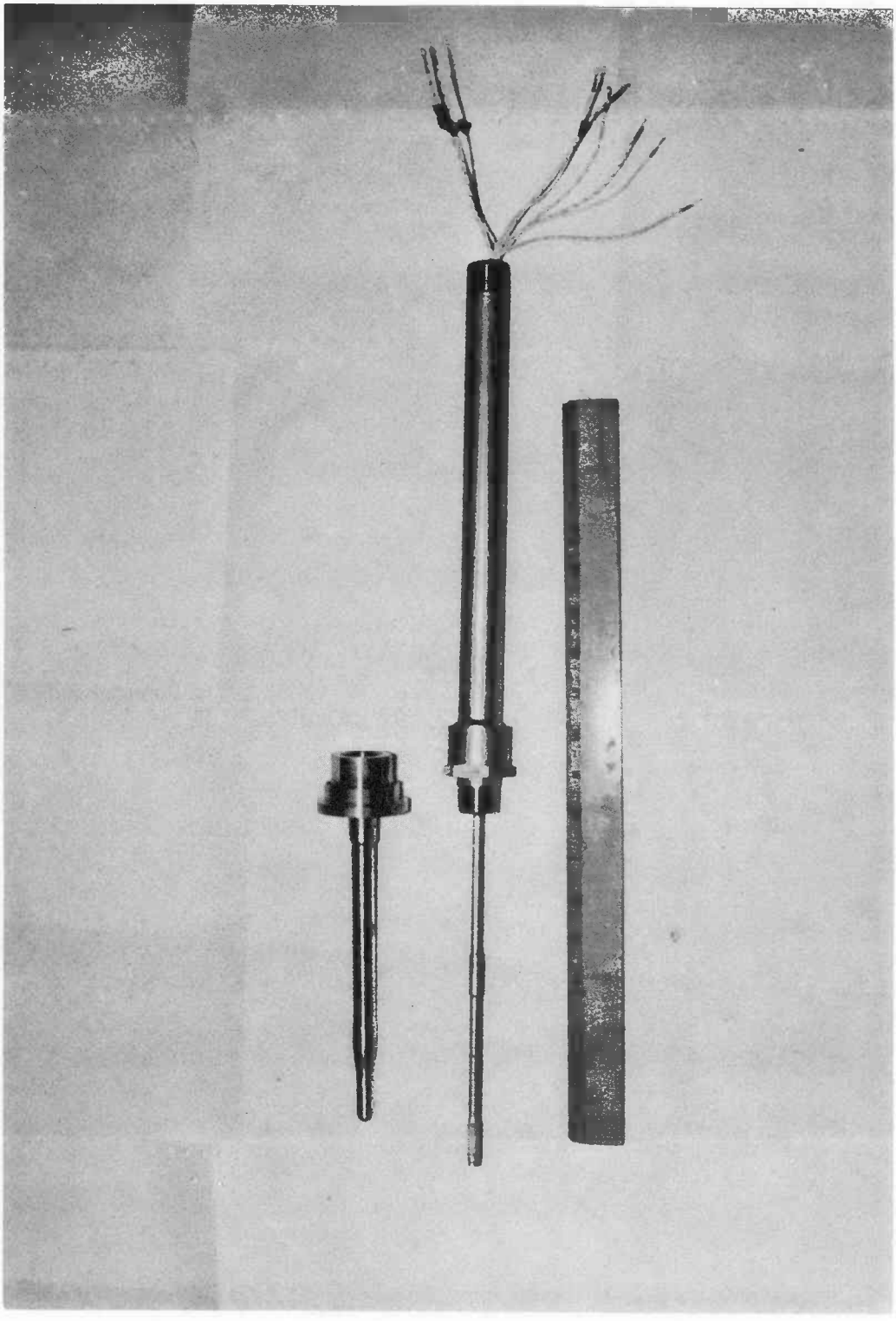

Figure 2.2b Picture of the Rosemount 177-HW Sensor.

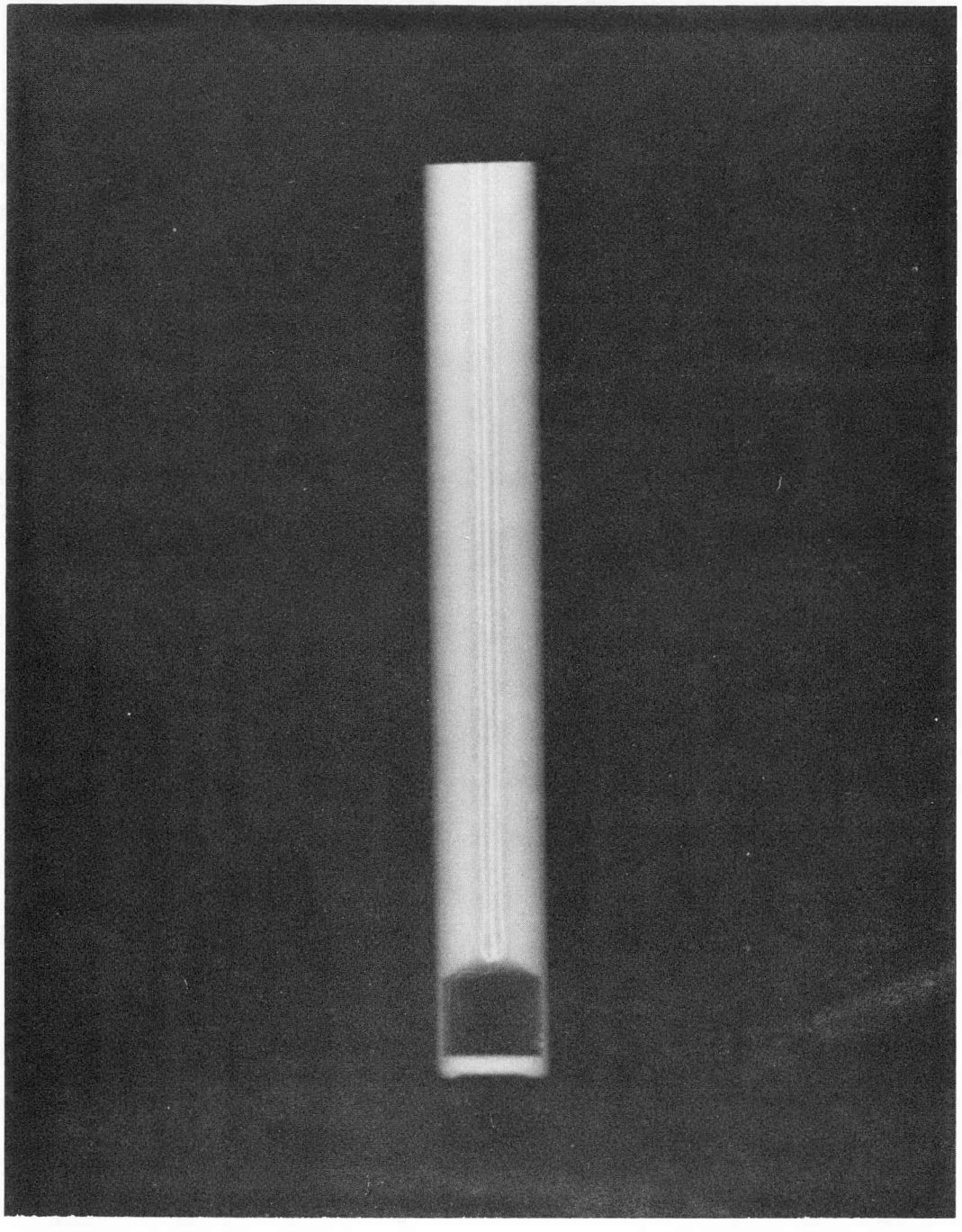

Figure 2.3a X-Ray of the Rosemount 176-KF Sensor.

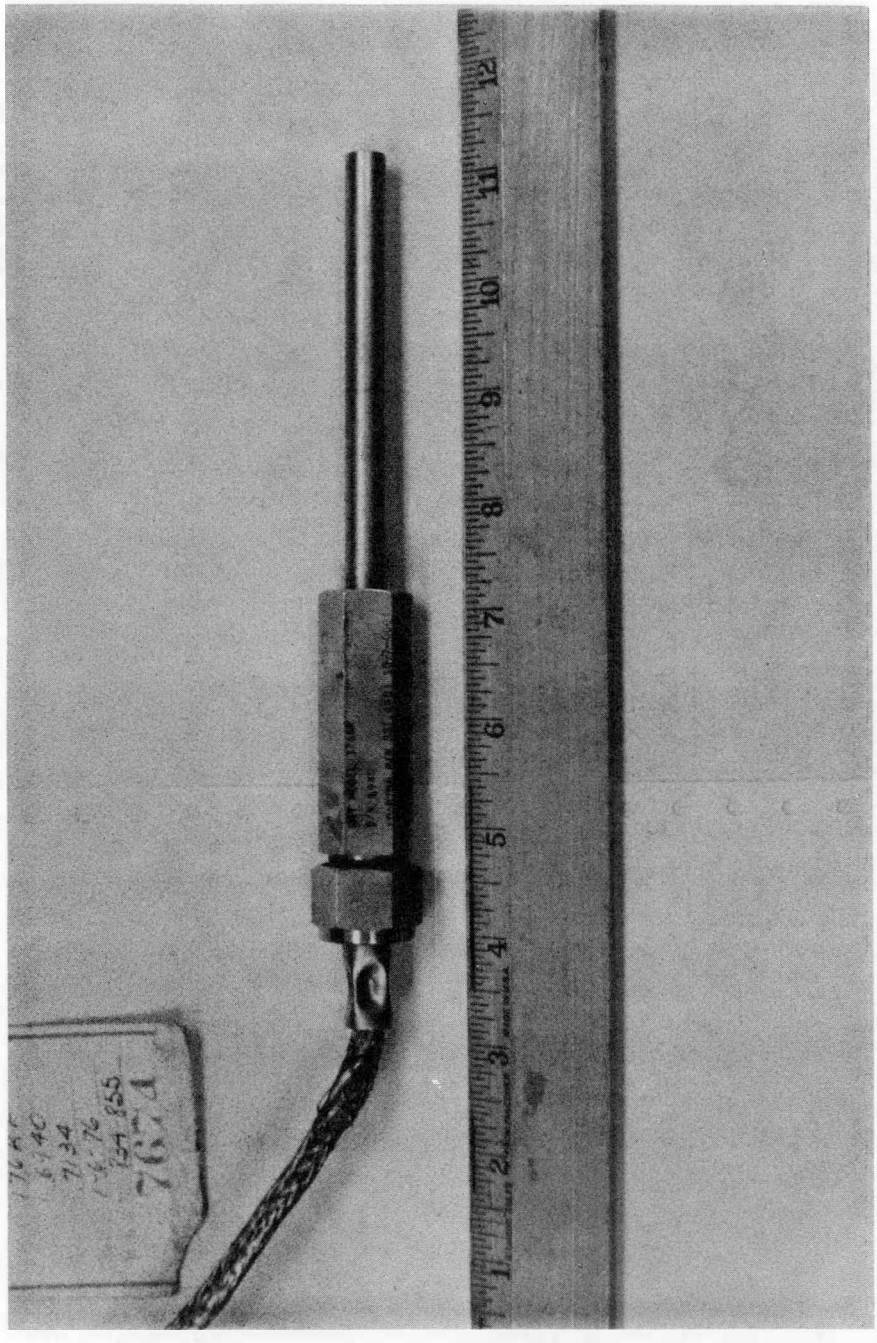

Figure 2.3b Picture of the Rosemount 176-KF Sensor.

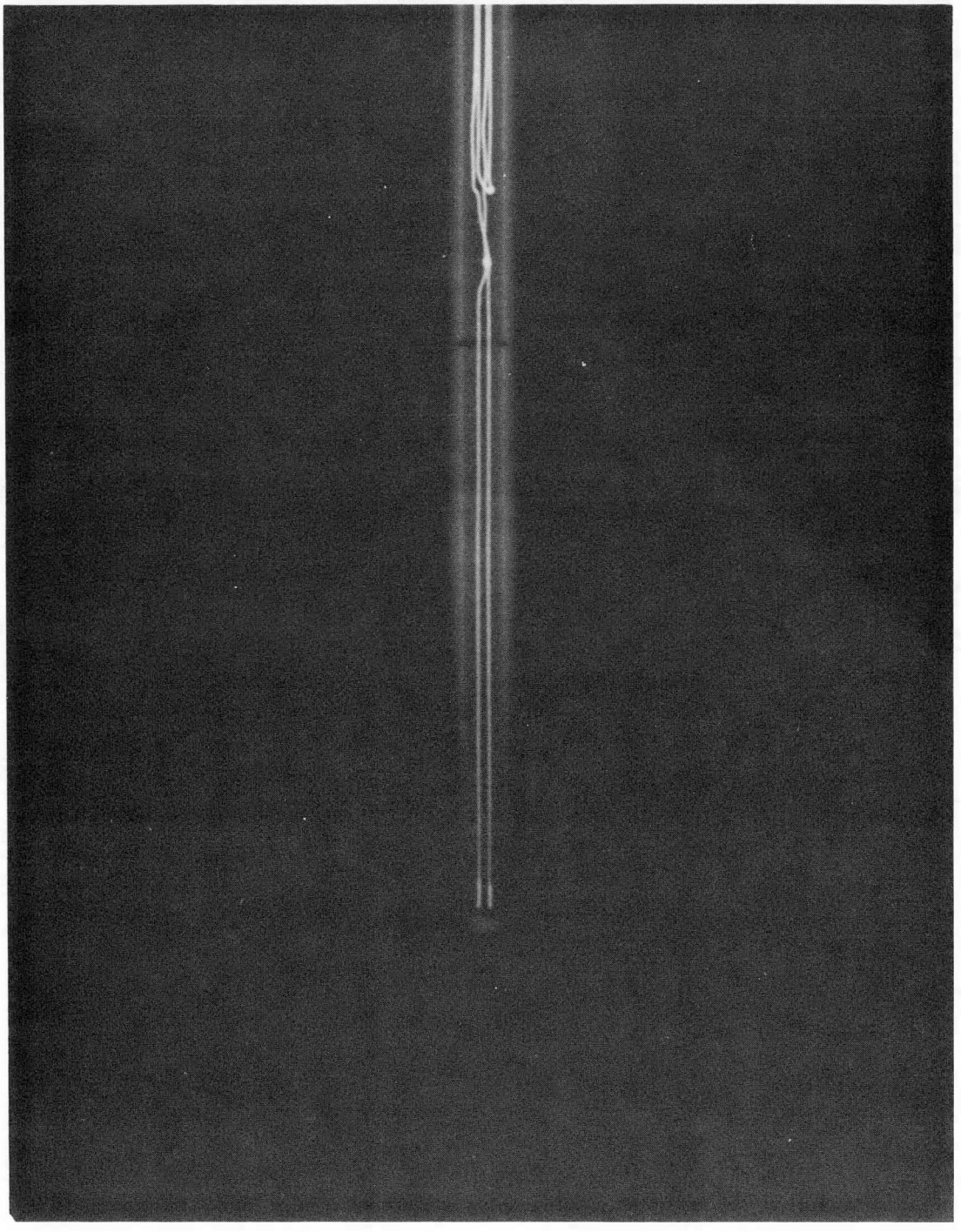

Figure 2.4 X-Ray of the Rosemount 104-AFC Sensor.

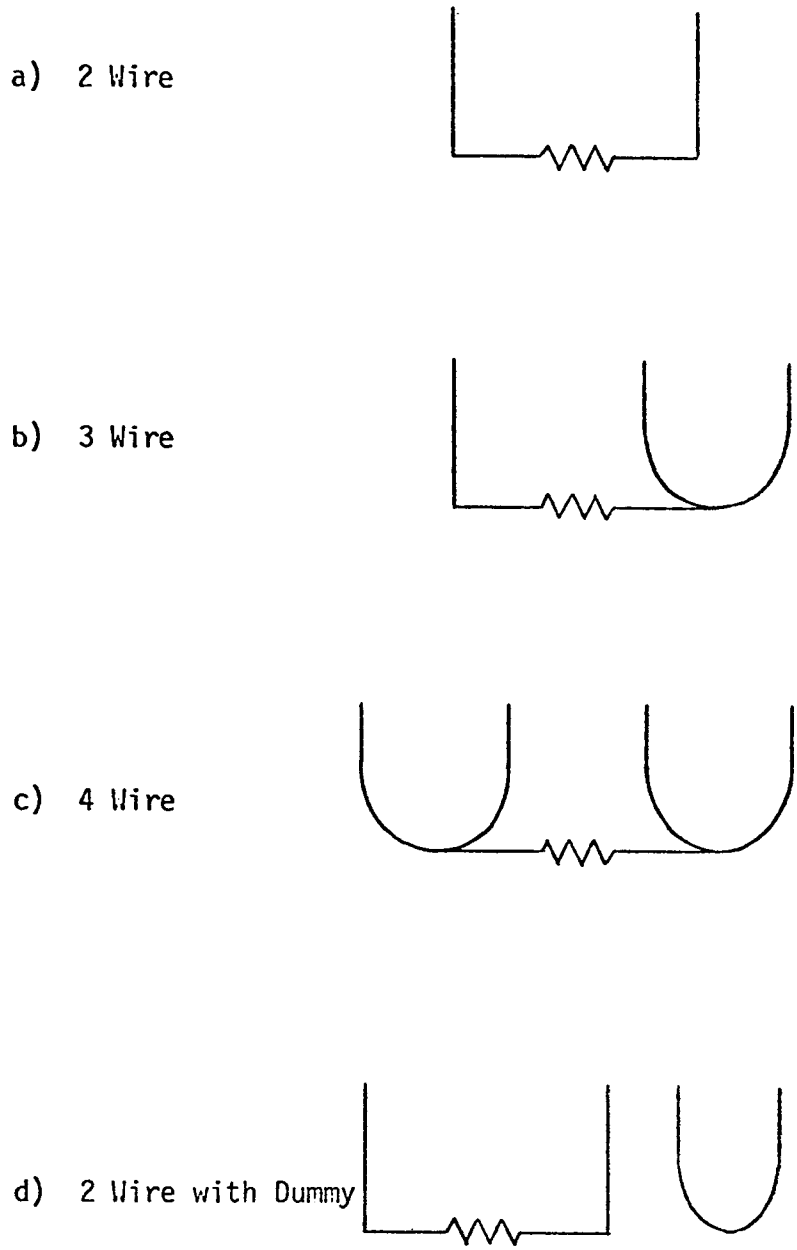

Figure 2.5. Possible Lead Wire Configurations for RTDs.

sensor would have a temperature coefficient of 0.7850 ohms/°C (0.4361 ohms/°F). Temperature coefficients for commercial sensors are typically 80 to 90 percent as large as for those with pure platinum elements.

2.3 RTD Instrumentation

The instrumentation used in resistance thermometry is usually a bridge circuit as shown in Figure 2.6. Various special methods for connecting multiple-wire RTDs are available, but all use the same basic Wheatstone bridge circuit. If the two fixed resistors have the same resistance, R_a, then the RTD resistance can be determined by finding the value for the variable resistance, R_d, that nulls the voltage drop, ΔV. If the bridge is used in the non-nulling mode then changes in the RTD resistance are related to the voltage drop across the two arms of the bridge by

$$\Delta V = \frac{(R_d - R_{RTD})R_a}{(R_a+R_d)\ (R_a+R_{RTD})}\ E. \qquad (2.1)$$

Note that the voltage drop is approximately linearly related to the RTD resistance for bridges in which the change in the sensor resistance is small compared to the sum of the original RTD resistance and the fixed resistance, R_a.

The voltage, E, used in normal applications is selected to give insignificant ohmic heating in the RTD. The self heating effect is quantified by the self heating index expressed in ohms/w. A typical value is 8 ohm/w for a 100 ohm sensor. For such a sensor with a 2 ma sensing current, the heat generation rate is 0.4 mw. This gives a resistance change of 3.2×10^{-3} ohms with a resulting temperature measurement error of 8.15×10^{-3}°C. Similar calculations show that a 50 ma current would give a temperature increase of 5.09°C (9.17°F).

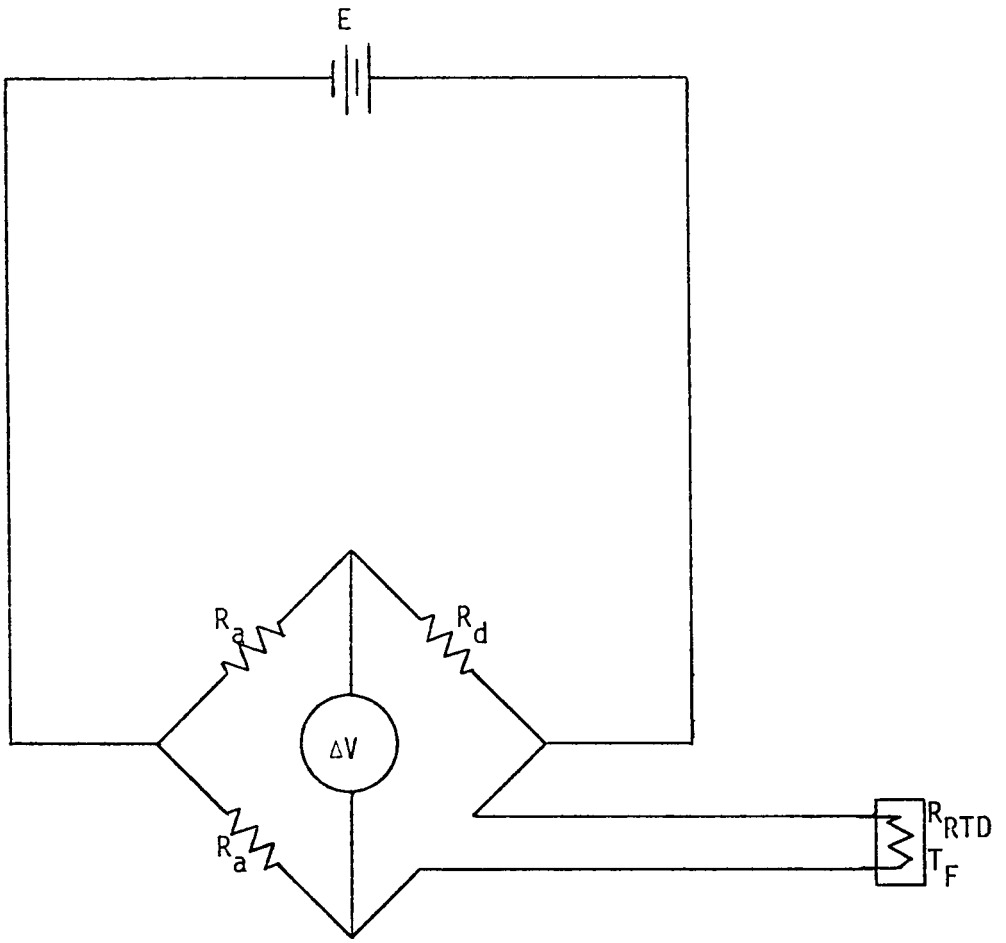

Figure 2.6. A Typical Bridge Circuit Used in Conjunction with an RTD.

2.4 Time Response Characterization of Sensors

2.4.1 The Concept of Time Constant

The time constant is commonly used to represent the response characteristics of a dynamic system. It has unambiguous meaning only for first order systems (described by a first order differential equation or equivalently, a first order transfer function):

$$\frac{dx}{dt} + ax = au \tag{2.2}$$

or

$$G(s) = \frac{x(s)}{u(s)} = \frac{1}{\frac{1}{a}s+1} \quad . \tag{2.3}$$

If Equation 2.3 is solved for a unit step change in the input, u; one obtains

$$x(t) = 1 - e^{-at} \quad . \tag{2.4}$$

If the response is evaluated for $t = \frac{1}{a}$, then

$$x(t = \frac{1}{a}) = 0.632. \tag{2.5}$$

The quantity, $\frac{1}{a}$, is defined as the time constant, τ. It is easily identified from test data by measuring the time required for the response to achieve 63.2 percent of its final value following a step change in the input.

2.4.2 Higher Order Dynamic Systems

The first order approximation is usually inadequate to represent the dynamics of typical temperature sensors. This means that higher

order differential equations or transfer functions are required to represent the dynamics. As will be shown in Section 3.2, a transfer function without zeroes (no numerator dynamics) is usually adequate:

$$G(s) = \frac{a_o}{s^n + a_1 s^{n-1} + \ldots + a_1 s + a_o} \tag{2.6}$$

or

$$G(s) = \frac{a_o}{(s-s_1)(s-s_2) \ldots (s-s_n)} \tag{2.7}$$

For a step change in the input, the response is

$$x(t) = \frac{a_o}{(-s_1)(-s_2) \ldots (-s_n)} + \frac{a_o e^{s_1 t}}{s_1(s_1-s_2) \ldots (s_1-s_n)}$$

$$+ \frac{a_o e^{s_2 t}}{s_2(s_2-s_1) \ldots (s_2-s_n)} + \ldots \tag{2.8}$$

or

$$x(t) = \frac{a_o}{(-s_1)(-s_2) \ldots (-s_n)} \left[1 + \frac{(-s_1)(-s_2) \ldots (-s_n) e^{s_1 t}}{s_1(s_1-s_2) \ldots (s_1-s_n)} \right.$$

$$\left. + \frac{(-s_1)(-s_2) \ldots (-s_n)}{s_2(s_2-s_1) \ldots (s_2-s_n)} e^{s_2 t} + \ldots \right] \tag{2.9}$$

The s_i are the poles of the system transfer function. They are all negative real numbers for transfer functions for temperature sensors. It is common to introduce the concept of a time constant for each mode of the solution:

$$e^{s_i t} = e^{-t/\tau_i} . \tag{2.10}$$

Thus, we may write:

$$\frac{x(t)}{x(\infty)} = 1 + \frac{\frac{1}{\tau_1\tau_2 \cdot \cdot \cdot \tau_n}}{\frac{1}{-\tau_1}\left(\frac{1}{-\tau_1}+\frac{1}{\tau_2}\right) \cdot \cdot \cdot \left(\frac{1}{-\tau_1}+\frac{1}{\tau_n}\right)} e^{-t/\tau_1}$$

$$+ \frac{\frac{1}{\tau_1\tau_2 \cdot \cdot \cdot \tau_n}}{\frac{1}{-\tau_2}\left(\frac{1}{-\tau_2}+\frac{1}{\tau_1}\right) \cdot \cdot \cdot \left(\frac{1}{-\tau_2}+\frac{1}{\tau_n}\right)} e^{-t/\tau_2} + \cdot \cdot \cdot \tag{2.11}$$

It is clear that there is no simple relation between the multiple time constants in the response equation. However, it is still accepted practice to define an overall time constant, τ, as the time required to achieve 63.2 percent of the final response following a step change in the input.

It is possible to develop an expression that relates the overall time constant, τ, to the individual time constants, τ_i, using an assumption that is well satisfied in typical temperature sensors. The faster time constants have a decreasing effect on the response compared to the slowest one as time progresses since they decay faster. For example, if we let τ_1 be the slowest time constant and evaluate the second exponential at $t/\tau_1 = 1$, we obtain the following:

τ_1/τ_2	e^{-t/τ_2} (at $t = \tau_1$)
2	.135
3	.050
4	.018
5	.007

Since τ_1/τ_2 is typically about 4 for a sensor, the τ_2 term contribution is small by the time $t = \tau_1$. Since the τ_1 term has the most important effect on τ, we can also assert that τ_2 and higher terms have a small influence when $t = \tau$. Thus, we may write

$$\frac{x(t)}{x(\infty)} \approx 1 + \frac{\frac{1}{\tau_1\tau_2 \cdot \cdot \cdot \tau_n}}{\frac{1}{-\tau_1}\left(\frac{1}{-\tau_1} + \frac{1}{\tau_2}\right) \cdot \cdot \cdot \left(\frac{1}{-\tau_1} + \frac{1}{\tau_n}\right)} e^{-t/\tau_1} \qquad (2.12)$$

Now, we can set $x(\tau)/x(\infty) = 0.632$ and solve for τ to obtain:

$$e^{-\tau/\tau_1} = .368\left(1 - \frac{\tau_2}{\tau_1}\right)\left(1 - \frac{\tau_3}{\tau_1}\right) \cdot \cdot \cdot \left(1 - \frac{\tau_n}{\tau_1}\right) \qquad (2.13)$$

or

$$\tau = \tau_1 \left(1 - \ell n\left(1 - \frac{\tau_2}{\tau_1}\right) - \ell n\left(1 - \frac{\tau_3}{\tau_1}\right) - \cdot \cdot \ell n\left(1 - \frac{\tau_n}{\tau_1}\right)\right. \qquad (2.14)$$

To illustrate the effect of the faster time constants on the overall time constant, the ratio, τ/τ_1, was evaluated for various values of

τ_2/τ_1 with $\tau_i = 0$ for i greater than 2. The results are shown in Figure 2.7.

2.4.3 Ramp Response

The ramp response of sensors is of interest because safety studies generally involve ramp changes. The ramp response is obtained readily from the transfer function of a system. First, let us consider a first order system:

$$G(s) = \frac{1}{\tau s + 1} \tag{2.15}$$

The ramp response is evaluated using the Laplace transform of a ramp with ramp rate K as follows:

$$L\{Kt\} = \frac{K}{s^2} \tag{2.16}$$

Then:

$$x(s) = \frac{K}{s^2(\tau s + 1)} \tag{2.17}$$

The response may be obtained by inverse Laplace transformation:

$$x(t) = K\left[t - \tau + \tau e^{-t/\tau}\right] \tag{2.18}$$

For $t \gg \tau$, the exponential term is insignificant. The response is as shown in Figure 2.8. The output, x(t), is delayed relative to the true process value, Kt, by a time that is less than or equal to τ. The asymptotic delay is called the system ramp time delay and is equal to the time constant for a first order system. Note that the ramp time

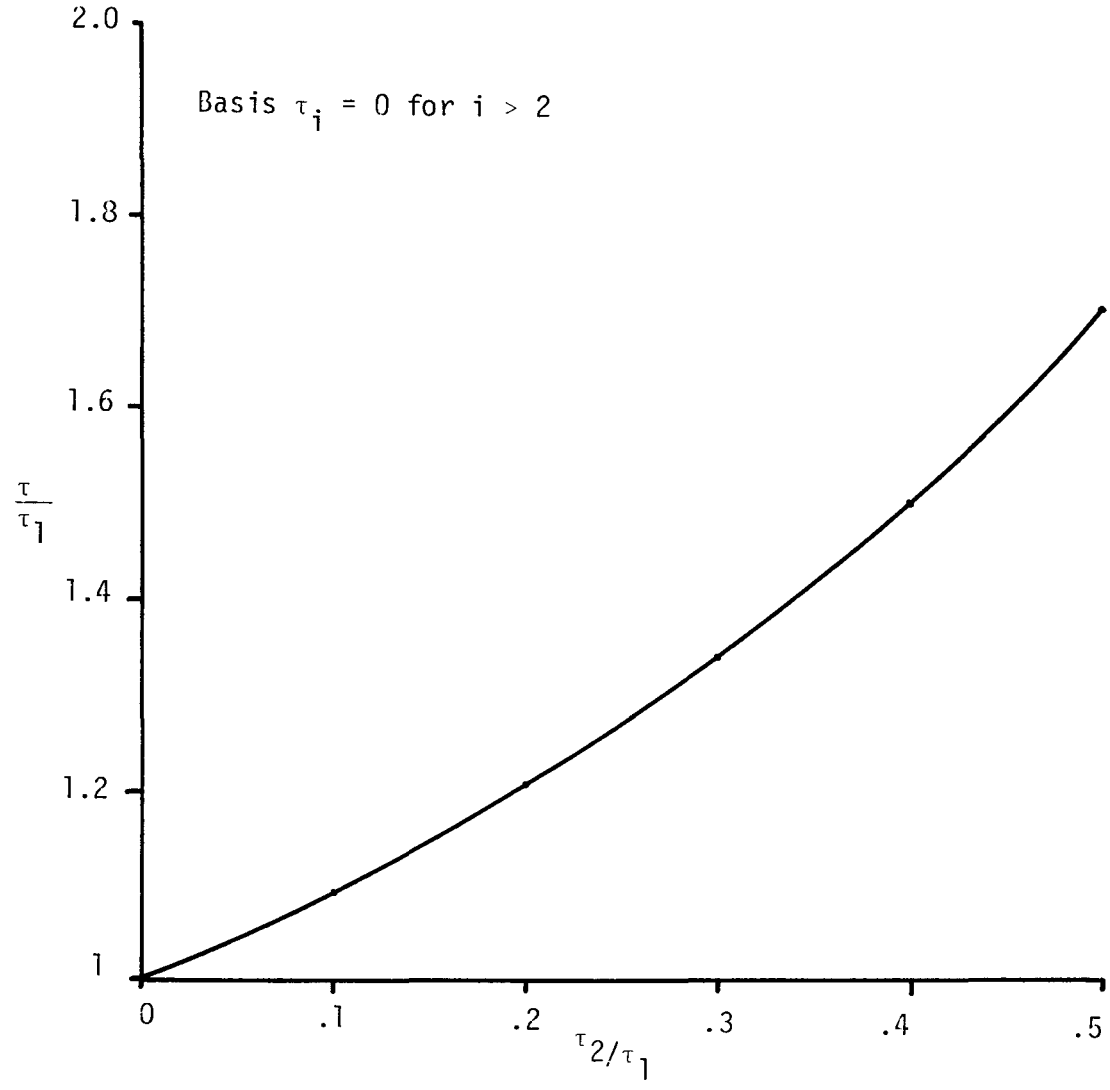

Figure 2.7. Effect of Faster Time Constant on Overall Time Constant.

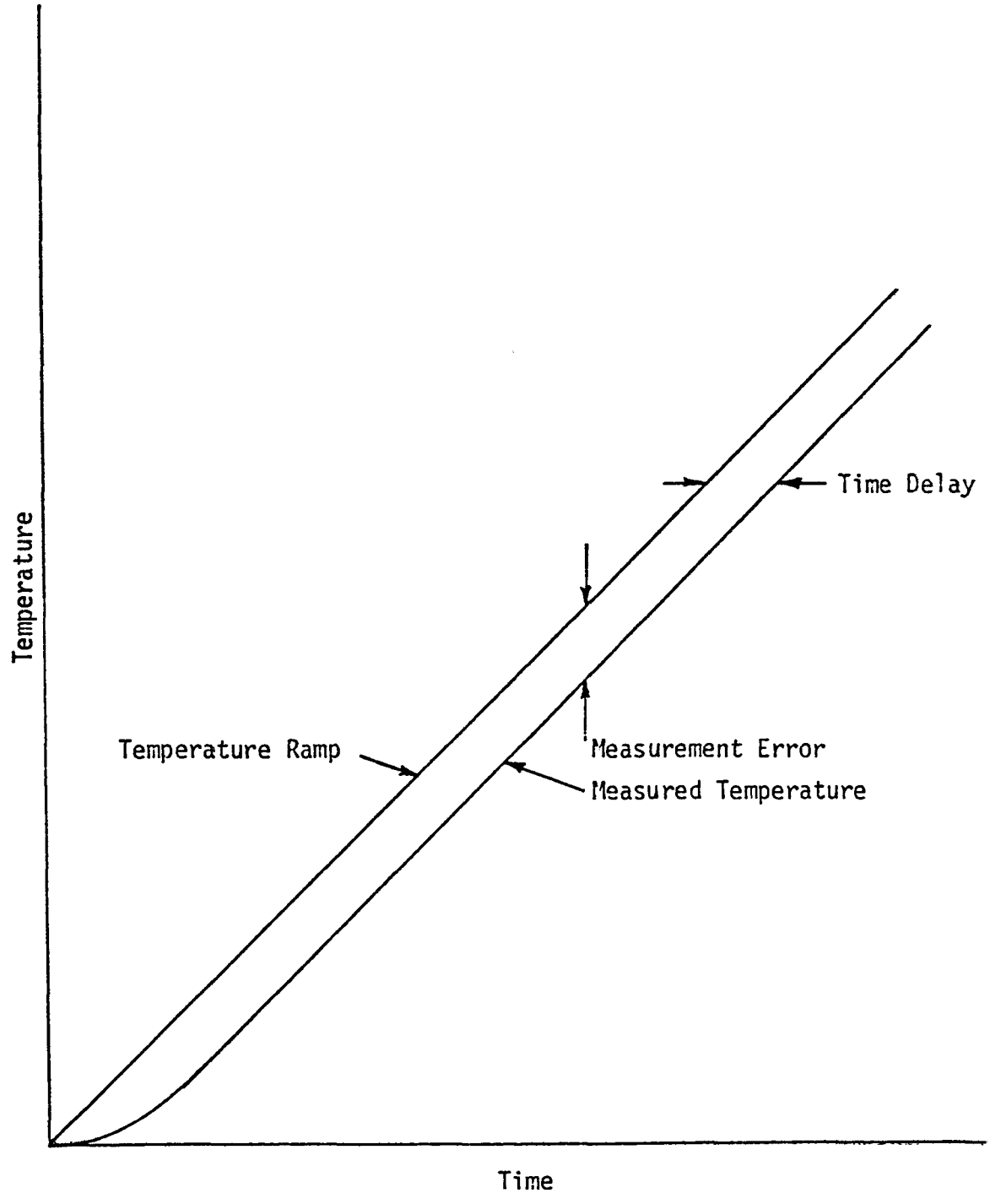

Figure 2.8. Typical Ramp Response and Illustration of Ramp Time Delay and Measurement Error.

delay is independent of the ramp rate. The asymptotic measurement error is $K\tau$.

Now, we will evaluate the ramp time delay and measurement error for sensors described by higher order dynamic models. Consider the transfer function:

$$G(s) = \frac{a_o}{(s-s_1)(s-s_2) \ldots (s-s_n)} \tag{2.19}$$

$$a_o = (-s_1)(-s_2) \ldots (-s_n)$$

and the input, Kt, with Laplace transform, $\frac{K}{s^2}$. The Laplace transform of the output is

$$x(s) = \frac{Ka_o}{s^2(s-s_1)(s-s_2) \ldots (s-s_n)} \tag{2.20}$$

The sensor response may be evaluated by inverse Laplace transformation. The partial fraction method gives

$$x(s) = \frac{A_1}{s^2} + \frac{A_2}{s} + \frac{A_3}{s-s_1} + \frac{A_4}{s-s_2} + \ldots \tag{2.21}$$

The arbitrary constants must be evaluated if the complete response is required. However, we are interested only in determining the ramp delay time and the asymptotic measurement error. Consequently, the exponential terms are of no interest, and we can concentrate on A_1 and A_2. These may be evaluated to give the following result (see Appendix A for the derivation of this result):

$$A_1 = K \tag{2.22}$$

$$A_2 = -K\,[\tau_1 + \tau_2 + \ldots \tau_n] \tag{2.23}$$

Therefore

$$x(t) \sim K[t-(\tau_1 + \tau_2 + \ldots + \tau_n)] \tag{2.24}$$

In this case, we obtain:

$$\text{ramp time delay} = \tau_1 + \tau_2 + \ldots \tau_n \tag{2.25}$$

and

$$\text{asymptotic measurement error} = K[\tau_1 + \tau_2 + \ldots + \tau_n] \tag{2.26}$$

2.4.4 Relation Between Time Constant and Ramp Time Delay

The time constant and the ramp time delay are given by:

$$\text{time constant} = \tau_1\,[1 - \ell n(1 - \frac{\tau_2}{\tau_1}) - \ell n(1 - \frac{\tau_3}{\tau_1}) - \ldots\,] \tag{2.27}$$

and

$$\text{ramp time delay} = \tau_1[1 + \frac{\tau_2}{\tau_1} + \frac{\tau_3}{\tau_1} + \ldots\,]. \tag{2.28}$$

Insertion of numerical values into these expressions shows that the ramp delay time is always less than the time constant, but the difference is small for values of the τ_i that are typical of temperature sensors. To illustrate this, the percent difference between the time constant and the ramp time delay was evaluated for a two-term representation (τ_1 and τ_2). The error is shown in Figure 2.9. We note that for a typical ratio of 0.20, the difference is less than two percent.

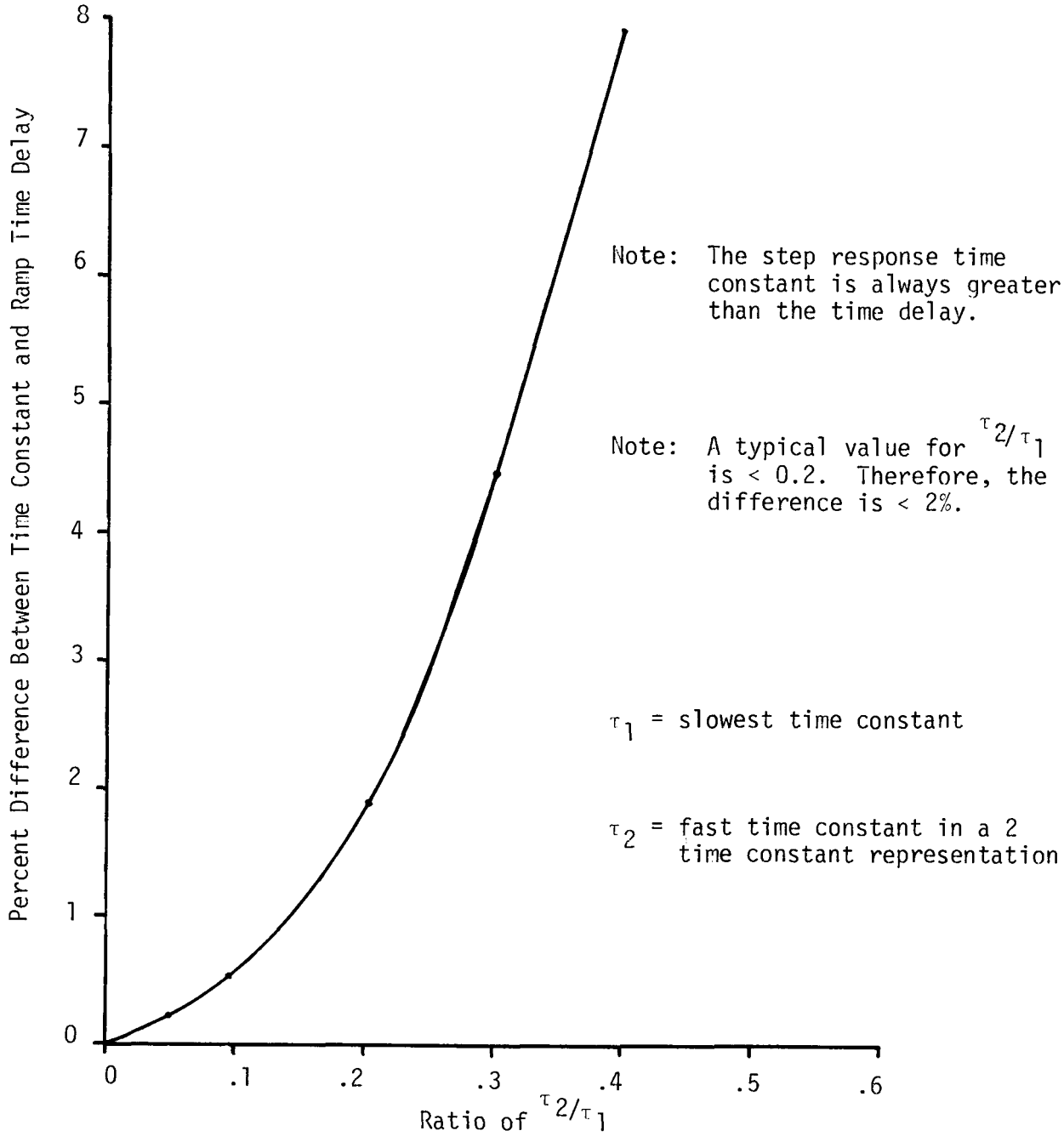

Figure 2.9. Relation Between Plunge Time Constant and Ramp Time Delay.

2.5 Factors Affecting the Steady State and Transient Performance of RTDs

2.5.1 Introduction

A change in physical, electrical or thermal properties of the sensor materials may cause errors in steady state and/or changes in the transient performance of an RTD. The sources of errors in steady state performance and the factors affecting the transient response of RTDs are discussed in this section.

2.5.2 Errors in Steady State Performance

Some of the possible sources of errors in the temperature measured with an RTD are covered in the following sections.

2.5.2.1 Self Heating Errors

Measurement of temperature with resistance thermometers using a Wheatstone bridge requires a small electric current called the sensing current. This current causes a small temperature rise in the sensor and results in an increase in the resistance of the sensing filament. The increase in the resistance of the sensing element indicates a false increase in the temperature being measured. The error in temperature measurement due to the sensing current is called the self heating error. The self heating error may be compensated by measuring the resistance at two different currents to permit an extrapolation to zero power input to the RTD to get the resistance at the temperature being measured. Usually, the sensing current used is small enough so that negligible self heating errors occur.

2.5.2.2 Errors Due to Stem Losses

The transfer of heat from the region of the sensing filament along the axis of the sensor's sheath is usually called a stem loss. Stem losses reduce the amount of heat transferred to the sensing filament and introduce errors in temperature measurements. Stem losses are minimized by filling the sheath with insulating materials such as MgO powder or placing mica disks along the leads inside the sheath.

The errors due to stem losses for several industrial resistance thermometers were measured by Carr[6]. He measured the resistance of the thermometers as a function of immersion depth in an oil bath with a temperature of about 100°C. He demonstrated that the resistance of these thermometers will not change more than the equivalent of .09°C when the immersion depth is varied from 10 to 25 cm.

2.5.2.3 Errors Due to Drifting Resistance

According to Dutt, [7] when an RTD is exposed to a wide range of temperature for a long period of time, the resistance at a reference temperature increases. This is due to dimensional changes and contamination from the materials used for supporting the wires. Therefore, periodic calibration of resistance thermometers is required for accurate measurement of temperature.

2.5.3 Factors Affecting the Transient Response of RTDs

The response of an RTD to a temperature transient depends on the physical and thermal properties of the sensor and its environment. Industrial resistance thermometers are usually exposed to a wide range of temperature, pressure, flow, vibration and corrosive materials.

These parameters have an influence on the properties by which a sensor response is characterized. A discussion of the effect of process parameters on the dynamic performance of an RTD is given in the following sections.

2.5.3.1 Effect of Temperature

As temperature rises, the dimensions of materials in the sensor change. If dimensional changes caused expansion of gas-filled gaps, the resistance to transfer of heat to the sensing filament would increase and result in a slower response. Reduction of gaps would occur if expansion of other materials compressed the gap spaces. This would decrease the heat transfer resistance of the sensor and cause a faster response. Therefore, the net effect may be either a faster or a slower response.

For the well-type RTDs with air in the thermowell, higher temperature reduces the heat transfer resistance in the air. This is due to the fact that the conductivity of air increases with temperature (see Figure 2.10) and results in a smaller heat transfer resistance for the sensor. As mentioned earlier, the air gap inside the thermowell of well-type RTDs is sometimes filled with a thermal bonding material to improve the response time. The effect of temperature on the well-type sensors with a thermal bonding material in the thermowell appears to be significant. Experience based on laboratory testing of a substance called Never-Seize that is sometimes used for thermal bonding indicated that this substance changes to a powder when it is exposed to a temperature of about 600°F in air for less than half an hour. The result of degradation of Never-Seize with temperature may result in a slower response of the sensor.

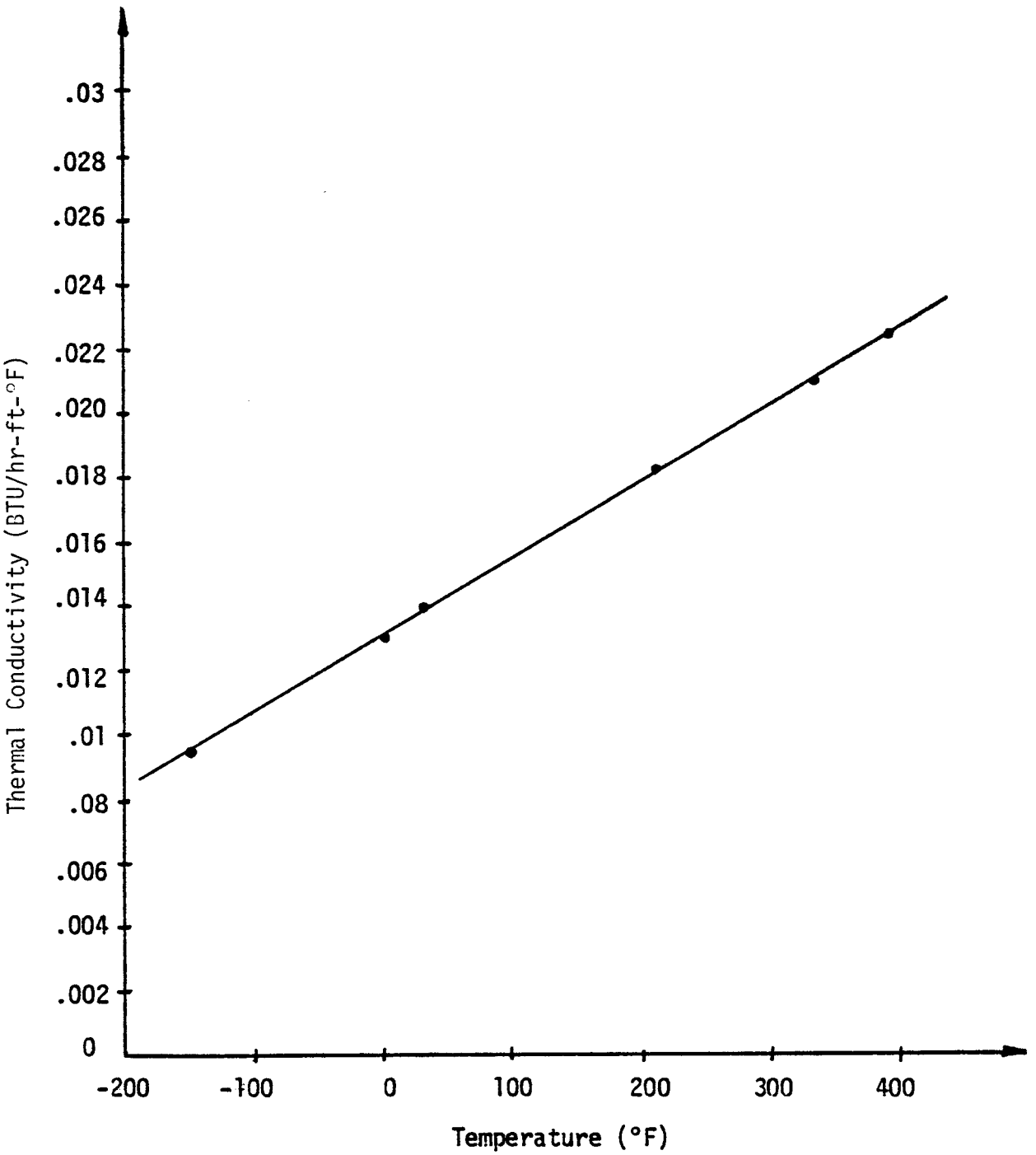

Figure 2.10. **Thermal Conductivity of Air Versus Temperature.**

2.5.3.2 Effect of Pressure

A faster response is expected for an RTD operating in a high pressure environment. This is because pressure can compress the sensor and fill up the gaps (if any) in construction materials. However, for typical sensors for PWR applications, this effect is expected to be negligible.

2.5.3.3 Effect of Flow

The surface heat transfer resistance of an RTD depends on the flow velocity to which the sensor is exposed. A high flow velocity increases the heat transfer coefficient of the surface and improves the sensor response time. This is understood from the heat transfer correlation for flow over submerged bodies.[8]

$$\frac{h_m D_o}{k_f} [Pr]^{-1/3} = b \left[\frac{D_o G}{\mu_f}\right]^n \qquad (2.29)$$

where

G = the mass flow rate

D_o = outside diameter of submerged body

μ_f = viscosity of the fluid

Pr = Prandtl number ($\frac{C_p \mu_f}{k_f}$; C_p = specific heat capacity of fluid)

h_m = the surface heat transfer coefficient

k_f = thermal conductivity of the fluid

b and n = constants that depend on the Reynolds number ($\frac{D_o G}{\mu}$).

These constants for different values of Reynolds numbers are given in Table 2.2. The effect of fluid flow rate on the surface heat transfer resistance is illustrated for a typical case where the body is submerged in water for which the flow rate changes from 3 ft/sec to 40 ft/sec.

$$\frac{\left[\frac{h_{m1} D_o Pr^{-1/3}}{k_f}\right]_{3 \text{ ft/sec}}}{\left[\frac{h_{m2} D_o Pr^{-1/3}}{k_f}\right]_{40 \text{ ft/sec}}} = \frac{b_1 \left(\frac{D_o G_1}{\mu_f}\right)^{n_1}}{b_2 \left(\frac{D_o G_2}{\mu_f}\right)^{n_2}} \tag{2.30}$$

This equation reduces to

$$\frac{h_{m1}}{h_{m2}} = \frac{b_1 \left(\frac{D_o G_1}{\mu_f}\right)^{n_1}}{b_2 \left(\frac{D_o G_2}{\mu_f}\right)^{n_2}} \tag{2.31}$$

in which

G_1 = the mass flow rate at 3 ft/sec

G_2 = the mass flow rate at 40 ft/sec

h_{m1} = surface heat transfer coefficient at 3 ft/sec

h_{m2} = surface heat transfer coefficient at 40 ft/sec

TABLE 2.2

CONSTANTS OF EQUATION 2.29

$D_o G/\mu$	n	b
1-4	.330	.891
4-40	.385	.821
40-4000	.466	.615
4000-40,000	.618	.174
40,000-250,000	.805	.0239

b_1 and n_1 = constants for a Reynolds number at 3 ft/sec

b_2 and n_2 = constants for a Reynolds number at 40 ft/sec.

Since

mass flow rate = fluid flow rate x density

and the density of water at room temperature (70°F) is about 62.27 lbm/ft^3 then:

$$G_1 = 3 \times 62.27 = 186.81 \text{ lbm/sec-ft}^2$$

$$G_2 = 40 \times 62.27 = 2490.8 \text{ lbm/sec-ft}^2$$

The viscosity of water at room temperature is 2.37 lbm/ft-hr. If D_o is assumed to be about .5 inch, then

$$Re_1 = \frac{D_o G_1}{\mu_f} = 1.18 \times 10^4$$

$$Re_2 = \frac{D_o G_2}{\mu_f} = 1.58 \times 10^5$$

From Table 2.2 the values of n_1, n_2, b_1 and b_2 for these values of Reynolds numbers are:

$n_1 = .618$ $\qquad$ $n_2 = .805$

$b_1 = .174$ $\qquad$ $b_2 = .0239$

substituting the Reynolds numbers and the values of n_1, n_2, b_1 and b_2 into Equation 2.31 will result in:

$$\frac{h_{m1}}{h_{m2}} = .157$$

$$\frac{h_{m2}}{h_{m1}} = 6.37$$

Thus, the surface heat transfer coefficient and therefore the overall heat transfer coefficient increases when the fluid flow rate is increased from 3 ft/sec to 40 ft/sec. On the other hand, the relation between overall heat transfer coefficient and response time is approximately given by

$$\tau \approx \frac{MC}{UA} \tag{2.32}$$

When the fluid flow rate to which a sensor is exposed increases, the surface heat transfer coefficient of the system increases and results in an increase in the overall heat transfer coefficient which reduces the sensor response time.

Equation 2.29 may also be used to study the effect of temperature on the surface component of the response time of an RTD. A typical case in which the sensor is submerged in water and temperature changes from 70°F (room temperature) to about 500°F is considered:

$$\frac{\left[\frac{h_{m1}D_o}{k_{f1}}\,[Pr1]^{-1/3}\right]_{500°F}}{\left[\frac{h_{m2}D_o}{k_{f2}}\,[Pr2]^{-1/3}\right]_{70°F}} = \frac{b_1\left[\frac{D_oG_1}{\mu_{f1}}\right]^{n_1}}{b_2\left[\frac{D_oG_2}{\mu_{f2}}\right]^{n_2}} \tag{2.33}$$

where

h_{m1} = the surface heat transfer coefficient at 500°F

h_{m2} = the surface heat transfer coefficient at 70°F

Pr1 = Prandtl number at 500°F

Pr2 = Prandtl number at 70°F

k_{f1} = thermal conductivity of water at 500°F

k_{f2} = thermal conductivity of water at 70°F

G_1 = mass flow rate at 500°F

G_2 = mass flow rate at 70°F

μ_{f1} = viscosity of water at 500°F

μ_{f2} = viscosity of water at 70°F

b_1 and n_1 = constants for a Reynolds number at 500°F

b_2 and n_2 = constants for a Reynolds number at 70°F.

The following data were obtained for water:[9]

At 500°F

1) k_{f1} = .356 BTU/hr-ft-°F

2) Pr1 = .83

3) μ_{f1} = .26 lbm/ft-hr

4) density = ρ_1 = 49.02 lbm/ft^3

At room temperature (70°F)

1) k_{f2} = .349 BTU/hr-ft-°F

2) Pr2 = 6.78

3) μ_{f2} = 2.37 lbm/ft-hr

4) density = ρ_2 = 62.27 lbm/ft^3

If the water flow rate assumed to be 3 ft/sec, then:

$$G_1 = 3 \times 49.02 = 147.06 \text{ lbm/sec-ft}^2$$

$$G_2 = 3 \times 62.27 = 186.81 \text{ lbm/sec-ft}^2$$

For D_o = .5 inch:

$$Re_1 = \frac{(.5/12)(147.06)(3600)}{.26} = 8.48 \times 10^4$$

$$Re_2 = \frac{(.5/12)(186.81)(3600)}{2.37} = 1.18 \times 10^4$$

The values of n_1, n_2, b_1 and b_2 for these Reynolds numbers are

n_1 = .805 $\qquad$ n_2 = .618

b_1 = .0239 $\qquad$ b_2 = .174

Upon substitution of these data into Equation (2.31) one will obtain:

$$\frac{h_{m1}}{h_{m2}} = 1.963$$

Therefore, the surface heat transfer resistance and the overall heat transfer resistance of a sensor decrease with temperature and result in a smaller response time.

The effect of the surface resistance on response time depends on the relative importance of internal heat transfer and surface heat transfer. This is discussed in section 3.4.

2.5.3.4 Effect of Corrosion

Corrosion on the sheath or on the well of an RTD forms an insulating film that results in a slower response.

2.5.3.5 Effect of Vibration

The effect of vibration on the performance of temperature sensors is of critical importance. Response time degradation and failure of the sensor may result from operating in a severe vibrating condition. Degradation of response time due to vibration occurs if the sensing structure (sensing element and/or supporting structure) or the insulating materials are displaced or gaps are opened inside the sheath of the sensor. The displacement of the sensing structure or insulating materials and expansion of gaps in the sensor affects the internal heat transfer resistance and introduces response time degradation. On the other hand, vibration may detach the sensing coil from the connecting wires inside the sensor and result in a complete failure of the system. Also, stresses imposed on the sensing coil by vibration may cause changes in the resistivity of the sensing filament which affects the performance of the sensor. If the sensor is subjected to periodic stresses that have frequency components matching the natural frequency of the sensor, the sensor can be vibrated to destruction.

3.0 THE LOOP CURRENT STEP RESPONSE TRANSFORMATION

3.1 Introduction

The result of interest is the time constant associated with a step change in fluid temperature external to the sensor. The time constant is defined to be the time required for the sensor output to reach 63.2 percent of its final steady-state value after a step change in fluid temperature. This time constant is usually obtained from a plunge test in a laboratory environment. Since the plunge test cannot be used to obtain the time constant of an installed RTD, the LCSR test is proposed as one method to obtain an estimate of the desired plunge test time constant.

A transformation is needed to convert LCSR data into a prediction of the response that would occur following a fluid temperature step change. The transformation may be developed using a general nodal model for sensor heat transfer. The development is independent of the number of nodes included in the model, so use of this approach does not imply any restrictive assumptions. The following sections give some details on RTD heat transfer that permit formulation of a transformation and that define the conditions for validity of the transformation.

3.2 Mathematical Development of the LCSR Transformation

An analytical transformation for converting loop current step response (LCSR) test results into plunge test results may be developed using a general nodal model for sensor heat transfer. Consider first a system with predominantly one-dimensional heat transfer. In this case, the nodal model may be represented schematically as shown in Figure 3.1.

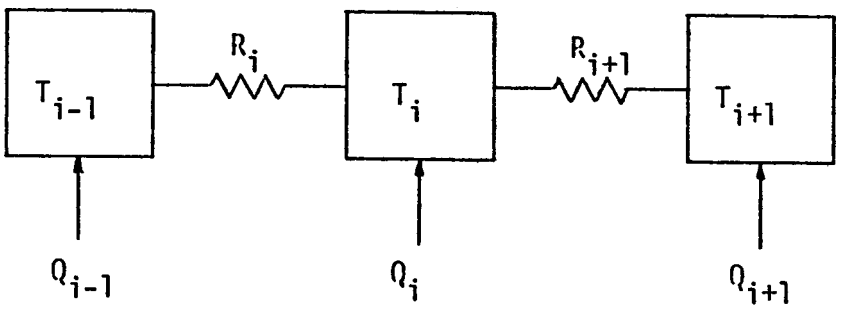

Figure 3.1. Schematic of a One-Dimensional Node-to-Node Heat Transfer Model.

The accuracy of such a model may be made as great as desired by using enough nodes.

The dynamic heat transfer equation for node i is:

$$(MC)_i \frac{dT_i}{dt} = \frac{1}{R_{i-1}} (T_{i-1} - T_i) - \frac{1}{R_i} (T_i - T_{i+1}) + Q_i \qquad (3.1)$$

where Q_i = heat generation rate in node i

M_i = mass of material in node i

C_i = specific heat capacity of material in node i

R_i = heat transfer resistance for node i-1 to node i

T_i = temperature of node i.

Dividing through by $(MC)_i$ and defining constants gives

$$\frac{dT_i}{dt} = a_{i,i-1} T_{i-1} - a_{i,i} T_i + a_{i,i+1} T_{i+1} + b_i Q_i \qquad (3.2)$$

where

$$a_{i,i-1} = \frac{1}{(MC)_i R_{i-1}}$$

$$a_{i,i} = \frac{1}{(MC)_i} \left(\frac{1}{R_{i-1}} + \frac{1}{R_i}\right)$$

$$a_{i,i+1} = \frac{1}{(MC)_i R_i}$$

$$b_i = \frac{1}{(MC)_i}$$

The nodal equations may be applied to a series of nodes, starting at the node closest to the center (i=1) and ending with the node closest to the surface (i=N). The equations have the form:

$$\frac{dT_1}{dt} = -a_{11} T_1 + a_{12} T_2 + b_1 Q_1$$

$$\frac{dT_2}{dt} = a_{21} T_1 - a_{22} T_2 + a_{23} T_3 + b_2 Q_2$$

$$\frac{dT_3}{dt} = a_{32}\,T_2 - a_{33}\,T_3 + a_{34}\,T_4 + b_3\,Q_3$$

.

.

.

$$\frac{dT_N}{dt} = a_{N,N-1}\,T_{N-1} - a_{N,N}\,T_N + C_{N,F}T_F + b_N\,Q_N$$

where

T_F = fluid temperature.

These equations may be written in matrix form:

$$\frac{d\bar{x}}{dt} = A\,\bar{x} + B\,\bar{q} + \bar{c}\,T_F \qquad (3.3)$$

where

$$\bar{X} = \begin{bmatrix} T_1 \\ T_2 \\ T_3 \\ . \\ . \\ . \\ T_N \end{bmatrix} \qquad A = \begin{bmatrix} -a_{11} & a_{12} & 0 & 0 & \cdots & \\ a_{21} & -a_{22} & a_{23} & 0 & \cdots & \\ 0 & a_{32} & -a_{33} & a_{34} & \cdots & \\ . & & & & & \\ . & & & & & \\ . & & & & & \\ & & & & & a_{N,N-1} - a_{N,N} \end{bmatrix}$$

$$B = \begin{bmatrix} b_1 & 0 & 0 & \cdots & \\ 0 & b_2 & 0 & \cdots & \\ 0 & 0 & b_3 & \cdots & \\ & & & & b_N \end{bmatrix} \qquad \bar{q} = \begin{bmatrix} Q_1 \\ Q_2 \\ Q_3 \\ . \\ . \\ . \\ Q_N \end{bmatrix}$$

Laplace transformation gives:

$$[sI-A]\ \bar{x}(s) = \bar{c}\ T_F(s) + B\ \bar{q}(s). \qquad (3.4)$$

The Laplace transform solution for the response of any node, x_i, may be found using Cramer's rule. Let us consider several cases:

1--no heat capacity in region between the filament and the center of the sensor*, no heat generation in any nodes, fluid temperature perturbation, one dimensional heat transfer

$$T_1(s) = \frac{F(s)}{|sI-A|} \qquad (3.5)$$

where

$$F(s) = \begin{vmatrix} 0 & -a_{12} & 0 & 0 & \cdots & & \\ 0 & (s+a_{22}) & -a_{23} & 0 & \cdots & & \\ 0 & -a_{32} & (s+a_{33}) & -a_{34} & \cdots & & \\ 0 & 0 & -a_{34} & (s+a_{44}) & \cdots & & \\ \cdot & \cdot & \cdot & \cdot & \cdots & & \\ \cdot & \cdot & \cdot & \cdot & \cdots & & \\ \cdot & \cdot & \cdot & \cdot & \cdots & & \\ C_{N,F}T_F(s) & \cdot & \cdot & \cdot & \cdots & -a_{N,N-1} & (s+a_{N,N}) \end{vmatrix} \qquad (3.6)$$

*In the interim report (EPRI Report NP-459), this was referred to as a central node. The specification used here is more general and applies to the configuration of some sensors.

This may be written

$$F(s) = C_{N,F}\, T_F(s)\, (-1)^{(N+F)} \begin{vmatrix} -a_{12} & 0 & 0 & \cdots & \\ (s+a_{22}) & -a_{23} & 0 & \cdots & \\ -a_{32} & (s+a_{33}) & -a_{34} & \cdots & \\ \cdot & \cdot & \cdot & \cdots & \\ \cdot & \cdot & \cdot & \cdots & \\ \cdot & \cdot & \cdot & & -a_{N-1,N-1} \end{vmatrix} \qquad (3.7)$$

This determinant is for a matrix in lower triangular form (all elements above the diagonal are zero). The determinant is given by the product of the diagonals, all of which are constants. Therefore, for a fluid temperature perturbation in a one-dimensional heat transfer system, the response of the innermost node is characterized by a transfer function with no zeroes. If the sensing element in an RTD is centrally located, or if there is insignificant heat capacity between the filament and the center of the sensor, then this type of transfer function describes the response characteristics of the sensor.

The transfer function may be written

$$\frac{T_1(s)}{T_F(s)} = \frac{K}{|sI-A|}$$

$$= \frac{K}{(s-p_1)\,(s-p_2)\,\cdots} \qquad (3.8)$$

where

p_i = poles (identical to eigenvalues of A).

For a unit step change in T_F, $T_F(s) = \frac{1}{s}$, and we may write:

$$T_1(s) = \frac{K}{s(s-p_1)\,(s-p_2)\,\cdots} \quad . \qquad (3.9)$$

Inversion of this Laplace transform using the residue theorem gives:

$$T_1(t) = K\left[\frac{1}{(-p_1)\ (-p_2)\ \ldots\ (-p_N)} + \frac{e^{p_1 t}}{(p_1)\ (p_1-p_2)\ \ldots}\right.$$

$$\left. + \frac{e^{p_2 t}}{(p_2)\ (p_2-p_1)\ \ldots} + \ldots\right]. \qquad (3.10)$$

Thus, we make the following important observation:

> For an RTD with predominantly one-dimensional heat transfer and with insignificant heat capacity between the sensing element and the center of the sensor, the poles alone (no zeroes) are adequate to characterize the response due to a fluid temperature change.

The implication is that if one can identify the poles by some other test (such as the LCSR), then he can construct the response to a fluid temperature step.

2--significant heat capacity between the filament and the center of the sensor, no heat generation in any nodes, fluid temperature perturbation, one dimensional heat transfer

This case may be analyzed for the response of any non-central node, but for notational simplicity, let us consider the response of the second node. In this case

$$T_2(s) = \frac{F(s)}{|sI-A|} \qquad (3.11)$$

where

$$F(s) = \begin{vmatrix} (s+a_{11}) & 0 & 0 & 0 & \cdots \\ -a_{21} & 0 & -a_{23} & 0 & \cdots \\ 0 & 0 & (s+a_{33}) & -a_{34} & \cdots \\ \cdot & \cdot & \cdot & \cdot & \cdots \\ \cdot & \cdot & \cdot & \cdot & \cdots \\ \cdot & \cdot & \cdot & \cdot & \cdots \\ \cdot & C_{N,F}T_F(s) & \cdot & \cdot & \cdots \end{vmatrix} \tag{3.12}$$

This may be written

$$F(s) = C_{N,F}\, T_F(s)\, (-1)^{(2+N)} \begin{vmatrix} (s+a_{11}) & 0 & 0 & 0 & \cdots \\ -a_{21} & -a_{23} & 0 & 0 & \cdots \\ 0 & (s+a_{33}) & -a_{34} & 0 & \cdots \\ \cdot & \cdot & \cdot & \cdot & \cdots \\ \cdot & \cdot & \cdot & \cdot & \cdots \\ \cdot & \cdot & \cdot & \cdot & \cdots \end{vmatrix} \tag{3.13}$$

Again, we observe that the matrix is triangular, but the diagonals are not all constant. In this case, the transfer function will have one zero. For the response of nodes further from the center, there will be more zeroes. Thus, the poles alone are not adequate to construct the response for an RTD if the sensing element is not located at a position with insignificant heat capacity between the filament and the center of the sensor.

3--insignificant heat capacity between the filament and the center of the sensor, heat generation in central node, constant fluid temperature, one-dimensional heat transfer

$$T_1(s) = \frac{F(s)}{|sI-A|} \tag{3.14}$$

where

$$F(s) = \begin{vmatrix} b_1 Q_1 & -a_{12} & 0 & 0 & \cdots \\ 0 & (s+a_{22}) & -a_{23} & 0 & \cdots \\ 0 & -a_{32} & (s+a_{33}) & -a_{34} & \cdots \\ \cdot & \cdot & \cdot & \cdot & \cdots \\ \cdot & \cdot & \cdot & \cdot & \cdots \\ \cdot & \cdot & \cdot & \cdot & \cdots \end{vmatrix} \tag{3.15}$$

This may be written

$$F(s) = b_1 Q_1 \begin{vmatrix} (s+a_{22}) & -a_{23} & 0 & 0 & \cdots \\ -a_{32} & (s+a_{33}) & -a_{34} & 0 & \cdots \\ 0 & -a_{43} & (s+a_{44}) & -a_{45} & \cdots \\ \cdot & \cdot & \cdot & \cdot & \cdots \\ \cdot & \cdot & \cdot & \cdot & \cdots \\ \cdot & \cdot & \cdot & \cdot & \cdots \end{vmatrix} \tag{3.16}$$

In this case, the matrix is not triangular, and the transfer function will have zeroes.

The transfer function may be written:

$$\frac{T_1(s)}{Q_1(s)} = K^1 \frac{(s-z_1)\ (s-z_2)\ \ldots\ (s-z_M)}{(s-p_1)\ (s-p_2)\ \ldots\ (s-p_N)} . \tag{3.17}$$

For a unit step change in Q_1 ($Q_1(s) = \frac{1}{s}$), we obtain

$$T_1(s) = \frac{K^1(s-z_1)\ (s-z_2)\ \ldots\ (s-z_M)}{s(s-p_1)\ (s-p_2)\ \ldots\ (s-p_N)} . \tag{3.18}$$

Inversion by the residue theorem gives:

$$T_1(t) = K^1\left[\frac{(-z_1)\ (-z_2)\ \ldots\ (-z_M)}{(-p_1)\ (-p_2)\ \ldots\ (-p_N)} + \frac{(p_1-z_1)\ (p_1-z_2)\ \ldots\ (p_1-z_M)}{(p_1)\ (p_1-p_2)\ \ldots\ (p_1-p_N)} e^{p_1 t}\right.$$

$$\left. + \frac{(p_2-z_1)\ (p_2-z_2)\ \ldots\ (p_2-z_M)}{(p_2)\ (p_2-p_1)\ \ldots\ (p_2-p_N)} e^{p_2 t} + \ldots\right]. \tag{3.19}$$

Note that the response is determined by the zeroes as well as the poles. However, the poles are the same as for the fluid temperature change case. Thus, if we can identify the poles from a LCSR test, we can construct the equivalent fluid perturbation response using Equation (3.10).

4--insignificant heat capacity between the filament and the center of the sensor, no heat generation in any nodes, fluid temperature perturbation, multi-dimensional heat transfer

In this case, there is branching in the heat transfer (see Figure 3.2). This means that the temperature of a node may be influenced by more than just two neighboring nodes as in the one-dimensional case. In the one-dimensional case, all of the elements of the A matrix are on the diagonal or in the position adjacent to the diagonal. In the multi-dimensional case, coupling terms appear in other positions (always symmetrically positioned around the diagonal). Thus F(s) may be written

$$F(s) = \begin{vmatrix} 0 & -a_{12} & * & * & \cdots \\ 0 & (s+a_{22}) & -a_{23} & * & \cdots \\ \cdot & -a_{32} & (s+a_{33}) & -a_{34} & \cdots \\ \cdot & * & * & * & \cdots \\ \cdot & \cdot & \cdot & \cdot & \cdots \\ \cdot & \cdot & \cdot & \cdot & \cdots \\ \cdot & \cdot & \cdot & \cdot & \cdots \\ C_{N,F}T_F(s) & \cdot & \cdot & \cdot & \cdots \end{vmatrix} \qquad (3.20)$$

where

* = possible new coupling terms.

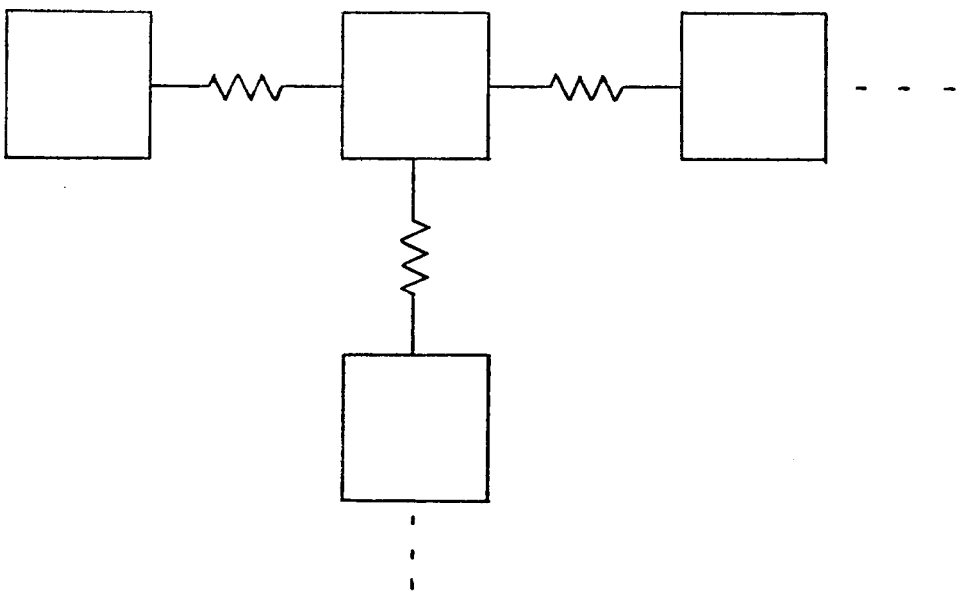

Figure 3.2 Schematic of a Multi-Dimensional Node-to-Node Heat Transfer Model.

In this case, the matrix is not triangular and zeroes can occur. This means that the availability of the poles through some sort of measurement is not sufficient for construction of the response to a fluid temperature step.

3.3 Steps in Implementing the LCSR Transformation

The steps for obtaining the plunge test time constant are:

1. perform a LCSR test
2. identify the poles associated with the LCSR data
3. construct the step response for a fluid temperature perturbation using Equation (3.10).

A key element is identification of the poles by analysis of the LCSR transient data. This is accomplished by minimizing the sum of the squares of the residual error between the model and the LCSR data. Although other methods have been used and are adequate, a nonlinear minimization algorithm that yields unbiased estimates of the model parameters is preferred. The computer program that estimates the poles and the plunge time constant is described in Appendix B.

One method to help in the pole-fitting problem has been proposed by Carroll of Oak Ridge National Laboratory. He observed that for a centrally located sensor in a cylindrical sensor with small surface heat transfer resistance compared to internal heat transfer resistance, the following relation approximately defines the poles:

$$p_i = p_1[1 + (i-1)\ R]^2. \qquad (3.21)$$

This relation is useful because it allows one to estimate higher poles using fitted values for only two parameters (p_1 and R).

3.4 Validity of the LCSR Transformation for RTDs With Noncentral Filaments

It is shown in Section 3.2 that the plunge test response can be characterized by only the system eigenvalues when the filament is centrally located or when the heat capacity interior to the filament is small compared to the heat capacity exterior to the filament. If neither of these criteria is satisfied, additional dynamical information is needed to characterize the response.

In order to demonstrate the effect of heat capacity in the region between the filament and the center of the sensor on the LCSR transformation, the RTD is modeled as a homogeneous structure with the filament represented by a delta function. For this case, an analytical solution is available for investigating the response.

3.4.1 Analytical Results for a Homogeneous RTD

Analytical solutions for three cases are presented: 1) a homogeneous RTD plunged into a fluid bath, 2) a homogeneous RTD subjected to a step change in the filament current, and 3) a homogeneous RTD with a hollow interior plunged into a fluid bath.

The partial differential equation which governs the response for each case is

$$\frac{\partial T(r,t)}{\partial t} = \alpha \left(\frac{\partial^2 T(r,t)}{\partial r^2} + \frac{1}{r} \frac{\partial T(r,t)}{\partial r}\right) + \dot{Q}(r,t) \qquad (3.22)$$

subject to the applicable boundary conditions where:

$\alpha = k/\rho c$

k = thermal conductivity

ρ = density

c = heat capacity

$\dot{Q}$ = heat source.

The generic procedure for solving the problems of interest is: 1) use the property that the space and time variables are separable, 2) use the transcendental equation obtained from the boundary conditions to determine the system eigenvalues, and 3) use the orthogonality property of the eigenfunctions (determined from the Sturm-Liouville problem) to obtain the expansion coefficients associated with each eigenfunction.

First, the key results for the case of plunging the RTD into a fluid bath are presented. The filament is treated as a cylindrical shell, located at R*, and is represented mathematically by a delta function. The outside radius of the RTD is denoted by R. Boundary conditions are: 1) finite temperature at the center of the RTD, and 2) Newton's Law of cooling at the RTD surface. For the initial condition, it is assumed that the RTD is in thermal equilibrium with its surroundings. The result for this case is [10]

$$\frac{T(R^*,t) - T_\infty}{T(R^*,0) - T_\infty} = \sum_{n=1}^{\infty} K_n \, e^{-M_n^2 \, \alpha t/R^2} \tag{3.23}$$

where

$$K_n = 2 \, \frac{J_1(M_n) \, J_o(M_n(R^*/R))}{[\, J_o^2(M_n) + J_1^2(M_n)]} \tag{3.24}$$

$$M_n = \lambda_n R \tag{3.25}$$

and the system eigenvalues are defined through the transcendental equation,

$$\frac{J_o(\lambda_n R)}{J_1(\lambda_n R)} = \frac{\lambda_n R}{hR/k} = \frac{\lambda_n R}{N_{Bi}} \quad . \tag{3.26}$$

The Biot modulus, N_{Bi}, is defined by

$$N_{Bi} = \frac{h}{k/R} \quad . \tag{3.27}$$

It is the ratio of internal heat transfer resistance to external heat transfer resistance. In other words, it is the ratio of conductive resistance to convective resistance.

The theoretical response of the RTD due to a step change in filament heating current is now considered. Although the generic procedure for obtaining the analytical solution for a change in the heating current is similar to the problem of plunging the RTD into a fluid bath, there are minor differences. In particular, the expansion coefficients are not the same. If the filament heating current undergoes a step change, one can obtain the expression,

$$T(r,t) - T_i(r,0) = \sum_{n=1}^{\infty} L_n \, e^{-M_n^2 \, \alpha t/R^2} \tag{3.28}$$

where

$$L_n = \frac{\dot{Q}_o - \dot{Q}_\infty}{\pi k} \frac{J_o(\lambda_n r)\, J_o(\lambda_n R^*)}{(\lambda_n R^2)[J_1^2(\lambda_n R) + J_o^2(\lambda_n R)]} \tag{3.29}$$

$\dot{Q}_o$ = the heat source before the step change

$\dot{Q}_\infty$ = the heat source after the step change

$T_i(r,0)$ = the initial temperature distribution.

The response of the filament is obtained by setting r equal to R*.

The eigenvalues for the response due to a step change in filament heating current are the same as for the response due to a step in external fluid temperature (plunging the RTD into a fluid bath). This follows since the boundary conditions are the same for both cases.

The forcing functions are not the same for the two problems presented. Consequently, the expansion coefficients are altered for a step change in heating current as compared to a step change in external fluid temperature.

Analytical results were also obtained for an RTD modeled as a hollow cylinder with the filament on the inside surface. Since both the forcing function and the boundary conditions are not the same as for the homogeneous cases already presented, both the system eigenvalues and the expansion coefficients must be determined for this case.

This problem can also be solved by separation of variables; hence the result can be written as an infinite sum,

$$T(r,t) - T(r,o) = \sum_{n=1}^{\infty} C_n\, e^{-\alpha\lambda_n^2 t}\, R_n(r) \tag{3.30}$$

where: 1) the C_n are the expansion coefficients (evaluated according to the Sturm-Liouville problem), 2) the $e^{-\alpha\lambda_n t}$ are the time dependent components of the eigenfunctions, and 3) the $R_n(r)$ are the space dependent components of the eigenfunctions. The transcendental equation defining the eigenvalues is,[10]

$$\frac{J_o'(\lambda_n a)}{\lambda_n K J_o'(\lambda_n b) + h J_o(\lambda_n b)} = \frac{Y_o'(\lambda_n a)}{\lambda_n k Y_o'(\lambda_n b) + h Y_o(\lambda_n b)} \tag{3.31}$$

where

a = the inside radius

b = the outside radius.

The primes on the Bessel functions denote differentiation with respect to the argument.

3.4.2 Numerical Results for a Homogeneous RTD

The effect of heat capacity between the filament and the sensor may be investigated using the homogeneous RTD model. This is accomplished easily by simply evaluating the plunge test time constant at various specified positions in the homogeneous sensor. Since the boundary conditions are the same for all of these cases, the eigenvalues are the same. These eigenvalues uniquely define the plunge test estimate from the LCSR transformation, and the transformation applies only for the center of a homogeneous sensor. Therefore the time constant obtained for a central position is equivalent to a perfectly performed LCSR transformation. This is the time constant that would be obtained from the

LCSR transformation regardless of the position of the filament. The error due to a non-central filament in a homogeneous sensor may be obtained by comparing the time constant obtained from Equation 3.23 for r=0 and for some position, $r=R^*$. Numerical results were obtained for various filament locations and for various values of the Biot modulus.

If the RTD filament is near the surface, the response time of the RTD will be faster than if it is near the center. If the surface resistance to heat transfer is much greater than the internal resistance, the location of the filament will not affect the response time significantly. This corresponds to a sensor with a small Biot modulus. Thus, if the filament of a homogeneous RTD is noncentrally located and the internal resistance approximates the surface resistance (or is less), the LCSR transformation should give good results. On the other hand, if the internal resistance is relatively high (large Biot modulus), the LCSR transformation should give poor results for a homogeneous RTD with a noncentral filament.

As the filament is moved toward the surface, the response time becomes shorter. The magnitude of this effect depends strongly on the Biot modulus. Figure 3.3 and Table 3.1 show the relative effect (ratio of the response time with the filament at R*/R to the response time with the filament at the center) on the response time due to moving the filament from the center to the surface. This effect is illustrated parametrically in the Biot modulus. Note that use of the LCSR transformation for a homogeneous sensor with $R^*/R \tilde{=} 0.8$ and with a Biot modulus near unity results in a theoretical error of about 20% in the time constant.

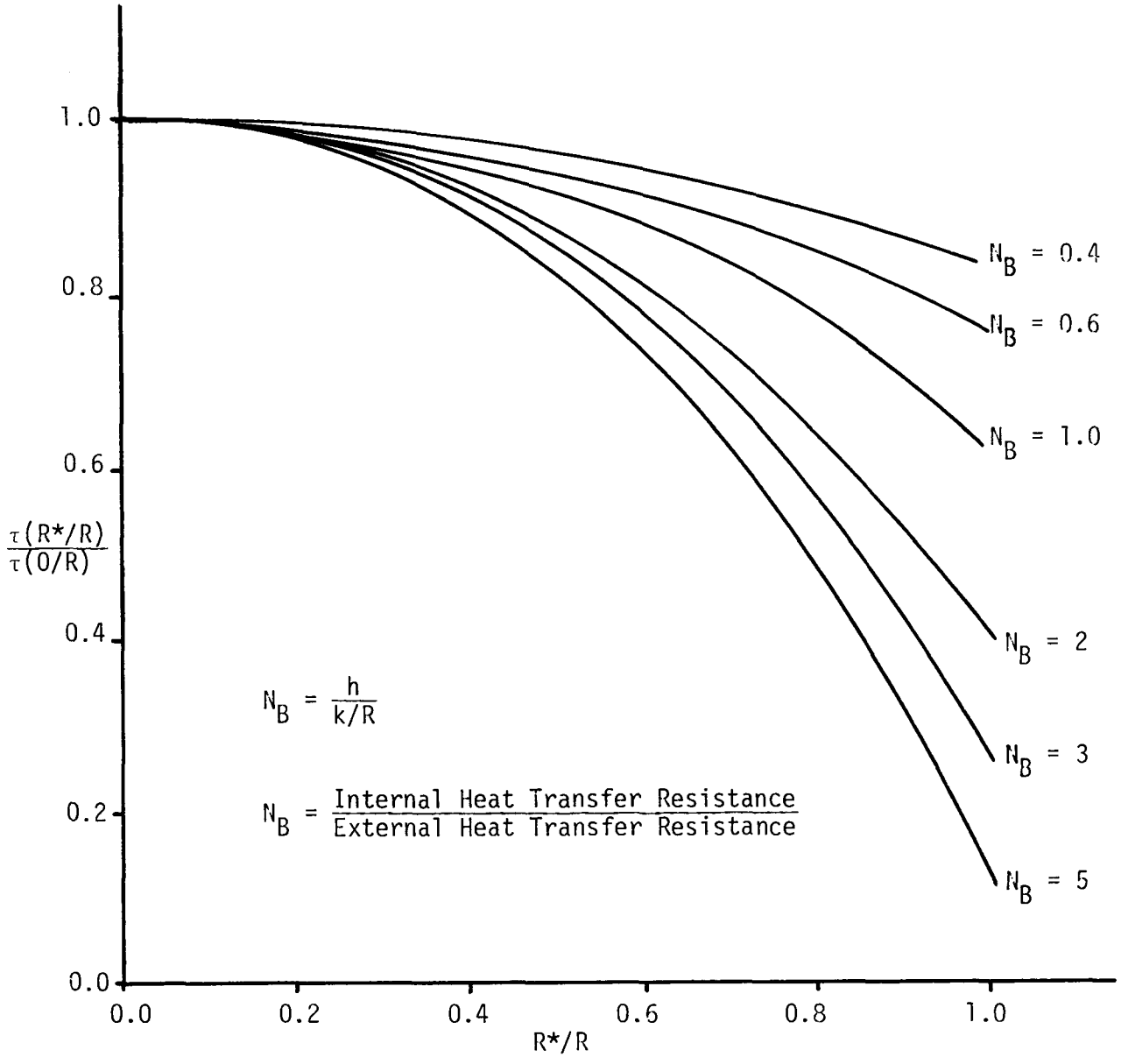

Figure 3.3. Ratio of the time constant with the filament at R* to the time constant with the filament at the center versus the ratio of the filament radius to the sensor radius (R*/R).

TABLE 3.1

RATIO OF THE TIME CONSTANT WITH THE FILAMENT AT R* TO THE TIME CONSTANT WITH THE FILAMENT AT THE CENTER ((R*/R)/(0/R)) FOR VARIOUS VALUES OF THE BIOT MODULUS AND OF THE FILAMENT RADIUS TO SENSOR RADIUS (R*/R)

R^*/R \ N_{Bi}	5	3	2	1	0.8	0.6	0.4
0.0	1.0	1.0	1.0	1.0	1.0	1.0	1.0
0.2	0.973	0.976	0.980	0.986	0.988	0.9907	0.993
0.4	0.888	0.901	0.923	0.946	0.954	0.962	0.973
0.6	0.727	0.799	0.810	0.876	0.894	0.915	0.939
0.8	0.467	0.561	0.643	0.775	0.809	0.848	0.889
1.0	0.133	0.263	0.3995	0.623	0.687	0.754	0.828

4.0 TEST PROCEDURES AND DATA ANALYSIS

4.1 Introduction

The test procedures and data analysis methods for testing RTDs by the loop current step response or the self heating methods are described in this chapter.

4.2 The LCSR Test

4.2.1 Description of the LCSR Test

A loop current step response test is based on an internal step change in temperature caused by a sudden change of electric current through the sensing filament. Typically, the current through the sensor is increased suddenly from its normal level of few milliampers to a level of 40 to 60 milliampers or higher. The increased current produces I^2R heating in the filament and results in a temperature transient which settles slightly above the temperature of the sensor surroundings. The details of the test procedure for in-plant measurements are given in Appendix C. A typical loop current step response output is shown in Figure 4.1 for a heating transient. A cooling transient is obtained when the sensor current is suddenly decreased. This is shown in Figure 4.2. Experiments indicate that the heating or cooling transient of a loop current step response test carries the same information about the response characteristics of a sensor (though the quality of the test data may differ).

A loop current step response test provides the response to an internal step change in temperature while the response to a temperature change outside the sensor is desired. An analytical transformation has been developed to convert the loop current step response data to give

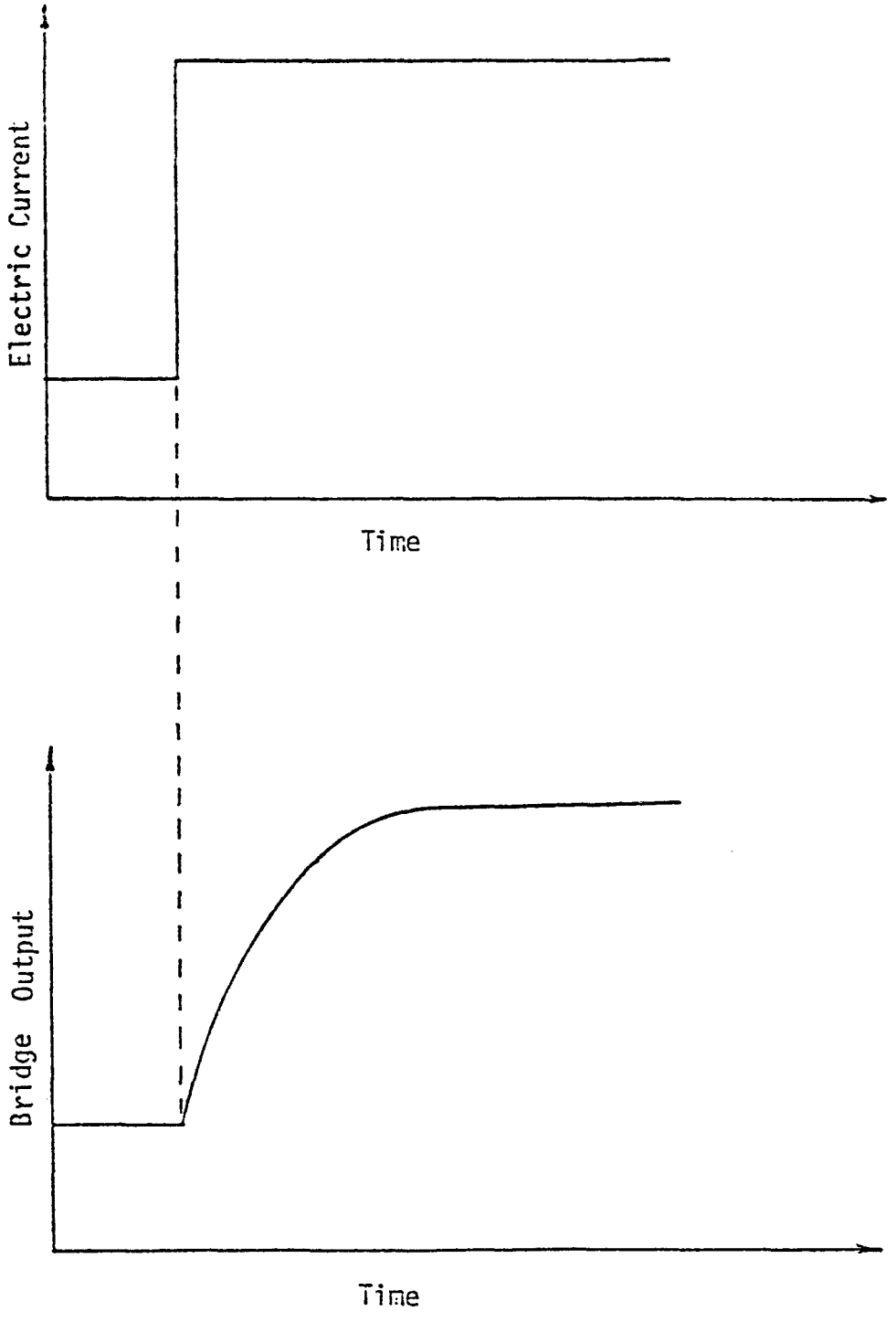

Figure 4.1. A Typical LCSR Heating Transient.

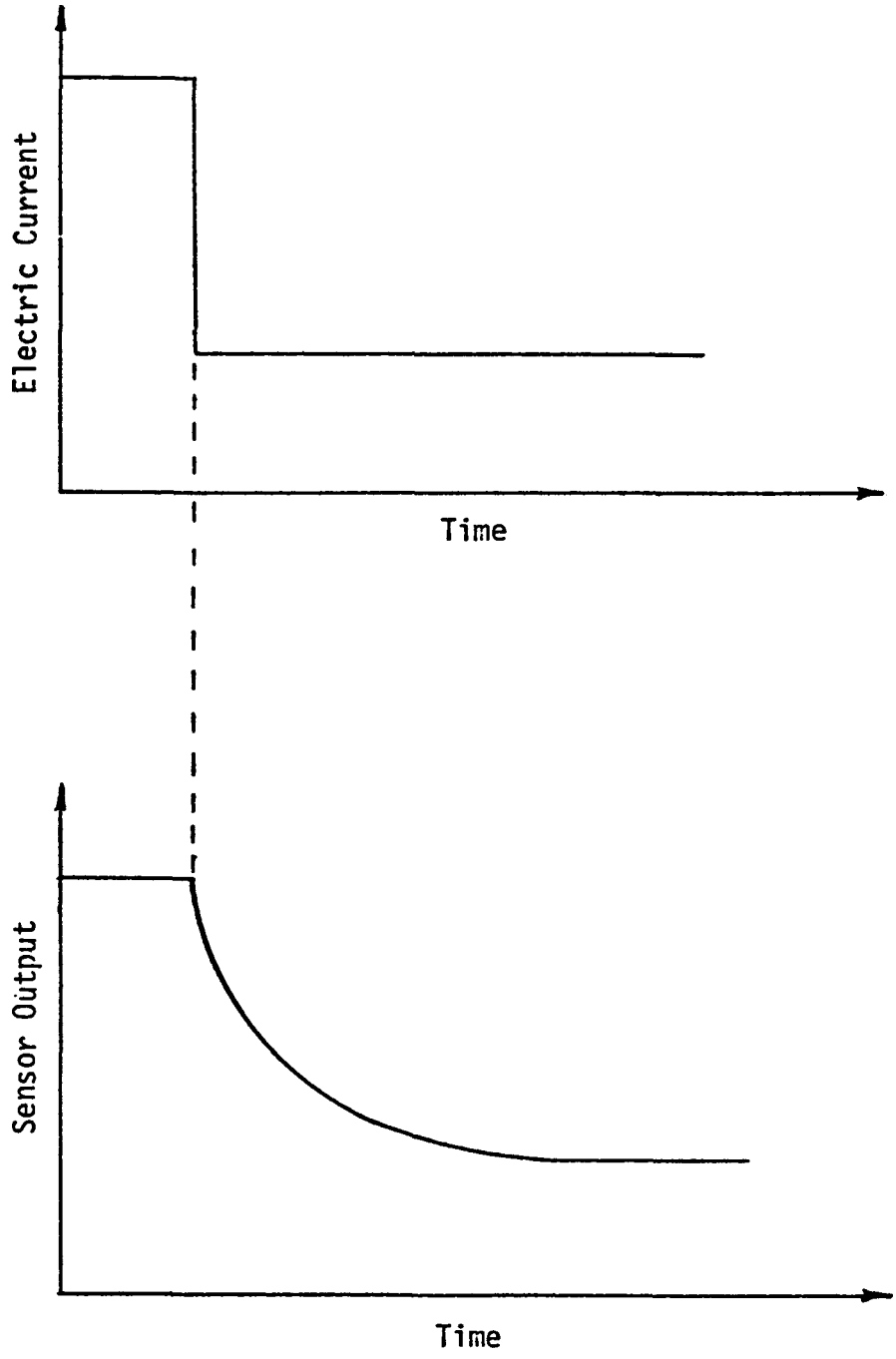

Figure 4.2. A Typical LCSR Cooling Transient.

the response of a sensor to an external change in temperature. This transformation is valid for sensors with the following characteristics (see Chapter 3 of this report):

1. Predominantly one-dimensional heat transfer: This requirement is often satisfied because all of the industrial temperature sensors are designed for a minimum axial heat conduction in order to improve their steady state performance.
2. Negligible heat capacity between filament and the center of sensor assembly.

4.2.2 LCSR Test Procedure

The LCSR test equipment is a bridge with current switching capability. This is illustrated in Figure 4.3. The switch can be opened or closed to decrease or increase the current. A detailed typical test procedure for in-plant tests is given in Appendix C.

There are two basic methods for performing a LCSR test. One involves initial balancing of the bridge to give zero output at low current (switch open). The other involves initial balancing to give zero output at high current (switch closed). The balancing at low current is usually preferred because the data are taken during high current operation where the signal-to-noise ratio is higher. The steps in these procedures are outlined below.

4.2.2.1 Balance at Low Current

1. Adjust the decade box resistance to give a zero output with the switch open.
2. Adjust the power supply voltage to give the desired current when the switch is closed (usually 40 to 60 ma).

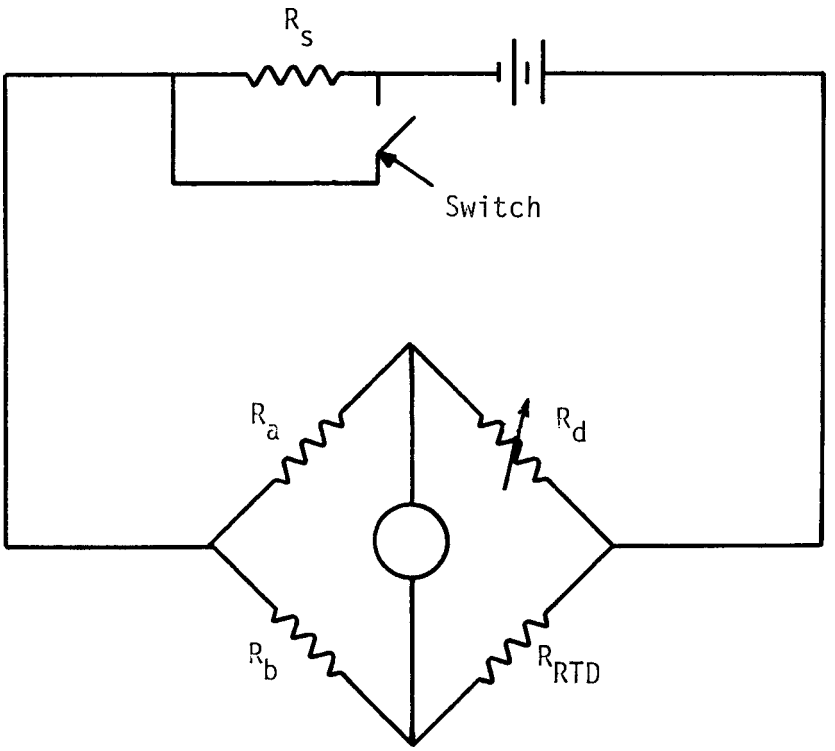

Figure 4.3. Schematic of the Loop Current Step Response Test Equipment.

3. Close the switch and monitor the sensor output. The response will be shown in Figure 4.1.

The interpretation follows from the bridge equation

$$\Delta V = \left[\frac{(R_d - R_{RTD})\ R_a}{(R_a + R_d)(R_a + R_{RTD})}\right] \quad E \tag{4.1}$$

Since $R_d = R_{RTD}$ when E changes, ΔV remains zero at the instant of switching. As the RTD resistance changes as a result of the heating, ΔV is given by:

$$\Delta V = C \quad \Delta R_{RTD} \quad E_H$$

where

$$C = \frac{R_a}{(R_a + R_d)(R_a + R_{RTD})} \tag{4.2}$$

E_H = impressed voltage at the high level.

If ΔR_{RTD} is small compared to $R_a + R_{RTD}$, then C is essentially constant and $\Delta V \propto \Delta R_{RTD}$.

One can also assess the effect of imperfect initial balancing of the bridge on the output signal. If $R_d \neq R_{RTD}$, then Equation 4.1 shows that at the instant of switching to the high current the bridge output will change (instantaneously) by

$$\Delta V = \frac{(R_d - R_{RTD})\ \ R_a}{(R_a + R_d)(R_a + R_{RTD})} \quad (E_H - E_L) \tag{4.3}$$

where

E_L = impressed voltage at the low level

Thus, the effect of imperfect balancing can give an output voltage of the type shown in Figure 4.4.

4.2.2.2 Balance at High Current

There are two approaches for initial balancing at high current. One involves the following steps:

1. Adjust the decade box resistance to give a zero output with the switch closed and the power supply voltage set to give a current of 40 to 60 ma.
2. Open the switch and monitor the output. The output will be as shown in Figure 4.2.

Equation 4.1 can be used to interpret Figure 4.2. Since $R_d = R_{RTD}$ when E changes, ΔV remains zero at the instant of switching. The output signal is given by

$$\Delta V = C \quad \Delta R_{RTD} \quad E_L \tag{4.4}$$

where

E_L = impressed voltage at the low level.

The ΔR_{RTD} change is the same as in the previous case except for a sign change. However, one should note that the output signal is proportional to E as well as the change in R_{RTD}. Since the transient is measured in this case with E at the low level, the signal will be smaller than in the previous case. Therefore more amplification is required and noise may be a problem. Because of this difficulity, this method usually is not used.

Another procedure involving initial balancing at high current can be used. It involves the following steps:

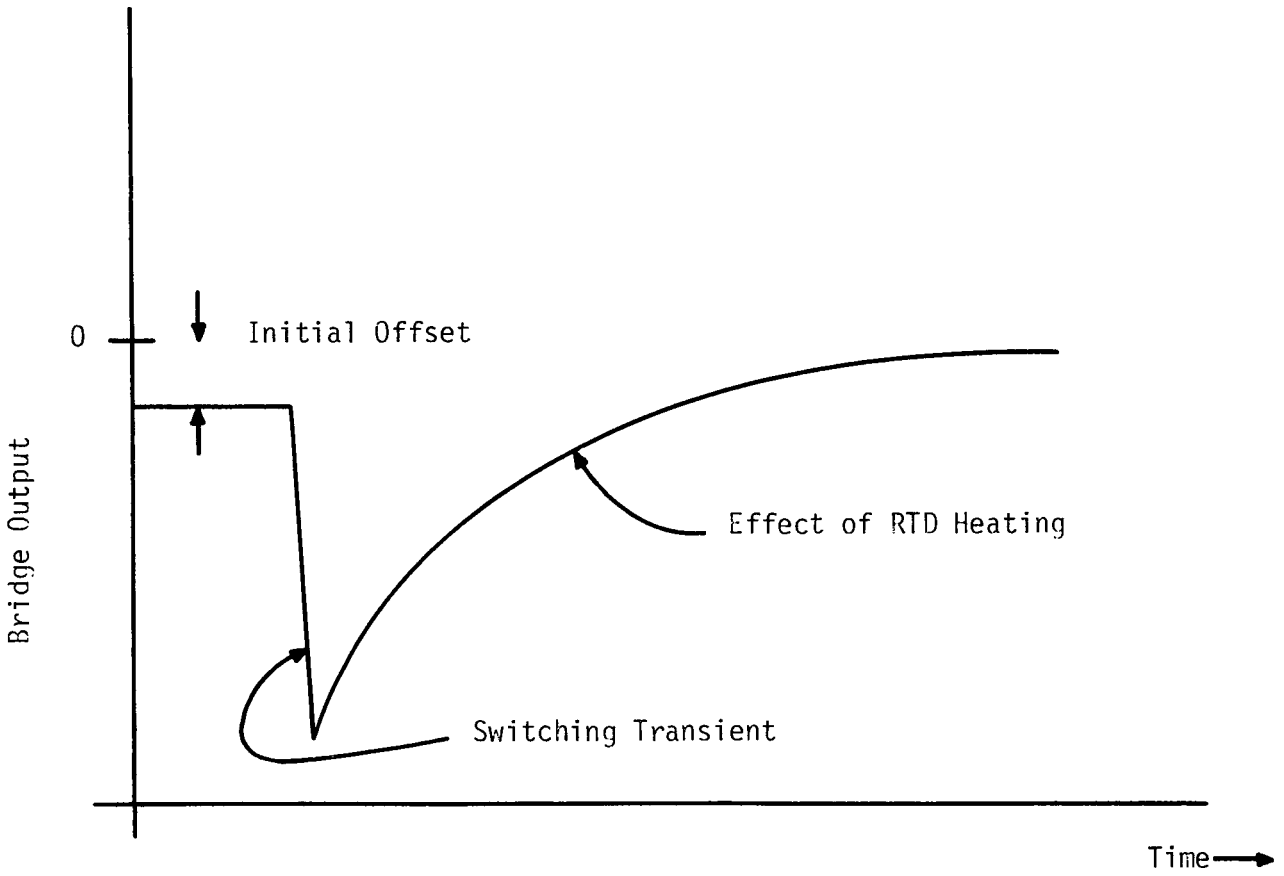

Figure 4.4. Illustration of a Switching Transient Due to An Initially Imbalanced Bridge.

1. Adjust the decade box resistance to give a zero output with the switch closed and the power supply voltage set to give a current of 40 to 60 ma.
2. Open the switch and let the output go to steady state. The bridge will now be out of balance.
3. Close the switch again and monitor the output signal. The response will be as shown in Figure 4.5.

The interpretation of this also follows from Equation 4.1. Since the bridge is out of balance, the output before the start of the test transient is:

$$\Delta V = \frac{(R_d - R_{RTD})\ R_a}{(R_a + R_d)(R_a + R_{RTD})}\ E_L \qquad (4.5)$$

where

$$R_d \neq R_{RTD}.$$

At the instant the impressed voltage is switched the value of R_{RTD} is still essentially unchanged, and ΔV jumps to

$$\Delta V = \frac{(R_d - R_{RTD})\ R_a}{(R_a + R_d)(R_a + R_{RTD})}\ E_H. \qquad (4.6)$$

Then R_{RTD} starts to change because of the heating effect. The output signal will return to zero since the bridge was set for a balanced condition at high current.

4.2.3 Steps in Implementing the LCSR Transformation

The plunge test response of a temperature sensor can be determined from a LCSR test by the following procedure:

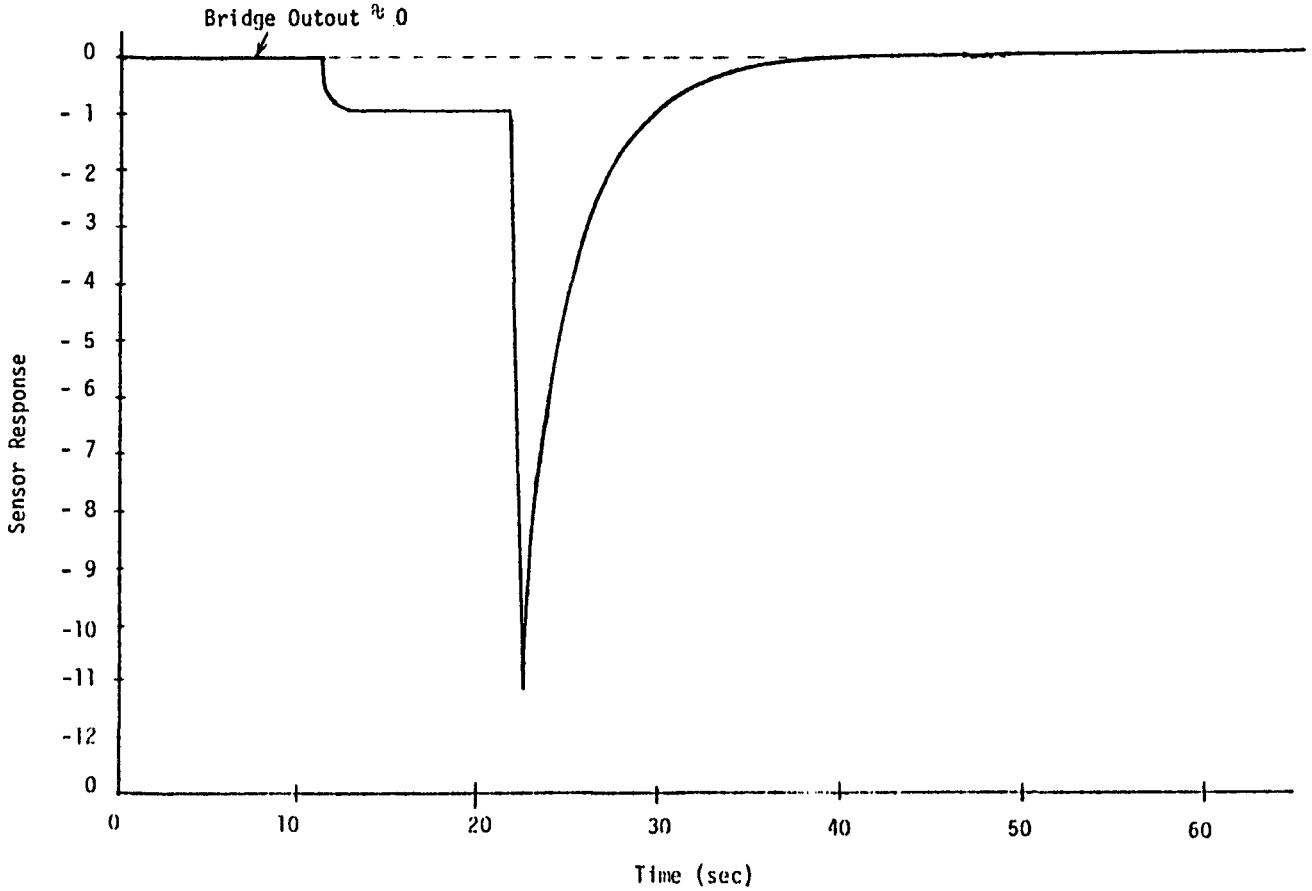

Figure 4.5. A Typical LCSR Output when Bridge is Balanced at a High Current Prior to Performance of the Test.

1. Perform a LCSR test.
2. Fit the LCSR test data to Equation 4.7:

$$T(t) = B_o + B_1 e^{p_1 t} + B_2 e^{p_2 t} + \ldots + B_n e^{p_n t} \qquad (4.7)$$

This provides the eigenvalues (p_i) necessary for predicting the plunge test response. A number of methods are available for performing this fit. Graphical exponential stripping or computer optimization routines are often used.

3. Subsitute the eigenvalues in Equation 3.10:

$$T(t) = A_o + A_1 e^{p_1 t} + A_2 e^{p_2 t} + \ldots + A_n e^{p_n t} \qquad (4.8)$$

where A_i are obtained from Equation 3.10:

$$A_0 = \frac{1}{(-p_1)(-p_2) \ldots (-p_n)}$$

$$A_1 = \frac{1}{(p_i)(p_1 - p_2) \ldots (p_1 - p_n)}$$

$$A_2 = \frac{1}{p_2(p_2 - p_1) \ldots (p_2 - p_n)}$$

etc.

Equation 4.8 gives the response of the sensor to a sudden change in the surrounding fluid temperature.

Special problems in obtaining a good fit occur when the LCSR data are contaminated with noise. A special procedure has been developed for handling this case and is described in Appendix D.

4.3 The Self Heating Test

The self heating test is a method of detecting the changes in the response time of an RTD installed in a process. This method is based on steady state measurement of temperature rise versus I^2R heating in the sensing filament. The steady state relation between temperature and I^2R heating generated in the sensor is:

$$Q = UA\,(T-\theta) \tag{4.9}$$

where

Q = heat generation rate in sensor by I^2R heating

U = overall heat transfer coefficient

A = heat transfer area

T = sensor temperature

θ = temperature of surrounding fluid

For constant fluid temperature:

$$\Delta Q = UA\,\Delta T \tag{4.10}$$

Therefore the temperature rise per unit power generated in the sensor is:

$$\frac{\Delta T}{\Delta Q} = \frac{1}{UA} \tag{4.11}$$

Since the resistance of a platinum filament is approximately proportional to its temperature ($\Delta R = G\,\Delta T$):

$$\frac{\Delta R}{\Delta Q} = \frac{1}{GUA} = \frac{\text{Constant}}{G\,UA} \tag{4.12}$$

On the other hand, the response time of a sensor is approximately given by:

$$\tau = \frac{MC}{UA} \tag{4.13}$$

where

M = mass

C = specific heat capacity

U = overall heat transfer coefficient (includes internal resistance as well as film resistance)

A = heat transfer area.

If the heat capacity C remains constant, then:

$$\tau = \frac{\text{Constant}}{UA} \tag{4.14}$$

Comparing Equations 4.12 and 4.14 leads to the conclusion that:

$$\tau \propto \frac{\Delta R}{\Delta Q} \tag{4.15}$$

Therefore, a change in the response time of a sensor can be identified by a change in the slope of the curve of ΔR versus ΔQ. This slope is called the self heating index and is usually expressed in ohms per watt. A procedure for evaluating the self heating index is explained in the following section.

4.3.1 Self Heating Test Procedure

A self heating curve is usually generated by the following procedures:

1. Increase the sensor current incrementally from 1-6 milliampers to 20-60 milliampers.
2. Measure the sensor resistance when the steady state is attained after each increment in current.
3. Calculate the amount of power generated in the sensor from:

$$P = I^2R$$

4. Plot the values of resistance as a function of electric power dissipated in the sensor (R versus P).

Experience indicates that the value of the self heating index ($\frac{\Delta R}{\Delta P}$) is quite different from one sensor to another, even when they are the same design. Therefore, each sensor must be identified by its own self heating index, i.e., the self heating index of a sensor should not be used to specify another sensor of the same type. Thus, the application of self heating method for monitoring the changes in response time of a RTD requires determination of its self heating index at the time of installation. Subsequent self heating measurements permit comparisons with respect to the as-new case.

5.0 LABORATORY RESULTS FOR LCSR AND SELF HEATING TESTS

5.1 Introduction

In the course of the response time testing program six different reactor-type RTDs were tested. The instrumentation and data acquisition are described in Appendix E and the Equipment Specifications are given in Appendix F. A listing of these sensors and their characteristics were given in Table 2.1. The response characteristics of these sensors were determined by several plunge, LCSR and self heating tests performed in a rotating tank at about 3 ft/sec. The test results are listed in Tables 5.1 and 5.2. The results are the average value of about 10 tests per sensor. The standard deviation included in the self heating index is obtained using a standard propagation of error approach that relates fitting errors to the error in the slope.[11] The time constant results are based on the following analyses:

1. Analysis of the plunge test response.
2. Graphical exponential stripping from the plot of the LCSR test data on semi-log paper (Appendix G).
3. Computer analysis of the LCSR test data (Appendix B).

The time constant estimates obtained by the graphical exponential stripping method are smaller than the pertinent plunge test time constant. This is apparently due to inaccurate determinations of the faster time constants and of the final steady state signal.

TABLE 5.1

RESPONSE TIME VERIFICATION RESULTS

RTD Manufacturer and Model Number	Time Constant (sec)		
	Plunge Test±S.D.	LCSR Test (Graphical Exponential Stripping)±S.D.	LCSR Test (Computer Analysis)±S.D.
Rosemount 176KF	.37±.02	.31±.02	.34±.02
Rosemount 177GY* Element #1	5.77±.13	4.17±.14	5.10±.10
Rosemount 177GY* Element #2	6.07±.18	4.13±.11	5.20±.12
Rosemount 104VC in Thermowell**	5.44±.14	3.63±.03	4.54±.07
Rosemount 104VC without Thermowell	2.27±.04	1.73±.07	2.25±.14

TABLE 5.1 (continued)

RTD Manufacturer and Model Number	Time Constant (sec)		
	Plunge Test±S.D.	LCSR Test (Graphical Exponential Stripping)±S.D.	LCSR Test (Computer Analysis)±S.D.
Rosemount 104ADA in Thermowell**	7.44±.22	4.90±.04	5.94±.13
Rosemount 104ADA without Thermowell	3.12±.10	2.50±.09	3.17±.087
Sostman 8606	2.01±.09	1.97±.09	1.72±.05
Rosemount 104AFC	6.08	5.1	****
Rosemount 104AFC without Thermowell***	3.00	3.10	****

*The 177GY is a dual element sensor. Separate measurements were made for each element.

**With air in thermowell.

***Thermowell not available.

****Data not available.

TABLE 5.2

SELF HEATING TEST RESULTS

RTD Manufacturer and Model Number	Self Heating index±S.D. (ohms/watt)
Rosemount 176KF	6.089±.15
Rosemount 177GY* Element #1	7.634±.20
Rosemount 177GY* Element #2	8.778±.18
Rosemount 104VC in Thermowell	6.148±.15
Rosemount 104VC without Thermowell	4.675±.112

TABLE 5.2 (continued)

RTD Manufacturer and Model Number	Self Heating index ± S. D. (ohms/watt)
Rosemount 104ADA in Thermowell	8.76±.11
Rosemount 104ADA without Thermowell	6.66±.11
Sostman 8606	11.60±.02
Rosemount 104AFC in Thermowell	6.45
Rosemount 104AFC without Thermowell	5.64
Rosemount 177HW in Thermowell	7.320

Table 5.1 shows that the time constant estimates from the computer program are within twenty percent of the plunge test result and that the time constant estimates obtained by transforming LCSR data are all too small. Figures 5.1 through 5.5 show computer plots that demonstrate the LCSR raw data, the result of the exponential fit, and the constructed plunge test estimate for several of the cases that provided data for Table 5.1. There are three curves on each figure, but the curves for raw data and the fitted curves are usually too close to be distinguished.

The self heating indices shown in Table 5.2 vary considerably for different sensors. This is due to the fact that the value of the self heating index depends on the details of the construction of the sensor. Typical self heating curves are shown in Figures 5.6 through 5.10.

5.2 Self Heating Test for Measuring the Temperature Rise in An RTD

The amount of temperature rise per unit of electric power in an RTD is given by

$$\frac{\Delta T}{\Delta P} = \frac{\Delta R}{\Delta P} \cdot \frac{\Delta T}{\Delta R}$$

If the self heating index $(\frac{\Delta R}{\Delta P})$ is known, the temperature rise in the sensor per unit of input electric power $(\frac{\Delta T}{\Delta P})$ can be determined. Table 5.3 gives the temperature rise per unit of electric power in the sensors tested in this work. The tabulated results are based on the self heating indices of Table 5.2.

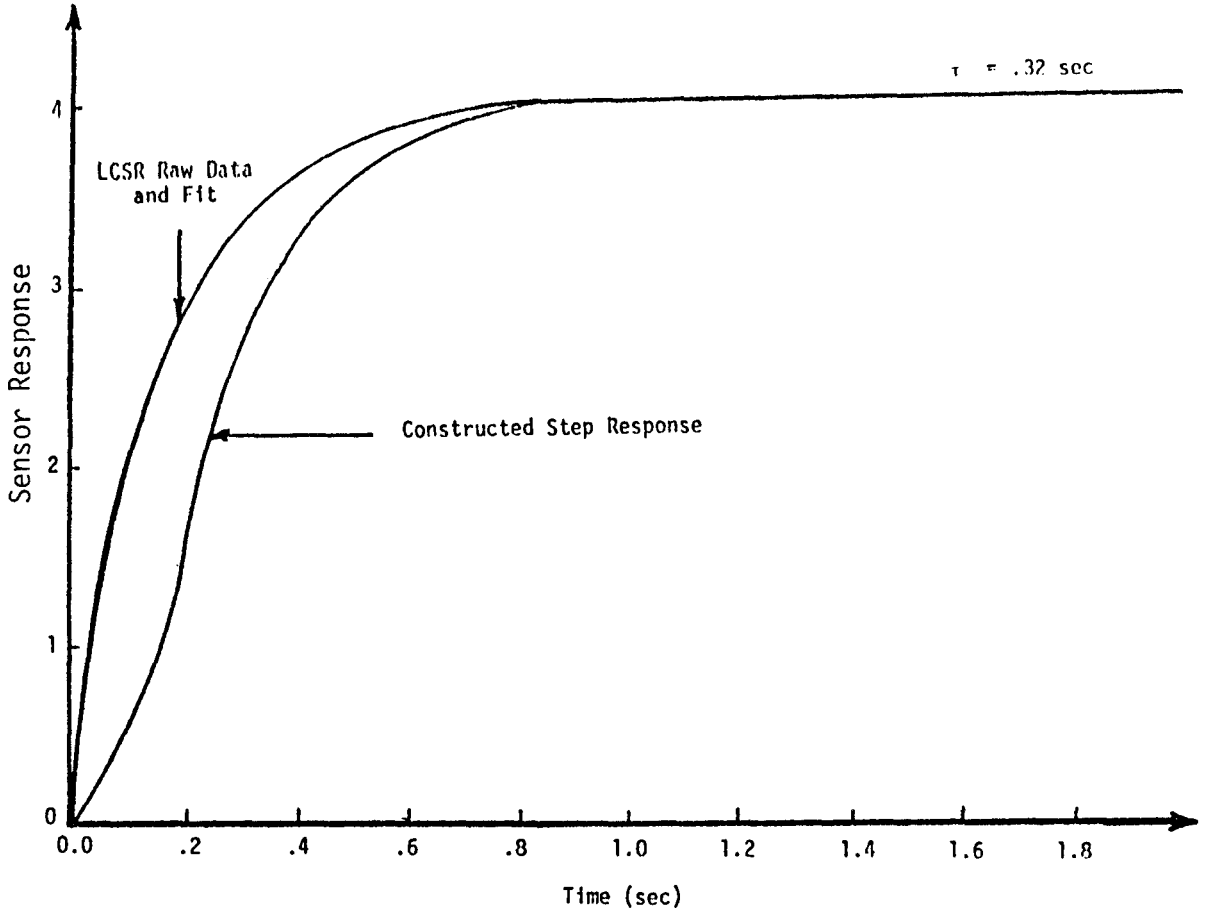

Figure 5.1. LCSR Raw Data, LCSR Fit and Step Response for Rosemount 176KF.

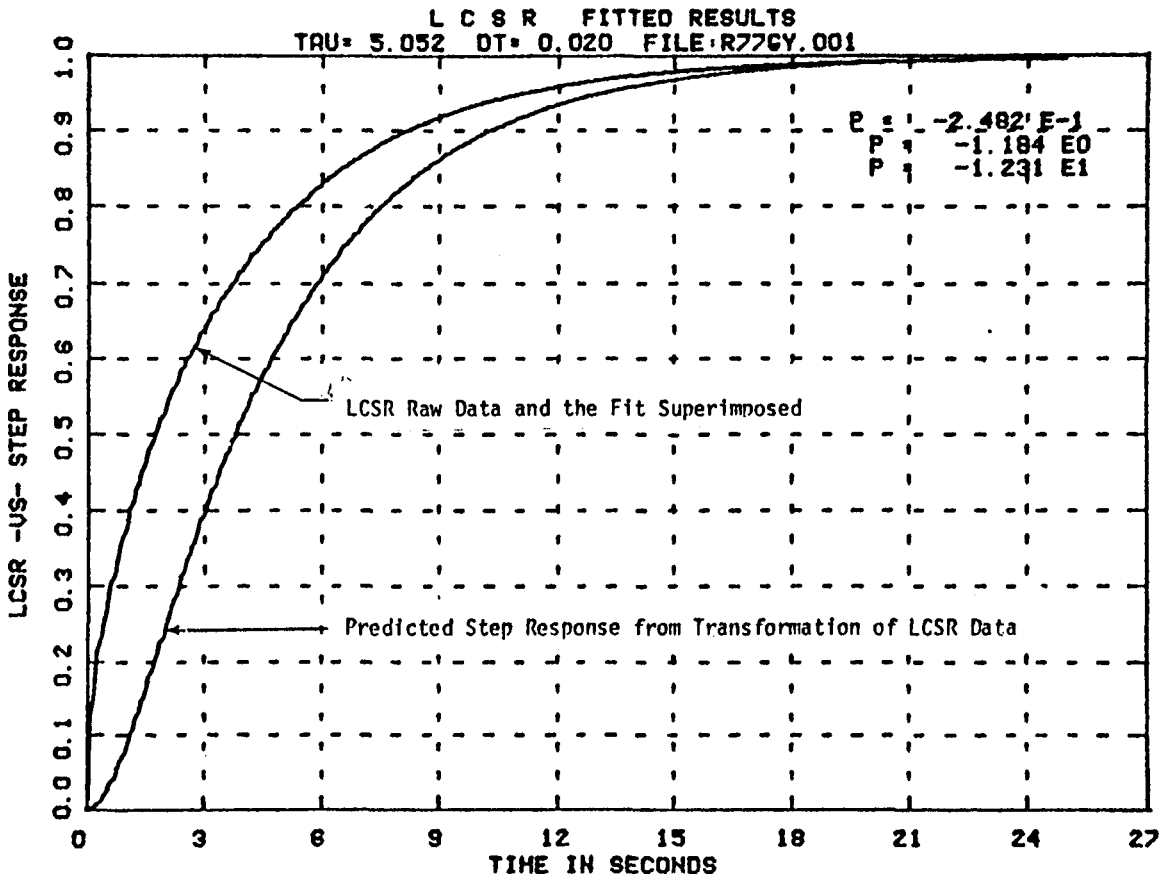

Figure 5.2. LCSR Raw Data, LCSR Fit and Predicted Step Response for Rosemount 177GY Filament No. 1.

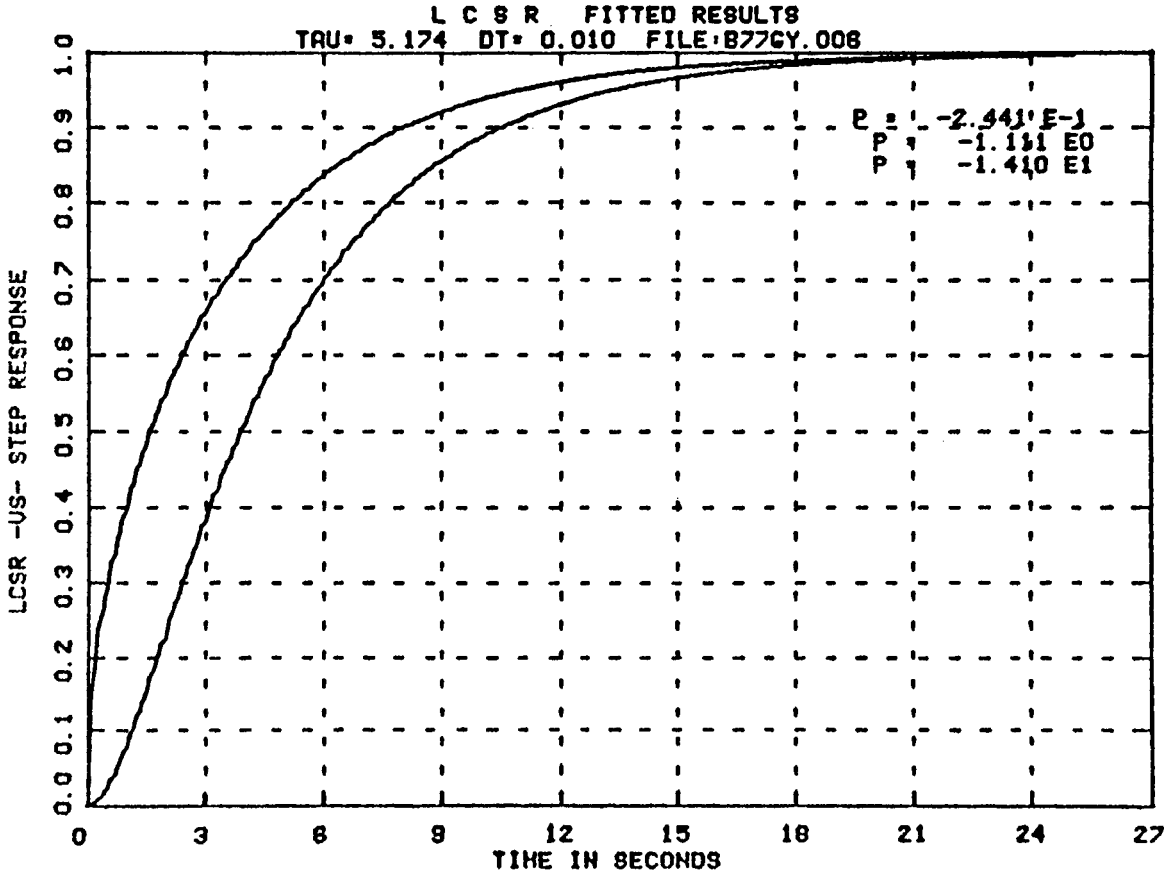

Figure 5.3. LCSR Raw Data, LCSR Fit, Predicted Step Response for Rosemount 177GY Filament No. 2.

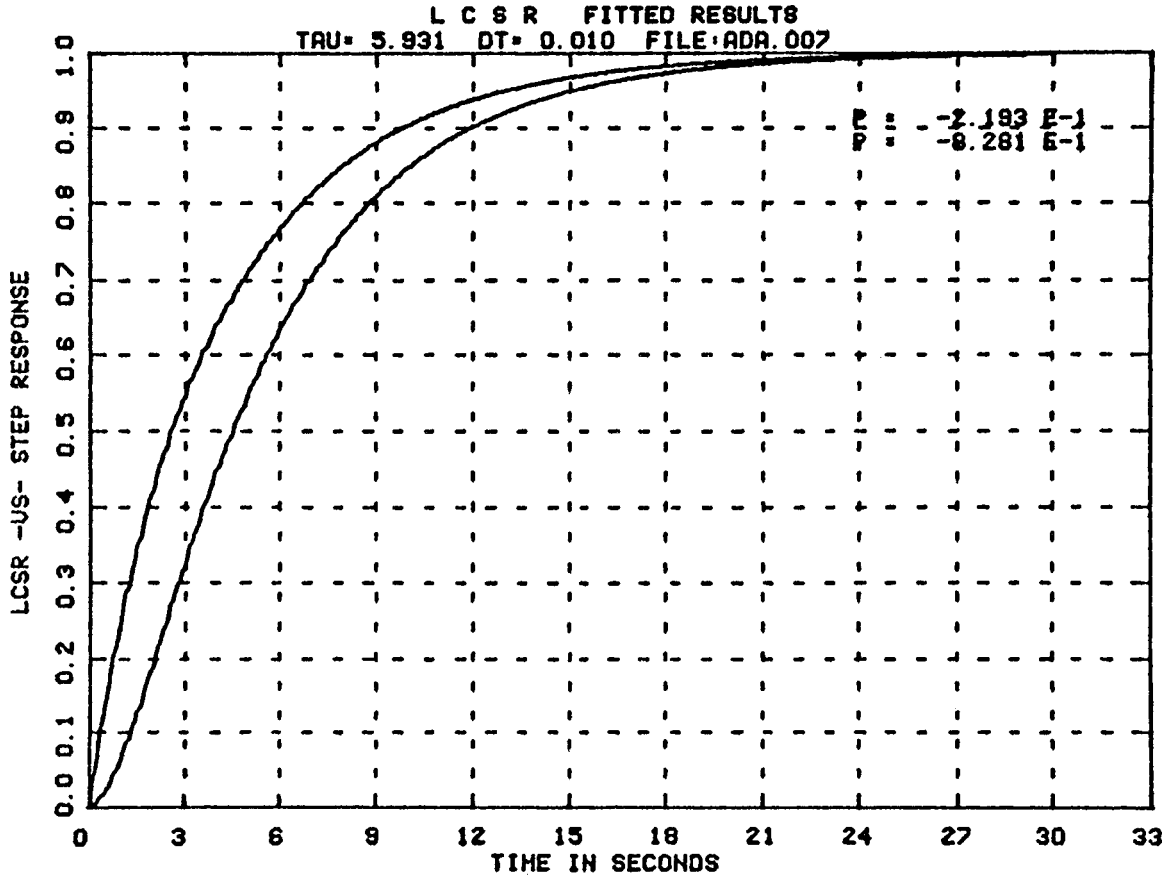

Figure 5.4. LCSR Raw Data, LCSR Fit, Predicted Step Response for Rosemount 104ADA.

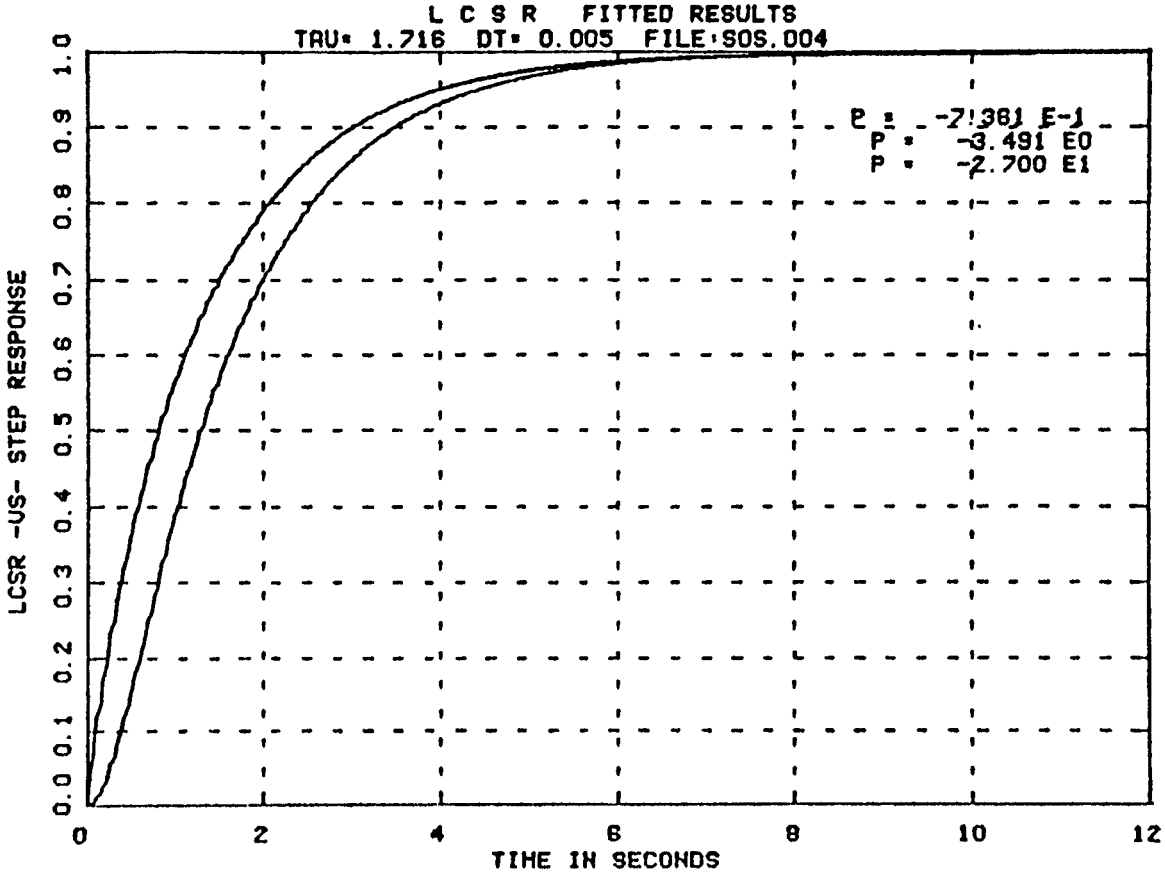

Figure 5.5. LCSR Raw Data, LCSR Fit, Predicted Step Response for Sostman 8606.

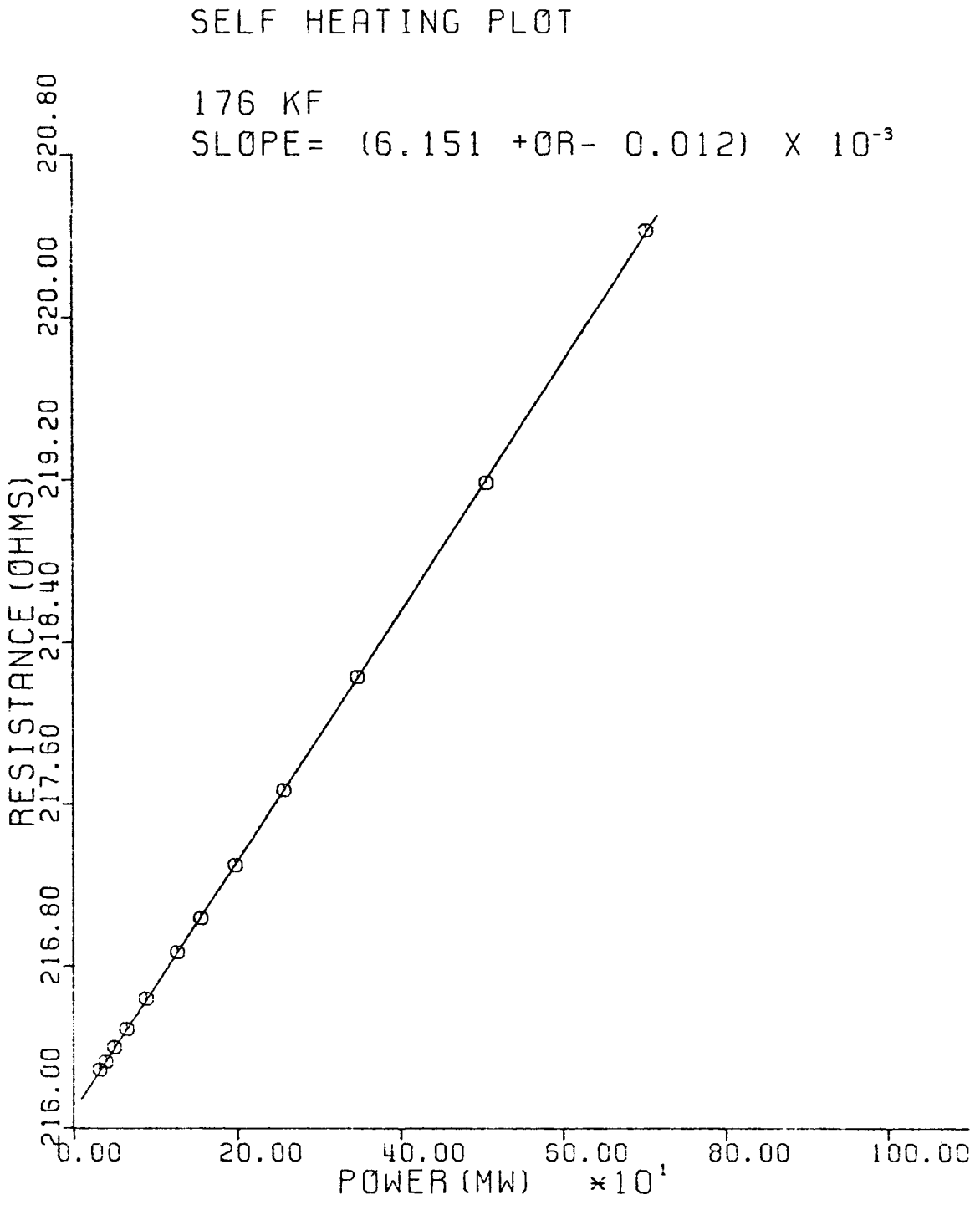

Figure 5.6. Self Heating Curve for Rosemount 176KF.

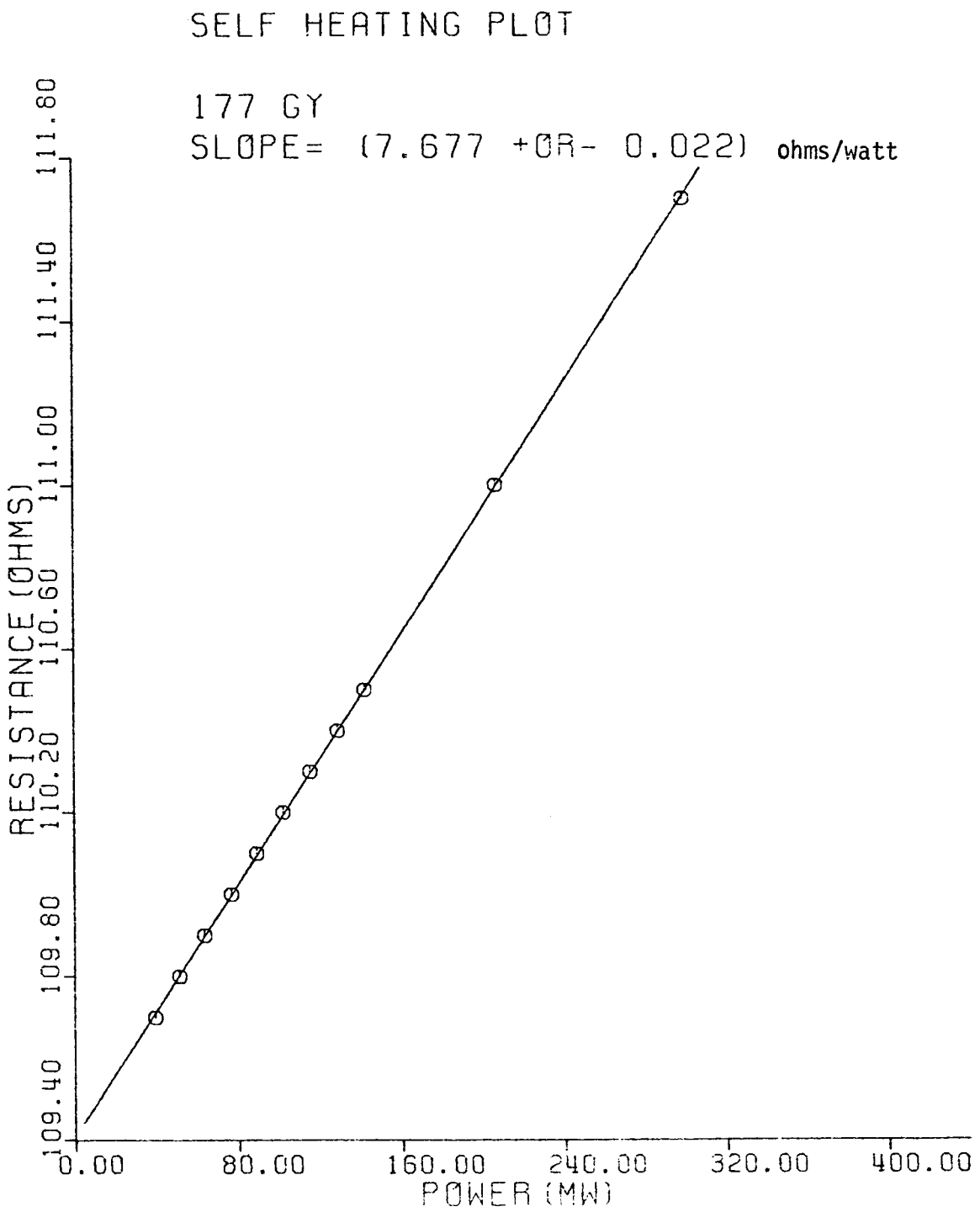

Figure 5.7. Self Heating Curve for Rosemount 177GY Filament No. 1.

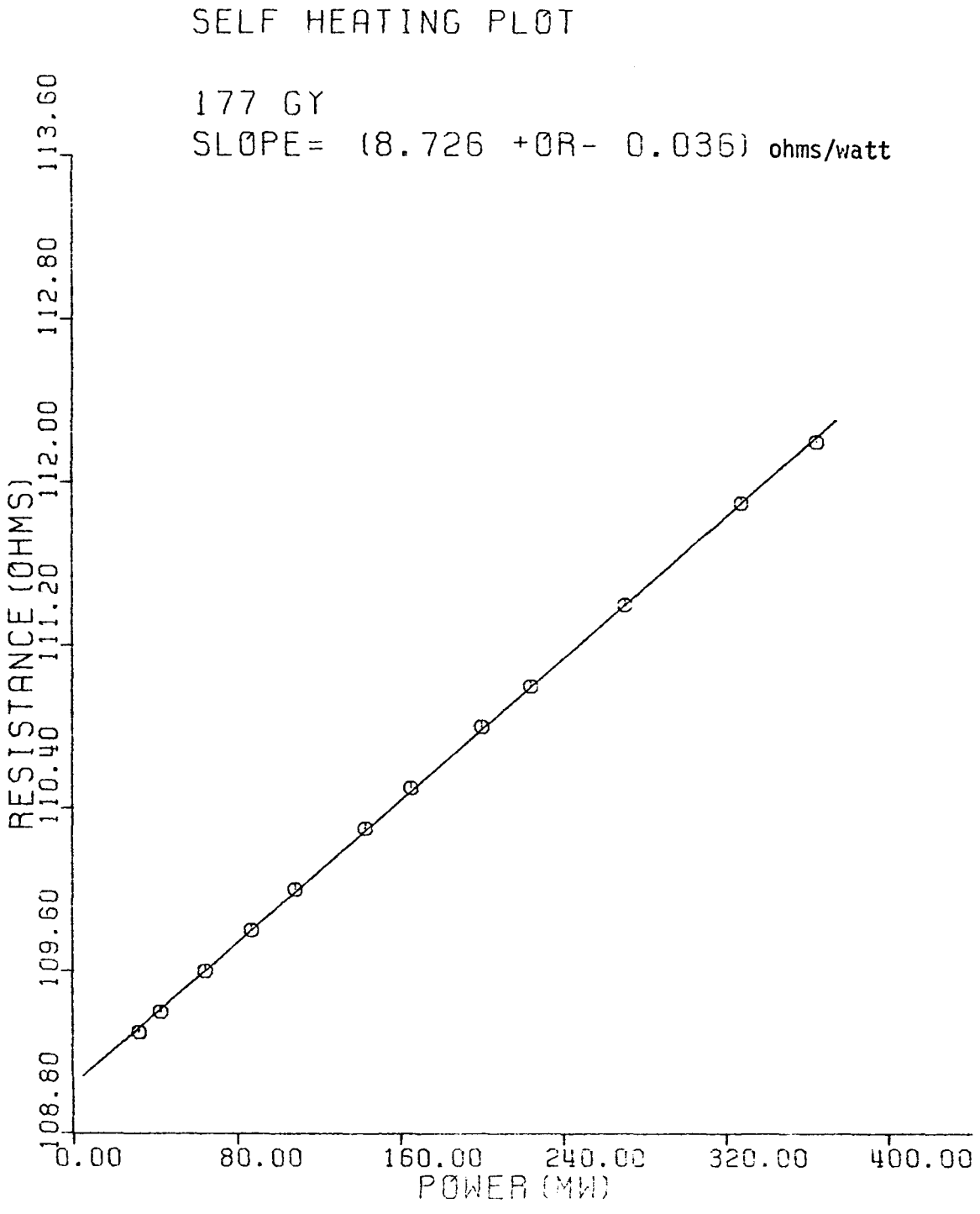

Figure 5.8. Self Heating Curve for Rosemount 177GY Filament No. 2.

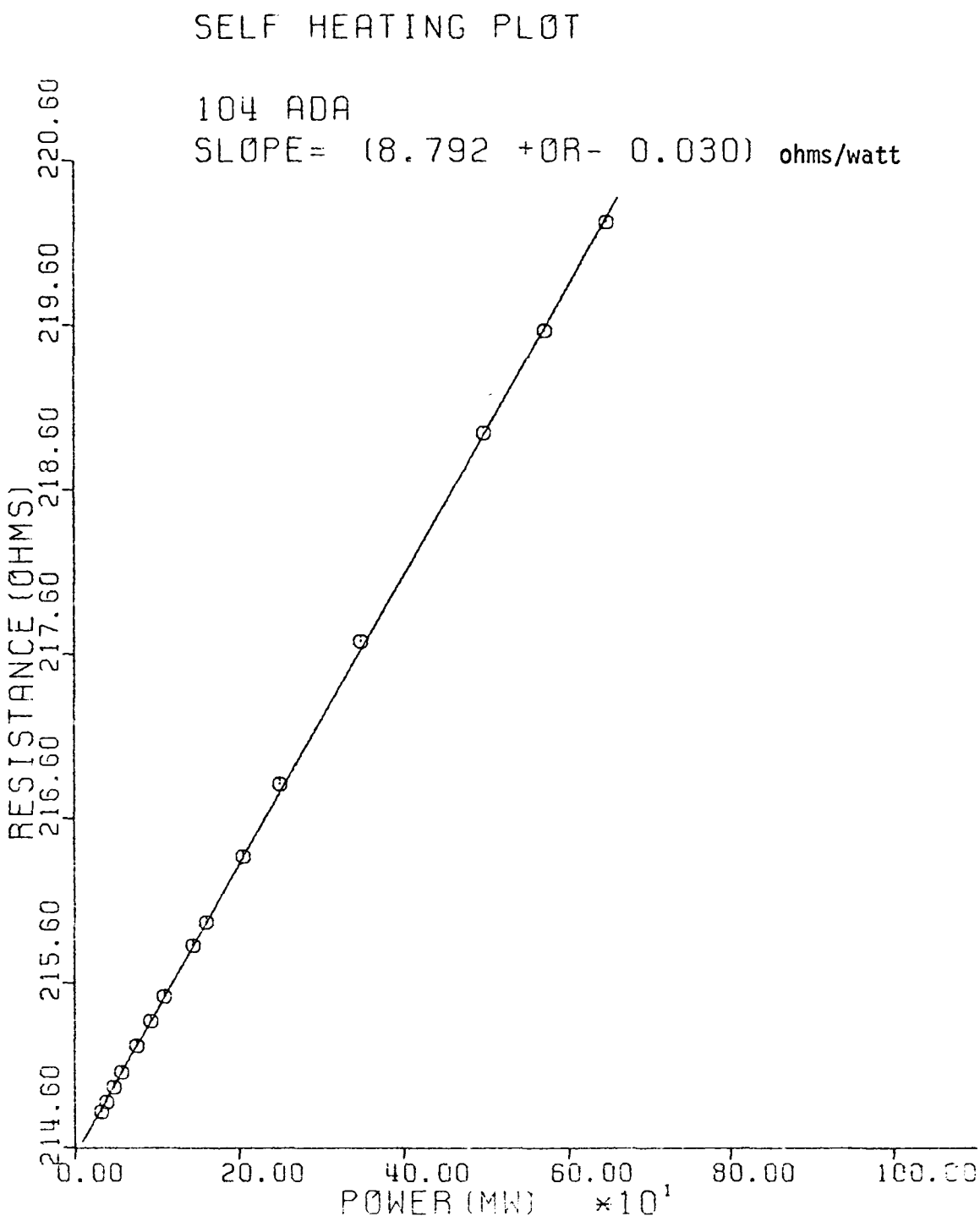

Figure 5.9. Self Heating Curve for Rosemount 104ADA.

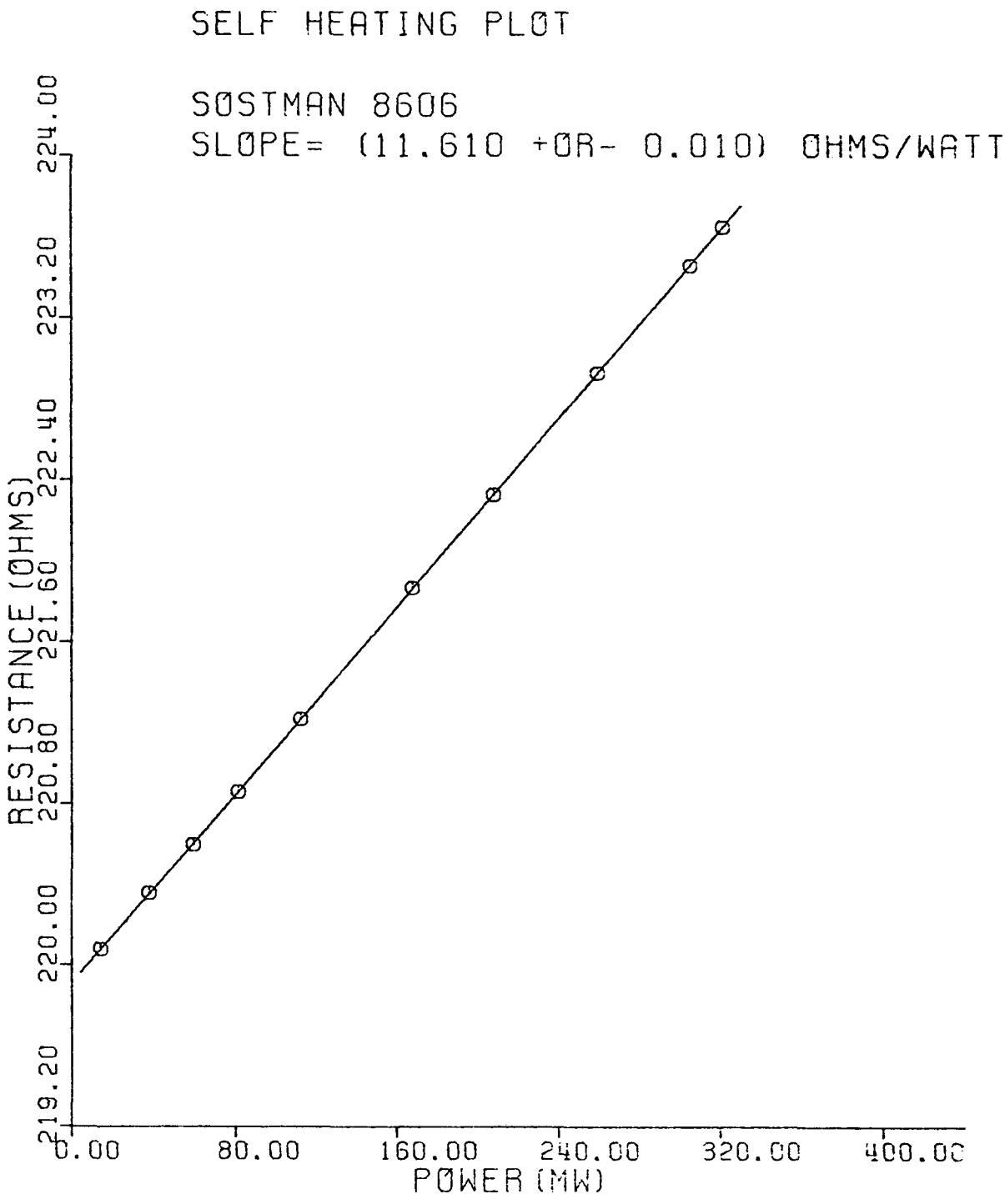

Figure 5.10. Self Heating Curve for Sostman 8606.

TABLE 5.3

TEMPERATURE RISE PER UNIT OF ELECTRIC POWER GENERATED IN RTDS

Sensor Manufacturer and Model Number	Temperature Rise Per Unit of Electric Power Input °C/watt
Rosemount 176KF	7.76
Rosemount 177GY Element #1	19.45
Rosemount 177GY Element #2	22.36
Rosemount 104VC in Thermowell	7.83
Rosemount 104VC without Thermowell	5.96
Rosemount 104ADD in Thermowell	11.16
Rosemount 104ADA without Thermowell	8.48
Sostman 8606	14.78
Rosemount 104AFC in Thermowell	8.22
Rosemount 104AFC without Thermowell	7.19
Rosemount 177HW in Thermowell	18.65

5.3 Effect of Thermal Bonding Material

The response time of well-type RTDs may be improved by using a thermal bonding material to fill up the air gap inside the thermowell. This was verified by using a thermal bonding material called Never-Seize inside the thermowell of a Rosemount 104AFC RTD. The sensing portion of the sensor was completely covered with a thin layer of Never-Seize before installation in its thermowell. As a result, the sensor time constant decreased from 6.08 sec to 4.65 sec for a water flow rate of 3 ft/sec and the self heating index decreased from 6.45 ohms/watt to 6.20 ohms/watt for a water flow rate of 3 ft/sec.

5.4 Special Tests

5.4.1 Effect of Current on the LCSR Test Results

Experience based on numerous laboratory experiments indicates that the time constant obtained from a LCSR test is independent of the amount of electric current used for generating the test transient up to at least 90 ma.

5.4.2 Test for Degradation of RTD Caused by LCSR Test

The LCSR test was investigated to determine whether a failure or a degradation of response time can occur by the application of this method on an RTD. A typical laboratory type RTD was selected for this study. The response time and the self heating index of the sensor was carefully determined, then the following tests were performed:

1. Test for Degradation or Failure of Sensor from Electric Current Used to Perform a LCSR Test: A current of about 120 milliamperes was input for 48 hours to the sensing filament of the RTD immersed in still water at room temperature. No failure occurred (sensor was operating after the 48 hour period). Plunge and self heating tests were performed. The results indicated that no degradation of response time had occurred.
2. Test for Degradation or Failure of Sensor from Sudden Change of Current in the Sensing Filament: A signal generator was used to produce pulses for actuating a relay to cause sudden changes of current through the sensing filament of the RTD immersed in still water. The system was adjusted to give signals of 40 second interval to step the sensor current from about 6 to 60 milliamperes and vice versa. This test was run for 12 hours to give more than 1000 step changes in current. The sensor did not fail as the result of this test (it was operating after the 12 hour test) and degradations were not observed (the time constant and self heating index were the same as before).

As a result of these investigations it appears that the LCSR test can not cause any failure or degradation of sensors unless current levels of much more than 120 milliamperes are used. However, exhaustive tests of all reactor-type RTDs have not been performed yet.

5.4.3 Experimental Verification of the Affect of Fluid Velocity on Response Time of an RTD

The response of an RTD is affected by the fluid flow rate to which the sensor is exposed. The affect of flow velocity on the response time of a Rosemount 176KF RTD was investigated by performing plunge tests in two different fluid flow rates in a rotating tank and by conducting a plunge test in a liquid metal bath. The results of these plunge tests are given in Table 5.4. The liquid metal (Galium-Indium eutectic) was used to achieve a high heat transfer rate to simulate a high flow velocity. A high heat transfer rate results from the high thermal conductivity of the liquid metal compared with water.

Table 5.4 shows that the response time of this sensor is significantly affected by the surface resistance; however, this is not a general rule for all the sensors unless the surface heat transfer resistance is relatively large compared with the internal heat transfer resistance.

TABLE 5.4

EFFECT OF FLUID FLOW VELOCITY ON THE RESPONSE TIME OF A ROSEMOUNT 176KF RTD

Fluid Flow Rate (ft/sec)	Sensor Time Constant
2.5	.42
3.5	.34
∞^*	.22

*Result from tests in liquid metal bath that simulate high flow conditions for surface heat transfer.

6.0 USE OF LCSR AND SELF HEATING TESTS FOR MONITORING RESPONSE TIME DEGRADATION

6.1 LCSR Test for Monitoring Response Time Degradation

The LCSR transformation provides a quantitative estimate of the time constant of a sensor. However, in some cases it may be desirable to seek only an indication of change in the time constant. In these cases, the need for computer analysis of the test data is avoided. The indication of change can be obtained by direct inspection of an LCSR test transient. A quantity called the LCSR time constant is defined to be used for diagnosis of RTD response time degradation. This quantity is denoted by τ_{LCSR} and defined as the time required for the sensor to respond to 63.2 percent of the final value following a step change in the sensor current. The definition is illustrated in Figure 6.1 using a typical LCSR test transient.

The LCSR time constant (as the plunge test time constant) depends on the heat transfer resistances and heat capacities of the sensor. The same heat transfer resistances and heat capacities control the plunge test response and the LCSR test response. Therefore, a change in heat transfer characteristics of a sensor results in a change in the plunge test time constant and also a change in the LCSR time constant. A change in the LCSR time constant indicates a change in the plunge test response resulting from a change in the heat transfer properties of the sensor. Thus, a measurement of the LCSR time constant can be used for diagnosis of sensor response time degradation. This method

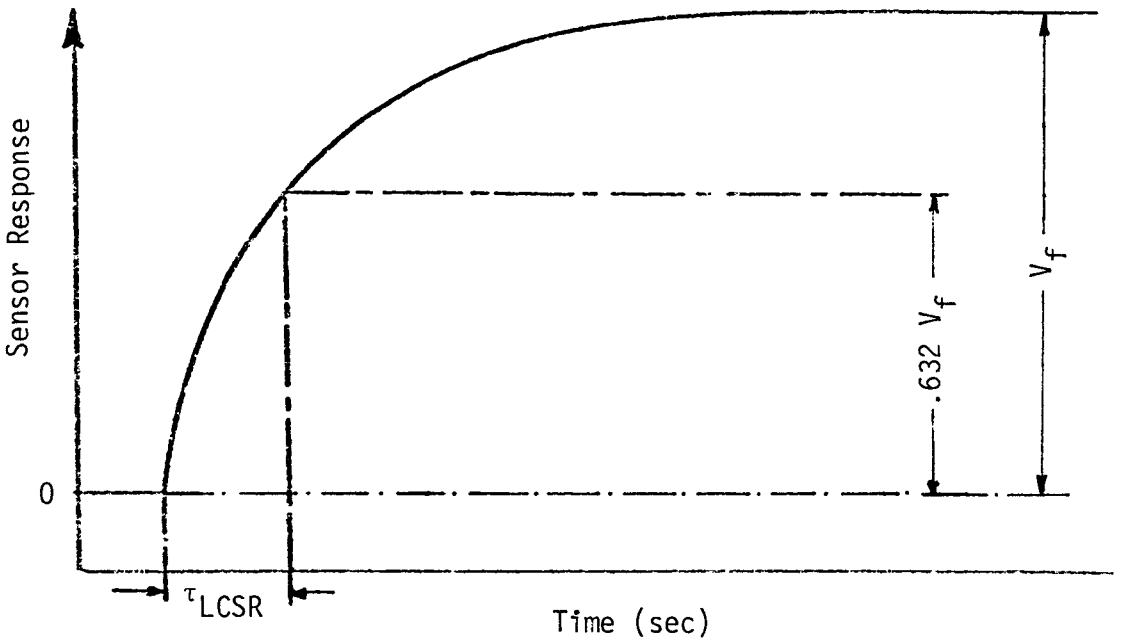

Figure 6.1. Determination of LCSR Time Constant from Test Data.

does not provide quantitative measurement of sensor response time, but it is presented as a simple technique for detecting sensor response time degradation.

Once an increase in the LCSR time constant is observed, response time degradation is indicated. The change in the LCSR time constant must be related to corresponding changes in the plunge time constant to determine whether the degradation is significant. The significance of a change in the LCSR time constant depends on the correlation between the response of a sensor to a step change in surrounding temperature and the response to a step change in internal heating of the sensor. Experimental results from laboratory tests of two RTDs (Rosemount 104AFC and Rosemount 176KF) indicated that a unique correlation exists between the LCSR time constant and plunge test time constant for a given sensor. An empirical correlation curve was established for each sensor to assist in relating the changes in the LCSR time constant to corresponding changes in the plunge test time constant to aid in estimating the amount of the response time degradation. The empirical correlation curves were constructed by performing several LCSR and plunge tests on each sensor for several different simulated surface heat transfer resistances. Different values of heat transfer resistances were achieved by varying the amount and/or position of insulating materials added to the surface of each sensor. The following procedures were used to establish the technique:*

---

*Tests were performed in a rotating tank at a fluid flow rate of about 3 ft/sec.

1. Perform a LCSR test and record the output on a strip chart recorder.
2. Determine the LCSR time constant (τ_{LCSR}).
3. Perform a plunge test.
4. Determine the plunge test time constant (τ_{PL}).
5. Plot τ_{PL} versus τ_{LCSR} on a cartesian coordinate system.
6. Add some form of insulating material (such as a portion of rubber tube or tape) around the surface at the sensing end (see Figure 6.2) of the sensor. This introduces an artificial degradation of the heat transfer and increases the plunge test time constant as well as the LCSR time constant.
7. Perform a new LCSR test and record the output on a strip chart recorder to determine the LCSR time constant of the artificially degraded sensor.
8. Perform a new plunge test and determine the new time constant.
9. Plot the new values of τ_{PL} and τ_{LCSR} on the coordinate system of step 5.
10. Change the heat transfer resistance of the surface. This may by done by changing the position or the amount of the insulating material added to the surface of the sensor.
11. Repeat until enough data are obtained to yield an empirical correlation curve.

These procedures are illustrated in Figure 6.3.

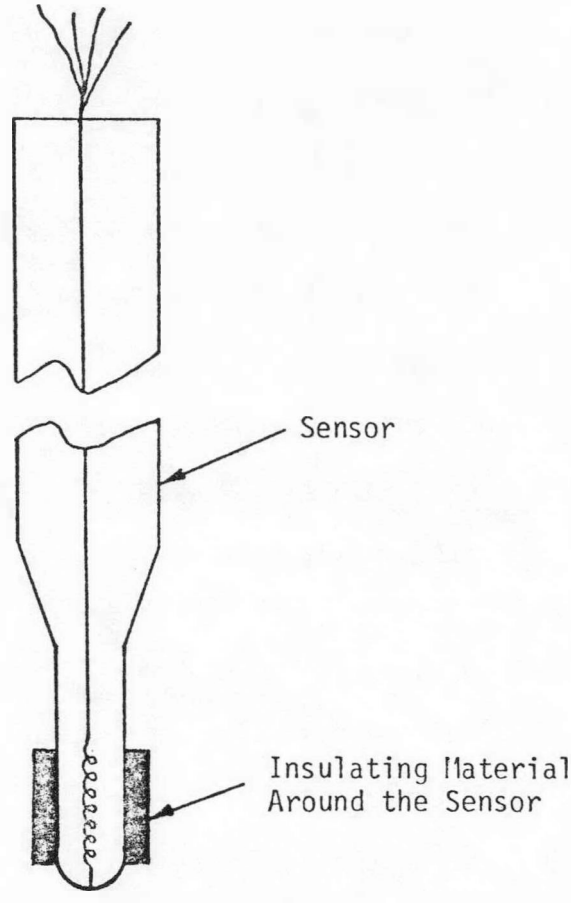

Figure 6.2. Configuration of an RTD with Augmented Surface Heat Transfer Resistance.

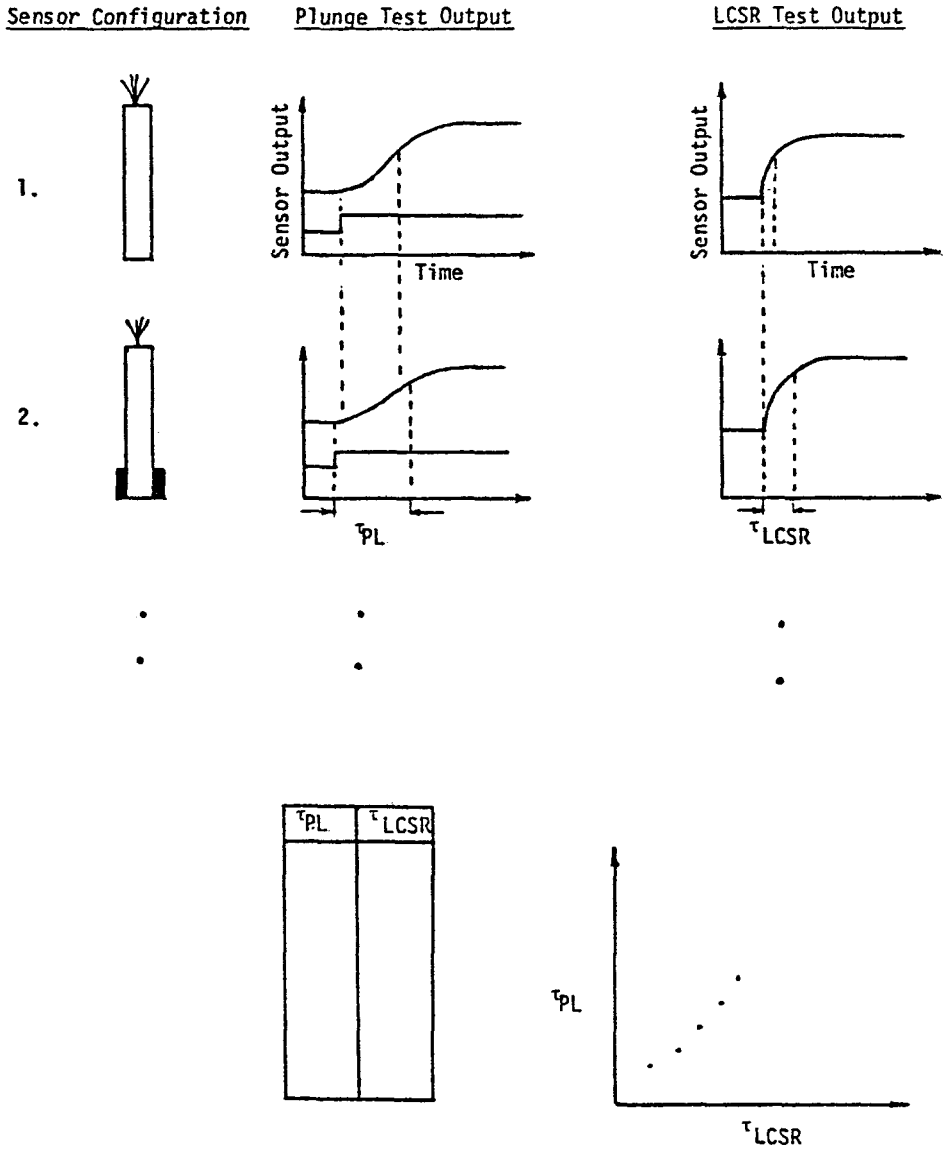

Figure 6.3. Illustration of Procedures for Establishment of an Empirical Correlation between Plunge and LCSR Time Constants.

The empirical correlation of τ_{PL} versus τ_{LCSR} developed for the Rosemount RTD Model 104AFC is shown in Figure 6.4. The data for this correlation were obtained from tests on the sensor inside its thermowell as well as tests with the sensor out of its thermowell (bare). Figure 6.4 indicates that the data from the bare sensor satisfy the same correlation as the in-well configuration and therefore, they are included in the empirical curve. Since the LCSR and plunge time constants of a sensor with no heat transfer resistance are expected to be zero, the empirical curve is extrapolated to zero to provide a range for monitoring the response time degradation in high flow and temperature enviornments where the sensor response time is usually less than the minimum value of the response that can be measured in a laboratory environment. A similar curve for the Rosemount 176KF sensor is shown in Figure 6.5

In order to relate the changes in the LCSR time constant to corresponding changes in the plunge test time constant, the ratio of the relative changes in these quantities ($\frac{\delta\tau_{PL}/\tau_{PL}}{\delta\tau_{LCSR}/\tau_{LCSR}}$) is determined.

From Figure 6.4 (around the sensor time constant of τ_{PL} = 6 sec):

$$\frac{\delta\tau_{PL}/\ PL}{\delta\tau_{LCSR}/\tau_{LCSR}} \approx 2.60 \qquad \text{(Rosemount Model 104AFC)}$$

For example, a 10 percent change in the LCSR time constant indicates a 26% change in the plunge test time constant of this sensor. This ratio for a Rosemount RTD Model 176KF is (around the sensor time constant τ_{PL} = 0.4 sec):

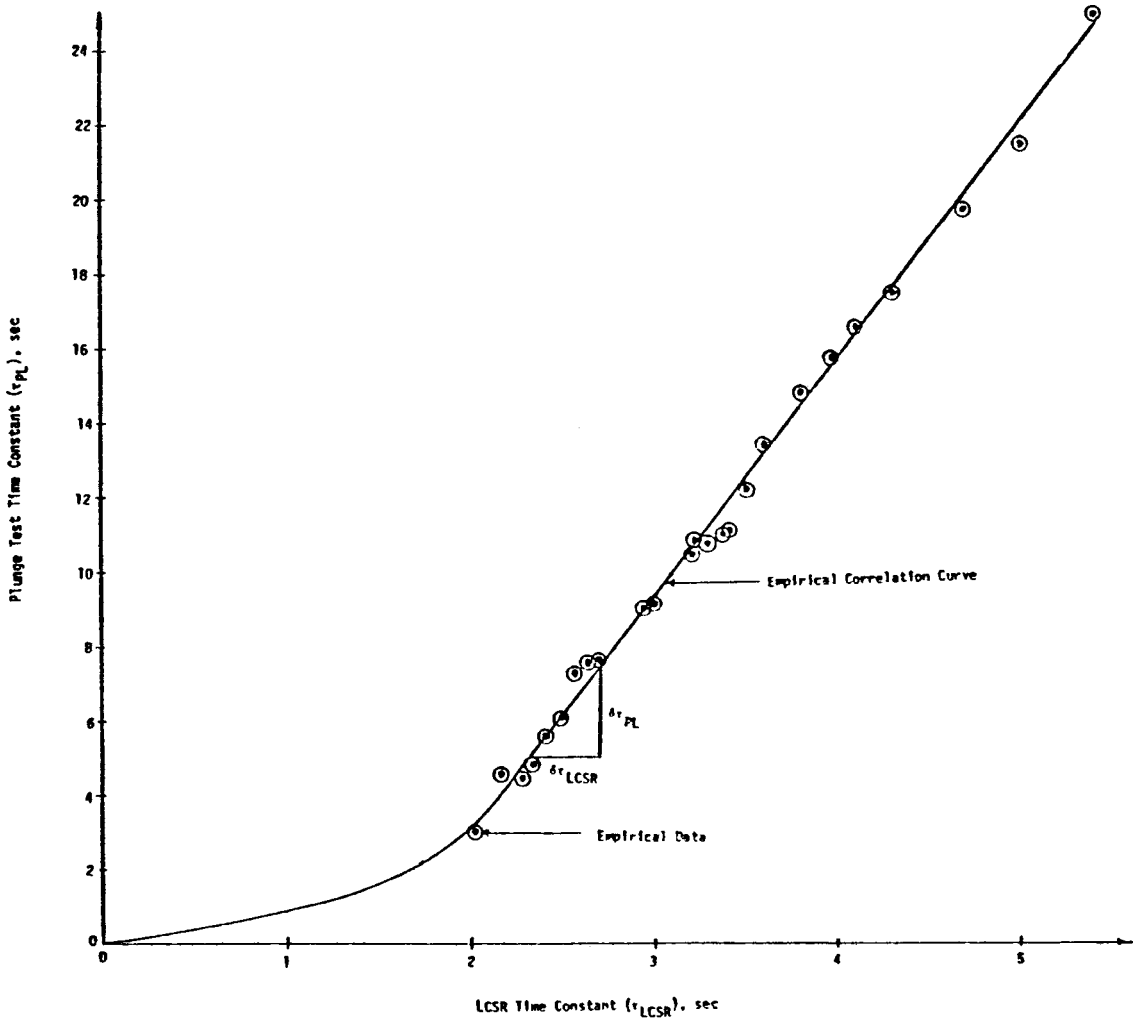

Figure 6.4. Empirical Correlation Curve for τ_{PL} versus τ_{LCSR} (for Rosemount RTD Model 104AFC).

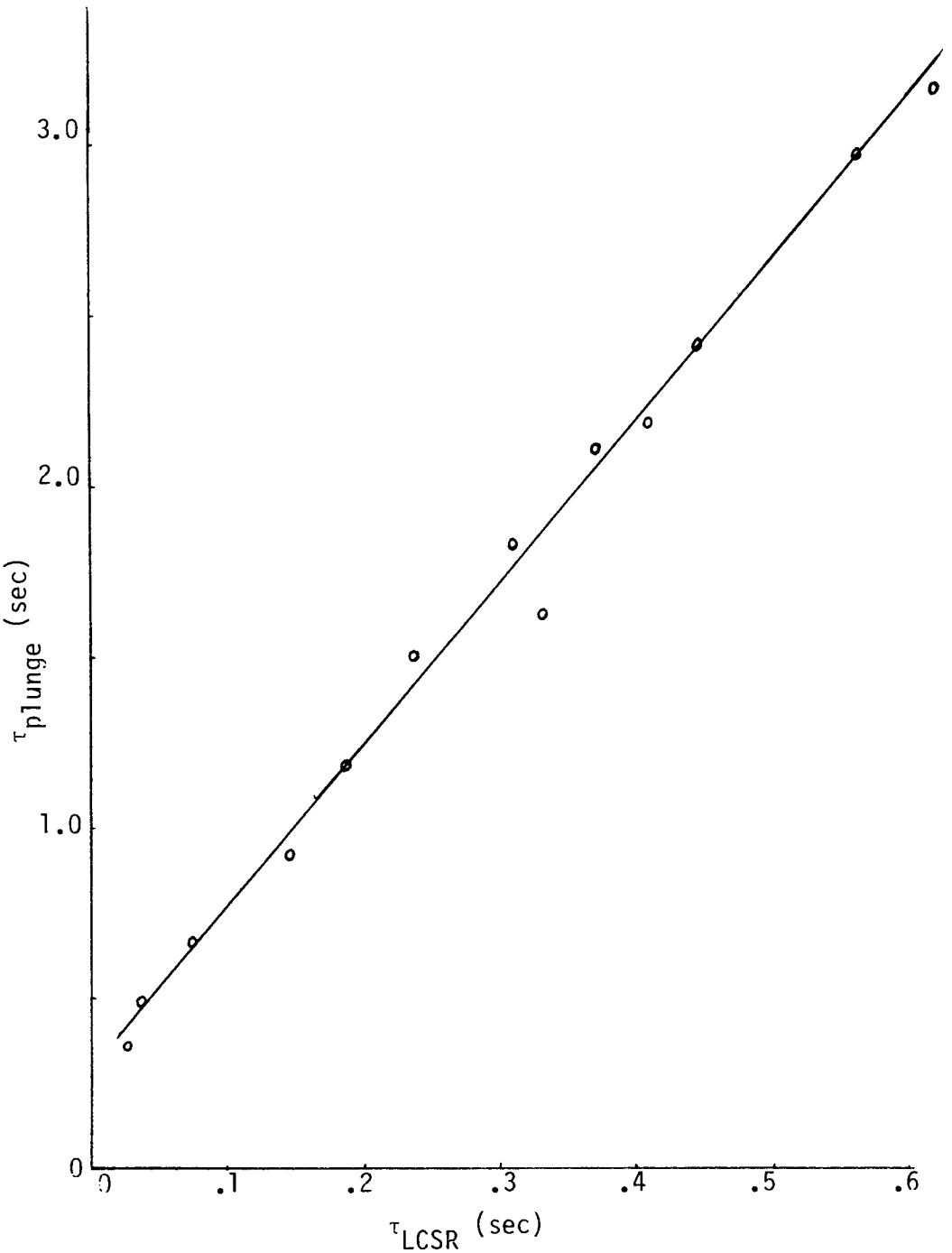

Figure 6.5. Empirical Correlation Curve for τ_{PL} versus τ_{LCSR} (for Rosemount Model 176KF).

$$\frac{\delta\tau_{PL}/\tau_{PL}}{\delta\tau_{LCSR}/\tau_{LCSR}} = .692 \quad \text{(Rosemount Model 176KF)}$$

Thus a 10 percent change in the LCSR time constant of this sensor corresponds to a 6.92 percent change in its plunge test time constant.

For a sensor installed in a process, response time changes may occur as a result of various response time degradation mechanisms. The empirical correlation curve can be used to detect the response time degradation of installed RTDs. The following procedures may be used:

1. Determine the LCSR time constant shortly after the sensor is installed in the process.
2. Perform a LCSR test whenever the response of the sensor is required to be checked. Determine the LCSR time constant.
3. Compare the values of the new LCSR time constant with the LCSR time constant of the sensor that was recorded shortly after the installation of the sensor.
4. If the LCSR time constant is changed, use the empirical correlation curve of the sensor to estimate the significance of the degradation.
5. If a significant degradation is shown or if the new value of the sensor response time is desired, the LCSR test data must be analyzed (using the LCSR transformation) to give the time constant of the sensor after degradation.

6.2 Self Heating Test for Diagnosis of Sensor Response Time Degradation

A self heating test can also be used as a method for diagnosis of response time degradation of RTDs. The parameters of interest in this method are the self heating index ($\frac{\Delta R}{\Delta P}$) and the plunge test time constant (τ_{PL}). An increase in the self heating index of a sensor is an indication of a response time degradation. (This is true if the heat capacity of the sensor has not changed since this would not be revealed by a self heating test.)

In order to determine the approximate change in the response time of a sensor by a measurement of its self heating index, one needs an estimate of the correlation between the plunge test time constant and the self heating index. Experimental results based on laboratory testing of two RTDs (Rosemount 104AFC and Rosemount 176KF) revealed that a unique correlation exists between the plunge test time constant and the self heating index. Empirical data were obtained by numerous plunge and self heating tests performed on the sensor with simulated heat transfer degradation at the surface (see Figure 6.6). The self heating indices and the corresponding plunge test time constants were measured and the results were plotted in a cartesian coordinate system to yield an empirical curve representing τ_{PL} versus $\frac{\Delta R}{\Delta P}$. The empirical correlation curve of the Rosemount RTD Model 104AFC is shown in Figure 6.7. The correlation curve may be extrapolated to zero because a self heating index of zero is expected for a plunge test time constant of zero. The extrapolation of the empirical curve to zero provides a range for monitoring the response time degradation in operating conditions

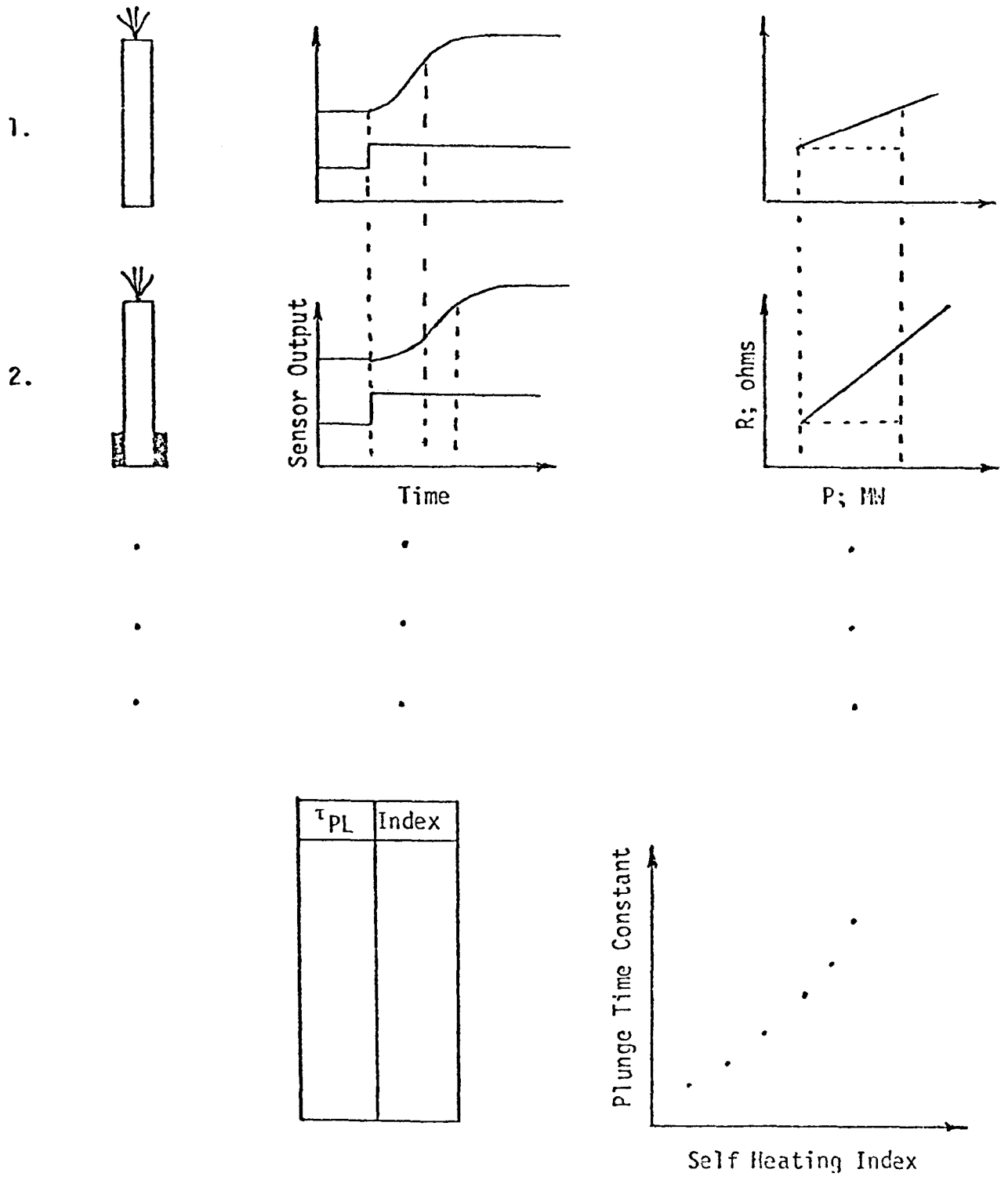

Figure 6.6. Illustration of Procedures for the Development of Empirical Correlation between Plunge Test Time Constant and Self Heating Index.

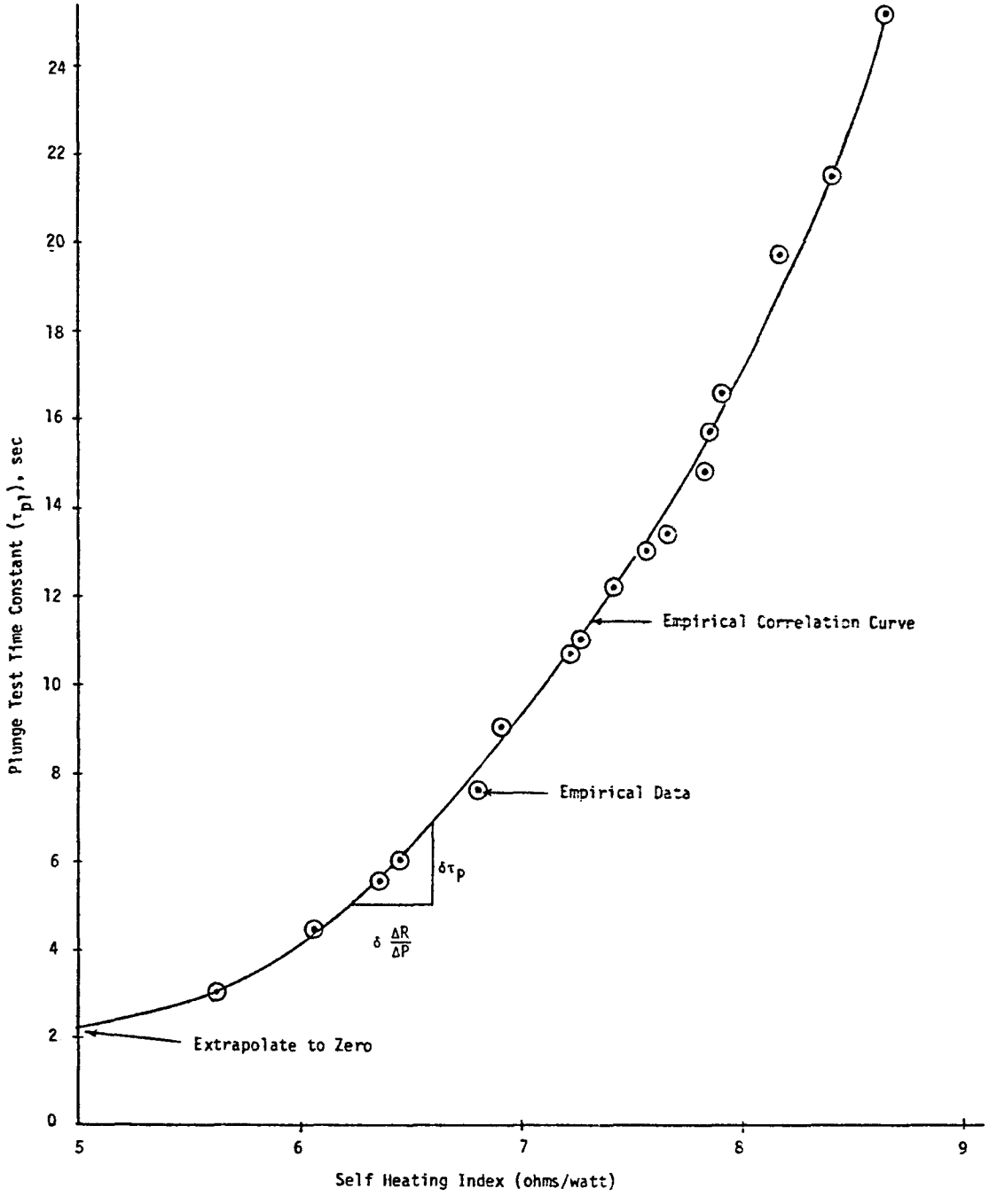

Figure 6.7. Empirical Correlation Curve for τ_{PL} versus Self Heating Index (for Rosemount RTD Model 104AFC).

(high temperature and flow) where the sensor response time is usually less than a minimum value that can be measured in a laboratory environment. Similar results for the Rosemount 176KF sensor are shown in Figure 6.8.

In order to relate the changes in the slope of the self heating index to corresponding changes in the plunge test time constant, the ratio of relative changes in these quantities ($\frac{\delta\tau_{PL}/\tau_{PL}}{\frac{\delta\Delta R/\Delta P}{\Delta R/\Delta P}}$) may be determined. From Figure 6.7 (around the sensor time constant of τ_{PL} = 6 sec):

$$\frac{\frac{\delta\tau_{PL}}{\tau_{PL}}}{\frac{\delta\Delta R/\Delta P}{\Delta R/\Delta P}} = 5.38$$

Thus, a change of, for example 10 percent, in the self heating index indicates a change of about 54 percent in the plunge time constant of this sensor. This ratio for a Rosemount RTD Model 176KF is (around the sensor time constant of τ_{PL} = 0.4 sec):

$$\frac{\frac{\delta\tau_{PL}}{\tau_{PL}}}{\frac{\delta\Delta R}{\Delta P} / \frac{\Delta R}{\Delta P}} = 5.87$$

This indicates that a 10 percent change in the self heating index of this RTD is related to about a 59 percent change in the plunge test time constant. These results show that the plunge test time constant is very sensitive to the changes in the self heating index. Therefore, a small change in the self heating index is an indication of a significant change in the plunge test time constant of an RTD.

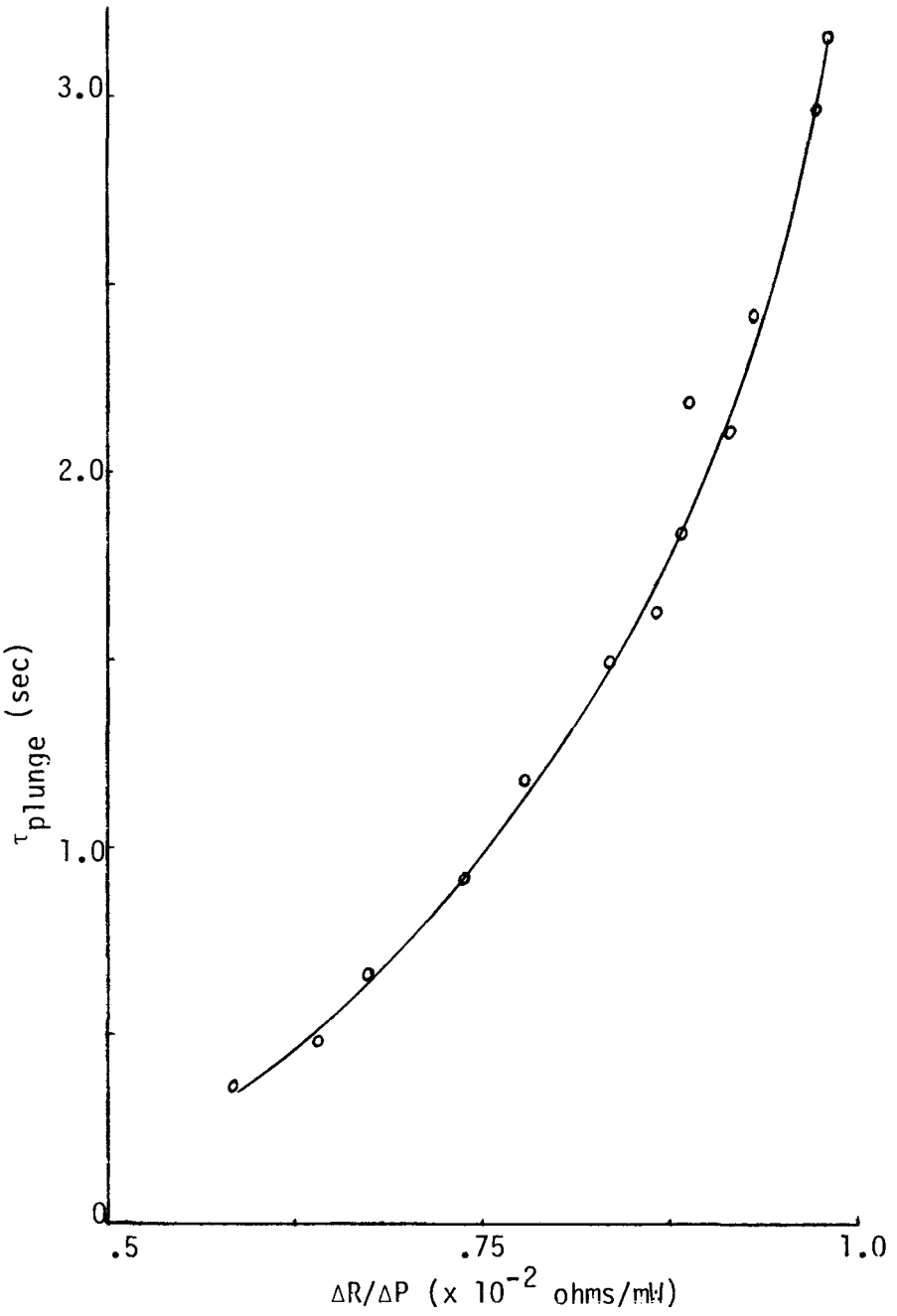

Figure 6.8. Empirical Correlation Curve for τ_{PL} versus Self Heating Index (for Rosemount 176KF).

The application of the self heating technique for monitoring the response time degradation of RTDs installed in a process requires an estimate of the empirical correlation of τ_{PL} versus self heating index prior to installation of the sensor in the plant. Once this empirical correlation is established for a sensor in laboratory conditions (limited temperature and flow velocity) it can be used to estimate the degradation of response time after the sensor is installed in a plant.

7.0 IN-PLANT TEST RESULTS

7.1 Introduction

In-plant implementation of the LCSR and self heating test methods has taken place in three plants as part of this program. They are:

- Oconee (Duke Power Company)
- Turkey Point (Florida Power & Light Company)
- St. Lucie (Florida Power & Light Company)

Tests at Oconee and Turkey Point provided the initial in-plant experience that led to the standard testing and analysis procedures (See Appendix C and Chapter 4). The St. Lucie tests provided a full check-out of the standard testing and analysis procedures that were established in the earlier work.

7.2 Oconee Tests

LCSR tests were performed on three different control system RTDs (two in the cold legs and one in a hot leg), and two types of RTDs (Rosemount 177GY wet-type and Rosemount 177HW well-type). Figures 7.1 through 7.3 show typical raw data, fitted curves, and predicted plunge test results for each sensor. In these tests, the heating current was 40 ma. Clearly, the quality of the test data is good. The time constant estimates from the LCSR tests are given in Table 7.1.

Self heating tests were also performed on all three Oconee sensors. The self heating curves are shown in Figures 7.4 through 7.6 and the self heating indexes are listed in Table 7.2.

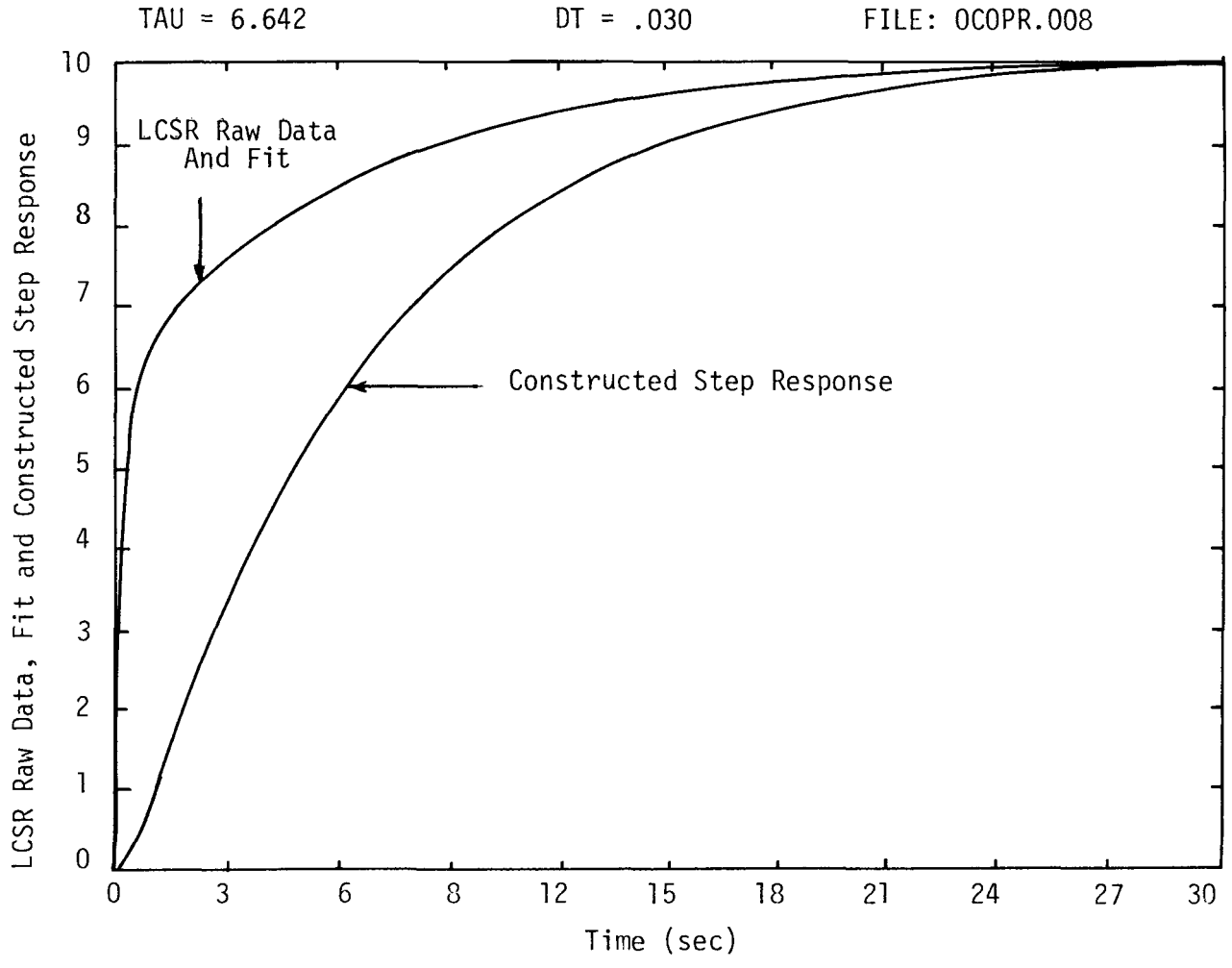

Figure 7.1. LCSR Test Results for Oconee 3 RTD (Rosemount 177HW, Tag #3RC5A-TE4).

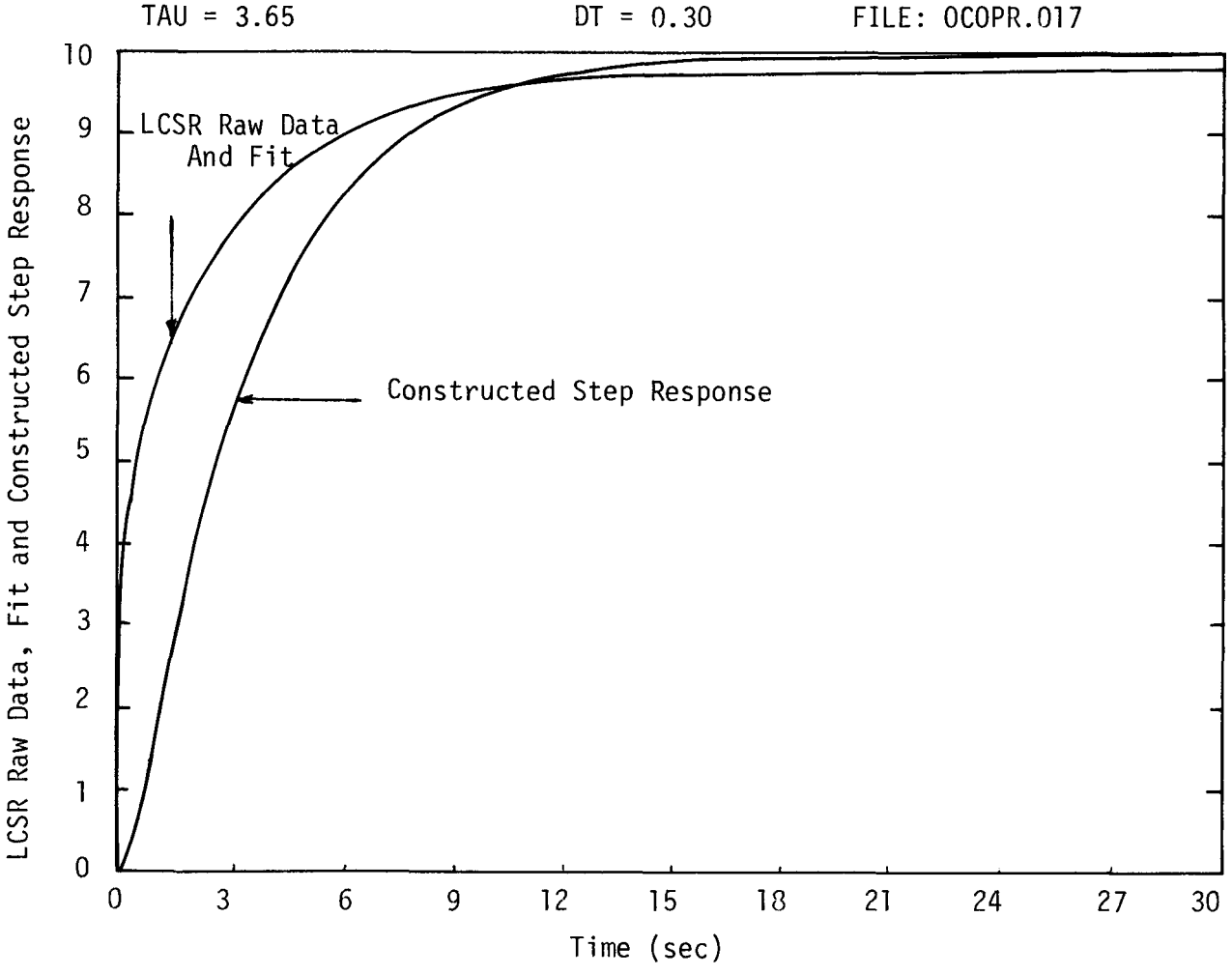

Figure 7.2. LCSR Test Results for Oconee 3 RTD (Rosemount 177GY, Tag #3RC5B-TE4).

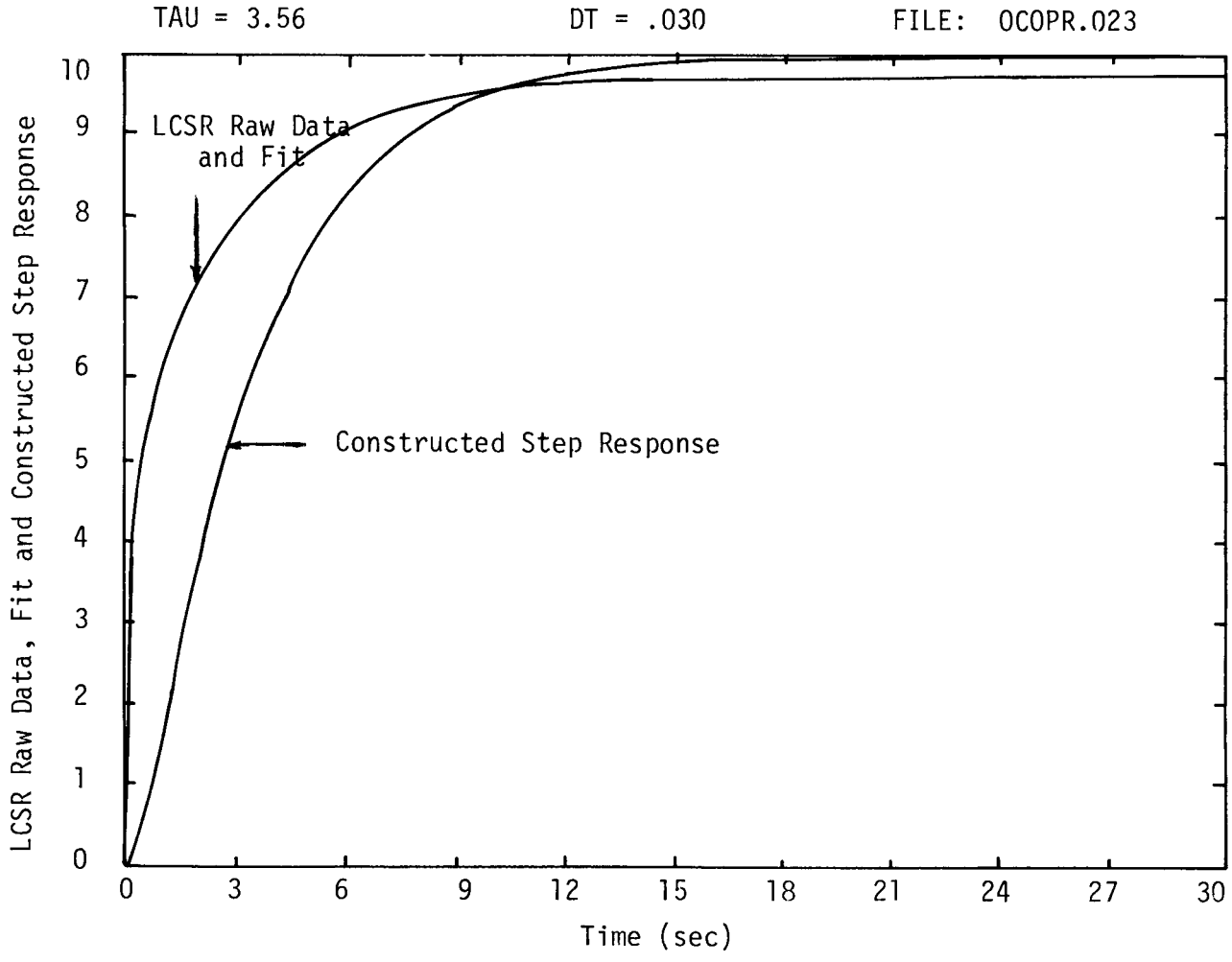

Figure 7.3. LCSR Test Results for Oconee 3 RTD (Rosemount 177GY, Tag #RC4A-TE2).

TABLE 7.1

LOOP CURRENT STEP RESPONSE TEST RESULTS FOR OCONEE 3 RTDS

Sensor Manufacturer: Rosemount

Plant Condition During Tests: Full Power

SENSOR IDENTIFICATION				RESULTS	
Sensor Model #	Sensor Tag #	Location in Plant	Number of Tests	Average Time Constant (sec)	Standard Deviation
177-HW	3RC5A-TE4	Cold Loop	7	6.59	±.77
177-GY	3RC5B-TE4	Cold Loop	8	3.26	±.60
177-GY	3RC4A-TE2	Hot Loop	4	3.38	±.27

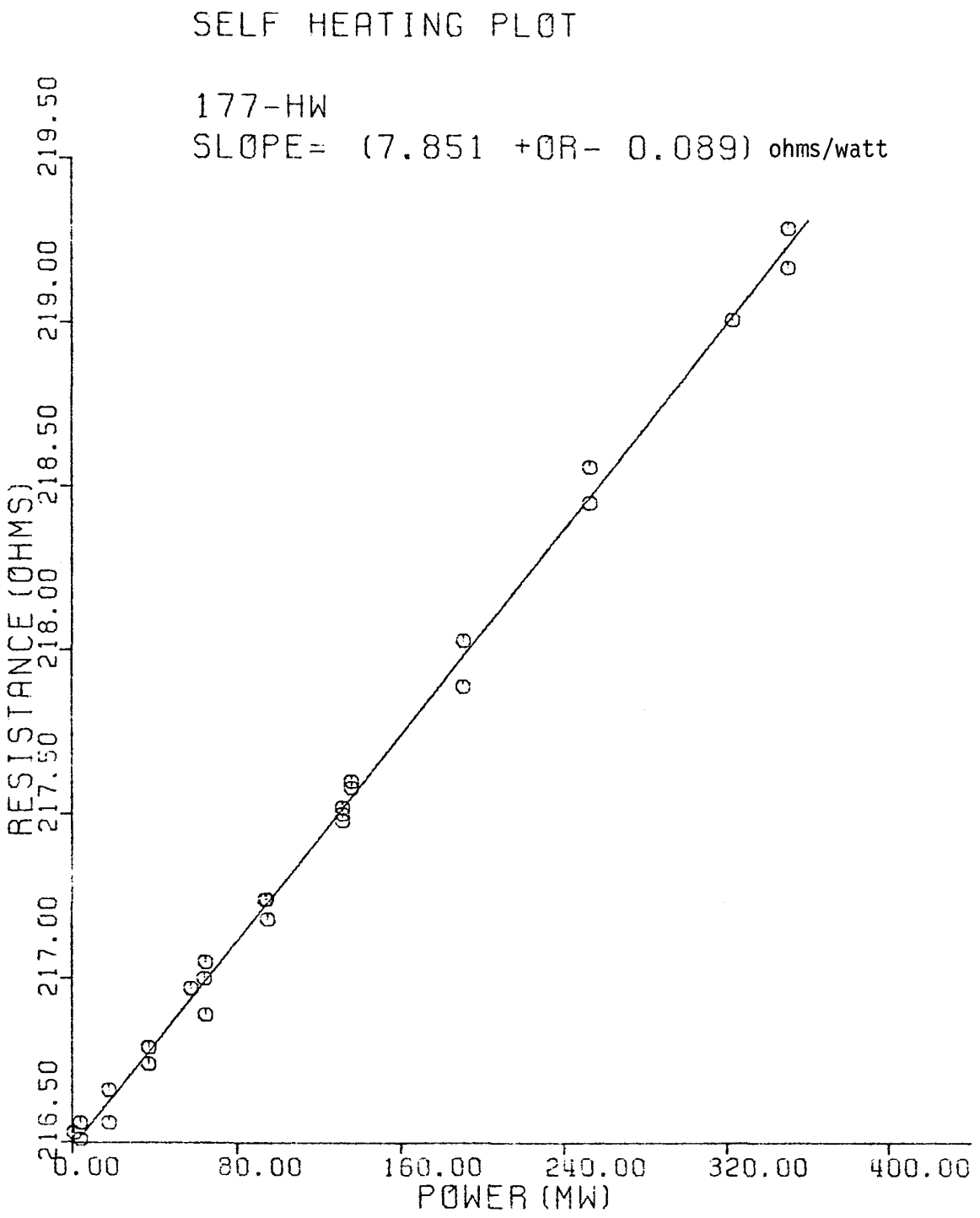

Figure 7.4. Self Heating Curve for Oconee 3 RTD (Rosemount 177-HW, Tag #3RC5A-TE4).

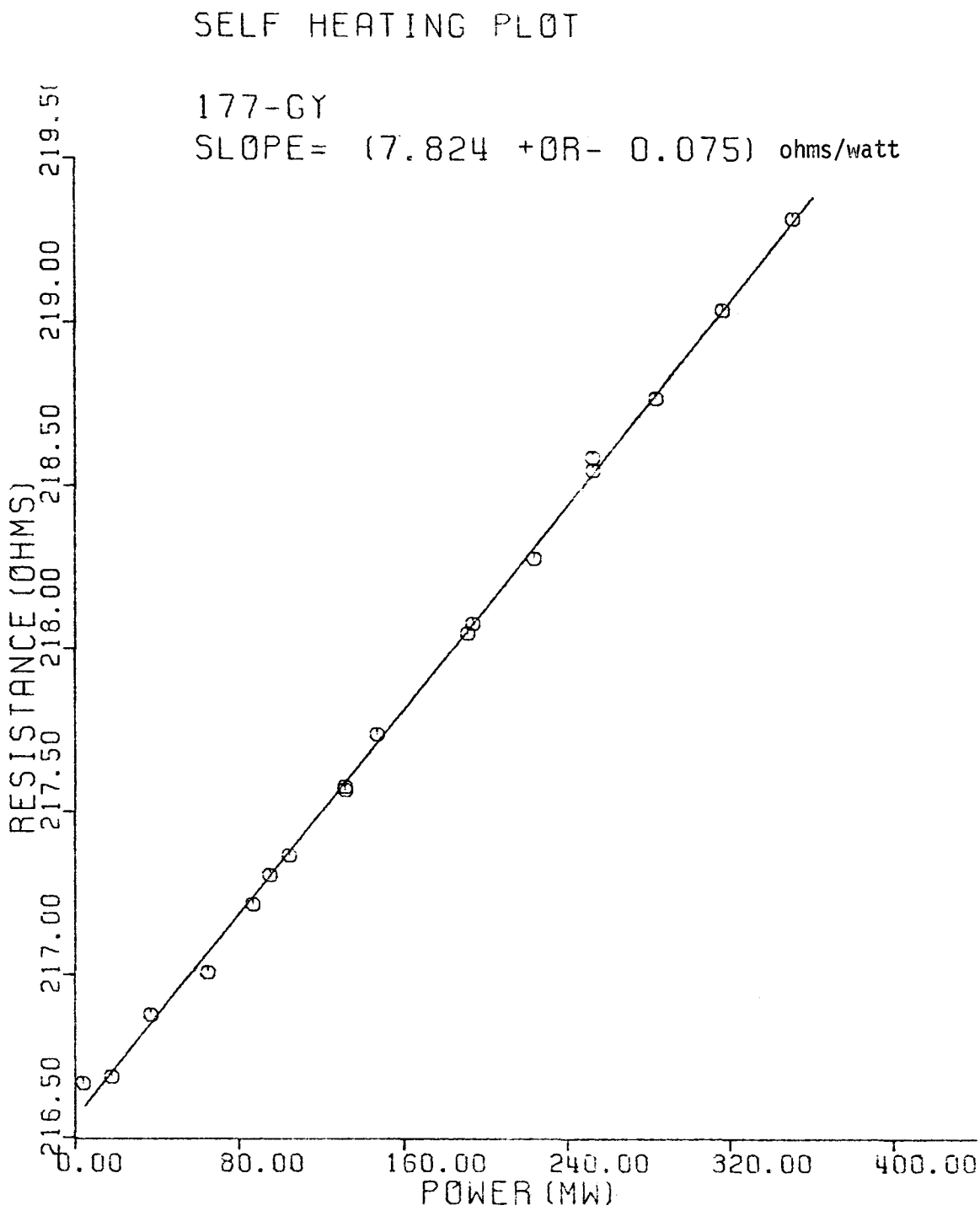

Figure 7.5. Self Heating Curve for Oconee 3 RTD (Rosemount 177-GY, Tag #3RC5B-TE4).

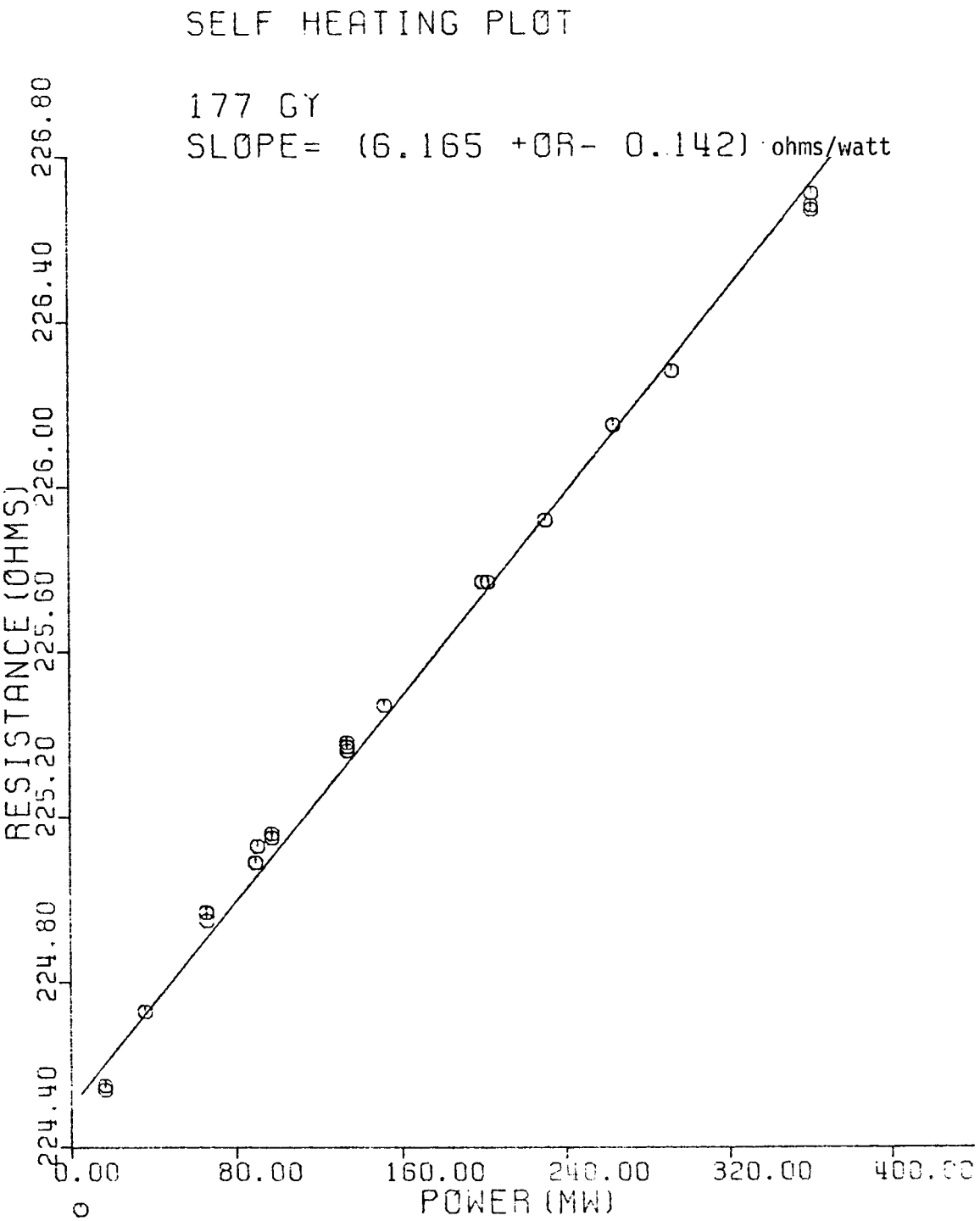

Figure 7.6. Self Heating Curve for Oconee 3 RTD (Rosemount T77-GY, Tag #3RC4A-TE2).

TABLE 7.2

SELF HEATING TEST RESULTS FOR OCONEE 3 RTDs

Sensor Manufacturer: Rosemount

Plant Condition During Tests: 100% Power

SENSOR IDENTIFICATION			RESULTS	
Sensor Model #	Sensor Tag #	Location in Plant	Self Heating Index (Ω/watt)	Standard Deviation
177-HW	3RC5A-TE4	Cold Loop	7.851	±.089
177-GY	3RC5B-TE4	Cold Loop	7.824	±.075
177-GY	3RC4A-TE2	Hot Loop	6.165	±.142

The Oconee results demonstrate the suitability of the test procedures in a plant environment.

7.3 Turkey Point

Two series of tests were performed at Turkey Point. The first Turkey Point test was the initial in-plant test in this project, and it was plagued by instrumentation problems. A voltmeter that was connected across a fixed resistor in the bridge caused spikes in the LCSR transient (see Figure 7.7). The effect of the voltmeter was discovered in the laboratory after the Turkey Point tests, so all of the data had this problem. Some effort was spent on analysis of the portion of the data record after the spike, but this was generally unsuccessful. Self heating tests had not been conceived at the time of the first Turkey Point test.

The second Turkey Point test also suffered from a testing problem, though not as serious. Through a procedural error, only 20 ma of heating current was used in the LCSR tests. This gave the expected LCSR transient, but the induced temperature rise was small and the variations in sensor output because of fluid temperature variations interferred significantly with the test results. A typical LCSR transient appears in Figure 7.8. There has not been a great effort to analyze the Turkey Point data (for example by using the averaging scheme of Appendix D). This is because the problem due to inadequate heating is not likely to be encountered in future tests performed to satisfy NRC requirements. It was decided that it is more fruitful to expend project effort on other activities rather than on this abnormal case.

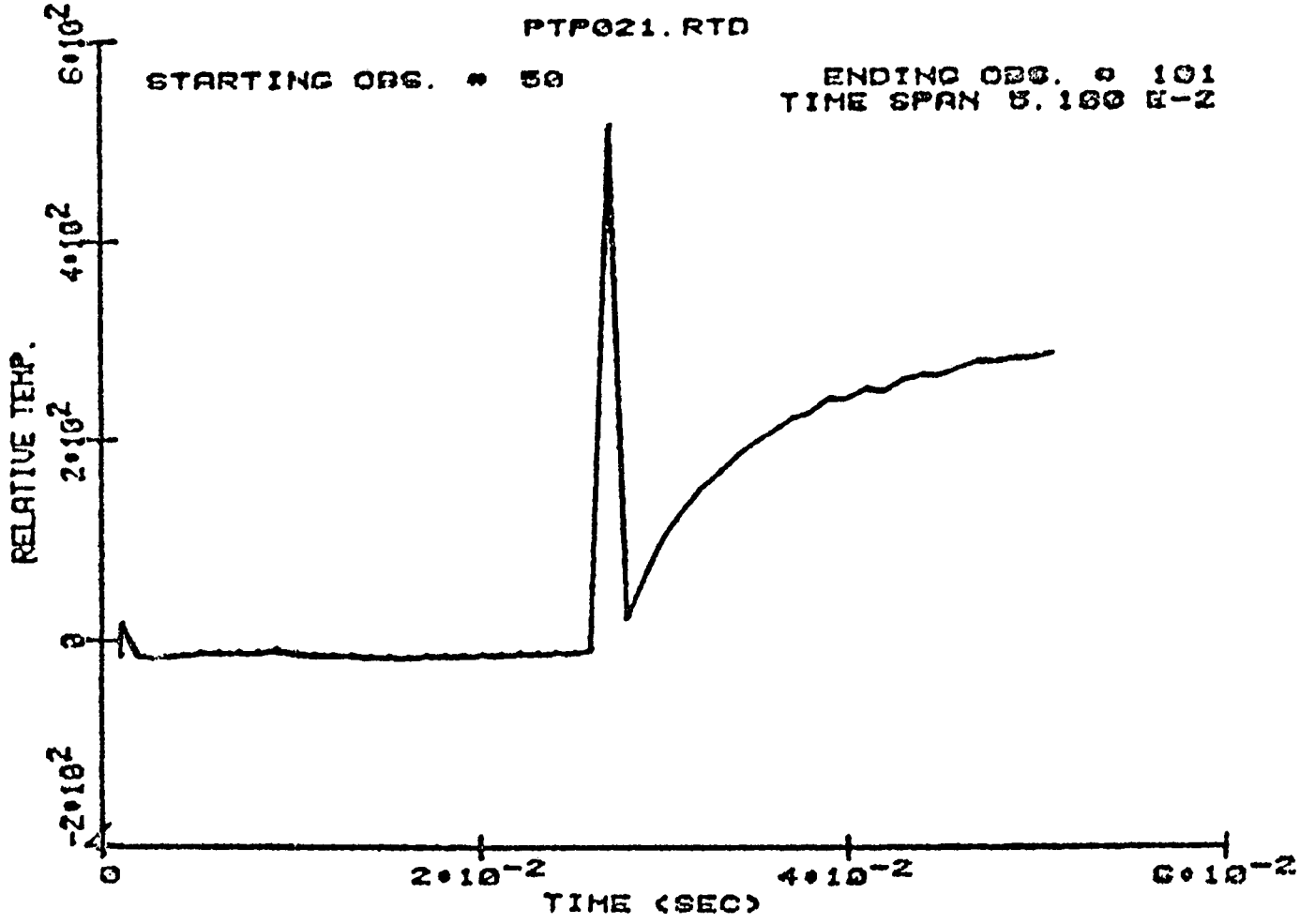

Figure 7.7. LCSR Test Data Showing Spike Encountered at Turkey Point 3.

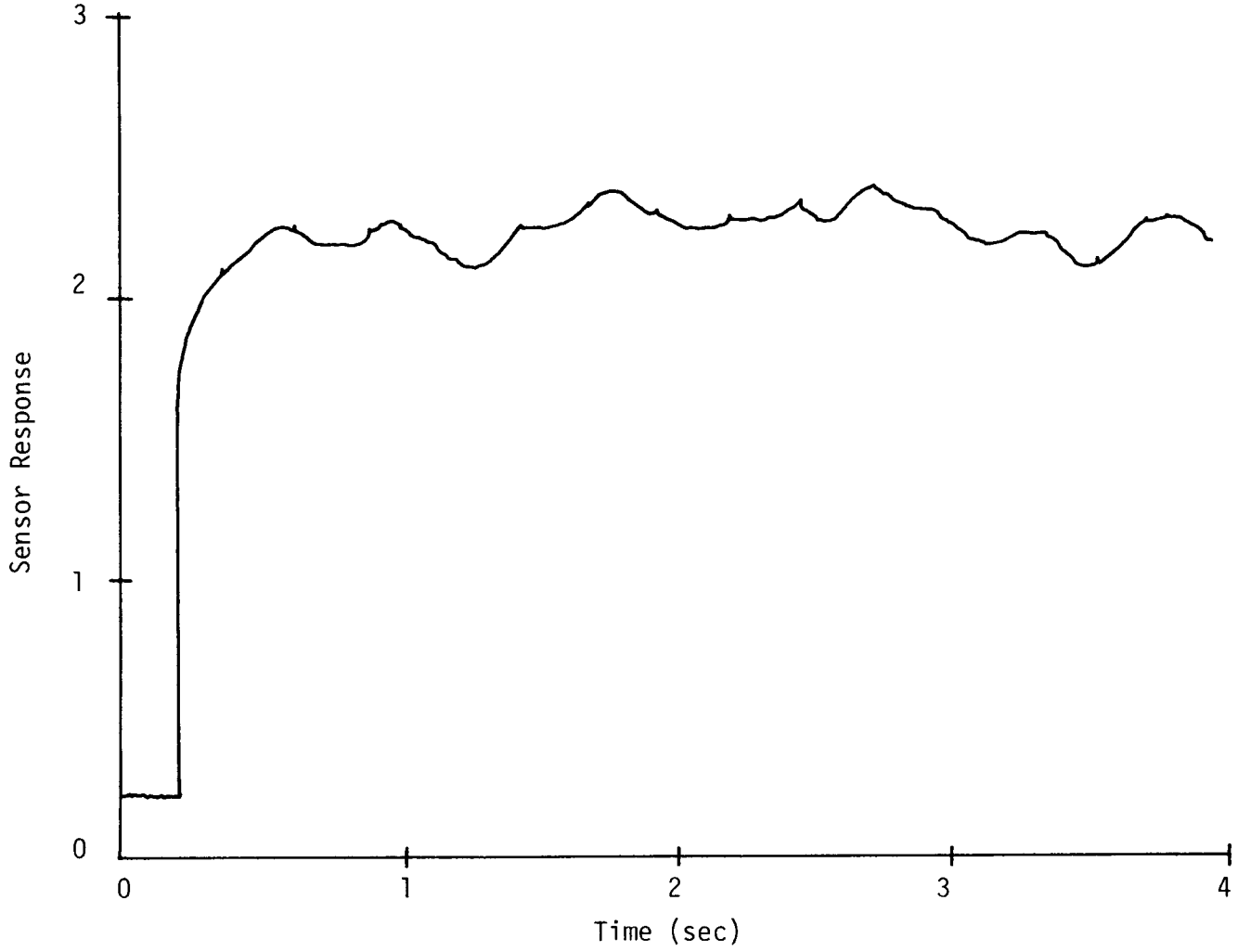

Figure 7.8. A Typical LCSR Data Set for Turkey Point 3 RTD (Rosemount 176KF).

The self heating tests at Turkey Point were not affected by the problem described above. The current determination error was corrected after it was discovered in post-test investigations. The resulting self heating curves are shown in Figures 7.9 through 7.11. The self heating results are summarized in Table 7.3.

7.4 St. Lucie

The St. Lucie tests included LCSR and self heating measurements. It was the final check of the testing procedures that evolved as a result of experience gained in earlier plant tests. Tests were made on four different control system sensors (hot leg and cold leg). All of the sensors were the Rosemount 104VC type. This is a well-type sensor and, at St. Lucie, the sensors had air in the gap between the sensor and the well.

Shortly after the start of the St. Lucie tests, a plant operational problem required a plant shut-down. LCSR tests were performed during plant cool-down and subsequently during cold stand-by (at approximately 130°F). Self heating tests were performed during cold stand-by.

After the plant returned to approximately full power (96 percent), the test program was completed. Figure 7.12 shows typical LCSR raw data, fitted data and predicted plunge test results. The LCSR test results are shown in Table 7.4. (Analysis of LCSR tests during cool-down were not reliable because the estimates are affected by the fluid temperature ramp.) One interesting point is the measured effect of ambient temperature on the response. Both of the sensors for which results were obtained at operating temperature and at cold stand-by temperature had shorter time constants at higher temperature.

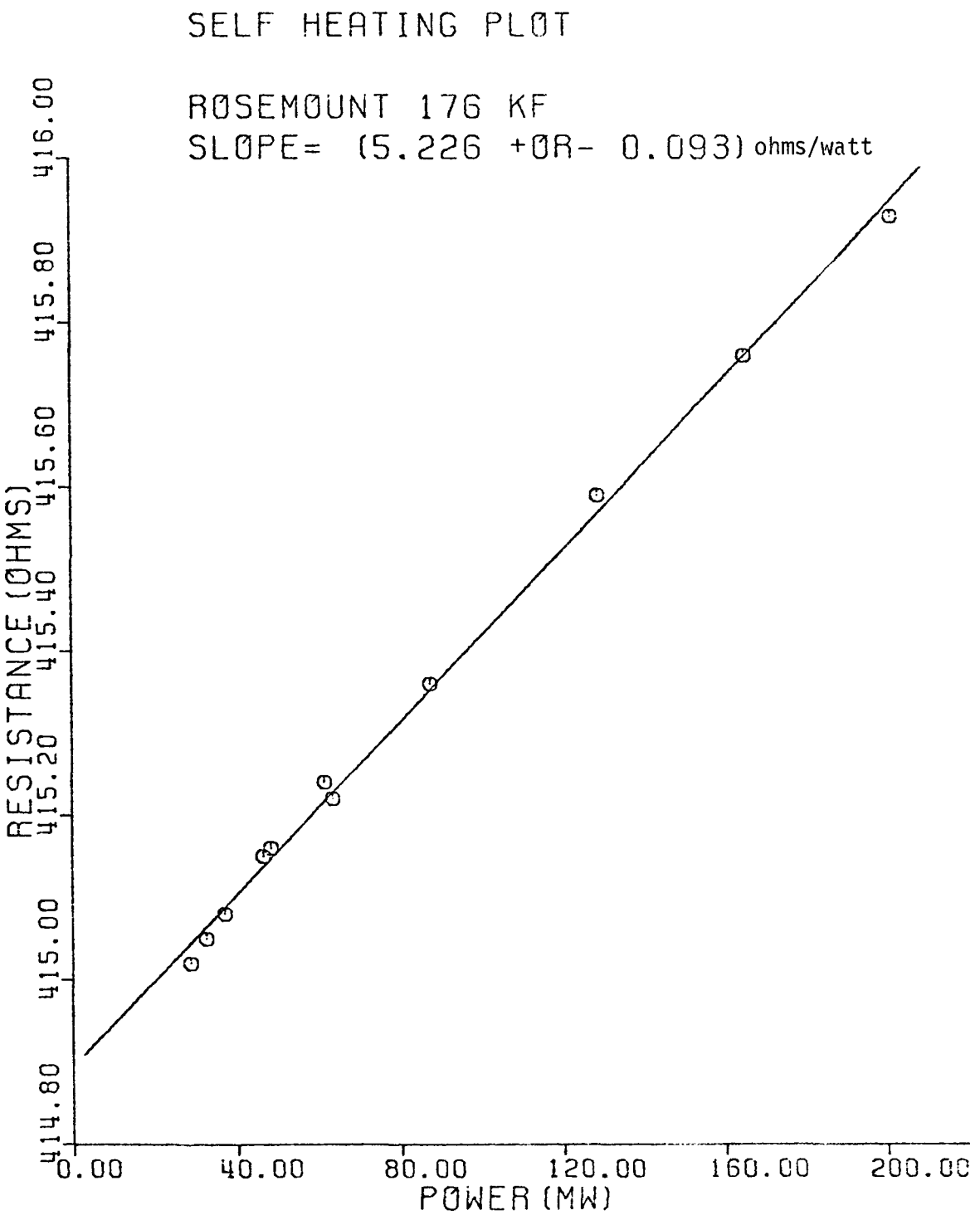

Figure 7.9. Self Heating Curve for Turkey Point 3 RTD (Rosemount 176-KF located at loop B cold).

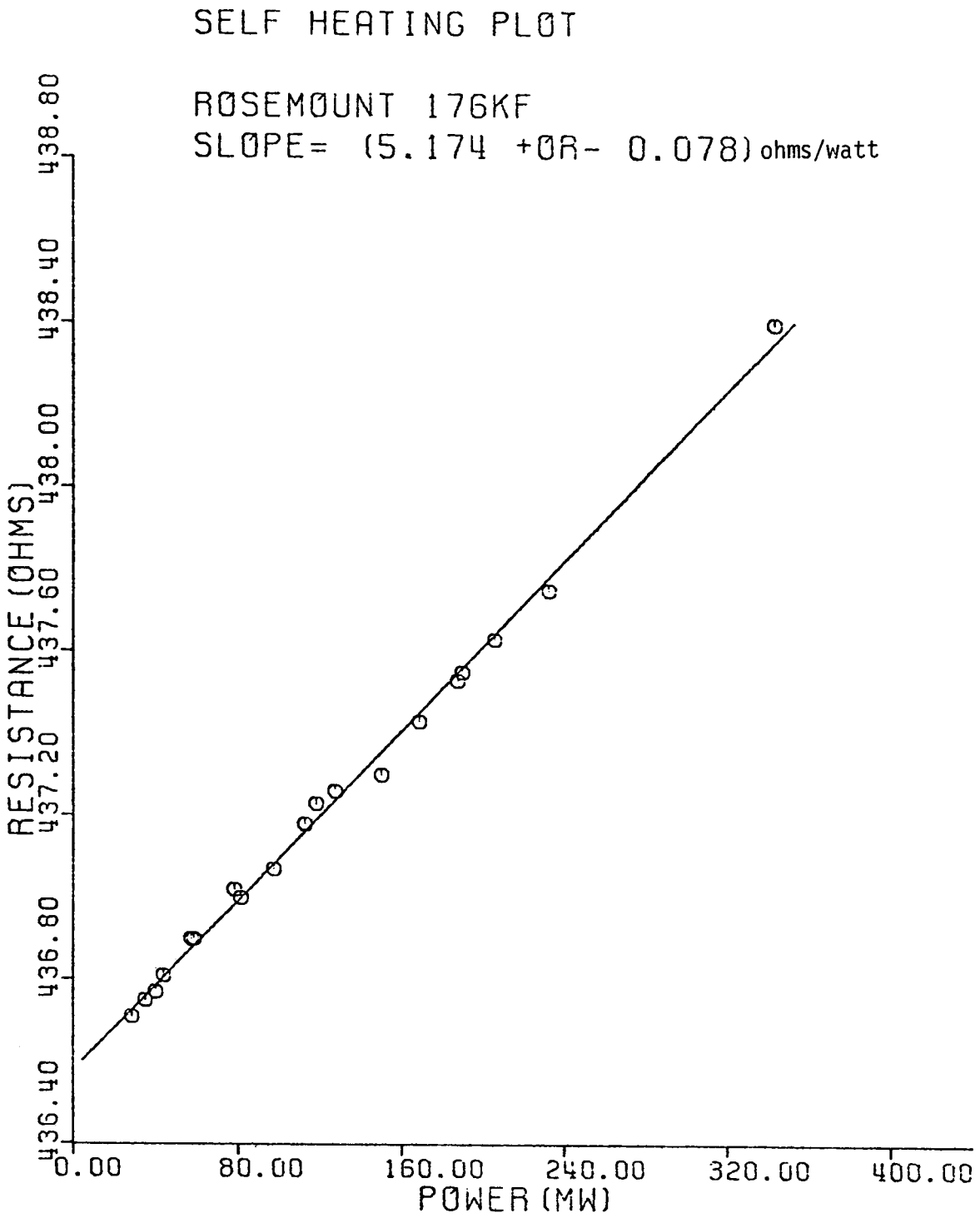

Figure 7.10. Self Heating Curve for Turkey Point 3 RTD (Rosemount 176-KF located at loop B hot).

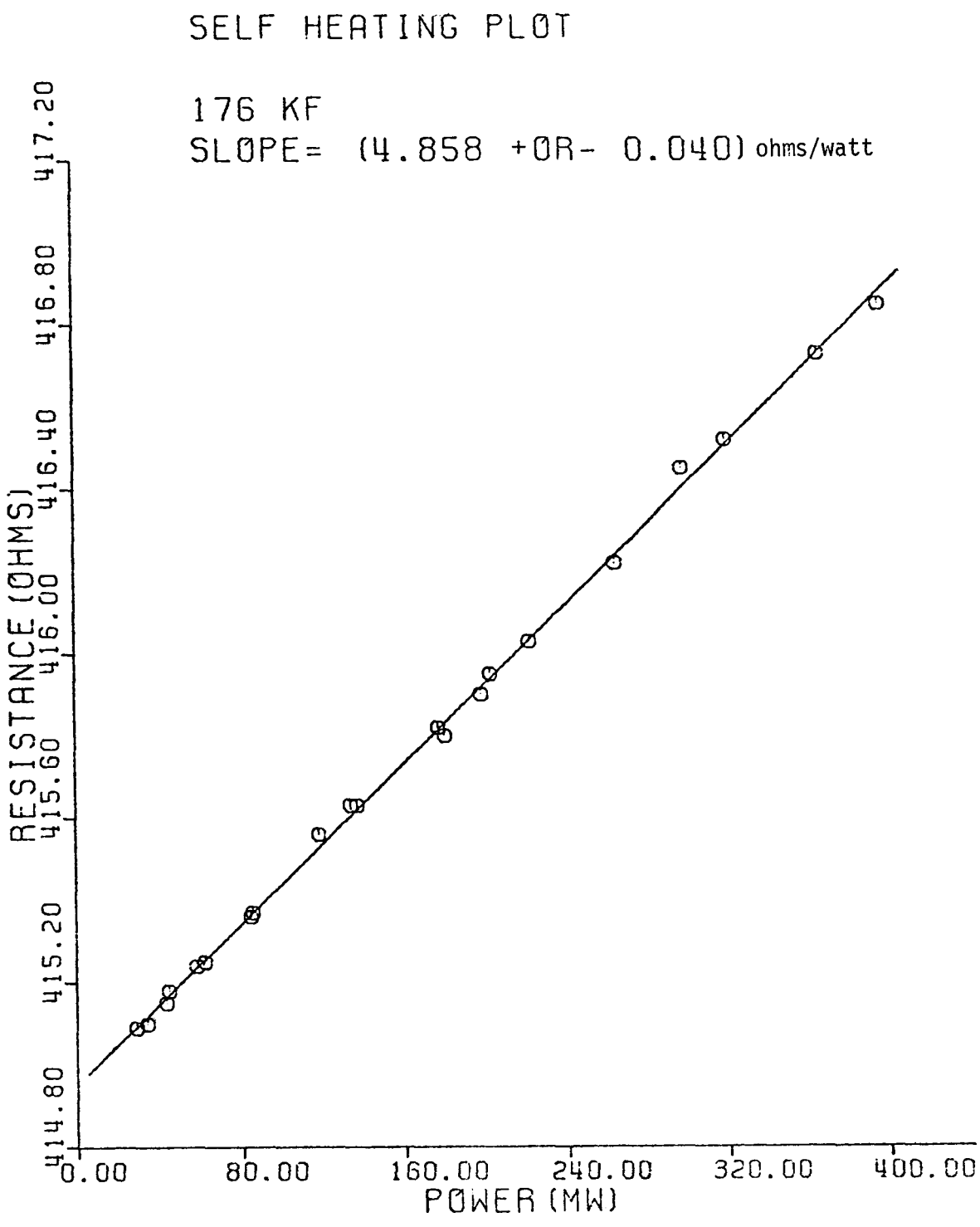

Figure 7.11. Self Heating Curve for Turkey Point 3 RTD (Rosemount 176-KF located at loop C cold).

TABLE 7.3

SELF HEATING TEST RESULTS FOR THE RTDS INSTALLED IN TURKEY POINT 3

Sensor Manufacturer: Rosemount

Plant Condition During Tests: 100% Power

SENSOR IDENTIFICATION		RESULTS	
Sensor Model #	Location In Plant	Self Heating Index (ohms/watt)	Standard Deviation
176-KF	Tcold, loop B	5.23	.09
176-KF	Thot, loop B	5.17	.08
176-KF	Tcold, loop C	4.86	.04

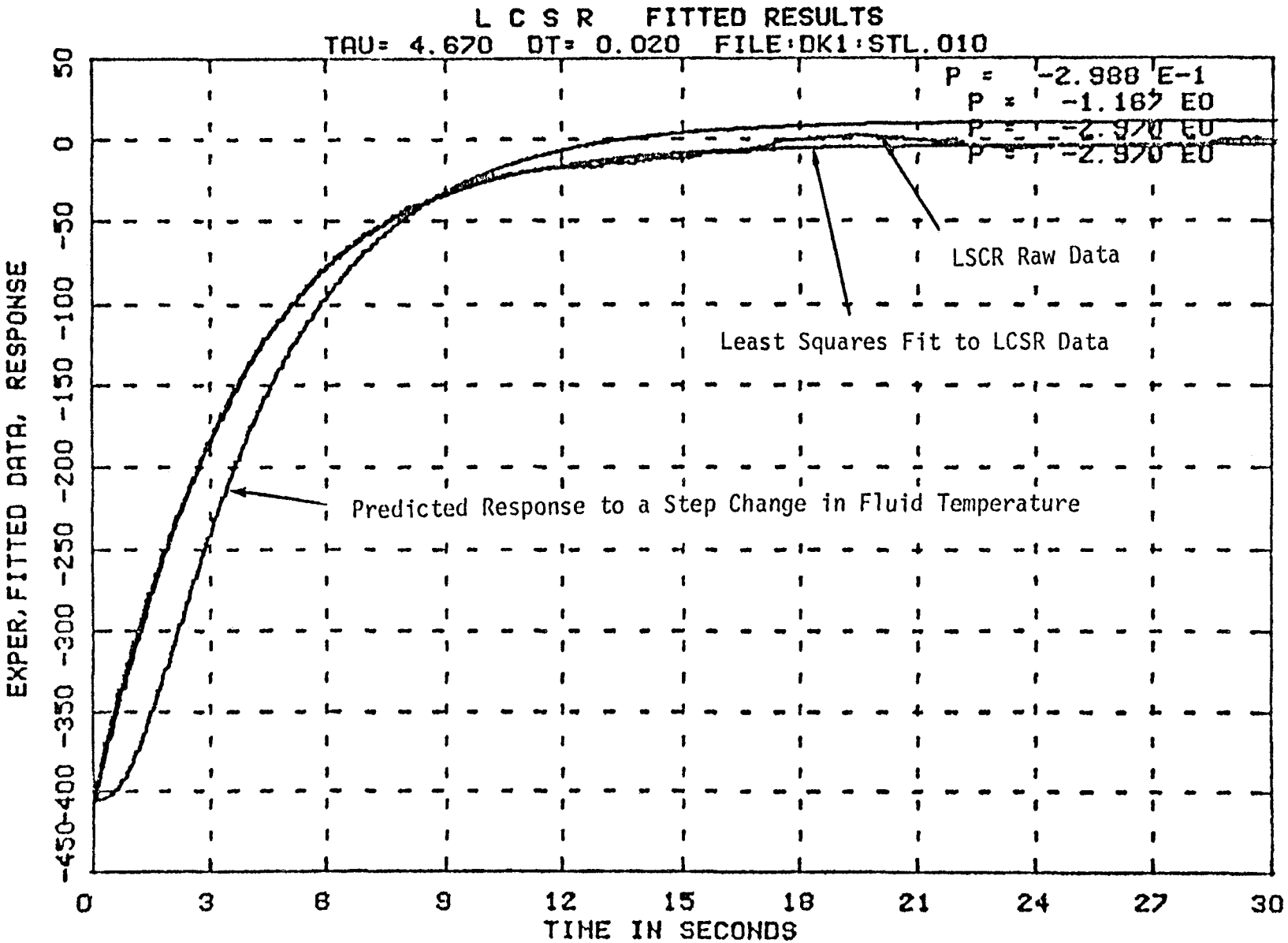

Figure 7.12. Typical Results from a Loop Current Step Response Test at St. Luice Nuclear Station.

TABLE 7.4

LOOP CURRENT STEP RESPONSE RESULTS FOR ST. LUCIE RTDS

Plant ID #	Location in Plant	Coolant Temp. °F	Number of Tests	Average Time Constant (sec.)	Standard Deviation (sec.)
TE 1125	Tcold 1B1	540	16	4.29	0.43
TE 1121Y	Tcold 1B2	540	18	5.28	0.52
TE 1121Y	Tcold 1B2	134	17	5.80	0.19
TE 1121X	Thot, loop B	583	25	4.47	0.79
TE 1121X	Thot, loop B	135	13	4.94	0.24
TE 1111Y	Tcold, 1A2	540	19	3.52	0.37

Self heating test results are shown in Figures 7.13 through 7.17. Table 7.5 gives a summary of the self heating test results. The self heating index is lower at the higher temperature for both of the sensors that were tested at two different temperatures. This gives the same conclusion as the LCSR tests. (These sensors responded faster as temperature increased.)

7.5 Conclusions Regarding In-Plant Test Experience

The in-plant testing program along with the laboratory testing program has yielded experience that led to development of equipment and procedures that are completely adequate for in-plant testing of RTDs. These were fully demonstrated in the tests at St. Lucie.

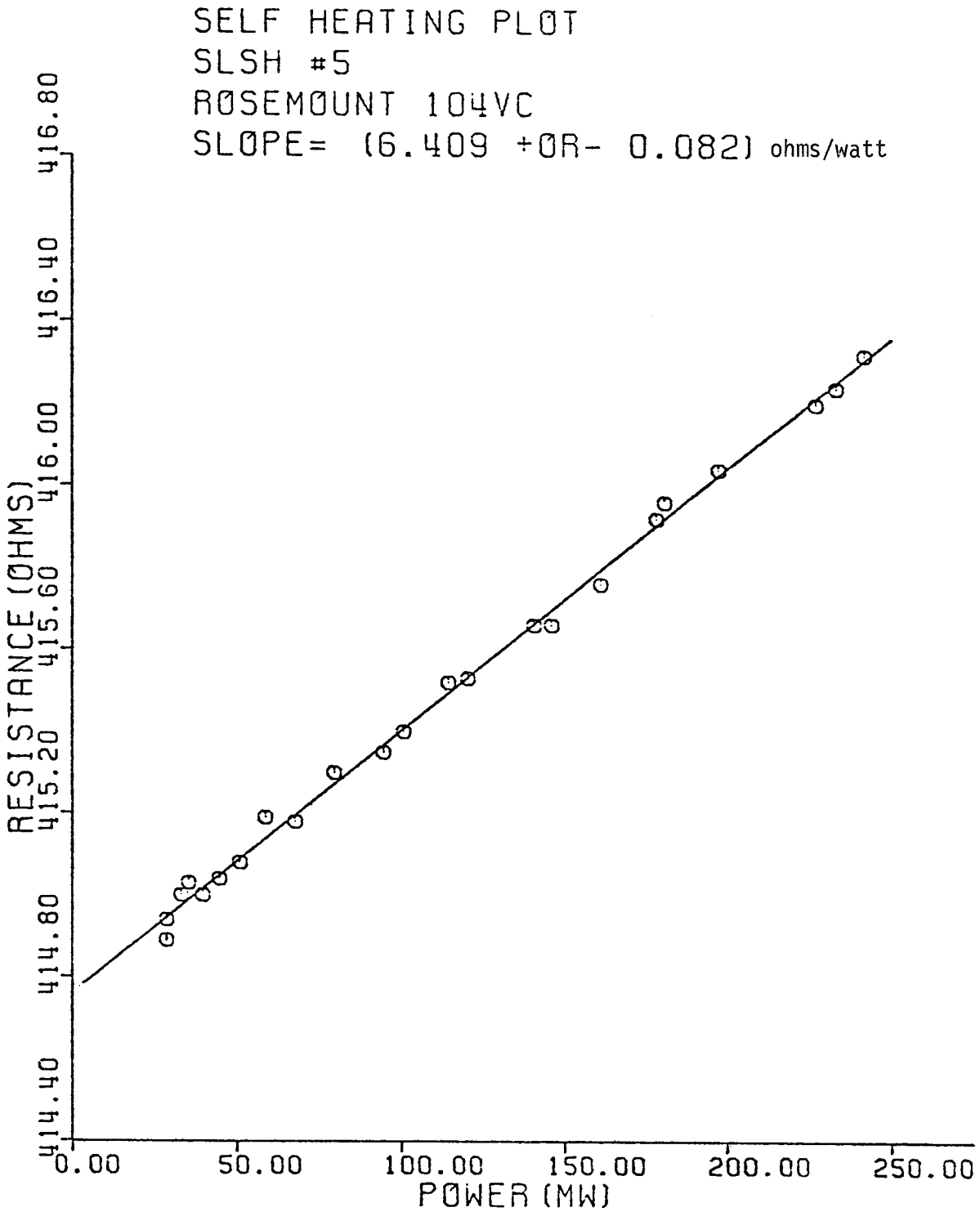

Figure 7.13. Self Heating Curve for St. Lucie RTD (TE 1125 at 540°F).

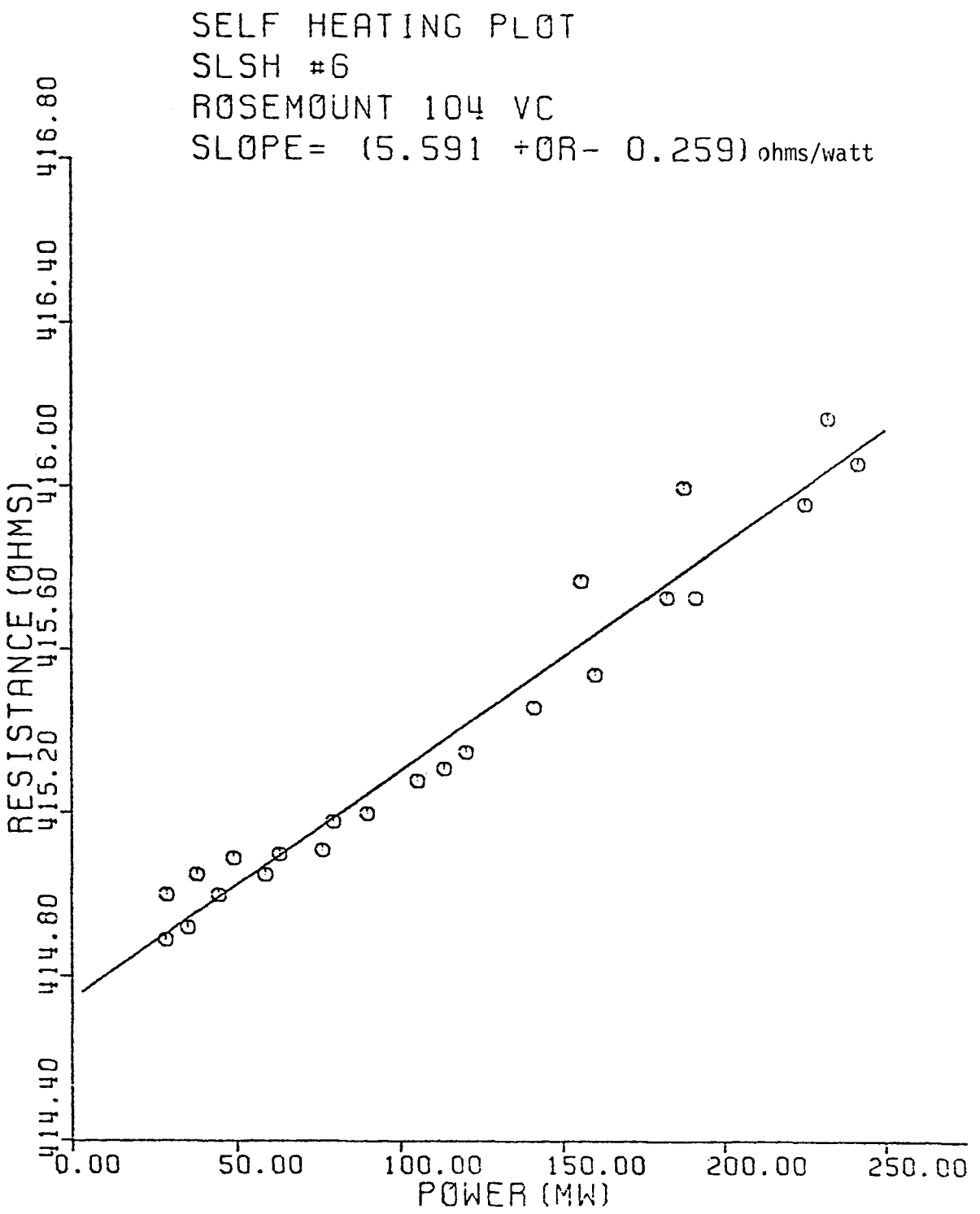

Figure 7.14. Self Heating Curve for St. Lucie RTD (TE 1121Y at 540°F).

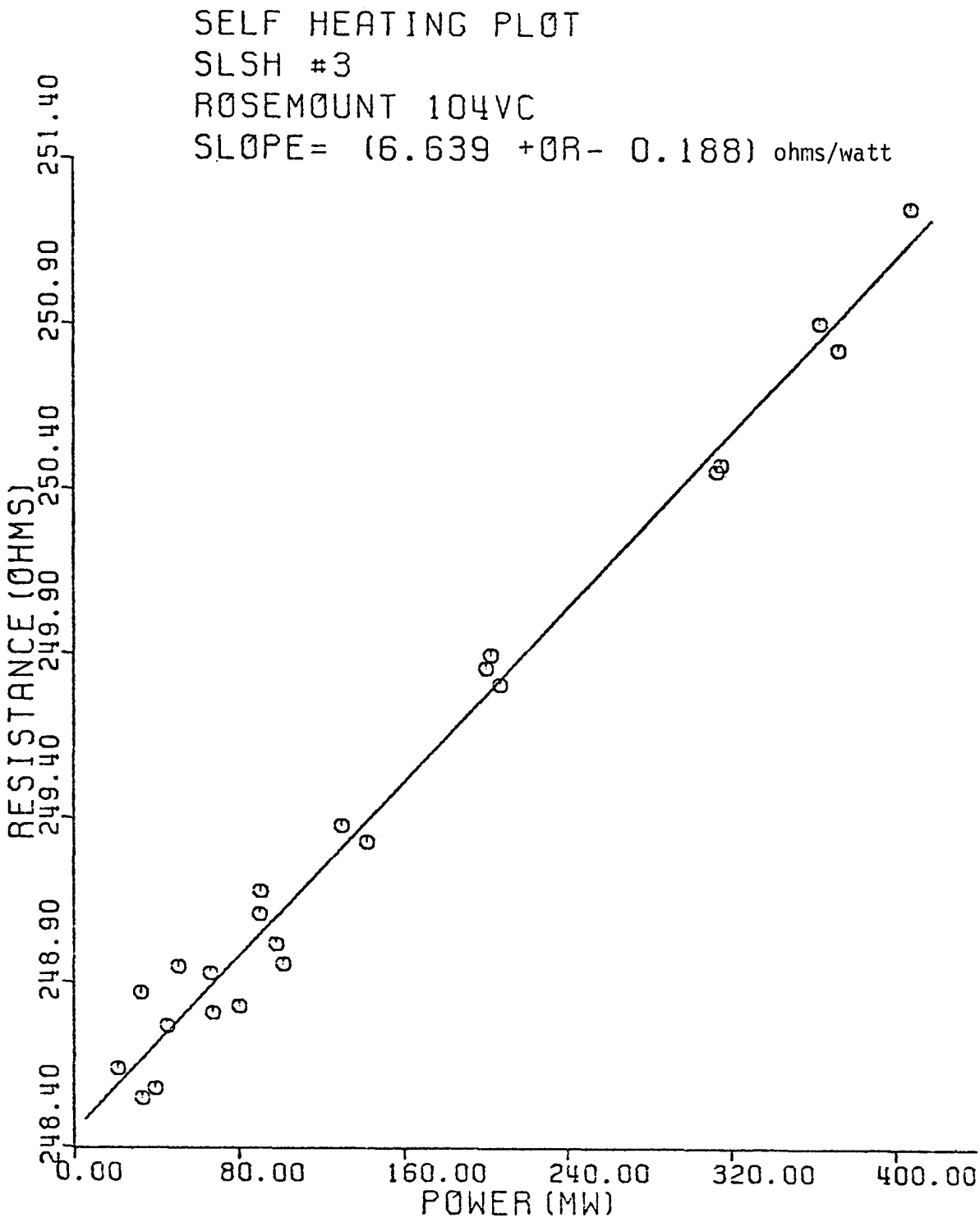

Figure 7.15. Self Heating Curve for St. Lucie RTD (TE 1121Y at 134°F).

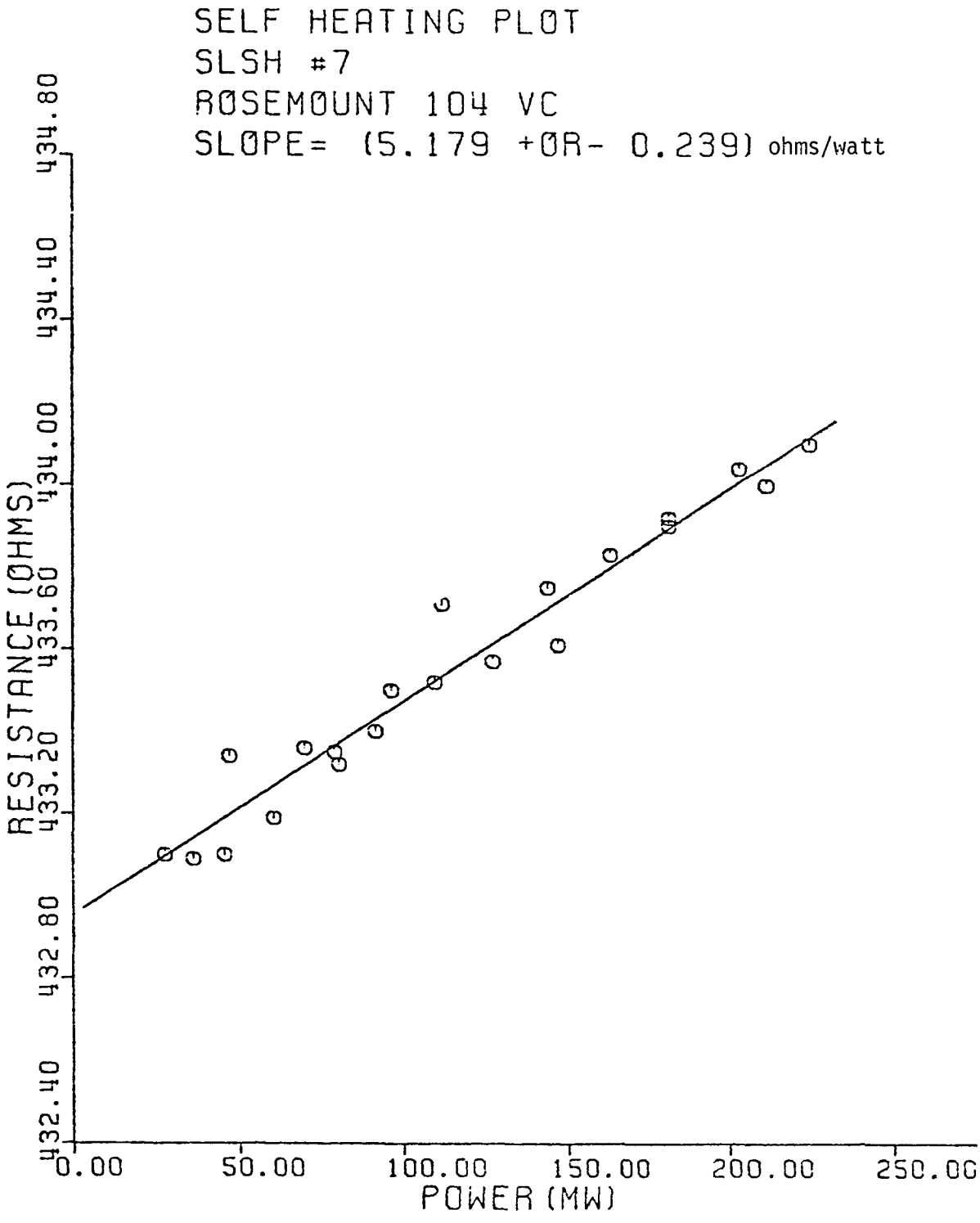

Figure 7.16. Self Heating Curve for St. Lucie RTD (TE 1121X at 583°F).

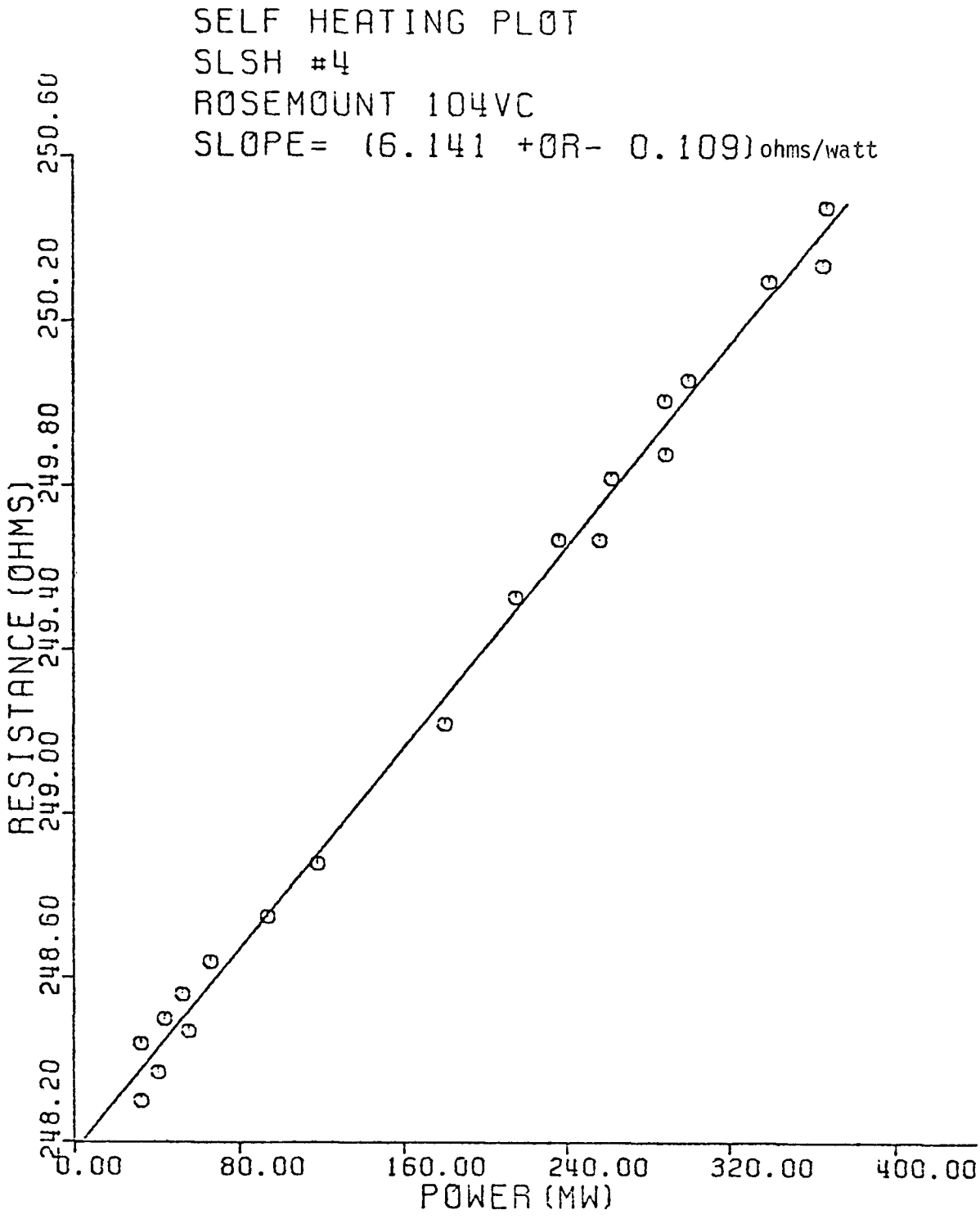

Figure 7.17. Self Heating Curve for St. Lucie RTD (TE 1121X at 135°F).

TABLE 7.5

SELF HEATING RESULTS FOR ST. LUCIE RTDs

Plant ID #	Location in Plant	Coolant Temp. °F	Self Heating Index (ohms/watt)	Standard Deviation
TE 1125	Tcold 1B1	540	6.41	0.08
TE 1121Y	Tcold 1B2	540	5.59	0.26
TE 1121Y	Tcold 1B2	134	6.64	0.19
TE 1121X	Thot, loop B	583	5.18	0.24
TE 1121X	Thot, loop B	135	6.14	0.11

8.0 SUMMARY AND CONCLUSIONS

Three methods for measuring the response time of installed platinum resistance thermometers have been developed. Experience with two of these methods (the loop current step response method and the self heating method) is described in this report. The methods have been tested in the laboratory and in four tests in three operating pressurized water reactors.

The loop current step response (LCSR) method involves analysis of the transient that occurs following a step increase in current through the sensor filament. Currents of 40 to 80 ma give temperature rises of 5 to 30 degrees Celsius. These values are suitable for in-plant testing and result in no deleterious effect on the sensor.

The loop current step response data gives the response of the sensor to an internal heating perturbation, but the response of interest is the one that results from a fluid temperature perturbation. An analytical transformation has been developed to predict the response to a fluid temperature perturbation by using information from the LCSR data record. Computer implementation of this procedure in the laboratory has been found to give time constant predictions within 10 to 20 percent of the true values. This is true for all sensors tested. This included sensors of the types commonly used in modern pressurized water reactors supplied by all PWR manufacturers.

Loop current step response testing procedures and analysis methods have been developed through laboratory tests and in-plant tests. The procedures and methods that evolved from this experience have been found to be suitable for practical in-plant measurements.

Loop current step response data can be used along with the transformation to provide quantitative time constant estimates. Also, the LCSR raw data can be used to detect changes in response characteristics from some reference condition. This may be accomplished by evaluating the LCSR time constant (different from the conventional plunge time constant) and comparing it with previous experimental evaluations on the same sensor.

The self heating method involves measurement of the steady state temperature (resistance) increase as a function of I^2R power generated in the sensor filament. Increased time constants resulting from increased heat transfer resistance are indicated by a larger temperature rise for a given power generation. Implementation of this method involves measurement of the slope of the self heating curve (electrical resistance increase vs. power generation). The slope of the self heating curve is called the self heating index and is usually expressed in ohms/watt. The self heating test may be used to detect changes in the heat transfer characteristics (and consequently the time constant) of sensors installed in an operating plant. Successful self heating tests were performed in three operating PWRs, indicating that the measurement is experimentally feasible in operating plants.

In general, the LCSR and self heating testing procedures provide methods for in-situ time response testing of platinum resistance thermometers that are safe, reliable, and inexpensive. The methods may be used to monitor changes or to obtain quantitative time constant estimates by additional analysis of test data. Thus, the test engineer can match the test effort (and cost) to the needs of the test program.

The research reported here provides the technology needed for in-situ response time testing of resistance thermometers. However, there are several different methods available that are capable of providing information of varying quality. Thus, the user must decide on the approach to time response testing that uses the available technology in the most reliable and efficient way. The experience of the authors in developing and implementing this technology has led to the following opinions on what constitutes a suitable test program.

1. The test program should be a mix of degradation monitoring and quantitative response time determination. Degradation testing provides adequate information on sensor response characteristics for less effort and cost than quantitative response time measurements.
2. The loop current step response method is the only suitable method for quantitative in-situ response time measurements for resistance thermometers. The data analysis should use a computer implementation of the transformation in order to obtain accurate time constant estimates.
3. Noise analysis (See Part B of this report) and self heating measurements are currently suitable only for degradation testing. They can indicate a change in sensor characterestics, but current technology does not provide a means to obtain reliable quantitative time response information from these methods.
4. The schedule for tests should not be set arbitarily. Rather, the test interval should be based on these factors:

- the experience on the maximum rate of change that is likely for the sensor under test
- the margin between current sensor response time and the maximum allowable response time

This information should be used to set a test interval that will detect a loss of some fraction (say half) of the margin between current conditions and maximum allowable conditions. This will help the industry by avoiding unnecessary testing, but will require industry cooperation in compiling information on degradation rates for typical sensors.

Blank Page

REFERENCES

1. M. Edelmann, "Two On-Line Methods for Routine Testing of Neutron and Temperature Instrumentation of Power Reactors," Kernforschungszentrum Karlsruhe report KFF 2316 (July 1976).

2. R. M. Carroll, R. L. Shepard, and T. W. Kerlin, "In-Situ Measurements of the Response Time of Sheathed Thermocouples," Trans. Amer. Nucl. Soc., 21, 427 (June 1975).

3. I. Warshawsky, "Heat Conduction Errors and Time Lag in Cryogenic Thermometer Installations," Trans. Instrum. Soc. Amer. 13 (4) 355 (1974).

4. T. W. Kerlin, et al, "In-Situ Response Time Testing of Platinum Resistance Thermometers," EPRI Report NP-459 (January 1977).

5. T. W. Kerlin, "Analytical Methods for Interpreting In-Situ Measurements of Response Times in Thermocouples and Resistance Thermometers," Oak Ridge National Laboratory Report ORNL/TM-4912 (March 1976).

6. K. R. Carr, "An Evaluation of Industrial Platinum Resistance Thermometers," Temperature, Its Measurement and Control in Science and Industry, Inst. Soc. of America, Part 2, pp. 971-982 (1972).

7. M. Dutt, "Practical Applications of Platinum Resistance Sensors," Temperature, Its Measurement and Control in Science and Industry, Inst. Soc. of America, Vol. 4, Part 2, pp. 1013-1019 (1972).

8. J. E. Myers, Momentum, Heat and Mass Transfer, McGraw-Hill Book Company, Inc., New York (1962).

9. J. P. Holman, Heat Transfer, McGraw-Hill Book Company, Inc., New York (1972).

10. M. N. Ozisik, Boundary Value Problems of Heat Conduction, International Text Book Company, Scranton, Pa., pp. 143-148 (1968).

11. Y. Beers, "Theory of Error," Addison-Wesley Publishing Company, Reading, Mass. (1962).

12. R. W. Hamming, Numerical Methods for Scientists and Engineers, McGraw-Hill Book Company, Inc., New York, p. 340 (1962).

13. Yonathan Bard, Nonlinear Parameter Estimation, Academic Press, New York, pp. 83-107 (1974).

14. N. R. Draper and H. Smith, Applied Regression Analysis, John Wiley & Sons, Inc., New York, p. 269 (1966).

15. C. Bayne, "Personal Communications," Oak Ridge National Laboratory (July 1977).

16. Yonathan Bard, Nonlinear Parameter Estimation, Academic Press, New York, pp. 176-179 (1974).

17. L. F. Miller, "Analysis of Loop Current Step Response Data Obtained from In-Situ Tests of Temperature Detectors," Oak Ridge National Laboratory Report ORNL/CF-77/467 (November 1977).

APPENDIXES

APPENDIX A

DERIVATION OF EQUATION 2.25

This appendix provides the derivation of the result given in Equation 2.25. It gives the relation between the asymptotic response to a ramp input and the modal time constants. Consider the Laplace transform of the ramp response of a sensor (described by a transfer function with n poles and no zeroes):

$$x(s) = \frac{Ka_o}{s^2(s-s_1)(s-s_2) \ . \ . \ . \ (s-s_n)} \tag{A.1}$$

where

K = ramp rate

$a_o = (-s_1)(-s_2) \ . \ . \ . \ (-s_n)$

The partial fraction approach involves the use of the following form:

$$x(s) = \frac{A_1}{s^2} + \frac{A_2}{s} + \frac{A_3}{s-s_1} + \frac{A_4}{s-s_2} \tag{A.2}$$

The general problem in the partial fraction approach is to find all of the A_i.

The A_i are evaluated by setting Equation A.1 equal to Equation A.2:

$$\frac{A_1}{s^2} + \frac{A_2}{s} + \frac{A_3}{s-s_1} + \frac{A_4}{s-s_2} + \ . \ . \ . = \frac{Ka_o}{s^2(s-s_1)(s-s_2) \ . \ . \ . \ (s-s_n)} \tag{A.3}$$

A common denominator is introduced on the left hand side and cancelled with the denominator on the right hand side.

$$A_1(s-s_1)(s-s_2) \ldots (s-s_n) + A_2 s(s-s_1)(s-s_2) \ldots (s-s_n)$$

$$+ \quad A_3 s^2(s-s_2)(s-s_3) \ldots (s-s_n) + A_4 s^2(s-s_1)(s-s_3) \ldots (s-s_n) + \ldots$$

$$= \quad Ka_o \qquad (A.4)$$

First we identify all of the constant terms on the left hand side. All of the factors with i>1 for A_i have s or s^2 as a multiplier, so they contain no constant terms. The term involving A_1 will have one constant term. It is:

$$A_1(-s_1)(-s_2) \ldots (-s_n)$$

Setting this equal to the constant term on the right hand side and inserting the definition of a_o gives:

$$A_1(-s_1)(-s_2) \ldots (-s_n) = K(-s_1)(-s_2) \ldots (-s_n)$$

or

$$A_1 = K. \qquad (A.5)$$

Now let us consider the terms involving s raised to the first power. When the factors in the coefficient of A_1 in Equation A.4 are multiplied out, the results are:

constant term = $(-s_1)(-s_2) \ldots (-s_n)$

coefficient of s^1 = $(-s_1)(-s_2) \ldots (-s_n)[\frac{1}{(-s_1)} + \frac{1}{(-s_2)}$

$$\ldots + \frac{1}{(-s_n)}]$$

Also, the coefficient of s^1 in the term in Equation A.4 involving A_2 is

$$K(-s_1)(-s_2) \ldots (-s_n).$$

There are no terms involving s^1 in any other terms in Equation A.4.

Since s^1 does not appear on the right hand side of Equation A.4, we obtain:

$$sA_1 [(-s_1)(-s_2) \ldots (-s_n)][\frac{1}{(-s_1)} + \frac{1}{(-s_2)} + \ldots + \frac{1}{(-s_n)}]$$

$$+ sA_2 (-s_1)(-s_2) \ldots (-s_n) = 0 \qquad (A.6)$$

Therefore

$$A_1 [\frac{1}{(-s_1)} + \frac{1}{(-s_2)} + \ldots + \frac{1}{(-s_n)}] + A_2 = 0 \qquad (A.7)$$

Since $A_1 = K$ and $(\frac{1}{-s_i}) = \tau_i$, we obtain

$$A_2 = K [\tau_1 + \tau_2 + \ldots + \tau_n]. \qquad (A.8)$$

Now, we note that the terms in Equation A.3 containing A_i for $i>2$ will all lead to terms in the inverse Laplace transform with negative exponentials. Therefore, they will die out with time and the remaining response is given by:

$$x(t) = L^{-1}\left[\frac{K}{s^2} - \frac{K(\tau_1 + \tau_2 + \ldots + \tau_n)}{s}\right] \quad \text{for } t>>0 \tag{A.9}$$

or

$$x(t) = K\,[\,t - (\tau_1 + \tau_2 + \ldots + \tau_n)] \quad \text{for } t>>0 \tag{A.10}$$

This is the result shown in Equation 2.25.

APPENDIX B

COMPUTER PROGRAM FOR ANALYSIS OF LOOP CURRENT STEP RESPONSE DATA

B.1 Introduction

Analysis of the LCSR data requires that unbiased estimates of the approximating function be obtained. In particular, the expansion coefficients and the exponents (eigenvalues) of the function

$$f(t) = a_0 + a_1 e^{\lambda_1 t} + \ldots + a_k e^{k^t}$$

must be evaluated so that f(t) is the function which optimally approximates the LCSR data. If the exponents are specified, the expansion coefficients can be determined by using the linear least squares method. However, if the eigenvalues are to be determined, a method of nonlinear functional minimization is required.

It is important to note that if the data are equally spaced, it is theoretically possible to estimate the eigenvalues by a linear method.[12] This procedure was evaluated and found to be impractical for analysis of LCSR data apparently due to the need for a precise elimination of the constant bias (if this shortcoming could be overcome, this method should be used instead of the functional minimization approach). Consequently, the discussion in this appendix is limited to: 1) some general comments on nonlinear minimization algorithms, 2) a method for estimating the variance of the unbiased parameter estimates, and 3) details regarding a computer program developed for analyzing LCSR data.

B.2 General Comments on Nonlinear Minimization Algorithms

Several nonlinear minimization algorithms commonly used for practical problems are:[13] 1) steepest descent in conjunction with a line search, 2) linearization of the functional or approximating function in conjunction with a variable stepsize (a generalization of Newton's method), and 3) Marquardt's method. The best algorithm for a particular application is usually not known a priori. Thus, three nonlinear minimization algorithms are evaluated for application to the LCSR data analysis: 1) linearization, 2) Marquardt's method, and 3) a combination of Marquardt's method and linearization. The linearization method is preferred to Marquardt's method or to the combined method for the LCSR data analysis since it is easier to implement and performs as well for the functional of interest.

Two basic problems associated with any iterative nonlinear search algorithm are: 1) determining a search direction vector, and 2) determining the optimal stepsize in the specified search direction. Most methods provide an implicit estimate of the stepsize in addition to determining the search direction. Nevertheless, it is frequently desirable to expend computational overhead to obtain an optimal (or suboptimal) estimate of the stepsize for at least two reasons: 1) to improve overall computational efficiency, and 2) to ensure convergence properties.

B.3 Nonlinear Minimization Using Linearization

One advantage of the linearization method over some second order methods is that the coefficient matrix for determining the search direction (the matrix formed during the least squares solution of

the equations specified by Equation B.8) is positive definite (at least semidefinite)[13]; consequently, the functional value decreases in the specified direction. Thus, if the optimal (or a suboptimal) stepsize is obtained for each iteration, the linearzation method is theoretically guaranteed to converge to a local minimum.[14] In practice, guaranteed convergence cannot always be achieved.[14] A disadvantage of the linearization method is that convergence is typically slow near the minimum compared to a second order methods. Some mathematical details follow.

The function which approximates the data is given by,

$$f(t) = a_o + \sum_{i=1}^{M} a_i \, e^{\lambda_i t} \tag{B.1}$$

Typically, two exponential terms (M=2) are sufficient to approximate LCSR data adequately. In order to estimate the model parameters $(a_o, \ldots, a_M \;\; \lambda_i, \ldots, \lambda_M)$, the variance of the residual is minimized; in particular, the following functional is minimized:

$$\Phi(\underline{\theta}; \underline{Y}_e) = \frac{1}{N-K} \sum_{k=1}^{N} (f_k - Y_{ek})^2 \;, \quad \underline{\theta} \epsilon R^K \tag{B.2}$$

where

$$\underline{\theta}^T = (a_o, \ldots, a_M \;\; \lambda_i, \ldots, \lambda_M), \; \underline{\theta} \epsilon R^{2M+1} \tag{B.3}$$

$$f_k = a_o + \sum_{i=1}^{M} a_i \, e^{\lambda_i t_k} \tag{B.4}$$

$$\underline{Y}_e = \text{vector of data points} \tag{B.5}$$

If the approximating function is expanded in a first order Taylor series, one obtains,

$$\tilde{\Phi}(\underline{\Theta}, \underline{Y}_e) = \frac{1}{N-K} \sum_{k=1}^{N} \left[f_k + \left(\frac{\partial f}{\partial \underline{\Theta}}\right)_k \underline{\partial\Theta} - Y_{ek} \right]^2 \qquad (B.6)$$

Minimization of $\tilde{\Phi}$ is equivalent to the linear least squares problem for the set of equations

$$\left(\frac{\partial f}{\partial \underline{\Theta}}\right)_k \underline{\delta\Theta} = Y_{ek} - f_k \; ; \quad k = 1, \ldots, N \qquad (B.7)$$

Thus, minimization of the functional given by Equation B.2 is converted into a sequence of linear least squares problems with a one-dimensional search for each iteration. At each iteration, the optimum stepsize is calculated so that $\Phi(\underline{\Theta} + \rho\underline{\delta\Theta}; \underline{Y}_e)$ is minimized; in particular, Φ is minimized with respect to ρ for each iteration.

The optimum stepsize is estimated by using: 1) the point where the functional minimum occurred for the previous iteration, 2) a point which reduces the functional value (this is found by halving the interval), and 3) a point which increases the functional value (this point is found by increasing the stepsize). A quadratic curve is defined by these three points; thus, the optimum stepsize is easily estimated. Since the search direction is obtained through the use of a positive definite coefficient matrix,[13] the functional can be reduced in the direction chosen.

Three criteria are used for terminating the minimization algorithm: 1) if the norm of the functional gradient is small with respect to the norm of the functional, 2) if the functional value cannot be

reduced in the selected direction by halving the interval a selected number of times, and 3) if the specified number of interations is exceeded.

B.4 Nonlinear Minimization Using Marquardt's Method

Marquardt's method uses the Hessian matrix of the functional (a matrix generated from the second partial derivative of the functional) to calculate the search direction and stepsize. Since this is a second order method, it has very good convergence properties near a local minimum. On the other hand, the Hessian matrix may be negative definite (and lead to a diverging sequence of functional values) as well as positive definite; thus, a method based only on the Hessian matrix could result in finding a maximum instead of a minimum. Marquardt has devised a method to circumvent this problem to ensure that the search algorithm always leads to decreasing the functional. Details of Marquardt's method are given by Bard.[13]

Marquardt's method requires the calculation of the second partial derivatives with respect to the model parameters as a preliminary step. The appropriate derivatives are as follows:

$$\frac{\partial \Phi}{\partial \theta_i}(\underline{\theta}; \underline{Y}_e) = \frac{2}{N-K} \sum_{k=1}^{N} R_k \left(\frac{\partial f}{\partial \theta_i}\right)_k \tag{B.8}$$

where

$$R_k = f_k - Y_{ek} \tag{B.9}$$

and

$$\frac{\partial^2 \Phi}{\partial \theta_j \partial \theta_i} = \frac{2}{N-K} \sum_{k=1}^{N} \left[\frac{\partial f}{\partial \theta_j}\right]_k \left[\frac{\partial f}{\partial \theta_i}\right]_k + R_k \left[\frac{\partial^2 f_k}{\partial \theta_j \partial \theta_i}\right] \tag{B.10}$$

The second partials of the approximating function are specified by:

$$\frac{\partial^2 f_k}{\partial\Theta_j \partial\Theta_i} = t_k \left[\frac{\partial f_k}{\partial\Theta_i}\right] \quad \begin{array}{l} i \leq M+1,\ j > M+1 \text{ and } j = M+i \\ i > M+1,\ j > M+1 \text{ and } i = j \end{array} \tag{B.11}$$

$$\frac{\partial^2 f_k}{\partial\Theta_j \partial\Theta_i} = t_k \left[\frac{\partial f_k}{\partial\Theta_j}\right] ; \quad i > M+1,\ j < M+1 \text{ and } i = M+j \tag{B.12}$$

otherwise, the second partials of the approximating function with respect to the model parameters are zero. The first partials are easily computed. For example, if k = 5:

$$\frac{\partial f_k}{\partial a_o} = 1 , \quad \frac{\partial f_k}{\partial a_1} = e^{\lambda_1 t_k} , \quad \frac{\partial f_k}{\partial a_2} = e^{\lambda_2 t_k} \tag{B.13}$$

$$\frac{\partial f_k}{\partial \lambda_1} = a_1 t_k e^{\lambda_1 t_k} , \text{ and } \frac{\partial f_k}{\partial \lambda_2} = a_2 t_k e^{\lambda_2 t_k} \tag{B.14}$$

where

$$(\Theta_1, \Theta_2, \Theta_3, \Theta_4, \Theta_5) = (a_o, a_1, a_2, \lambda_1, \lambda_2) \tag{B.15}$$

B.5 Variances of Model Parameters and Response Time

Data obtained from a LCSR test are analyzed to obtain unbiased estimates of the model parameters. Some of the estimated parameters are subsequently used to estimate the time constant that characterizes a temperature detector plunge test.

Uncertainty in the estimates of the model parameters that characterize the LCSR data arises from at least three factors: 1) noise contamination of the data, 2) the existance of modal responses in the data that are not included in the model, and 3) sensitivity of the functional to functional parameters (e.g. data sampling interval and sampling frequency). A method for estimating the variance of unbiased parameter estimates due to noise contamination has been discussed with Bayne[15] and is described by Bard.[16] If the variances of the parameter estimates are given, two methods for estimating the variance of the plunge test time constant are: 1) the propagation of error formula[11] in conjunction with an analytical approximation for the time constant, or 2) the parameters used to obtain the "plunge test time constant" could be randomly varied in conjunction with a direct calculation of the time constant. Although the second method is preferred, the first method is used for computational convenience.

In terms of the model and the residuals (noise), the observed data are given by

$$Y_j = f(\hat{\Theta}, t_j) + \varepsilon_j \; ; \; j = 1, \ldots, N \quad . \tag{B.16}$$

where

$\hat{\Theta}$ = the unbiased parameter estimates

Y_j = an observed datum

ε_j = a residual.

It is assumed that the expected value of the residual is near zero; in particular,

$$E(\varepsilon_j) \tilde{=} 0. \tag{B.17}$$

Also, the best estimate of the variance of the residuals is used to estimate the true variance of the residuals,

$$E(\varepsilon_j^2) = S^2 \tag{B.18}$$

and

$$S^2 \tilde{=} \sigma^2 \tag{B.19}$$

where σ^2 is the unknown variance of the residuals.

In order to obtain the variances of the parameter estimates, it is necessary to calculate the variance-covariance matrix of $(\mathrm{Var}(\hat{\Theta}))$. The diagonal elements of $\mathrm{Var}(\hat{\Theta})$ are the variances of the elements of the vector $\hat{\Theta}$. The variance-covariance matrix is approximated by

$$\mathrm{Var}\,(\hat{\Theta}) = S^2 \left[\sum_{j=1}^{N} \left[\frac{\partial f}{\partial \Theta}\right]_j \left[\frac{\partial f}{\partial \Theta}\right]_j^T \right]^{-1} \tag{B.20}$$

or

$$\mathrm{Var}\,(\hat{\Theta}) = [Z^T Z]^{-1} S^2 \tag{B.21}$$

where

$$Z = \begin{bmatrix} \frac{\partial f}{\partial \Theta_{11}} & \cdots & \frac{\partial f}{\partial \Theta_{k1}} \\ \cdot & & \\ \cdot & & \\ \cdot & & \\ \frac{\partial f}{\partial \Theta_{1N}} & \cdots & \frac{\partial f}{\partial \Theta_{KN}} \end{bmatrix} \tag{B.22}$$

The first subscript denotes the position vector of $\hat{\Theta}$ and the second subscript denotes the observation number. The estimate of the variance (S^2) is given by

$$S^2 = \frac{\sum_{j=1}^{N} [\, Y_o - f(\hat{\varepsilon}, t_j)]^2}{N - K} \tag{B.23}$$

It is of interest to point out that the elements of Z_{ij} are simple analytical expressions. Also, if the data are equally spaced, closed form expressions for the elements of $Z^T Z$ can be obtained. These closed form expressions are included in the computer program developed in this project.

An estimate of the plunge test response (obtained from the LCSR data) for a second order system is given by

$$Y_{p1}(t) \cong K \left[\frac{1}{(-\lambda_1)(-\lambda_2)} + \frac{e^{\lambda_1 t}}{\lambda_1(\lambda_1 - \lambda_2)} + \frac{e^{\lambda_2 t}}{\lambda_2(\lambda_2 - \lambda_1)} \right] \tag{B.24}$$

The time constant τ is defined through the expression

$$Y_{p1}(\tau) = Y_{p1}(\infty)\ (1 - e^{-1}), \tag{B.25}$$

and is accurately approximated by

$$\tau = \left[\ 1 - \ln(1 - \frac{\lambda_1}{\lambda_2})\right]\left[\frac{-1}{\lambda_1}\right] \tag{B.26}$$

The propagation of error formula is used to estimate the variance in τ as follows:

$$\sigma_\tau^{\,2} = (\frac{\partial\tau}{\partial\lambda_1})^2\ \sigma_{\lambda 1}^{\,2} + (\frac{\partial\tau}{\partial\lambda_2})^2\ \sigma_{\lambda 2}^{\,2} \tag{B.27}$$

where $\sigma_{\lambda_1}^{\,2}$ and $\sigma_{\lambda_2}^{\,2}$ are obtained from $\mathrm{Var}(\hat{\Theta})$.

B.6 Methods Evaluation and Computer Program Verification: Discussion

A number of test problems using theoretical data were studied during the computer program development. Several computer programs are available that analyze theoretical LCSR data correctly and also give the same results for experimental data. Some of the computational experiments performed while developing the program described were:[17]

1. Survey calculations to evaluate the linearization method, Marquardt's method and a Marquardt-linearization method.
2. Calculations to determine the effect of white noise and of 60 Hz in theoretical LCSR data parameter estimates and a standard deviation of parameter estimates.

3. Calculations for parameter estimates and for uncertainties of parameter estimates using experimental data.

Each of the three nonlinear minimization algorithms tested performed well. Although Marquardt's method (in theory) converges much faster than the linearization method near the minimum, the overall performance of the linearization method was better than Marquardt's method for the functional of interest (c.f. Eq. (B.2)). A combination of the two methods performed no better than the linearization method; consequently, the computer program listed uses only the linearization method.

Results (reported in Reference 17) relating to the effect of white noise and of 60 Hz on theoretical data illustrate that the parameter estimates are not affected by significant white noise or 60 Hz data contamination. A quantative evaluation to verify the accuracy of the uncertainty estimates would require a detailed simulation study which has not been performed.

B.7 Analysis of Experimental Data: Discussion

Theoretical considerations indicate that identification of two eigenvalues should be adequate to obtain a good estimate of the plunge test time constant. However, experimental data has been found to be contaminated with other functions: 1) fast transients due to data acquisition instrumentation, 2) significant process noise in the frequency range where the RTD spectral power is concentrated, and 3) ramp process transients.

Analysis of data contaminated with fast transients can be delt with in two ways: 1) use three to five exponentials in the approximating function, or 2) use only two or three exponentials in the approximating function but skip an appropriate portion of the initial data record. The second method is preferred. However, several calculations must be made by skipping different lengths of the initial transient to determine the appropriate amount of data to be skipped. Some results to show the effect of skipping initial data points are given in Figures B.1 and B.2. Note that more data must be skipped with the second order model than the third order model. Also, note that the time constant of interest (where the curve flattens out) is the same for the second and third order models. If too much data is skipped for a particular model, then information on a particular mode is discarded and again the time constant estimate will be incorrect.

If the data is contaminated with a ramp function, one needs only to include a ramp in the approximating function. Process noise can usually be delt with using appropriate filtering. However, frequencies in the range where the RTD spectral power is concentrated cannot be filtered.

B.8 Comments on the Computer Program Described Herein

An earlier version of this program is given in Reference 17. The version described herein has been modified to run on a PDP 11 and assumes that the data are equally spaced. Assuming that the data are equally spaced allows one to write closed form expressions for elements of the

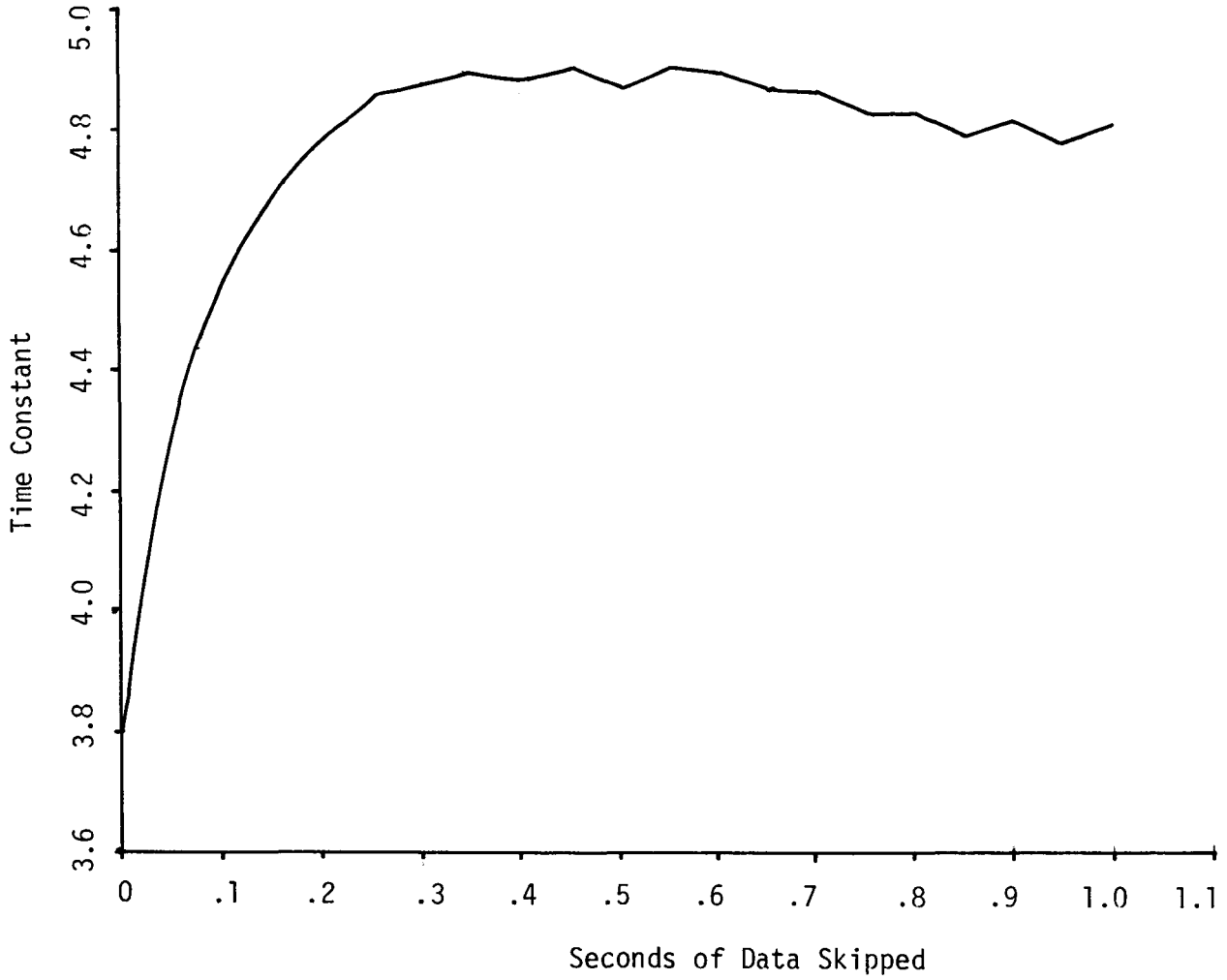

Figure B.1. Effect of Skipping Initial Data Points on the Time Constant Estimate (Second Order Model).

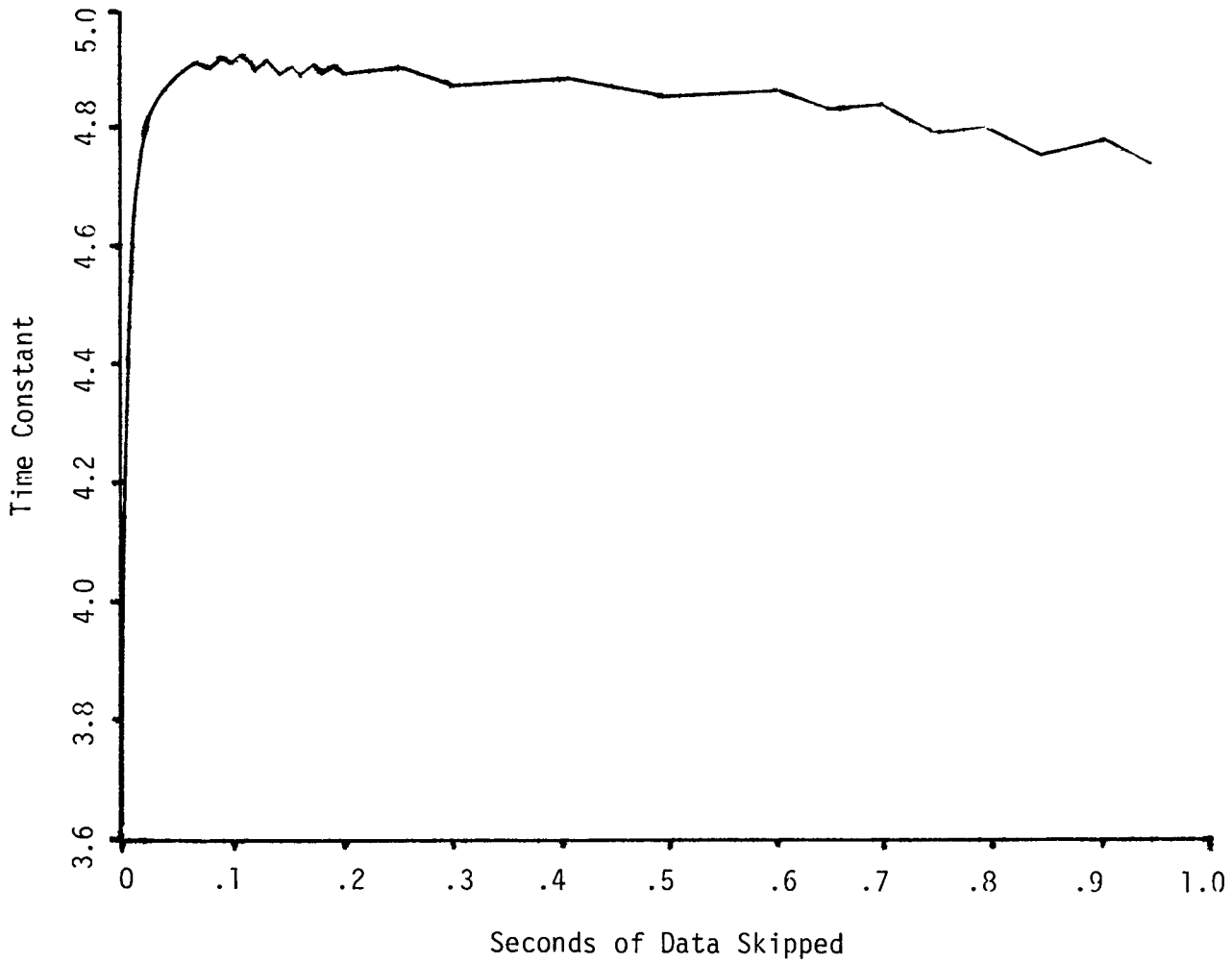

Figure B.2. Effect of Skipping Initial Data Points on the Time Constant Estimate (Third Order Model).

coefficient matrix used to determine the direction vector. This reduces the execution time by a factor of four to five.

Direction vectors are always calculated using the linearization method. However, two different methods are employed for the optimal line search. One uses the search direction as calculated and the other exploits the fact that the expansion coefficients can be obtained with a linear least squares technique.

Before any result is accepted, the influence of changing functional parameters (i.e. sampling frequency and data interval) should be evaluated since the uncertainty estimate does not take these variables into account. However, this evaluation is straightforward.

B.9 Sample Problem and Program Listing

The instructions for using the LCSR transformation program, the output of this program for a typical case, and the program listing are given in this section. Table B.1 gives the listing of the inputs to the LCSR program. Explanations of these inputs are:

1. "DO YOU WISH TO GENERATE A LIST FILE?". This input provides the user with the option of storing the results of the LCSR test analysis on a computer disk. The user types "Y" to invoke this option or types "N" otherwise.
2. "ENTER 0 FOR NO PLOTS, 1 FOR PLOTS, 2 FOR PLOTS AND AUTO-COPIES". Results of the analysis may be obtained in graphical form on a CRT as well as digital form on a line printer. The CRT may be connected to a hard copy unit to give a copy of the results displayed on the CRT. The user may type "0" to avoid plotting the results (to save time) or type "1" to only observe the plots of

Table B.1 Inputs to the Loop Current Step Response Computer Program

```
R LCFT2

DO YOU WISH TO GENERATE A LIST FILE? N

ENTER 0 FOR NO PLOTS, 1 FOR PLOTS, 2 FOR PLOTS AND AUTO-COPIES : 2

ENTER THE NAME OF THE FIRST DATA SET TO 'BE ANALYZED : DK1:PAVE.001

ENTER THE NUMBER OF DATA SETS TO BE ANALYZED : 1

ENTER 0 TO RUN SECOND ORDER CASES ONLY, ENTER 1
TO RUN SECOND AND THIRD ORDER CASES.
1

ENTER THE NUMBER OF SAMPLES TO BE SKIPPED : 10

ENTER DELTA T AND TMAX : .002,2
```

the LCSR results. If a "2" is entered a hard copy of the results can be obtained from the hard copy unit.

3. "ENTER THE NAME OF THE FIRST DATA SET TO BE ANALYZED". The LCSR program can analyze a sequence of LCSR data with a single set of inputs. This input specifies the name of the first data set to be analyzed. After the first data set is analyzed, the program will proceed to the next data set in the sequence and perform the analysis. This process will continue until all of the data sets specified by the inputs are analyzed.
4. "ENTER THE NUMBER OF DATA SETS TO BE ANALYZED". This input specifies the number of data sets to be analyzed in a sequence of LCSR data sets.
5. "ENTER 0 TO RUN SECOND ORDER CASE ONLY, ENTER 1 TO RUN SECOND AND THIRD ORDER CASES". This allows the use of a second order model or a third order model in analyzing of the LCSR data. If "0" is entered, the LCSR data will be fitted to a second order model yielding two eigenvalues (poles). If "1" is entered, the LCSR data will be fitted to a third order model yielding three eigenvalues.
6. "ENTER THE NUMBER OF SAMPLES TO BE SKIPPED". It is usually required to skip the first few milliseconds of the data that include a very fast transient. This initial transient is characteristic of the instrumentation and of the sensor filament rather than the sensor heat transfer characteristics. The appropriate number of points that should be skipped to eliminate the transient may be determined by plotting the time constant versus the number of points skipped (c.f. section B.7).

7. "ENTER DELTA T AND TMAX". The Delta T (T) is the reciprocal of the sampling frequency and TMAX is the duration of the data set to be analyzed.

The plot of LCSR data for a typical case is given in Figure B.3. The results of analysis of this data along with the plots of intermediate and final results are shown in Table B.2 and Figures B.4 and B.5. The program listing follows Figure B.5.

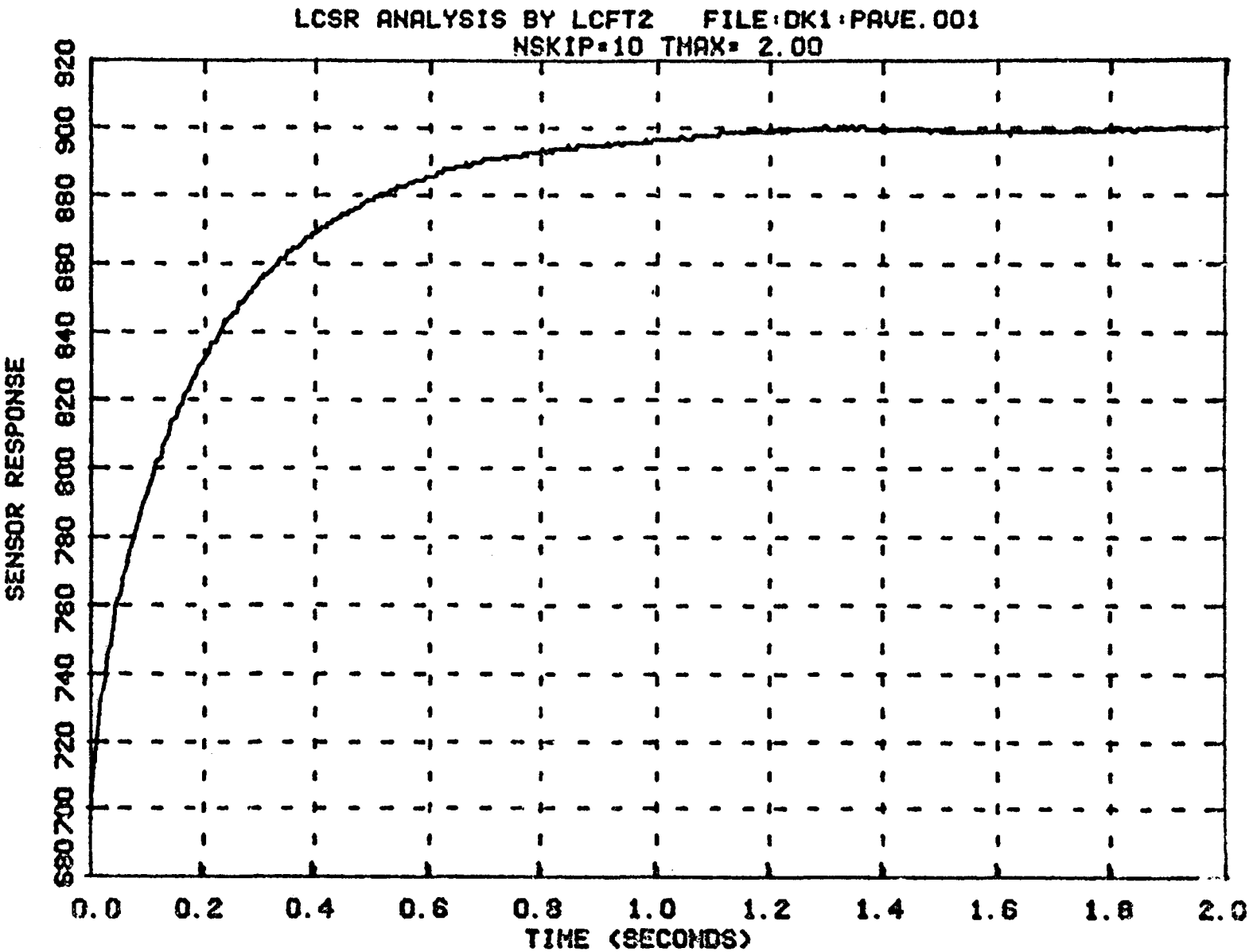

Figure B.3. Plot of a Typical LCSR Data Set

Table B.2. Listing of The Results of Analysis of a Typical LCSR Data Set

```
  RESULTS OF THE DIRECT SEARCH:

  THE FUNCTIONAL VALUE          =      0.57424E+00
  THE TIME CONSTANT             =      0.28608E+00
  THE EXPANSION COEFFICIENTS =      0.89990E+03    -0.15314E+03    -0.47367E+
02
  THE EIGENVALUES               =     -0.40344E+01    -0.28240E+02

  THE FOLLOWING RESULTS PERTAIN TO AN
APPROXIMATING MODEL WITH  2 EXPONENTIALS:

  NEW AND OLD FUNCTIONAL VALUES FOR ITERATION  1
    ARE    0.52719E+00  AND    0.57424E+00
  NEW AND OLD FUNCTIONAL VALUES FOR ITERATION  2
    ARE    0.52450E+00  AND    0.52719E+00
  NEW AND OLD FUNCTIONAL VALUES FOR ITERATION  3
    ARE    0.52441E+00  AND    0.52450E+00

  RESULTS FROM THE MINIMIZATION ALGORITHM:

  TERMINATED BY, NOPT =  0
```

Table B.2 (Continued)

```
EXPECTED VALUE OF RESIDUAL          =  0.51141E-04
STANDARD DEVIATION OF THE RESIDUAL =  0.72416E+00
VARIANCE OF THE RESIDUAL            =  0.52441E+00
THE NORMALIZED GRADIENT             =  0.18788E-03

EXPANSION COEFFICIENTS ARE:
    0.89988E+03 + OR -  0.49306E-01
   -0.15050E+03 + OR -  0.70066E+00
   -0.47739E+02 + OR -  0.70912E+00

EIGENVALUES ARE:
   -0.40037E+01 + OR -  0.16842E-01
   -0.23670E+02 + OR -  0.61314E+00

THE TIME CONSTANT =  0.29605E+00 + OR -  0.81241E-02
```

Table B.2 (Continued)

```
  THE FOLLOWING RESULTS PERTAIN TO AN
APPROXIMATING MODEL WITH  3 EXPONENTIALS:

  NEW AND OLD FUNCTIONAL VALUES FOR ITERATION  1
    ARE    0.46520E+00  AND    0.49715E+00
  NEW AND OLD FUNCTIONAL VALUES FOR ITERATION  2
    ARE    0.41917E+00  AND    0.46520E+00
  NEW AND OLD FUNCTIONAL VALUES FOR ITERATION  3
    ARE    0.37680E+00  AND    0.41917E+00
  NEW AND OLD FUNCTIONAL VALUES FOR ITERATION  4
    ARE    0.37115E+00  AND    0.37680E+00
  NEW AND OLD FUNCTIONAL VALUES FOR ITERATION  5
    ARE    0.37036E+00  AND    0.37115E+00

  RESULTS FROM THE MINIMIZATION ALGORITHM:

  TERMINATED BY, NOPT =  0
```

Table B.2 (Continued)

```
  EXPECTED VALUE OF RESIDUAL          =  0.14722E-03
  STANDARD DEVIATION OF THE RESIDUAL  =  0.60857E+00
  VARIANCE OF THE RESIDUAL            =  0.37036E+00
  THE NORMALIZED GRADIENT             =  0.39995E-05

  EXPANSION COEFFICIENTS ARE:
      0.90005E+03 + OR -  0.47649E-01
     -0.13938E+03 + OR -  0.18671E+01
     -0.44507E+02 + OR -  0.13774E+01
     -0.18840E+02 + OR -  0.15239E+01

  EIGENVALUES ARE:
     -0.38248E+01 + OR -  0.29432E-01
     -0.13621E+02 + OR -  0.82742E+00
     -0.80088E+02 + OR -  0.88482E+01

  THE TIME CONSTANT =  0.36043E+00 + OR -  0.13444E-01
STOP --
```

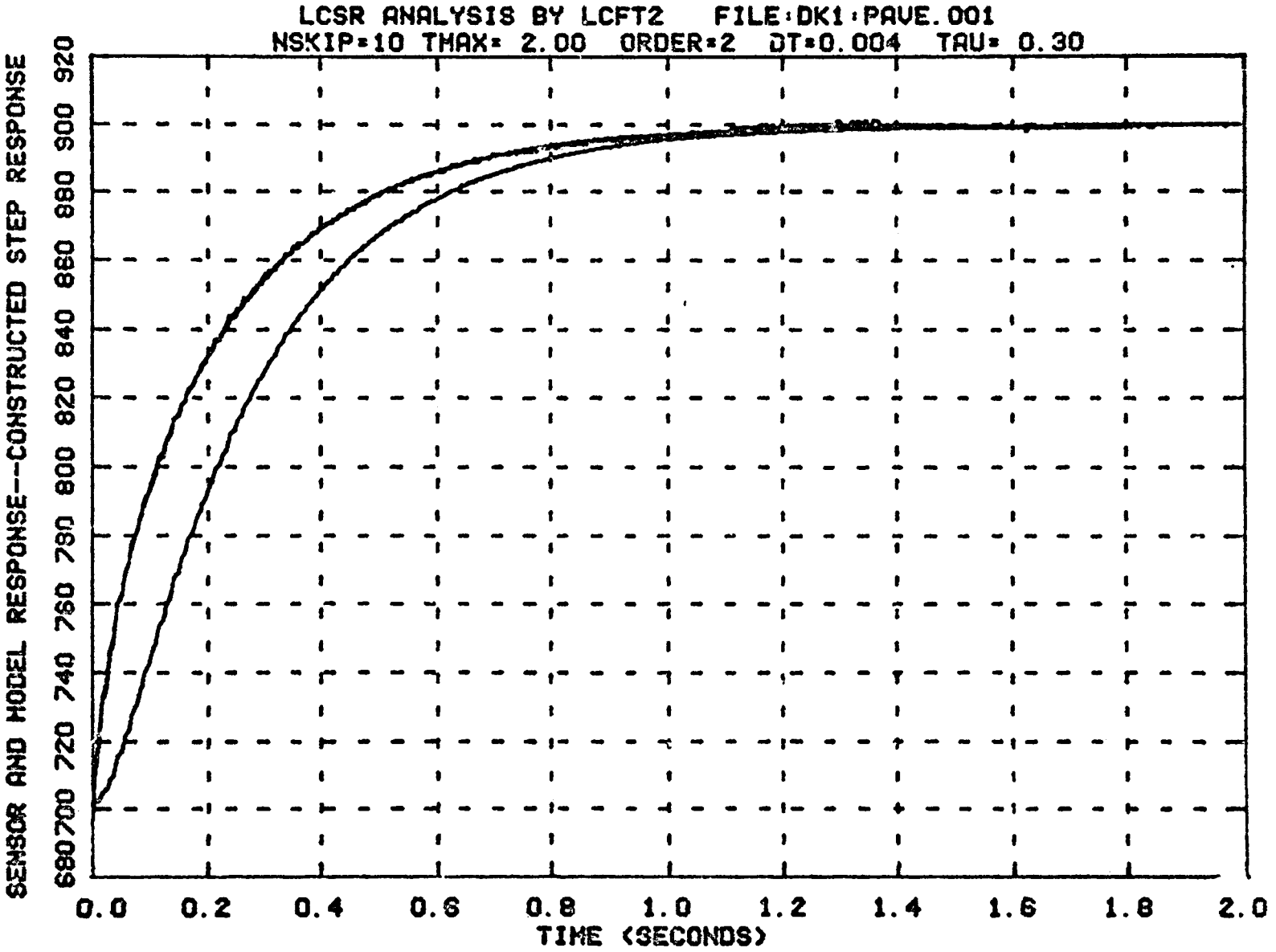

Figure B.4. Plot of Intermediate Analysis Result of a Typical LCSR Data Set

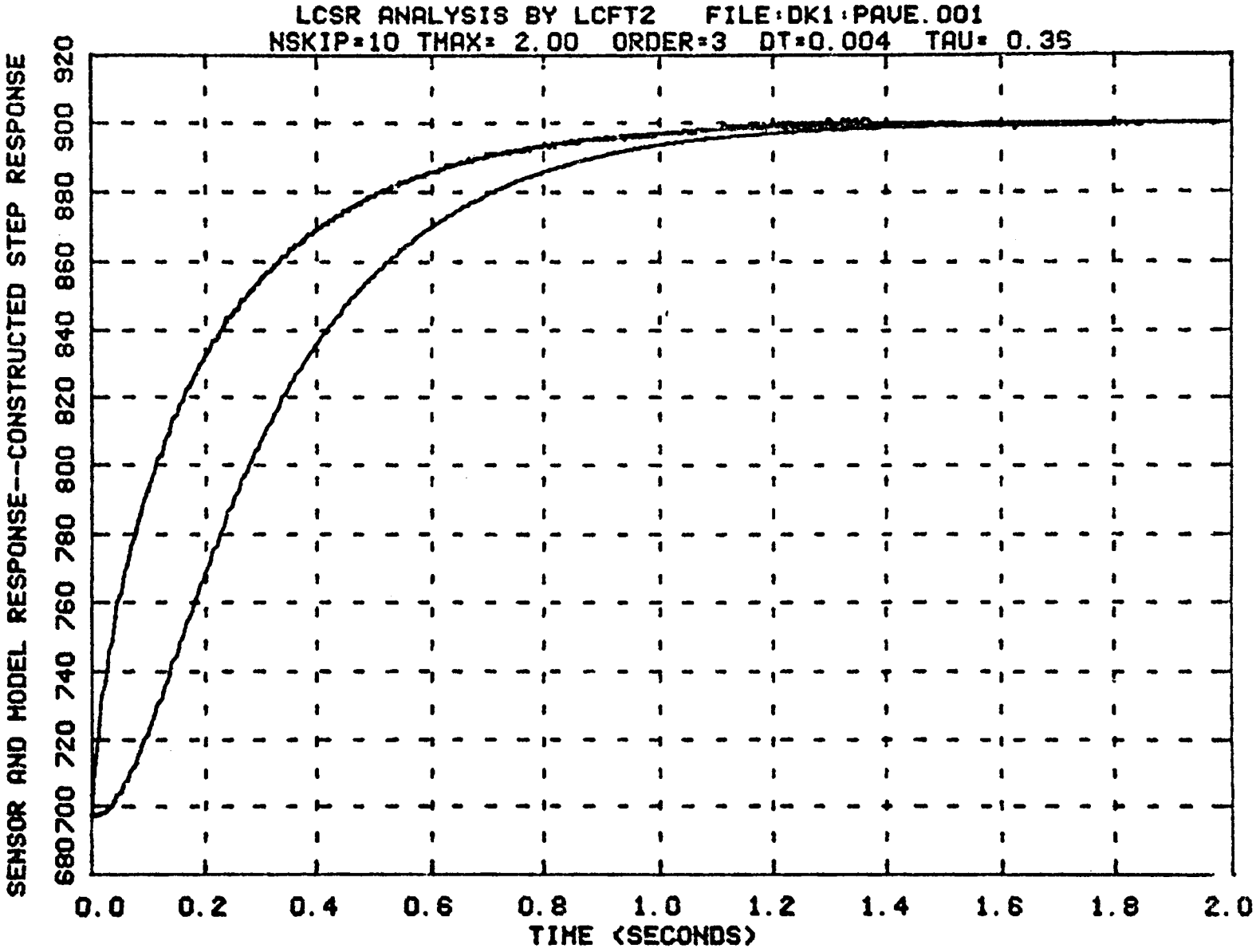

Figure B.5. Plot of Final Analysis Result of a Typical LCSR Data Set

```
      C-T  LCFT3.MUL
      C
      C-N  NOTE:  THIS VERSION OF DR. MILLER'S PROGRAM HAS BEEN MODIFIED TO
      C    RUN ON PDP 11 MINICOMPUTERS USING RT/11 FORTRAN.  ALSO THIS
      C    VERSION ASSUMES A CONSTANT SAMPLING RATE FOR THE DATA TO BE
      C    ANALYZED.  NO PLOTS ARE PRODUCED BY THIS VERSION.  SOME CORRECTIONS
      C    HAVE BEEN MADE TO THE ORIGINAL VERSION.  THESE CORRECTIONS HAVE
      C    BEEN INCLUDED IN THIS VERSION.  SUBROUTINE GTDAT HAS BEEN INCORPORATED
      C    INTO THIS VERSION SO THAT THE PROGRAM WILL HANDLE LCSR DATA AS
      C    STORED ON THE PDP 11.  THIS VERSION HAS BEEN MODIFIED TO RUN
      C    MULTIPLE CASES WHILE VARYING THE STARTING POINT  AND KEEPING TMAX
      C    CONSTANT.  THE TIME CONSTANT, THE UNCERTAINTY IN THE TIME CONSTANT,
      C    AND THE STANDARD DEVIATION OF THE RESIDUALS ARE OUTPUT TO A  DISK
      C    FILE.  THESE RESULTS MAY BE RETRIEVED AND PLOTTED BY TIMPLT.
      C
      C*************************************************************************
      C*************************************************************************
      C*************************************************************************
      C  THIS PROGRAM IDENTIFIES PARAMETERS OF AN EXPONENTIAL MODEL THAT
      C  APROXIMATES THE LOOP-CURRENT-STEP-RESPONSE(LCSR) DATA.  THE OVERALL
      C  PROGRAM LOGIC IS AS FOLLOWS:
      C   1. CONDUCT A DIRECT SEARCH FOR A STARTING POINT
      C   2. MINIMIZE THE VARIANCE OF THE RESIDUAL ERROR
      C   3. ESTIMATE THE STANDARD DEVIATION OF THE 63% RESPONSE TIME FROM
      C      THE VARIANCE-COVARIANCE MATRIX
      C*************************************************************************
0001          DIMENSION YG(2048),WORK(2048),X(7),Y(7),A(7,7),AIV(7,7),
             1 ASAV(7,7),P(7),G(7),WK(7),DIR(7),PSAV(7)
0002          INTEGER*2 JTEMP(100)
0003          LOGICAL*1 DSNAME(14),RSNAME(14)
0004          WRITE (7,3000)
0005     3000 FORMAT(' ENTER THE LCSR DATA FILE NAME : ',$)
0006          READ (5,3010) DSNAME
0007     3010 FORMAT (14A1)
0008          WRITE (7,2000)
0009     2000 FORMAT (' ENTER THE FILE NAME FOR THE RESULTS : ',$)
0010          READ (5,3010) RSNAME
0011          CALL ASSIGN(10,RSNAME,14,'OLD','NC',1)
0012          DEFINE FILE 10(100,6,U,JLOOK)
0013          WRITE (7,3020)
0014     3020 FORMAT (' ENTER 0 TO RUN SECOND ORDER CASES ONLY,'
            1 ' ENTER 1 TO RUN SECOND AND THIRD ORDER CASES : ',$)
0015          READ (5,3030) NEXP
0016     3030 FORMAT (I2)
0017          WRITE (7,1080)
0018     1080 FORMAT (' ENTER DTN, TMAX : ',$)
0019          READ (5,1090) DTN,TMAX
0020     1090 FORMAT (2F10.0)
0021          WRITE (7,1020)
0022     1020 FORMAT (' ENTER THE NUMBER OF CASES TO BE RUN : ',$)
0023          READ (5,1030) NCASES
0024     1030 FORMAT (I6)
0025          DO 10 I=1,NCASES
0026     30    WRITE (7,1040) I
```

```
0027   1040  FORMAT (' ENTER JSKIP(',I3,') : ',$)
0028         READ (5,1050) JTEMP(I)
0029   1050  FORMAT (I6)
0030         IF (JTEMP(I) .GE. 0) GO TO 20
0032         WRITE (7,1060)
0033   1060 FORMAT (' JSKIP MUST BE GREATER THAN OR EQUAL'
          1 ' TO ZERO!  TRY AGAIN!')
0034         GO TO 30
0035   20    IF (JTEMP(I) .LT. 100) GO TO 10
0037         WRITE (7,1070)
0038   1070  FORMAT (' JSKIP MUST BE LESS THAN 100!  TRY AGAIN!')
0039         GO TO 30
0040   10    CONTINUE
0041        NCASE=0
0042   100   NCASE=NCASE+1
0043        JSKIP=JTEMP(NCASE)
0044        DT=DTN
0045        TL=TMAX
0046         ND=7
0047         NOUT=50
0048         NMAX=10
0049         NSRH=16
0050         NCMX=2
0051         EPS=1.E-4
0052         TAU=1.0
      C*************************************************************************
      C  READ THE INPUT DATA FROM THE FILE SPECIFIED BY THE USER.
      C  NOMX: NUMBER OF OBSERVATIONS
      C  NEXP: IF SET TO 1, A THREE EXPONENTIAL CALCULATION IS PERFORMED
      D      PAUSE 'CALL GTDAT'
0053         CALL GTDAT(YO,WORK,NO,DT,T0,TL,DSNAME,JSKIP)
      D      PAUSE 'RETURN FROM GTDAT'
      D      WRITE (7,2010) NO
0054    2010 FORMAT (2X,I6)
0055         NOMX=NO
      C*************************************************************************
      C  CONDUCT A DIRECT SEARCH TO ESTIMATE A STARTING  POINT
0056         AR=1.0
0057         IOPT=0
0058         NX=2
0059         RHO=0.0
0060         FMIN=1.0E+12
0061         NV=2*NX+1
0062         BU=TAU*5.0
0063         BL=TAU*0.2
0064         RTO=(BU/BL)**(1.0/FLOAT(NSRH-1))
0065         NLP=NSRH
0066         DO 40 I=1,NLP
0067        CALL XSTOP
0068         P(4)=-BU/AR
0069         P(5)=P(4)*7.0
0070         IER=0
0071         CALL FUNCT(NO,NX,ND,A,X,Y,P,DT,YO,IOPT,IER,FVAL)
0072         IF(IER.EQ.0)GO TO 35
```

```
0074          PRINT 1013, IER
0075  1013    FORMAT('0',' ERROR IN THE COEFFICIENT CALCULATION, IER=',I5)
0076          STOP
0077  35      CONTINUE
0078          AR=AR*RTO
0079          IF(FVAL.GE.FMIN)GO TO 40
0081          FMIN=FVAL
0082          CALL VECDP(NV,RHO,P,WK,DIR)
0083  40      CONTINUE
0084          CALL VECDP(NV,RHO,WK,P,DIR)
      C*************************************************************************
      C  PRINT RESULTS OF THE DIRECT SEARCH
0085          EIG1=P(4)
0086          EIG2=P(5)
0087          CALL TAUA(TAU,EIG1,EIG2)
0088          PRINT 1000
0089          FVAL=FMIN
0090          PRINT 1001, FVAL,TAU,P(1),P(2),P(3),P(4),P(5)
0091  1000    FORMAT('0',' RESULTS OF THE DIRECT SEARCH:')
0092  1001    FORMAT('0',' THE FUNCTIONAL VALUE       = ',3X,E12.5/
             1' ',' THE TIME CONSTANT           = ',3X,E12.5/
             2' ',' THE EXPANSION COEFFICIENTS = ',3(3X,E12.5)/
             3' ',' THE EIGENVALUES             =  ',2(3X,E12.5))
      C*************************************************************************
      C  MINIMIZE THE RESIDUAL VARIANCE
0093          NX=2
0094  50      CONTINUE
0095          PRINT 1003, NX
0096  1003    FORMAT('0',' THE FOLLOWING RESULTS PERTAIN TO AN '/
             1 ' APPROXIMATING MODEL WITH ',I2,' EXPONENTIALS:'/)
0097          CALL LNR(NO,NX,ASAV,P,ND,WK,DIR,A,X,Y,YO,EPS,NMAX,NOUT,
             1 NOPT,FMIN,FVAL,DT,NLOOPS)
0098          PRINT 1004
0099  1004    FORMAT('0',' RESULTS FROM THE MINIMIZATION ALGORITHM:'/)
0100          PRINT 1010, NOPT
0101  1010    FORMAT(' ',' TERMINATED BY, NOPT = ',I2)
0102  60      CONTINUE
0103          CALL SWAP(NX,WK,P)
      C*************************************************************************
      C  CALCULATE THE STANDARD DEVIATIONS OF THE ESTIMATED PARAMETERS AND OF
      C  THE 63% TIME CONSTANT
0104          CALL TSD(A,ASAV,AIV,X,Y,YO,P,ND,NO,NX,DT,TAU,JSKIP,NEXP)
0105          IF(NEXP.NE.1)GO TO 70
0107          P(NV+2)=3.0*P(NV)
0108          P(NV+1)=P(NV)
0109          P(NV)=P(NV-1)
0110          NX=NX+1
0111          IF(NX.GT.3)GO TO 70
0113          IOPT=0
0114          CALL FUNCT(NO,NX,ND,A,X,Y,P,DT,YO,IOPT,IER,FVAL)
0115          FMIN=FVAL
0116          IF(IER.EQ.0)GO TO 65
0118          PRINT 1013,IER
0119  65      CONTINUE
```

```
0120          GO TO 50
0121   70     CONTINUE
0122         IF (NCASE .NE. NCASES) GO TO 100
0124    333  FORMAT ('0****  EXECUTION COMPLETE  ****')
0125          STOP
0126          END
```

```
      C*****************************************************************
      C*****************************************************************
0001          SUBROUTINE DRCHK(DIR,P,NX,RHO,WK,ITST)
0002          DIMENSION DIR(1),P(1),WK(1)
      C*****************************************************************
      C  THIS SUBROUTINE ENSURES THAT THE EIGENVALUES FOR THE SEARCH POINTS
      C  ARE ALWAYS NEGATIVE.
      C*****************************************************************
0003          NX2=NX+2
0004          NV=2*NX+1
0005          ITST=0
0006          TST=ABS(RHO)
0007          DO 10 K=NX2,NV
0008          IF(RHO.GT.0.0.AND.DIR(K).LE.0.0)GO TO 10
0010          IF(RHO.LT.0.0.AND.DIR(K).GE.0.0)GO TO 10
0012          TERM=ABS(P(K)/DIR(K))
0013          IF(TERM.GT.TST)GO TO 10
0015          TST=TERM
0016    10    CONTINUE
0017          TERM=ABS(RHO)
0018          IF(TST.LT.TERM) ITST=1
0020          IF(ITST.EQ.1)RHO=RHO*0.7*TST/TERM
0022          RETURN
0023          END
```

```
      C*******************************************************************
      C*******************************************************************
0001          SUBROUTINE FUNCT(NO,NX,ND,A,X,Y,P,DT,YO,IOPT,IER,FVAL)
0002          DIMENSION A(ND,ND),Y(1),P(1),YO(1),X(1),AE(10),R(10)
      C*******************************************************************
      C  THIS SUBROUTINE CALCULATES THE FUNCCTIONAL TO BE MINIMIZED  WHICH IS
      C  THE APPROXIMATE VARIANCE OF THE RESIDUALS.
      C  THE OPTIMUM EXPANSION COEFFICIENTS ARE CALCULATED.
      C*******************************************************************
0003          IF (IOPT .NE. 0) GO TO 40
      C  CALCULATE THE OPTIMUM EXPANSION COEFFICIENTS
0005          CALL COF(NO,NX,ND,A,X,Y,DT,YO,P,IER)
0006          IF (IER .NE. 0) GO TO 30
      C*******************************************************************
      C  EVALUATE THE FUNCTIONAL
0008    40    CONTINUE
0009          NX1=NX+1
0010          SUM=0.0
0011          DO 20 I=1,NX1
0012           AE(I)=P(I)
0013    20     SUM=SUM+AE(I)
0014          FVAL=(YO(1)-SUM)**2
0015          DO 25 I=1,NX
0016    25     R(I)=EXP(DT*P(NX1+I))
0017          DO 10 K=2,NO
0018           SUM=AE(1)
0019           DO 15 I=2,NX1
0020             AE(I)=AE(I)*R(I-1)
0021    15       SUM=SUM+AE(I)
0022    10     FVAL=FVAL+(SUM-YO(K))**2
0023          ANO=NO-(2*NX+1)
0024          FVAL=FVAL/ANO
0025    30    CONTINUE
0026           RETURN
0027           END
```

```
      C*****************************************************************
      C*****************************************************************
0001          SUBROUTINE COF(NO,NX,ND,A,X,Y,DT,YO,P,IER)
0002          DIMENSION A(ND,ND),X(1),Y(1),YO(1),P(1)
      C*****************************************************************
      C  THIS SUBROUTINE EVALUATES THE OPTIMUM EXPANSION COEFFICIENTS BY A
      C  LINEAR LEAST SQUARES ALGORITHM
      C*****************************************************************
      C  CALCULATE THE COEFFICIENT MATRIX
0003          A(1,1)=NO
0004          NX1=NX+1
0005          DO 20 I=1,NX1
0006          DO 20 J=I,NX1
0007          EX=P(NX+I)+P(NX+J)
0008          IF(J.EQ.1)GO TO 20
0010          IF(I.EQ.1)EX=P(NX+J)
0012         R=EXP(EX*DT)
0013         AL=EXP(EX*DT*FLOAT(NO-1))
0014         A(I,J)=(R*AL-1.)/(R-1.0)
0015    20    CONTINUE
0016          DO 25 I=2,NX1
0017          DO 25 J=1,I
0018    25    A(I,J)=A(J,I)
      C  COMPUTE THE INHOMOGENEOUS VECTOR
0019         Y(1)=0.0
0020         DO 45 I=1,NO
0021     45   Y(1)=Y(1)+YO(I)
0022          DO 30 I=2,NX1
0023          Y(I)=0.0
0024          XR=P(NX+I)
0025         FAC=1.0
0026         R=EXP(XR*DT)
0027          DO 30 K=1,NO
0028         XT=FAC
0029         FAC=FAC*R
0030    30    Y(I)=Y(I)+XT*YO(K)
      C  CHECK FOR A ZERO DIAGONAL ELEMENT
0031          IER=0
0032          DO 35 K=1,NX1
0033          IF(ABS(A(K,K)).GT.1.0E-12)GO TO 35
0035          IER=1
0036          GO TO 50
0037    35    CONTINUE
      C  CALCULATE THE EXPANSION COEFFICIENTS
0038          CALL GAUS(A,Y,X,ND,NX1)
0039          DO 40 I=1,NX1
0040    40    P(I)=X(I)
0041    50    CONTINUE
0042          RETURN
0043          END
```

```
      C*************************************************************************
      C*************************************************************************
0001          FUNCTION FAPR(P,NX,TM)
0002          DIMENSION P(1)
      C*************************************************************************
      C  THIS FUNCTION SUBROUTINE EVALUATES THE APPROXIMATING FUNCTION AT
      C  A SPECIFIED TIME
      C*************************************************************************
0003          NX1=NX+1
0004          FX=P(1)
0005          DO 10 I=2,NX1
0006    10    FX=FX+P(I)*EXP(P(NX+I)*TM)
0007          FAPR=FX
0008          RETURN
0009          END
```

```
      C*************************************************************************
      C*************************************************************************
0001          SUBROUTINE VECDP(K,RHO,X,Y,DIR)
0002          DIMENSION X(1),Y(1),DIR(1)
      C*************************************************************************
      C  THIS SUBROUTINE CALCULATES THE COORDINATES OF A POINT THAT LIES A
      C  SPECIFIED DISTANCE IN A SPECIFIED DIRECTION FROM A K-DIMENSIONAL
      C  VECTOR
      C*************************************************************************
0003          DO 10 I=1,K
0004    10    Y(I)=X(I)+RHO*DIR(I)
0005          RETURN
0006          END
```

```
      C*******************************************************************************
      C*******************************************************************************
0001          SUBROUTINE TAUA(TAU,E1,E2)
      C*******************************************************************************
      C  THIS SUBROUTINE CALCULATES THE APPROXIMATE TIME CONSTANT(63%) FROM
      C  AN ANALYTICAL EXPRESSION USING TWO EIGENVALUES.
      C*******************************************************************************
0002          TAU=(ALOG(1.00-E1/E2)-1.0)/E1
0003          RETURN
0004          END
```

```
      C*****************************************************************
      C*****************************************************************
0001        SUBROUTINE TSG(A,ASAV,AIV,X,Y,YO,P,ND,NO,NX,DT,TAU,
           1 JSKIP,NEXP)
0002        DIMENSION A(ND,1),ASAV(ND,ND),AIV(ND,1),X(1),Y(1),YO(1),
           1 P(1)
      C*****************************************************************
      C  THIS SUBROUTINE CALCULATES THE FOLLOWING:
      C     1. STANDARD DEVIATIONS OF THE MODEL PARAMETERS USING THE
      C        VARIANCE-COVARIANCE MATRIX
      C     2. AN ESTIMATE OF THE TIME CONSTANT USING AN ANALYTICAL
      C        EXPRESSION
      C     3. AN ESTIMATE OF THE STANDARD DEVIATION OF THE TIME CONSTANT
      C        USING THE VARIANCE-COVARIANCE MATRIX AND THE PROPAGATION OF
      C        ERROR FORMULA
      C*****************************************************************
      C  INPUT DATA REQUIRED BY THIS SUBROUTINE ARE AS FOLLOWS:
      C     1. THE NUMBER OF OBSERVARIONS
      C     2. UNBIASED PARAMETER ESTIMATES FROM THE LCSR MINIMIZATION
      C        PROGRAM
      C        (ITEMS 1. AND 2. ARE READ UNDER THE FILENAME 'TVDAT')
      C     3. OBSERVATION DATA AND TIME VALUES ASSOCIATED WITH THE
      C        OBSERVATION DATA
      C        (ITEM 3. IS READ FROM THE FILE SPECIFIED BY THE USER.  THIS IS
      C        THE SAME FILE USED BY THE LCSR MINIMIZATION PROGRAM)
      C*****************************************************************
0003        NV=2*NX+1
      C  CALCULATE THE MATRIX:  Z TRANSPOSE Z WHICH WILL BE INVERTED TO
      C  OBTAIN THE VARIANCE-COVARIANCE MATRIX
0004        CALL ZTZ(NO,NX,A,P,DT,ND)
      C  INVERT THE Z TRANSPOSE Z MATRIX TO OBTAIN THE VARIANCE-
      C  COVARIANCE MATRIX
0005        IER=0
0006        N=NV
0007        CALL INV(A,AIV,ASAV,X,Y,ND,N,IER)
0008        IF(IER.EQ.0)GO TO 30
0010        PRINT 1005, IER
0011  1005  FORMAT(' ',' A ZERO DIAGONAL ELEMENT WAS ENCOUNTERED '/
           1'       IER = ',I5)
0012  30    CONTINUE
      C*****************************************************************
      C  ESTIMATE THE STANDARD DEVIATIN AND THE EXPECTED VALUE OF THE
      C  RESIDUAL ERROR.  ALSO CALCULATE THE NORMALIZED GRADIENT.
0013        CALL VAR(P,NX,NO,DT,YO,NV,STD,EXV)
0014        AR=STD**2
0015        CALL GRAD(NO,NX,YO,P,DT,X,GRD)
0016        GRD=GRD/AR
0017        PRINT 1006, EXV,STD,AR,GRD
0018  1006  FORMAT('0',' EXPECTED VALUE OF RESIDUAL          = ',E12.5/
           1 '   STANDARD DEVIATION OF THE RESIDUAL = ',E12.5/
           2 '   VARIANCE OF THE RESIDUAL           = ',E12.5/
           3 '   THE NORMALIZED GRADIENT            = ',E12.5)
      C*****************************************************************
      C  CALCULATE THE STANDARD DEVIATIONS OF THE EXPANSION COEFFICIENTS
```

```
      C  AND OF THE EIGENVALUES
0019          DO 40 K=1,NV
0020          Y(K)=AIV(K,K)*STD**2
0021          XA=ABS(Y(K))
0022  40      Y(K)=SQRT(XA)
0023          NX1=NX+1
0024          PRINT 1007, (P(K),Y(K),K=1,NX1)
0025  1007    FORMAT('0','  EXPANSION COEFFICIENTS ARE: '/
             1 (' ',5X,E12.5,' + OR - ',E12.5))
0026          PRINT 1008,(P(NX1+K),Y(NX1+K),K=1,NX)
0027  1008    FORMAT('0','  EIGENVALUES ARE: '/
             1 (' ',5X,E12.5,' + OR - ',E12.5))
      C*************************************************************************
      C  CALCULATE THE TIME CONSTANT AND THE STANDARD DEVIATION OF THE
      C  TIME CONSTANT
0028          SG1=Y(NX1+1)
0029          SG2=Y(NX1+2)
0030          CALL TVAR(SG1,SG2,TAU,TSIG,P,NX)
0031          PRINT 1009, TAU,TSIG
0032  1009    FORMAT('0','  THE TIME CONSTANT = ',E12.5,' + OR - ',E12.5)
0033         IF (NX .EQ. 3) GO TO 50
0035         IF (NEXP .EQ. 1) RETURN
0037   50    IREC=JSKIP+1
0038         WRITE(10'IREC) STD,TAU,TSIG
0039          RETURN
0040          END
```

```
      C*********************************************************************
      C*********************************************************************
0001          SUBROUTINE GRAD(NO,NX,YO,P,DT,G,GRD)
0002          DIMENSION YO(1),P(1),G(1)
      C*********************************************************************
      C  THIS SUBROUTINE EVALUATES THE GRADIENT OF THE FUNCTIONAL WITH
      C  RESPECT TO EACH PARAMETER AND EVALUATES THE NORM OF THE GRADIENT.
      C*********************************************************************
0003          NV=2*NX+1
0004          DO 5 J=1,NV
0005    5     G(J)=0.0
0006          DO 15 K=1,NO
0007          TM=FLOAT(K-1)*DT
0008          RID=FAPR(P,NX,TM)-YO(K)
0009          G(1)=G(1)+RID
0010          DO 10 I=2,NV
0011          K1=I
0012          CALL DRV(K1,NX,TM,P,DIV)
0013   10     G(I)=G(I)+RID*DIV
0014   15     CONTINUE
0015          AT=2.0/FLOAT(NO-NV)
0016          DO 20 K=1,NV
0017   20     G(K)=G(K)*AT
0018          GRD=0.0
0019          DO 30 K=1,NV
0020   30     GRD=GRD+G(K)**2
0021          RETURN
0022          END
```

```
      C*****************************************************************
      C*****************************************************************
0001          SUBROUTINE DRV(K,NX,T,P,FVAL)
0002          DIMENSION P(1)
      C*****************************************************************
      C  THIS SUBROUTINE CALCULATES THE PARTIAL DERIVATIVES OF THE
      C  APPROXIMATING FUNCTION WITH RESPECT TO EACH OF THE MODEL PARAMETERS
      C  THE EXPANSION COEFFICIENTS ARE IN THE FIRST NX1 ELEMENTS OF THE
      C  P VECTOR AND THE EIGENVALUES ARE IN THE LAST NX ELEMENTS OF THE
      C  VECTOR.
      C*****************************************************************
0003          NX1=NX+1
0004          IF(K.GT.1)GO TO 10
0006          FVAL=1.0
0007          GO TO 30
0008  10      CONTINUE
0009          IF(K.GT.NX1)GO TO 20
0011          FVAL=EXP(T*P(NX+K))
0012          GO TO 30
0013  20      CONTINUE
0014          FVAL=P(K-NX)*T*EXP(T*P(K))
0015  30      CONTINUE
0016          RETURN
0017          END
```

```
      C*********************************************************************
      C*********************************************************************
0001          SUBROUTINE INV(A,AIV,ASAV,X,Y,ND,N,IER)
0002          DIMENSION A(ND,ND),AIV(ND,ND),ASAV(ND,ND),X(1),Y(1)
      C*********************************************************************
      C  THIS SUBROUTINE CALCULATES THE INVERSE BY REPEATED CALLS TO A
      C  LINEAR EQUATION SOLVER WHHICH USES DIRECT GAUSSIAN ELIMINATION.
      C  THUS, NONE OF THE DIAGONAL ELEMENTS CAN BE ZERO.  A CHECK IS
      C  MADE FOR ZERO DIAGONAL ELEMENTS EVEN THOUGH NONE SHOULD BE ZERO.
      C*********************************************************************
      C  TEST FOR ZERO DIAGONAL ELEMENTS
0003          DO 2 K=1,N
0004          IF(ABS(A(K,K)).GT.1.0E-12)GO TO 2
0006          IER=1
0007          GO TO 30
0008  2       CONTINUE
0009          NS=0
0010  10      NS=NS+1
      C  GENERATE THE APPROPRIATE UNIT VECTOR
0011          DO 15 K=1,N
0012          Y(K)=0.0
0013          IF(K.EQ.NS)Y(K)=1.0
0015  15      CONTINUE
0016          DO 16 I=1,N
0017          DO 16 J=1,N
0018  16      ASAV(I,J)=A(I,J)
0019          CALL GAUS(ASAV,Y,X,ND,N)
0020          DO 20 I=1,N
0021  20      AIV(I,NS)=X(I)
0022          IF(NS.LT.N)GO TO 10
0024  30      CONTINUE
0025          RETURN
0026          END
```

```
      C*****************************************************************
      C*****************************************************************
0001          SUBROUTINE GAUS(A,Y,X,ID,N)
0002          DIMENSION A(ID,ID),Y(1),X(1)
      C*****************************************************************
      C  THIS SUBROUTINE SOLVES A SET OF LINEAR EQUATIONS BY DIRECT ELININATION
      C*****************************************************************
0003          M=N-1
0004          DO 10 I=1,M
0005          L=I+1
0006          DO 10 J=L,N
0007          IF(A(J,I))6,10,6
0008    6     DO 8 K=L,N
0009    8     A(J,K)=A(J,K)-A(I,K)*A(J,I)/A(I,I)
0010          Y(J)=Y(J)-Y(I)*A(J,I)/A(I,I)
0011   10     CONTINUE
0012          X(N)=Y(N)/A(N,N)
0013          DO 30 I=1,M
0014          K=N-I
0015          L=K+1
0016          DO 20 J=L,N
0017   20     Y(K)=Y(K)-X(J)*A(K,J)
0018          X(K)=Y(K)/A(K,K)
0019   30     CONTINUE
0020          RETURN
0021          END
```

```
      C*****************************************************************
      C*****************************************************************
0001          SUBROUTINE VAR(P,NX,NO,DT,YO,NV,SUM,EXVAL)
0002          DIMENSION P(1),YO(1)
      C*****************************************************************
      C  THIS SUBROUTINE ESTIMATES THE VARIANCE OF THE DATA FROM THE RESIDUALS.
      C  IT ALSO CALCULATES THE EXPECTED VALUE OF THE RESIDUALS
      C*****************************************************************
0003          NX1=NX+1
0004          EXVAL=0.0
0005          SUM=0.0
0006          DO 10 K=1,NO
0007          TM=FLOAT(K-1)*DT
0008          S1=P(1)
0009          DO 5 J=1,NX
0010    5     S1=S1+P(J+1)*EXP(P(NX1+J)*TM)
0011          EXVAL=EXVAL+YO(K)-S1
0012   10     SUM=SUM+(YO(K)-S1)**2
0013          ANO=NO
0014          EXVAL=EXVAL/ANO
0015          SUM=SUM/(ANO-NV)
0016          SUM=SQRT(SUM)
0017          RETURN
0018          END
```

```
      C*********************************************************************
      C*********************************************************************
0001          SUBROUTINE SWAP(NX,WK,P)
      C*********************************************************************
      C  THIS SUBROUTINE ORDERS THE EIGENVALUES AND ASSOCIATED EXPANSION
      C  COEFFICIENTS.  THE TIME CONSTANT CALCULATION AND TIME CONSTANT
      C  VARIANCE CALCULATION ASSUMES ORDEREDD EIGENVALUES AND EXPANSION
      C  COEFFICIENTS.
      C*********************************************************************
0002          DIMENSIONWK(1),P(1)
0003          NX1=NX+1
0004          NV=2*NX+1
0005          DO 20 I=1,NX
0006          ETST=-1.E+12
0007          DO 10 J=1,NX
0008          IF(P(NX1+J).LE.ETST)GO TO 10
0010          ETST=P(NX1+J)
0011          JSAV=J
0012    10    CONTINUE
0013          WK(I+NX1)=P(JSAV+NX1)
0014          P(JSAV+NX1)=-2.0E+12
0015          WK(I+1)=P(JSAV+1)
0016    20    CONTINUE
0017          DO 30 I=2,NV
0018    30    P(I)=WK(I)
0019          RETURN
0020          END
```

```
      C*********************************************************************
      C*********************************************************************
0001          SUBROUTINE TVAR(SG1,SG2,TAU,TSIG,P,NX)
0002          DIMENSION P(1)
      C*********************************************************************
      C  THIS SUBROUTINE CALCULATES THE TIME CONSTANT USING THE FIRST TWO
      C  (ORDERED) EIGENVALUES IN AN ANALYTICAL EXPRESSION.  THE STANDARD
      C  DEVIATION IS CALCULATED USING THE PROPAGATION OF ERROR FORMULA
      C*********************************************************************
0003          NX1=NX+1
0004          X1=P(NX1+2)
0005          X2=P(NX1+1)
0006          X3=X1-X2
0007          X4=X3/X1
0008          IF (NX .NE. 3) GO TO 10
0010          X5=P(NX1+3)
0011          X6=X3/X5
0012    10        TAU=(ALOG(X4)-1.)/X2
0013          IF (NX .EQ. 3) TAU=TAU+ALOG(1.0-X6)/X2
0015          DV1=-(1./X3+TAU)/X2
0016          DV2=1./(X1*X3)
0017          SIG2=SG1*DV1**2+SG2*DV2**2
0018          TSIG=SQRT(SIG2)
0019          RETURN
0020          END
```

```
      C*********************************************************************
      C*********************************************************************
      C*********************************************************************
0001        SUBROUTINE GTDAT(Y,IWRK,NOP,DTN,T0,TMAX,DSNAME,JSKIP)
      C
      C-F   THIS SUBROUTINE OBTAINS THE LCSR DATA FROM THE DATA FILE
      C     SPECIFIED BY THE USER AND PLACES IT THE PROPER ARRAY FOR
      C     ANALYSIS.
0002        LOGICAL*1 LNM(9),THEAD(64),DSNAME(14)
0003        DIMENSION IWRK(4096),Y(2048)
0004        CALL ASSIGN(1,DSNAME,14,'OLD','NC',1)
0005        DEFINE FILE 1(1,6291,U,IWO)
0006        READ(1'1,ERR=20,END=20) THEAD,LNM,RL,NO,ITN,
           ?    (IWRK(K),K=1,4096)
0007  20    CONTINUE
0008        DT=RL/FLOAT(NO)
0009        T0=FLOAT(JSKIP)*DT
0010        IF(NO .GT. 4096) NO=4096
0012        CALL CLOSE(1)
0013        RL=FLOAT(NO-1)*DT
0014        NP=IFIX(TMAX/DTN+0.99)
0015        IF(NP .LE. 2048) GO TO 100
0017        WRITE(7,60)
0018  60    FORMAT('0***** TOO MANY POINTS--TMAX MODIFIED *****')
0019        TMAX=2048.0*DTN
0020        NP=IFIX(TMAX/DTN+0.99)
0021  100   ISKIP=IFIX(DTN/DT+0.99)
0022        IF(ISKIP .LE. 0) ISKIP=1
0024        DT0=FLOAT(ISKIP)*DT
0025        NPTS0=IFIX(TMAX/DT0)
0026        IF(NPTS0 .GT. 2048) NPTS0=2048
0028        IF(NPTS0*ISKIP+19 .GT. NO) NPTS0=(NO-19)/ISKIP
0030        DO 200 I=1,NPTS0
0031        J=(I-1)*ISKIP+1+19+JSKIP
0032  200   Y(I)=FLOAT(IWRK(J))
0033        DTN=DT0
0034        NOP=NPTS0
0035        RETURN
0036        END
```

```
      C*****************************************************************
      C*****************************************************************
      C*****************************************************************
0001          SUBROUTINE LNR(NO,NX,ASAV,P,ND,WK,DIR,A,X,Y,YO,EPS,NMAX,
     1    NOUT,NOPT,FMIN,FVAL,DT,NS)
0002          DIMENSION ASAV(ND,ND),P(1),WK(1),DIR(1),A(ND,1),X(1),
     1    Y(1),YO(1),F(7),R(7)
      C*************************************************************************
      C  THIS SUBROUTINE USES THE LINEARIZATION METHOD IN CONJUNCTION WITH
      C  A CONSTANT STEP SIZE.  SINCE THE COEFFICIENT MATRIX FOR CALCULATING
      C  THE SEARCH DIRECTION IS POSITIVE DEFINITE THE DIRECTION VECTOR
      C  SHOULD ALWAYS BE IN A DIRECTION THAT DECREASES THE FUNCTIONAL.  BY
      C  DETERMINING THE OPTIMUM STEP SIZE, THIS MINIMIZATION ALGORITHM
      C  SHOULD ALWAYS CONVERGE.
      C*************************************************************************
0003          NV=2*NX+1
0004          NOLSS=0
0005          FOLD=FVAL
0006          ZRO=0.0
0007         NOPT=-1
0008          NS=0
0009  5       NS=NS+1
0010          IOPT=0
0011          IF((NS/2)*2.EQ.NS)IOPT=1
      C*************************************************************************
      C  CALCULATE THE SEARCH DIRECTION
0013  10      CONTINUE
0014          CALL ZTZ(NO,NX,ASAV,P,DT,ND)
0015          DO 15 I=1,NV
0016  15      Y(I)=0.0
0017          DO 20 K=1,NO
0018          TM=FLOAT(K-1)*DT
0019          RID=YO(K)-FAPR(P,NX,TM)
0020          DO 20 I=1,NV
0021          K1=I
0022          CALL DRV(K1,NX,TM,P,DR)
0023  20      Y(I)=Y(I)+RID*DR
0024          CALL GAUS(ASAV,Y,DIR,ND,NV)
      C*************************************************************************
      C  DETERMINE THE OPTIMUM STEP SIZE
0025          NFAIL=0
0026          ISA=1
0027          RHO=1.0
0028  25      CONTINUE
      C  VERIFY THAT THE SEARCH POINT DOES NOT INCLUDE A POSITIVE EIGENVALUE
0029          CALL DRCHK(DIR,P,NX,RHO,WK,ISET)
0030          CALL VECDP(NV,RHO,P,WK,DIR)
0031  30      IER=0
0032          CALL FUNCT(NO,NX,ND,A,X,Y,WK,DT,YO,IOPT,IER,FVAL)
0033          IF(IER.EQ.0)GO TO 40
0035          IOPT=1
0036          GO TO 30
0037  40      CONTINUE
0038         FTST=FVAL*(1.+EPS)
```

```
0039          IF(FTST.GE.FMIN.AND.ISA.EQ.1)GO TO 45
0041         IF (FVAL .GT. 1.01*FMIN .AND. ISA .NE. 3) GO TO 42
      C  EXTEND THE LINE SEARCH UNTIL THE FUNCTIONAL VALUE IS INCREASED
0043         IF (FVAL .GE. FMIN) GO TO 41
0045          RSAV=RHO
0046          FMIN=FVAL
0047          CALL VECDP(NV,ZRO,WK,R,DIR)
0048    41    CONTINUE
0049          IF(ISA.EQ.3)GO TO 50
0051         IF (ISET .EQ. 1 .AND. ISA .NE. 1) GO TO 50
0053          ISA=2
0054          RHO=RHO*1.618
0055          GO TO 25
0056    42    CONTINUE
      C  CALCULATE THE OPTIMUM STEP SIZE USING A QUADRATIC APPROXIMATION
0057          ISA=3
0058          Y1=FMIN-FOLD
0059          Y2=FVAL-FOLD
0060          DET=RSAV*RHO**2-RHO*RSAV**2
0061          A1=(Y1*RHO**2-Y2*RSAV**2)/DET
0062          B1=(RSAV*Y2-RHO*Y1)/DET
0063          RHO=-0.5*A1/B1
0064          GO TO 25
      C  IF THE FUNCTIONAL IS NOT LOWERED, THE INTERVAL IS HALVED NMAX
      C  TIMES.
0065    45    NFAIL=NFAIL+1
0066         IF (NFAIL .GT. 2) IOPT=1
0068          RHO=RHO*0.5
0069          IF(NFAIL.LE.NMAX)GO TO 25
0071         NOLSS=NOLSS+1
0072          GO TO 60
      C*************************************************************************
      C  CHECK CONVERGENCE
0073    50    CALL VECDP(NV,ZRO,R,P,DIR)
0074          PCT=(FOLD-FMIN)/FOLD
0075         IF (PCT .LT. EPS) NOLSS=NOLSS+1
0077         IF (PCT .GE. EPS) NOLSS=0
0079          CALL GRAD(NO,NX,YO,P,DT,X,GRD)
0080         IF (GRD .LT. 10.0*EPS*FMIN) NOPT=0
0082    60    CONTINUE
0083          PRINT 1000, NS,FMIN,FOLD
0084    1000  FORMAT(' ',' NEW AND OLD FUNCTIONAL VALUES FOR ITERATION ',I2/
             1 '      ARE  ',E12.5,'  AND  ',E12.5)
0085          FOLD=FMIN
0086         CALL XSTOP
0087         IF (NOLSS .GE. 2) NOPT=1
0089         IF (NS .GE. NOUT) NOPT=2
0091         IF (NOPT .LT. 0) GO TO 5
0093    70    CONTINUE
0094          RETURN
0095          END
```

```
      C*******************************************************************************
      C*******************************************************************************
0001          SUBROUTINE ZTZ(NO,NX,A,P,DT,ND)
0002          DIMENSION A(ND,ND),P(1)
      C*******************************************************************************
      C  THIS SUBROUTINE CALCULATES THE SQUARE MATRIX NEEDED TO INVERT
      C  TO OBTAIN THE VARIANCE-COVARIANCE MATRIX
      C*******************************************************************************
0003          NV=2*NX+1
0004         NX1=NX+1
0005         NX2=NX+2
0006         XNOP1=FLOAT(NO+1)
0007         XNO=FLOAT(NO)
0008         XNOM1=FLOAT(NO-1)
0009         A(1,1)=XNO
0010         DO 10 I=1,NX1
0011          DO 10 J=I,NX1
0012            IF (J .EQ. 1) GO TO 10
0014            X=P(NX+J)
0015            IF (I .EQ. 1) GO TO 20
0017            X=X+P(NX+I)
0018   20       R=EXP(DT*X)
0019            RL=EXP(DT*X*XNO)
0020            A(I,J)=(RL-1.0)/(R-1.0)
0021   10       CONTINUE
0022         DO 30 I=1,NX1
0023          DO 30 J=NX2,NV
0024            X=P(J)
0025            IF (I .EQ. 1) GO TO 40
0027            X=X+P(NX+I)
0028   40       R=EXP(DT*X)
0029            RL=EXP(DT*X*XNO)
0030            RL1=EXP(DT*X*XNOP1)
0031            A(I,J)=(1.0+XNOM1*RL)/(R-1.0)
0032            A(I,J)=A(I,J)-(RL-1.0)/(R-1.0)**2
0033            A(I,J)=A(I,J)*P(J-NX)*DT
0034   30      CONTINUE
0035         DO 50 I=NX2,NV
0036          DO 50 J=I,NV
0037            X=P(J)+P(I)
0038            R=EXP(DT*X)
0039            RL=EXP(DT*X*XNO)
0040            A(I,J)=2.0*(1.0+XNOM1*RL)/(R-1.0)
0041            A(I,J)=A(I,J)-2.0*(RL-1.0)/(R-1.0)**2
0042            A(I,J)=A(I,J)-(RL-1.0)/(R-1.0)
0043            A(I,J)=A(I,J)+1.0
0044            A(I,J)=A(I,J)-XNOM1**2*RL
0045            A(I,J)=A(I,J)*1.0/(1.0-R)
0046            A(I,J)=A(I,J)*DT*P(I-NX)*P(J-NX)*DT
0047   50       CONTINUE
0048         DO 70 I=1,NV
0049          DO 70 J=I,NV
0050   70       A(J,I)=A(I,J)
0051          RETURN
```

```
0052          END
```

```
      C*************************************************************************
      C*************************************************************************
      C*************************************************************************
0001        SUBROUTINE XSTOP
      C-T   SUBROUTINE XSTOP
      C
      C-F   THIS SUBROUTINE CHECKS TO SEE WHETHER A REQUEST TO HALT
      C     THE RUN HAS BEEN MADE.  IF THE REQUEST HAS BEEN MADE
      C     THE OUTPUT LIST FILE IS CLOSED AND EXECUTION TERMINATES
      C     NORMALLY.  THE REQUEST IS MADE BY TYPING THE CHARACTERS
      C     ST FOLLOWED BY A CARRIAGE RETURN ON THE TELETYPE.
0002        CALL TTYABT(ISTOP)
0003        IF (ISTOP .NE. 1) RETURN
0005        CALL CLOSE (10)
0006        STOP ' EXECUTION TERMINATED BY OPERATOR REQUEST'
0007        END
```

APPENDIX C

A TYPICAL IN-PLANT TEST PROCEDURE

A typical test procedure for performing a combined self heating, loop current step response test program is presented below. Of course, it is not necessary to perform both tests. However, they both use the same test equipment and the test duration is short for both methods, so it is probably advisable to perform both types of test during this stage of implementing the technology. This makes it possible to compare two independent results for each sensor and obtain added confidence in the results. All tests should be made at identical flow, temperature, and pressure conditions.

The actual test procedure for a particular plant will depend on the format used by the utility and by its policy for special tests. Consequently, the test procedure will need to be tailored somewhat for a specific plant.

The procedure does not address the question of how to modify the safety system logic during the test or special instructions for plant operators during the tests. These will have to be specific to the plant being tested.

The procedure is:

1. Set up the equipment as near as possible to the cabinet where the RTD leads are connected to the plant transmitters. The equipment includes:
   - The test instrument (bridge, switchable power supply, adjustable decade resistors, adjustable-gain amplifier to amplify the voltage drop across the bridge, and a

digital voltmeter that can monitor the amplifier output or can be switched to measure the voltage drop across a fixed bridge resistor to provide the current).

- an oscilloscope connected to the bridge amplifier output.
- a strip chart recorder connected to the bridge amplifier output.
- a data recording system (analog or digital) connected to the bridge amplifier output and to the current switch status (open or closed) indicator output.

2. Connect a spare RTD to the test instrument. The RTD should be immersed in water (in a bucket) to within two inches of the top connector on the RTD.
3. Turn on the power supply with the current selector switch set to LOW and the power supply voltage at its lowest setting.
4. Adjust the power supply to give 1-5 ma.
5. Balance the bridge (adjust the decade resistor until the bridge amplifier output goes to zero).
6. Check to be sure that the resistance is correct for the water temperature.
7. Switch the current selector switch to HIGH.
8. Adjust the power supply to give 60 ma (typical through the sensor).
9. Adjust the amplifier gain to give an output voltage that is suitable for the recording equipment.

10. Switch the current selector switch to LOW.
11. Wait until the bridge amplifier output settles out.
12. Turn on the strip chart recorder.
13. Switch the current selector switch to HIGH.
14. Wait until the bridge amplifier output settles out.
15. Measure the time required for the output to reach 63.2 percent of its total variation.
16. Compare this time with a reference value (obtained on previous tests on the same sensor in still water).
17. If the difference in times is more than fifteen percent, check equipment and procedure.
18. If the difference in times is less than fifteen percent, set the current selector switch to LOW.
19. Turn off the power supply.
20. Disconnect the spare RTD.
21. Remove the selected plant RTD leads from its in-plant transmitter.
22. Connect the in-plant RTD leads to the test instrument. If the RTD has more than two leads, select only one from each side of the filament.
23. Turn on the power supply and adjust to give 1-5 ma through the RTD.
24. Balance the bridge.
25. Check the noise level at the bridge amplifier output.
26. Set the power supply to its lowest value.
27. Switch the current selector switch to HIGH.

28. Start the self heating test. Increase the power supply voltage to give a current through the RTD of about 10 ma.
29. Wait until the bridge amplifier output settles out.
30. Rebalance the bridge.
31. Calculate the power dissipated in the RTD filament.
32. Record the resistance and power.
33. Repeat steps 23 through 32 for current values up to 60 ma (typical).
34. Plot resistance versus power on linear graph paper. If the data indicate a well-defined straight line, go to step 35. If the data indicate scatter, repeat steps 23 through 32 for more data points.
35. Start the Loop Current Step Response (LCSR) tests. Balance the bridge at low current then set the current selector switch to HIGH.
36. Set the power supply voltage to give a current of 60 ma (typical) through the RTD.
37. Adjust the amplifier gain to give an input voltage that is suitable for the recording equipment.
38. Set the current selector switch to LOW.
39. Wait for the bridge amplifier output to settle out.
40. Start the strip chart recorder and the data recording equipment.
41. Switch the current selector switch to HIGH.
42. Wait until the bridge amplifier output settles out.
43. Switch the current selector switch to LOW.
44. Determine the time required for the bridge amplifier

output from step 41 to reach 63.2 percent of its total variation from the strip chart recorder trace.

45. Plot the data from step 41 on semi-log paper and use the exponential peeling technique (see Appendix G) to estimate the time constant.
46. If the results obtained from steps 44 and 45 agree reasonably well with prior experience or with tests on other sensors of the same design, continue to step 47. If not, check equipment and procedures before continuing.
47. Repeat steps 38 through 43 at least five times (more for noisy or unstationary data).
48. Set the current selector switch to LOW.
49. Turn off the power supply.
50. Disconnect the sensor.
51. Repeat steps 22 through 50 for the next sensor to be tested.
52. Complete tests on all sensors.
53. Remove test equipment.

APPENDIX D

A METHOD FOR SMOOTHING THE LCSR TEST TRANSIENTS

A LCSR test transient is naturally smooth unless fluctuations in fluid temperature or flow occur during the collection of the test data. A method was developed to smooth the LCSR test transients that are contaminated with noise. Since small fluctuations in temperature and flow of the coolant of a nuclear power plant are expected, the LCSR test transients for installed RTDs may be contaminated with noise. Plant data should be smoothed before analysis for prediction of response time if this occurs. The method is based on averaging a set of the LCSR tests performed on a sensor. A program called LCSRAV* is available that takes a set consisting of several noise-contaminated LCSR data sets and constructs a smoothed average transient. The program uses the following procedures:

1. Determine the average value (T_{AVE}) of the steady state portion of the transient (the portion of the LCSR transient in which the output does not change with time). This is done by fitting a straight line through the data in the steady state region (see Figure D.1).
2. To compensate for the possible offsets that may occur from one test to another, an arbitrary level (T_C) is selected, the difference (D) between T_{AVE} and T_C is determined ($D = T_C - T_{AVE}$) and the transient is shifted by adding

---

*Program is written by Mr. J. E. Jones of the Nuclear Engineering Department of The University of Tennessee.

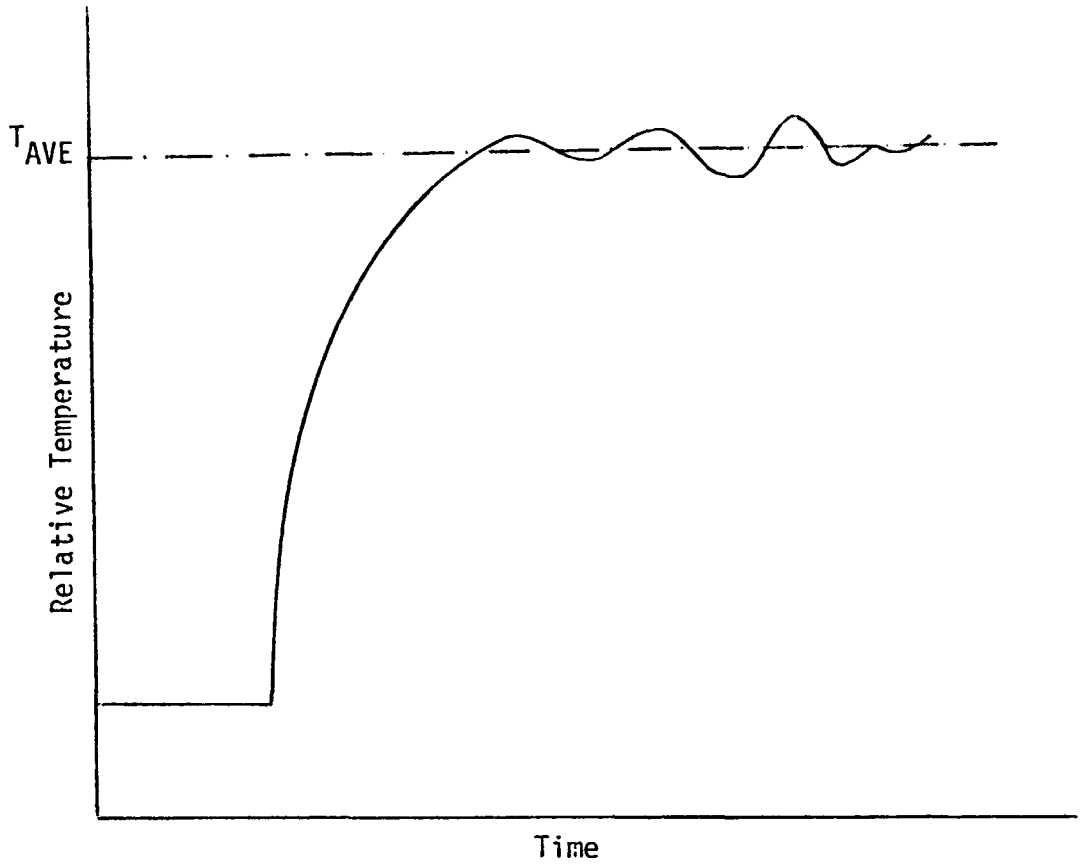

Figure D.1. A Noise Contaminated LCSR Test Output (Hypothetical Data).

D to each data point in the transient (see Figure D.2). This forces the data sets to have the same T_{AVE}. Since the correction is for possible offset rather than an amplitude scaling problem, an additive correction is used instead of a multiplicative factor.

3. Evaluate the average value of the response for each point on the reconstructed data sets. For example, if the value of the response at time = $t_o + \Delta t$ from the first, second and third data sets are 601, 602 and 603 respectively, the average value of the response at $t = t_o + \Delta t$ is equal to 602 (see Figure D.3).
4. Construct a transient from the average of each data point obtained in Step 3.

The smoothing algorithm is applicable only if:

1. The temperature of sensor surroundings has not changed during the LCSR tests.
2. The fluctuation of output is random.
3. The data set is sufficiently long to provide adequate data for evaluating the T_{AVE}.
4. Sufficient number of LCSR data sets are provided for a given sensor.

The capability of this procedure was evaluated by generating random noise on the LCSR test data and using the computer program to average a set of tests and provide a smooth transient. Figure D.4 shows a sample of a LCSR transient (for a Rosemount 176KF RTD) obtained

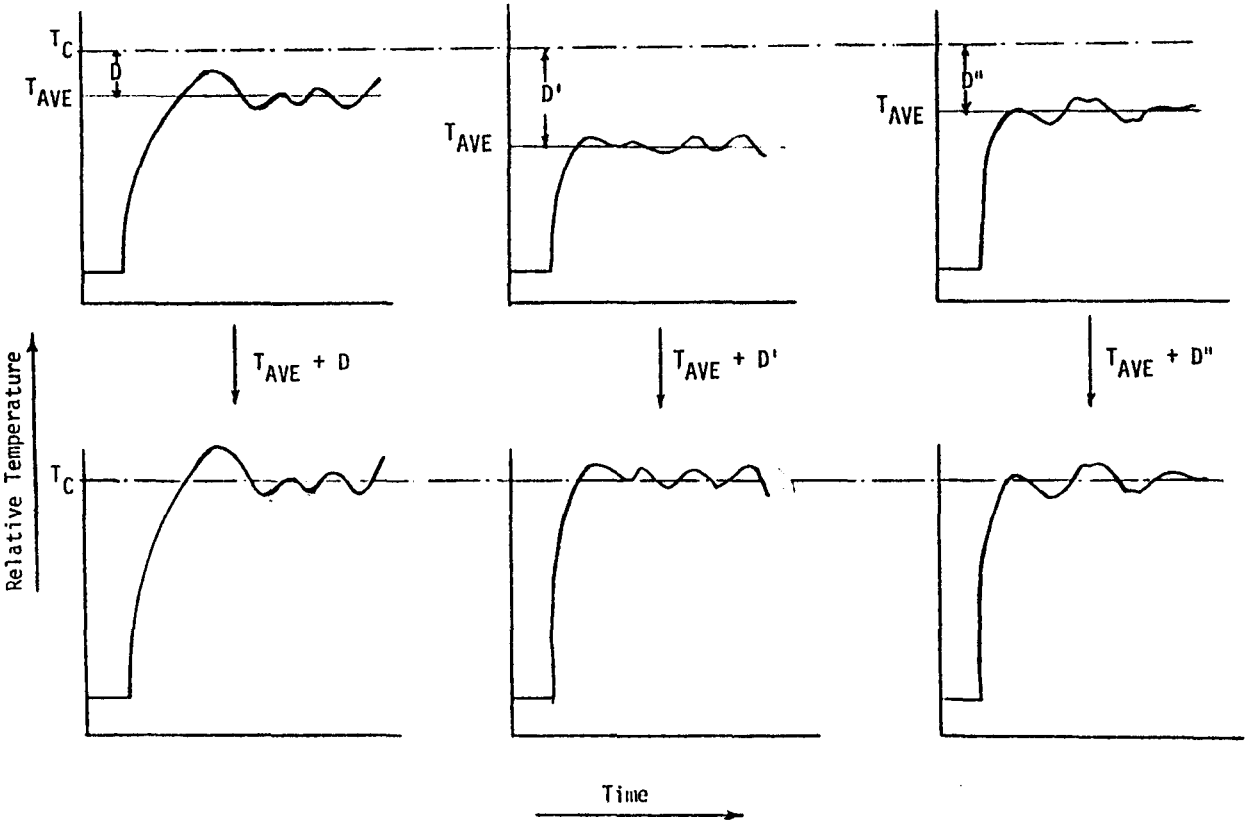

Figure D.2. Correction of LCSR Transient to Compensate for Possible Offsets (Hypothetical Data).

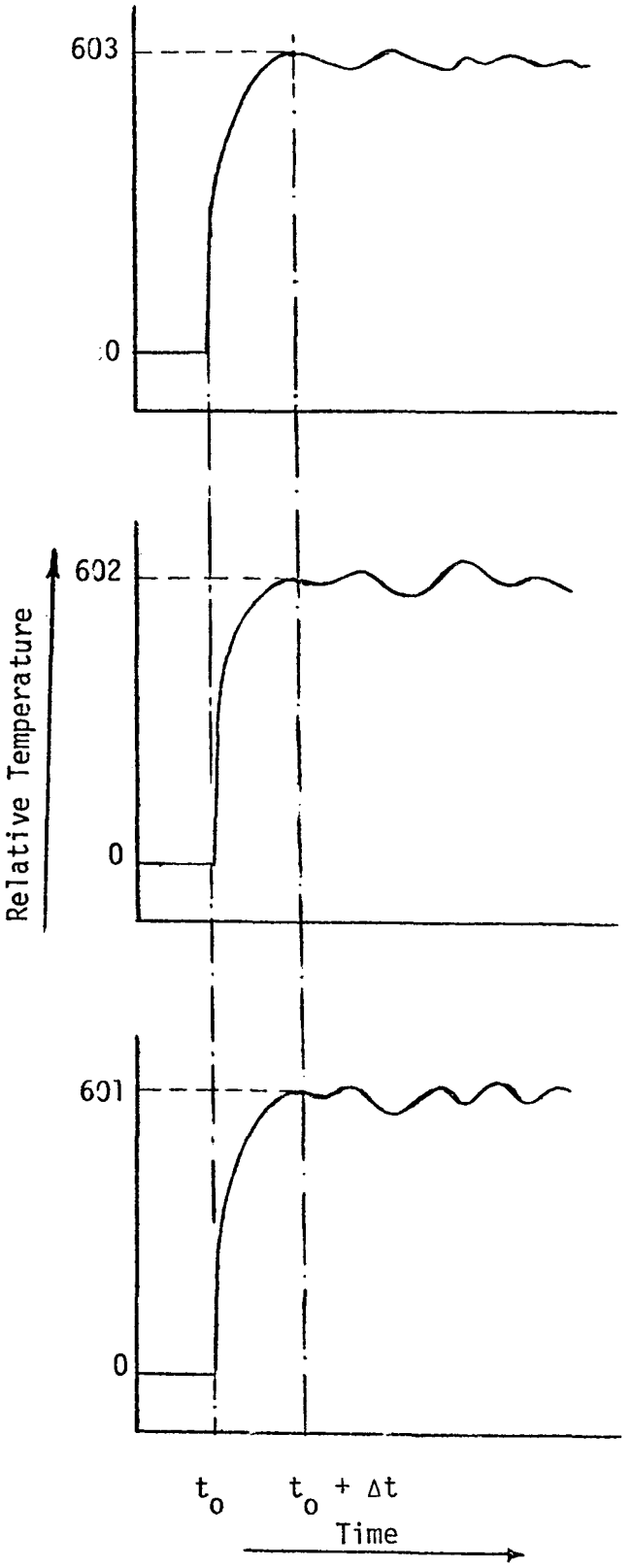

Figure D.3. Illustration of the Average Value of the LCSR Transient at a Time = $t_o + \Delta t$ (Hypothetical Data).

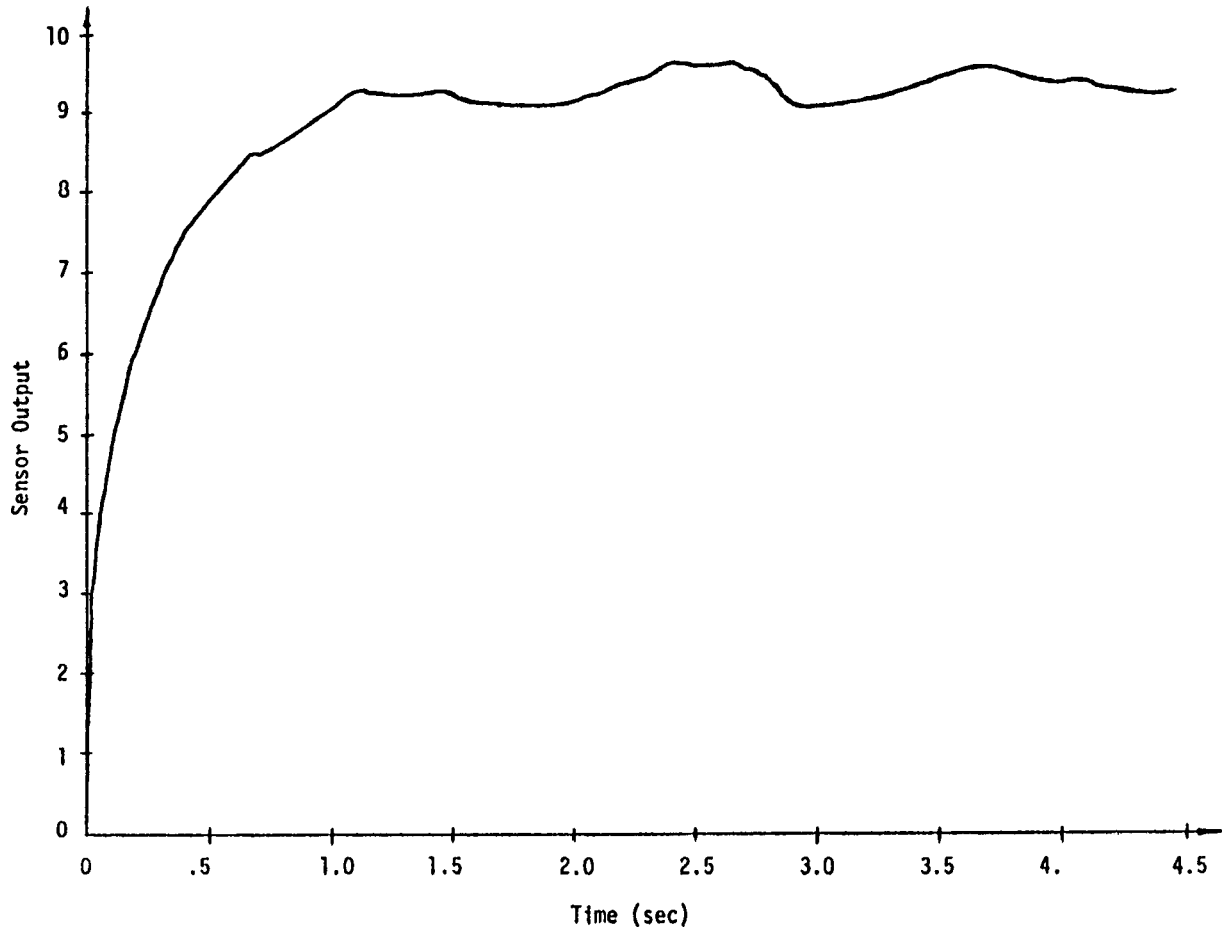

Figure D.4. A LCSR Test Data with Simulated Fluctuations (for Rosemount 176KF RTD).

by simulating random fluctuations on the data in the laboratory. The plot from the analysis of this data set is shown in Figure D.5. As indicated in this figure a time constant of .432 second is obtained from this data set for the sensor. This value compares with a time constant of .420 obtained from a plunge test in the same condition in the laboratory. Figure D.6 shows the smooth transient resulted from averaging 40 LCSR tests that had random fluctuations of the shape shown in Figure D.4. The plot from analysis of the smooth data set is given in Figure D.7. A time constant of about .422 second is obtained from this data set. This value compares with .432 second obtained from the contaminated data set and .420 from the plunge test.

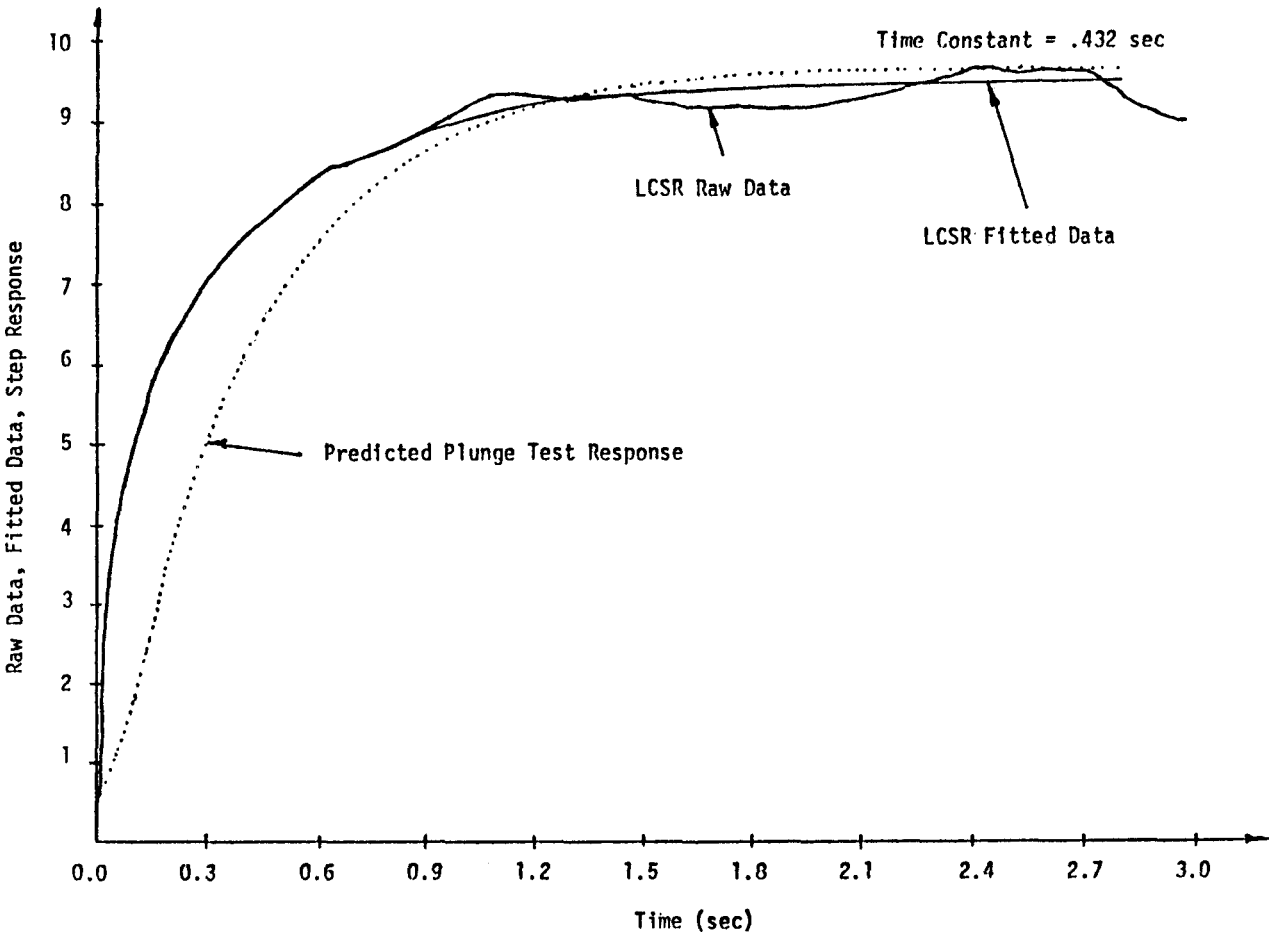

Figure D.5. Results of the Analysis of a Noise Contaminated LCSR Test Data (for Rosemount 176KF RTD).

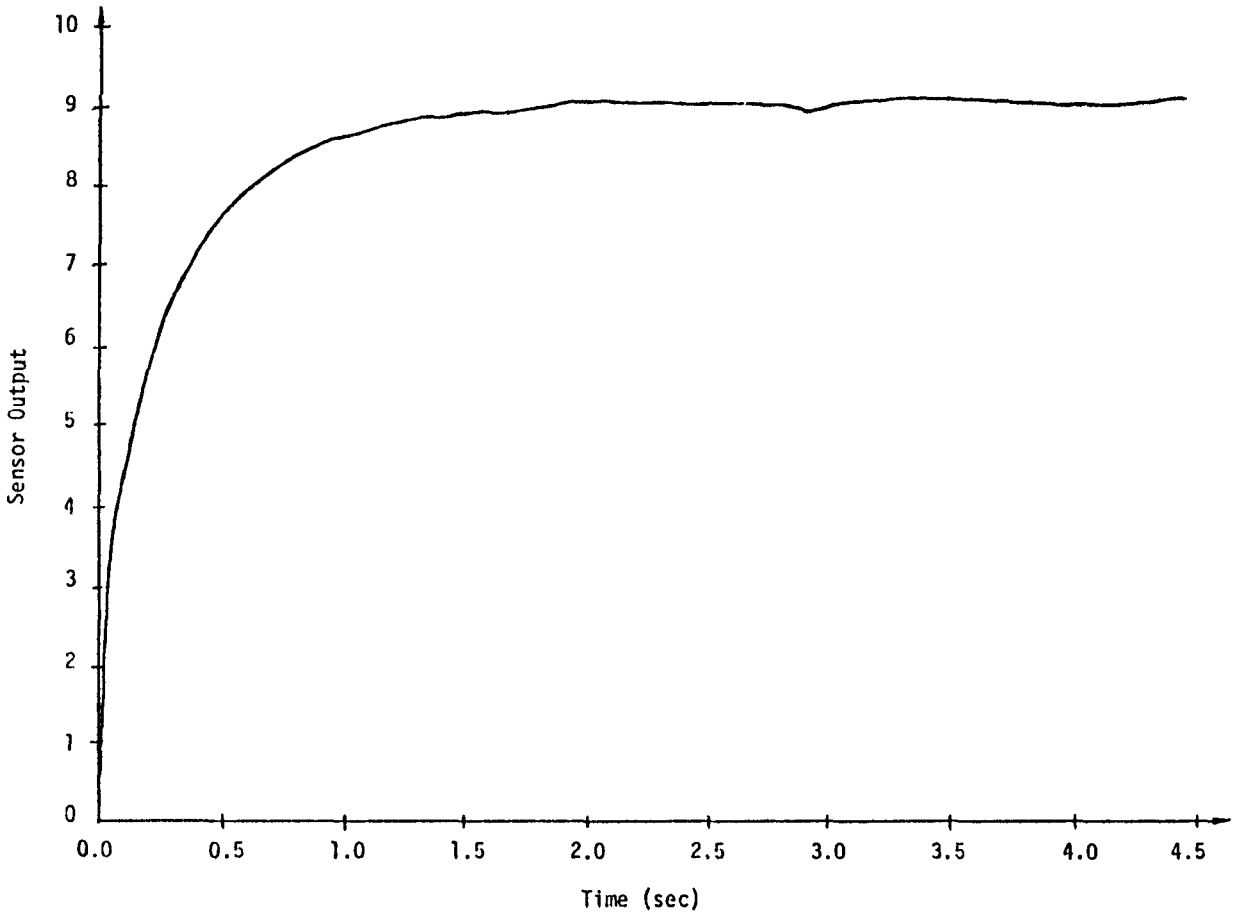

Figure D.6. A Smoothed LCSR Data Set (for Rosemount 176KF RTD).

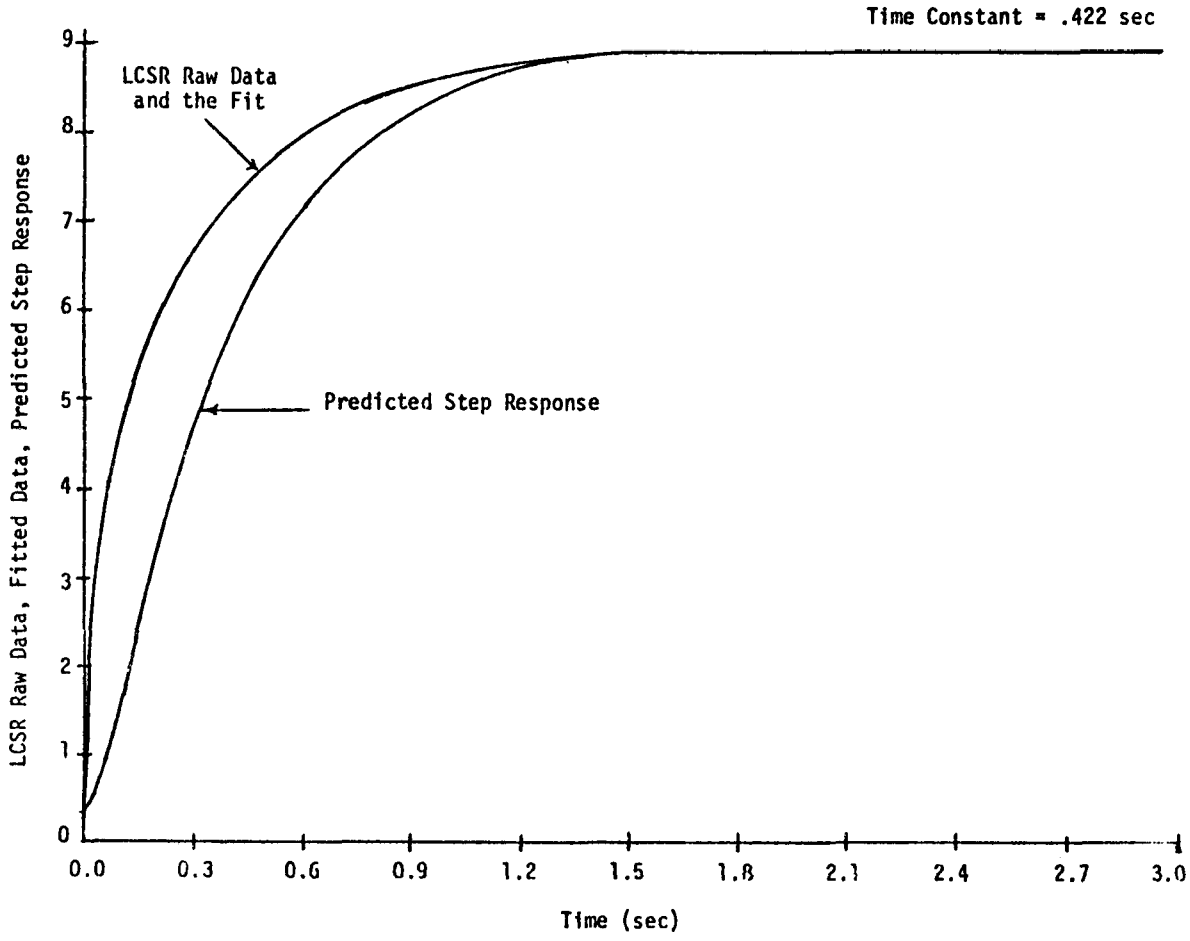

Figure D.7. Results of the Analysis of a Smoothed LCSR Test Data (for Rosemount 176KF RTD Tested at 2.5 ft/sec).

APPENDIX E

LABORATORY INSTRUMENTATION AND DATA ACQUISITION

E.1 Laboratory Facilities

A thermometry laboratory consisting of a rotating tank, response time test circuitry and recording facilities was established for evaluating the methods of in-situ response time testing of platinum resistance thermometers. The output signals from this equipment can be connected to a mini-computer system with remote access and control capability. A schematic of the response time test setup is given in Figure E.1. The components of this setup are described in the following sections.

E.1.1 Rotating Tank

The rotating tank consists of a drum of diameter = 22 inches and height = 13 inches. It is filled with water at room temperature to a depth of about 9 inches. A 1/12 HP motor rotates the drum to provide water velocities from zero at the center to 4 ft/sec at the edge of the drum. This system is shown in Figure E.2.

E.1.2 Measurement Circuit

A Wheatstone bridge with current switching capability is used for measuring the RTD response characteristics. The output of the bridge is amplified with a differential amplifier with adjustable gain. A potentiometer is included in the circuit to vary the output voltage of the power supply and provide a means for adjusting the current (see Figure E.3). For the variable resistance of the bridge, a seven-element decade box with a maximum resolution of .01 ohm is used. A

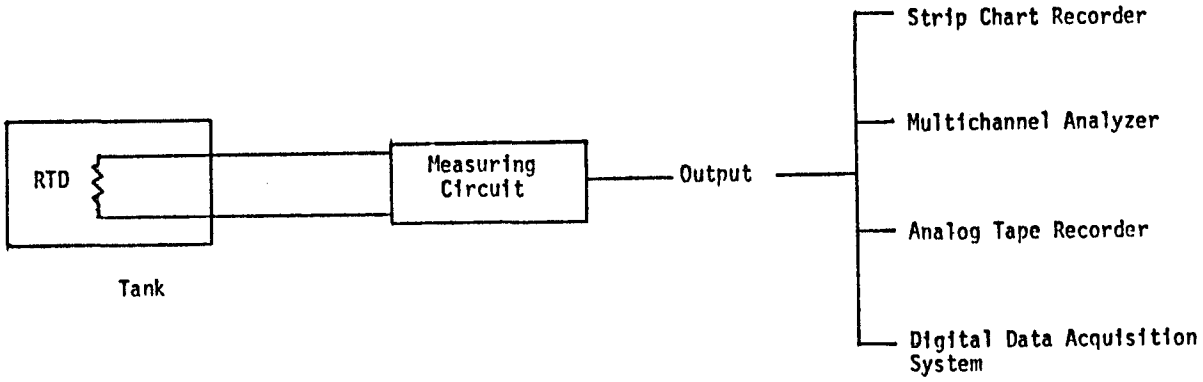

Figure E.1. Response Time Test Set Up.

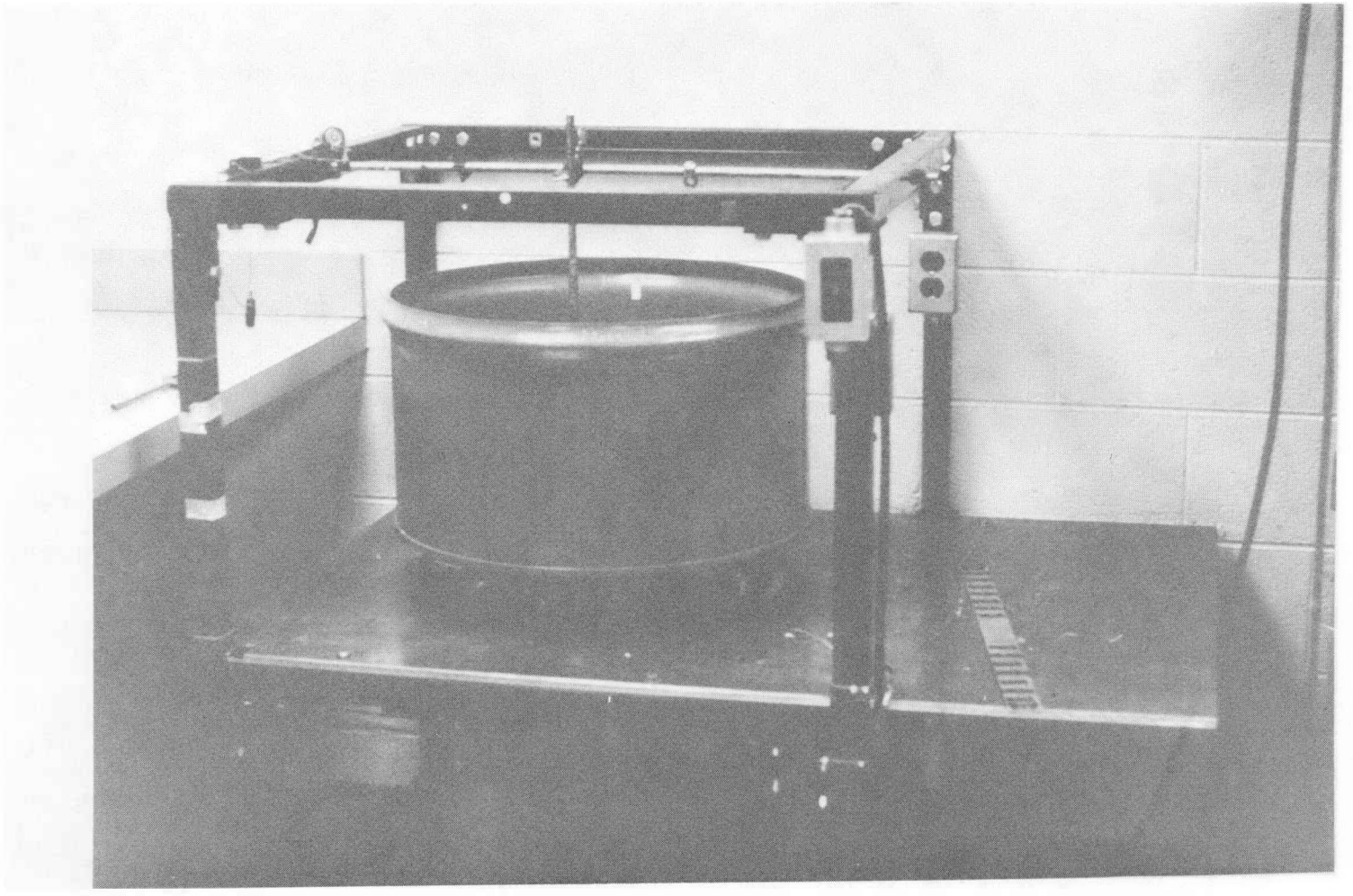

Figure E.2. Rotating Tank.

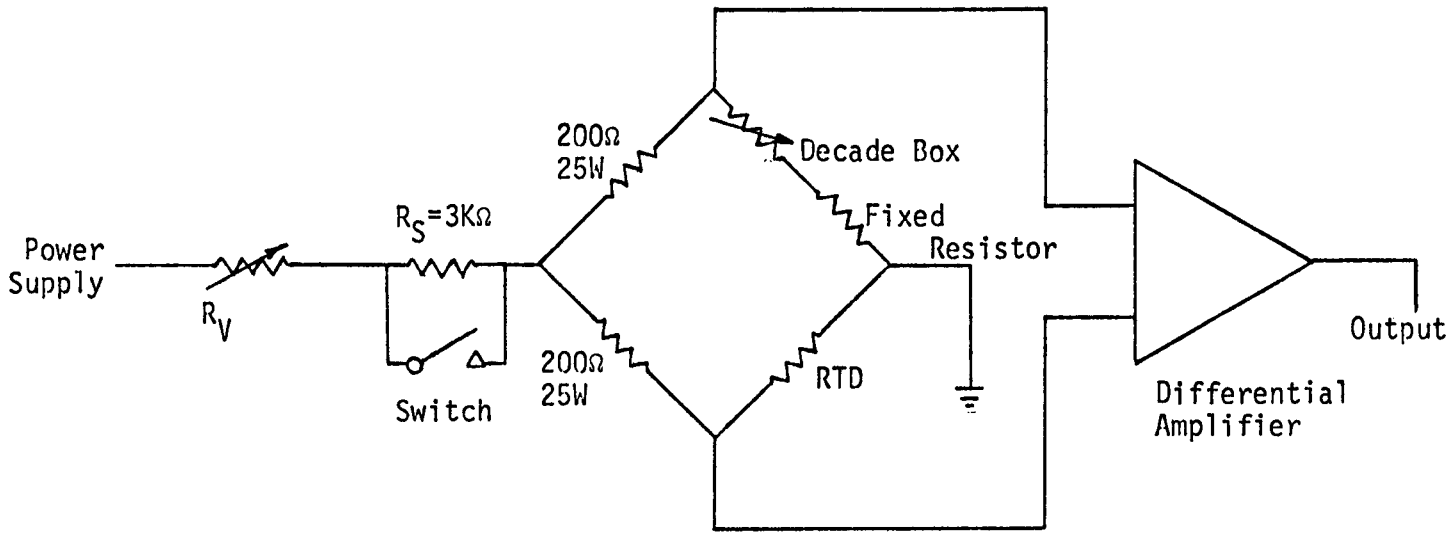

Figure E.3. Response Time Measuring Circuit.

fixed resistor with high current tolerance (high wattage resistor) is usually used in series with the decade box to avoid heating the elements of the decade box when large currents are passing through the bridge circuit. The fixed resistors of the bridge are 200 ohms with a rating of 25 watts to avoid heating due to high currents. A detailed diagram of the measuring circuit and specifications of its components are given in Appendix F.

E.1.3 Recording Devices

The transient data were recorded on one or more of the recording devices listed in Table E.1.

E.1.4 Miscellaneous Equipment

A list of miscellaneous equipment used during this work is given in Table E.2.

E.2 Data Collection Procedures

E.2.1 Plunge Test

Experimental Setup. The experimental setup for a plunge test is shown in Figure E.4. The sensor is held in air before being plunged into the rotating tank of water in a location where a desired water velocity is maintained. A step change in temperature is introduced either by plunging the sensor from room temperature air into warm water or by using a warm air blower to heat the sensor prior to immersion into the water at room temperature. A system was designed for dropping the sensor into the water in a manner to insure a minimum vibration of the sensor. The sensor drop assembly consists of a steel rod 7/8 inches in diameter

TABLE E.1

RECORDING INSTRUMENTS

Recording Device	Manufacturer	Model Number	Application In This Work
Strip Chart Recorder	Hewlett-Packard	7402A	Recording plunge and LCSR test transients
Multichannel Analyzer	Ino-Tech	IT-5200	Recording and Monitoring LCSR test output
Magnetic Tape Recorder	Ampex	PR-2200	Field Data Acquisition
Mini-Computer	Digital Equipment Corporation	PDP-11	Digital Data Acquisition

TABLE E.2

MISCELLANEOUS EQUIPMENT

Equipment	Manufacturer	Model Number
Power Supply (Adjustable Output)	Wanlass	Maverick II
Amplifier	University of Tennessee	100
	University of Tennessee	200
Digital Multimeter	Systron Donner	7004
	Hewlett-Packard	3476A
	Valballa Scientific	4440
	Sencore	37
Function Generator	Hewlett-Packard	3310A
Filter	Krohn-Hite	3323
Storage Display Unit	Tektronix	613
Computer Display Terminal	Tektronix	4006-1
Hard Copy Unit	Tektronix	4631
	Tektronix	4610
Computer Video Terminal	Digital Equipment Corp.	VT50

TABLE E.2 (continued)

Equipment	Manufacturer	Model Number
Line Printer	Centronics	101
	Digital Equipment Corp.	Decwriter II
	Versatec	1200A
Oscilloscope (with storage)	Tektronix	7633
	Hewlet-Packard	1220A
Teletype	Teletype Corp.	33TU
Voltage to Frequency Converter	University of Tennessee	NE

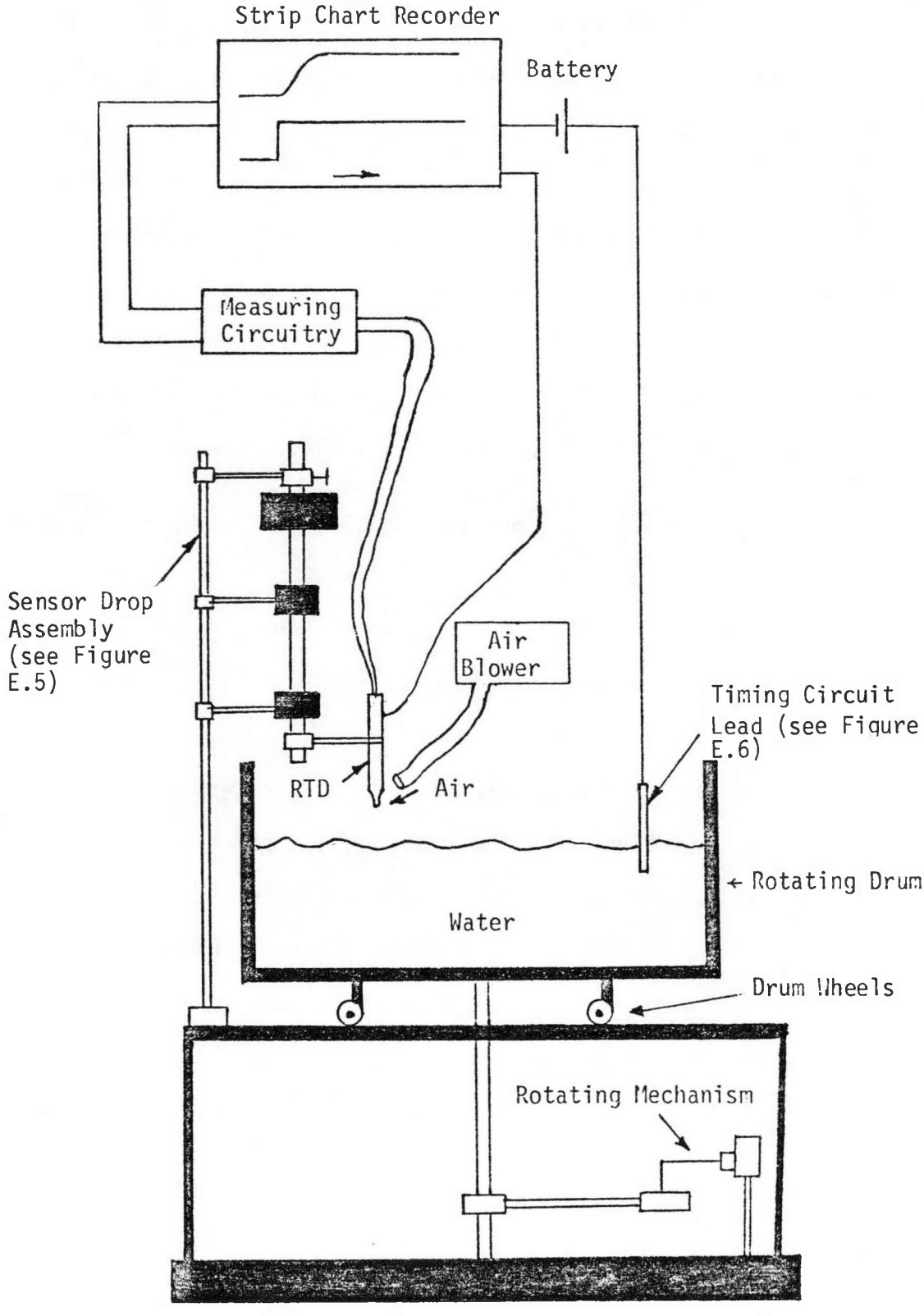

Figure E.4. Plunge Test Set Up.

and 20 inches in height with a holder to which the sensor is secured (see Figure E.5). The drop assembly falls into the water under gravitational force when a latch is removed. A cushion stop is used to reduce vibration. An adjustment can be made to stop the rod after a desired immersion depth is achieved. A timing circuit is provided in the setup to indicate the instant that the sensor touches the water. This circuit provides a timing signal using the conductivity of water to close a loop consisting of a battery and the recorder with connections to water and the body of the sensor (see Figure E.6).

Testing Procedures. The steps followed in performing a plunge test are:

1. Connect the RTD to the measuring circuit (keep the current switch on the low position).
2. Balance the bridge.
3. Adjust the output voltage of the power supply to give a low current level of 1 to 6 milliamperes.
4. Adjust the gain of the bridge amplifier and the gain of the chart amplifier* to obtain a useful output level.
5. Rebalance the bridge (if necessary).
6. Select a high chart speed (25 mm/sec or 125mm/sec) to be able to obtain an accurate measurement of response time.

---

*The strip chart recorder used in this study has a built-in amplifier with adjustable gain.

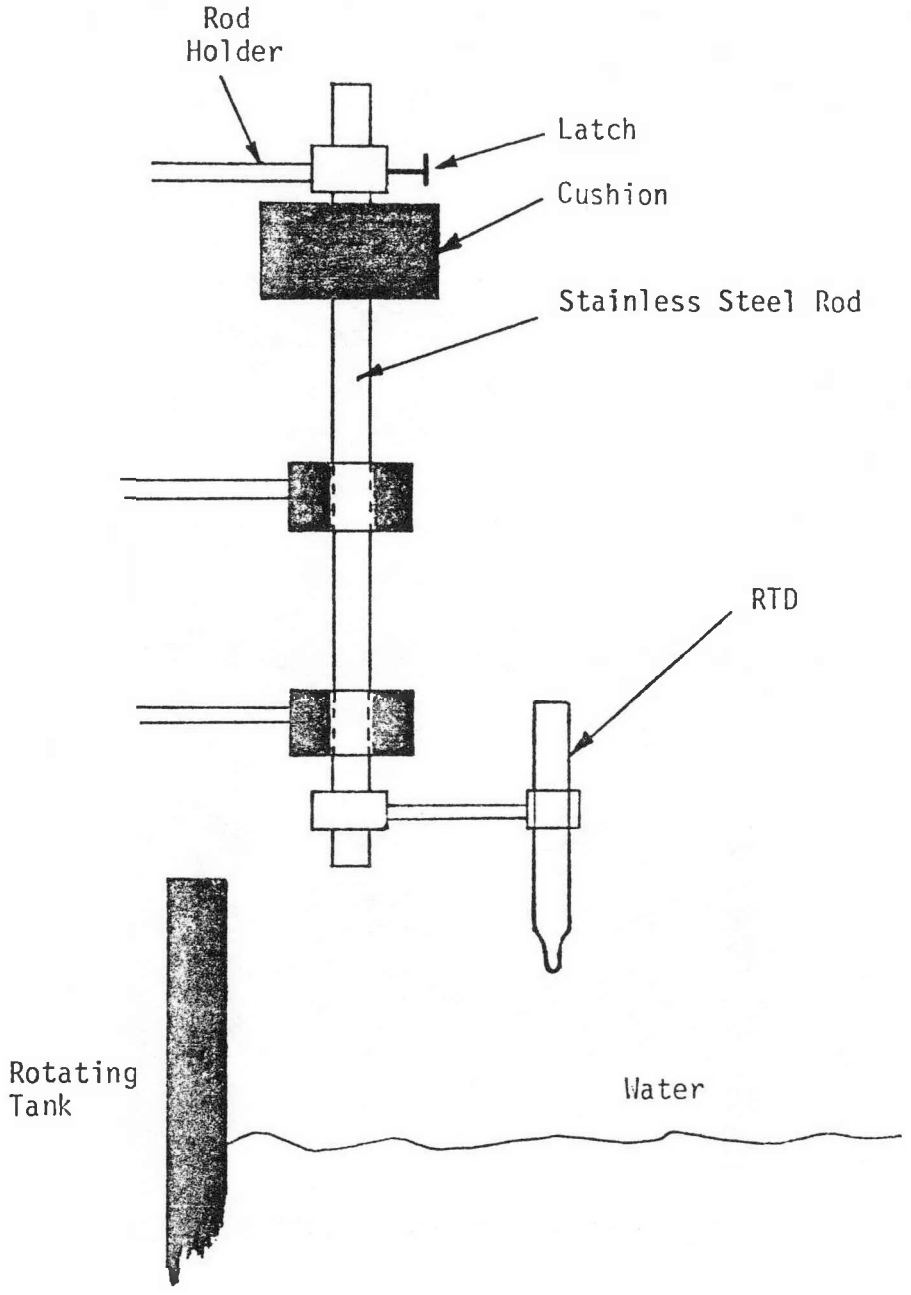

Figure E.5. Plunge Test Drop Assembly.

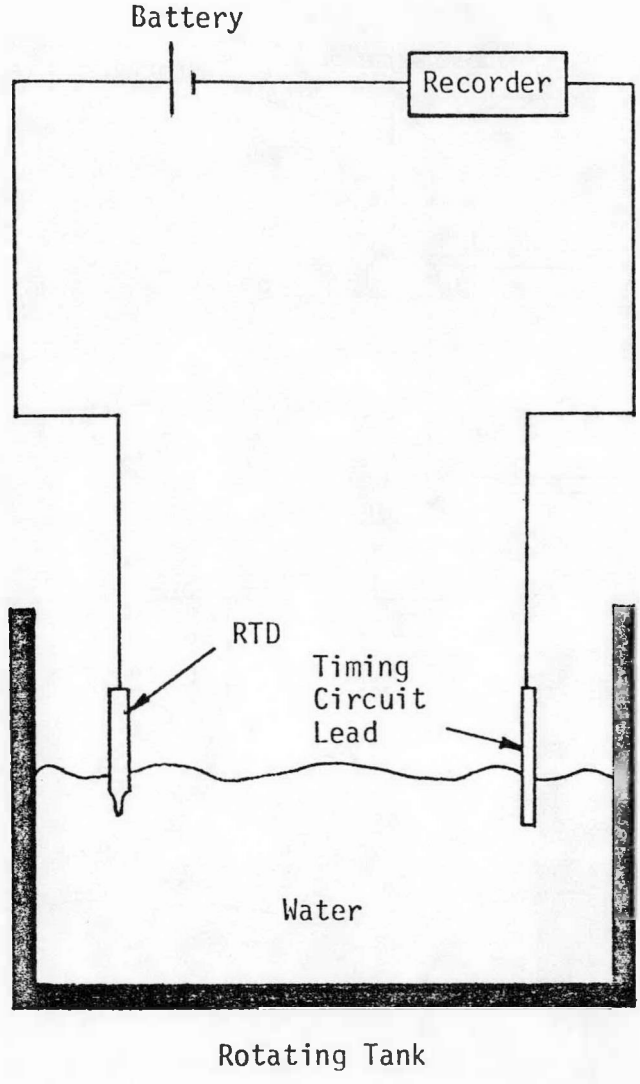

Figure E.6. Schematic of Plunge Test Timing Circuit.

7. Drop the sensor into the stirred tank and record the transient on the strip chart recorder until a steady state is attained.

A typical output of a plunge test is shown in Figure E.7.

E.2.2 LCSR Test

Experimental Setup. The equipment setup for a LCSR test depends on the method of recording the test data. Although the LCSR test data are usually stored on a mini-computer disk, a strip chart recorder and a multichannel analyzer also may be used to monitor the test output. Field data from operating plants may be stored on a magnetic tape and then transferred to a computer disk through an analog to digital converter (this is to avoid taking the computer for field data acquisition). The steps taken in recording the LCSR test data on each of these recording devices follows:

1. Strip Chart Recorder: The LCSR test data can be recorded directly on a strip chart recorder, i.e., no special equipment or procedure is required.
2. Multichannel Analyzer: For recording the LCSR test data on a multichannel analyzer a voltage to frequency (V to F) converter is necessary. The output voltage from the bridge circuit goes through a V to F converter before it can be recorded on the multichannel analyzer. The multichannel analyzer has the capability of converting the data into digital form that can be printed on a teletype (see Figure E.8).

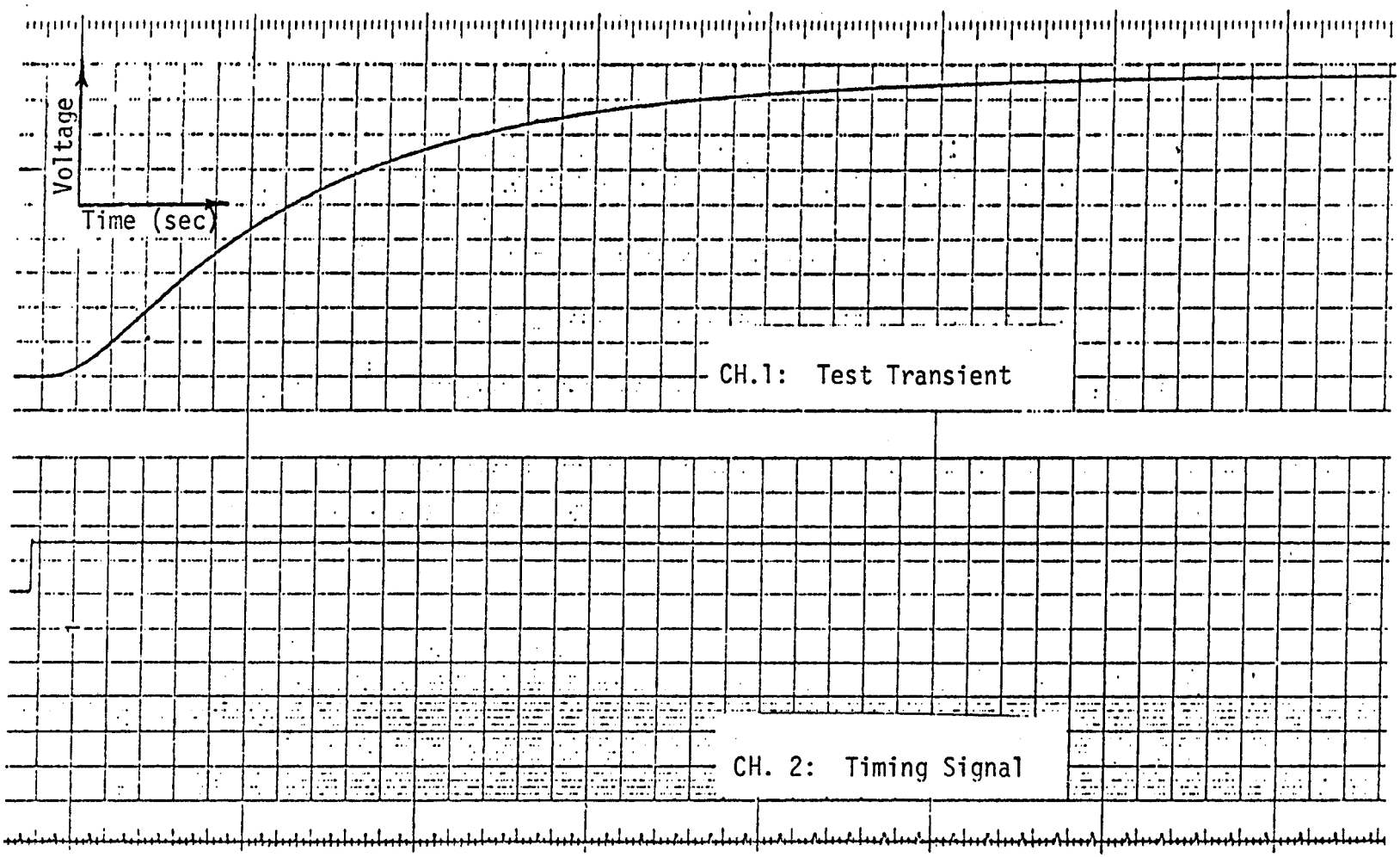

Figure E.7. A Typical Output of a Plunge Test.

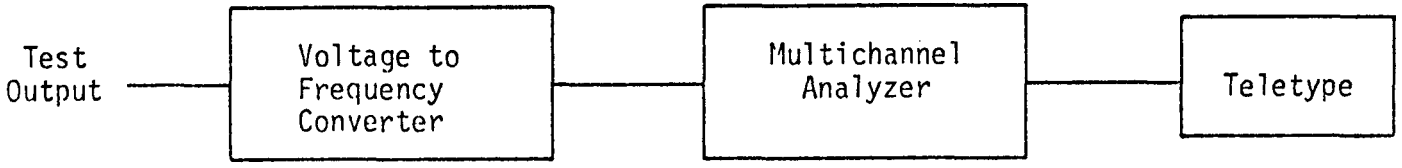

Figure E.8. Equipment Set Up for Recording the LCSR Test Data on a Multichannel Analyzer.

3. Analog Tape Recorder: The equipment setup for recording the LCSR test data on magnetic tape is shown in Figure E.9. Since the maximum limit of the voltage input to the tape recorder is about one volt, an attenuator system is used to drop the voltage to a value of less than one volt before it goes to the tape recorder. The output from the tape recorder is then amplified to provide desired voltage levels. The field data are usually contaminated with high frequency components that are not useful. A low pass filter is usually used to remove the unnecessary components of the data.
4. Mini-Computer: Figure E.10 shows the equipment setup for collection of LCSR test data with the mini-computer. The output of the measuring circuit passes through an analog to digital converter (A/D) before it can be taken by the computer. A timing circuit is used to provide a signal to initiate the collection of data at the instant a test starts. After a test is completed the data are automatically stored on a disk, displayed on a storage display unit and copied with a hard copy system.

Test Procedures. A LCSR test may be performed in two different manners. One in which the bridge circuit is initially balanced when a low current is passing through the sensing filament and another in which the bridge is initially balanced when a high current is used. The procedures for a LCSR test in which the bridge is balanced at a low current level are listed first:

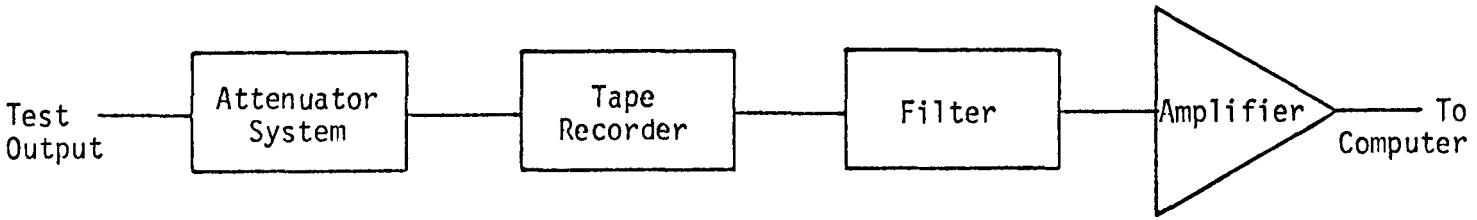

Figure E.9. Equipment Set Up for Field Data Acquisition.

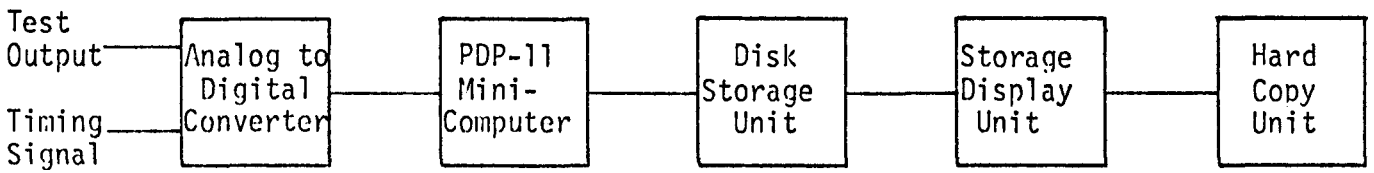

Figure E.10. Equipment Set Up for Collection of Data with the Mini-Computer.

1. Connect the sensor to the measuring circuit (keep the current on low level).
2. Place the sensor in the rotating tank at a location where a desired fluid flow rate can be obtained.
3. Balance the bridge.
4. Adjust the output voltage of the power supply to obtain a high current level of about 40 to 60* milliamperes.
5. Adjust the gain of the amplifier to give an output voltage of 5 to 10 volts when the high current is passing through the circuit.
6. Return the current to the low value.
7. Connect the measuring system to the recording device (if sampling the data with the mini-computer, connect the system to the analog to digital converter, set the timing signal, make certain that the input voltage to the analog to digital converter is less than 10 volts and run the sampling program).
8. Switch the current to the high level and record the output until a steady state is achieved.

A typical LCSR test transient is given in Figure E.11 for which the bridge has been balanced with a low current passing though the circuit.

---

*This is a typical range of current used in the course of this study. Higher or lower current levels can also be used.

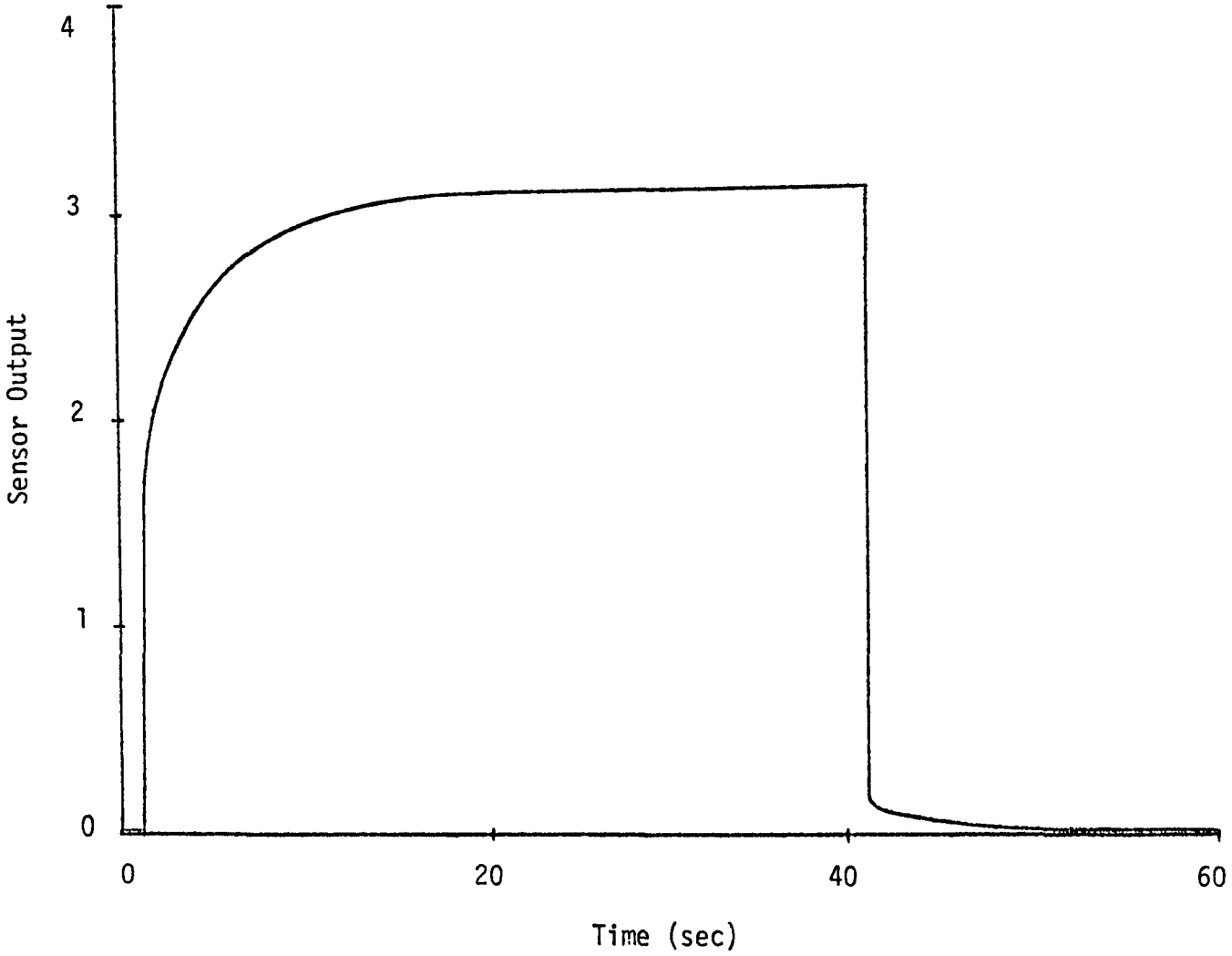

Figure E.11. A Typical LCSR Test Transient (for Rosemount 177GY RTD).

Another method of performing a LCSR test follows:

1. Balance the bridge while a high current is passing through the RTD.
2. Step the current back to its low level. This will give a negative output voltage.
3. Wait until a steady state output is obtained.
4. Switch the current to high level and record the transient.

The output of a LCSR test obtained by balancing the bridge at high current is given in Figure E.12.

E.2.3 Self-Heating Test

Experimental Setup. The experimental setup of Figure E.13 is used for a self heating test. The variable resistor R_V changes the voltage input to the bridge and gives different values of current through the circuit. Two digital voltmeters (DVM) are used, one to measure the voltage drop across a fixed resistor of the bridge and another for measuring the output of the system.

Testing Procedures. The following procedures are used to perform a self heating test in the laboratory:

1. Connect the RTD to the measuring circuit.
2. Place the RTD in the rotating tank at a location where it is exposed to a desired fluid flow rate.
3. Keep the current switch closed to have a high current level throughout the test.
4. Adjust the variable resistor R_V (potentiometer) to start with a minimum voltage input to the bridge.

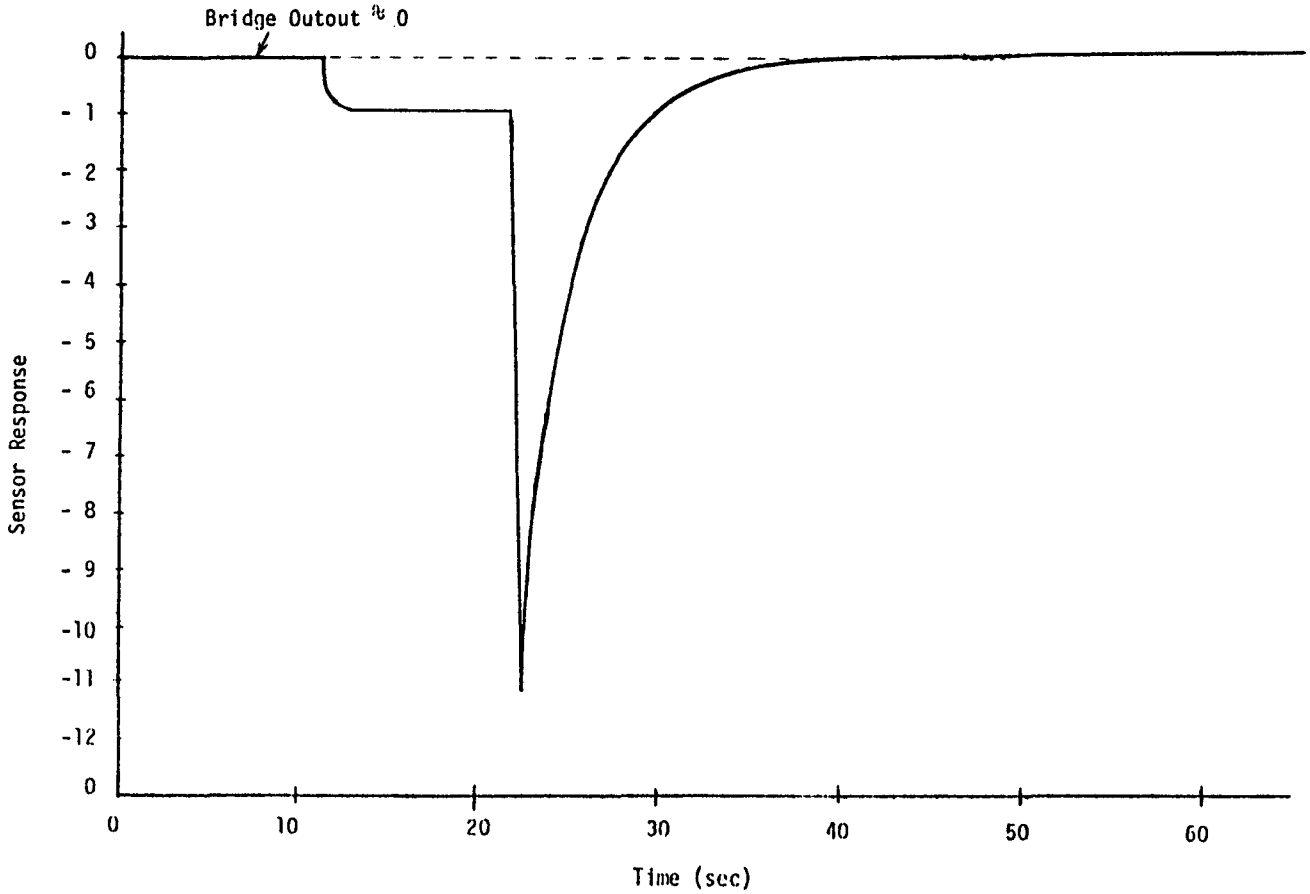

Figure E.12. A Typical LCSR Output when Bridge is Balanced at a High Current Prior to Performance of the Test.

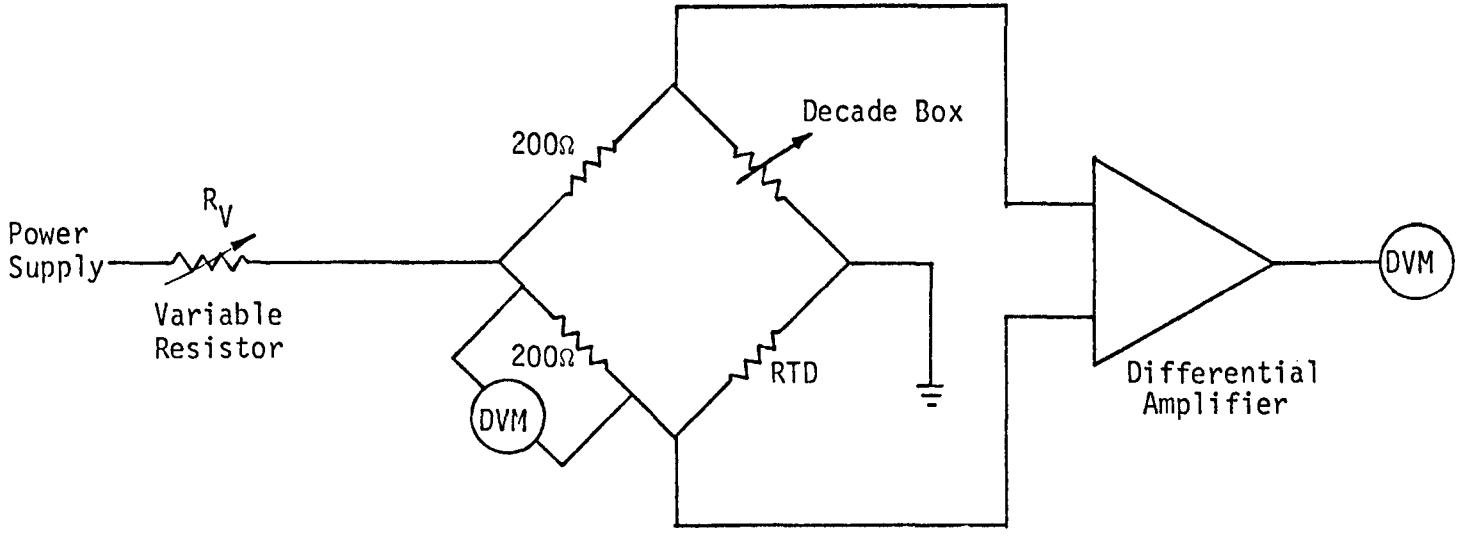

Figure E.13. Self Heating Test Circuit.

5. Balance the bridge and record the decade box resistance at which the bridge is balanced. This resistance is equal to the sensor's resistance ($R_{RTD} = R_D$).
6. Measure the voltage drop across one of the fixed resistors of the bridge. Calculate the current from $I_{RTD} = \frac{V_{Fixed\ Resistor}}{R_{Fixed}}$.
7. Calculate the power input to the RTD form: $P_{RTD} = R_{RTD} \cdot I^2_{RTD}$.
8. Increase the voltage input to the bridge using the potentiometer (R_V). This increases the current through the sensor. Repeat from step 5 on. Use small voltage increments to allow 15 to 20 measurements before the sensor current reaches its limit.
9. Plot the values of R_{RTD} versus P_{RTD} on a cartesian coordinate system.

The plot is called a self heating curve. A typical self heating curve is shown in Figure E.14.

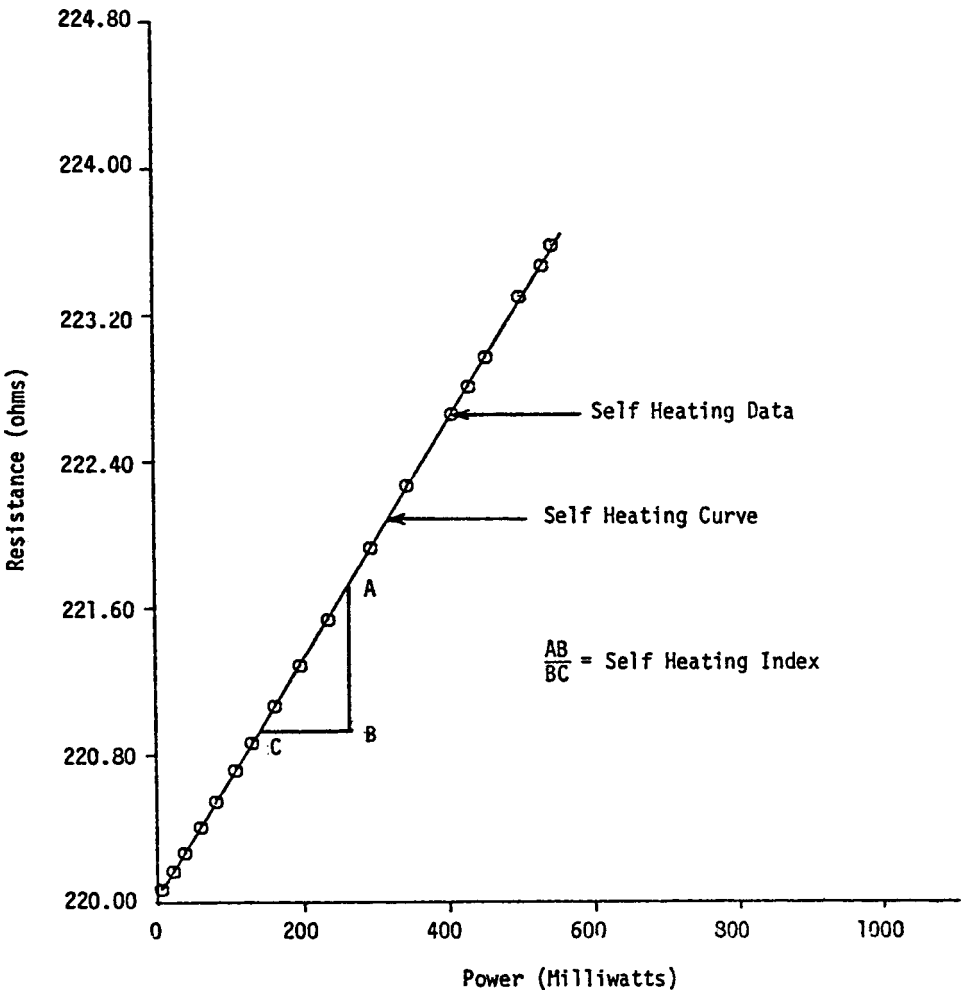

Figure E.14. A Typical Self Heating Test (for a Rosemount 176KF RTD).

APPENDIX F

COMPONENTS OF MEASURING CIRCUIT

A unit was built for response time testing of RTDs.* This unit consists of:

1. A DC power supply with adjustable voltage.
2. A Wheatstone bridge circuit with current switching capability.
3. A differential amplifier with adjustable gain.

A complete schematic of the unit is given in Figure F.1. The components of the unit along with their specification and approximate price for the specified quantity are listed in Table F.1.

---

*Unit was designed and built by Mr. J. T. Smith of Nuclear Engineering Department of The University of Tennessee.

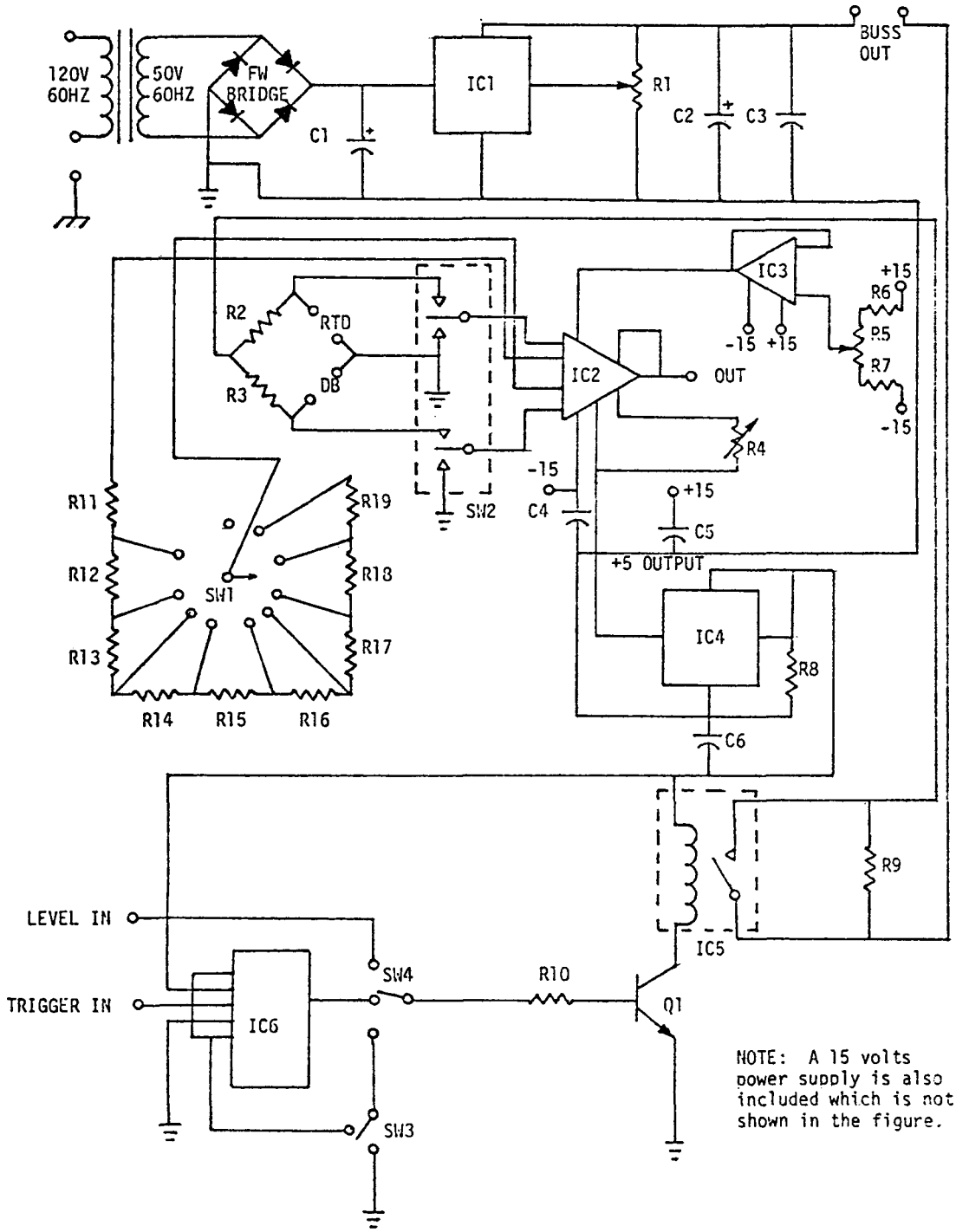

Figure F.1. Complete Schematic of the Response Time Testing Bridge and Amplifier.

TABLE F.1

COMPONENTS OF RESPONSE TIME TESTING UNIT

Component*	Specification or Part Number	Quantity	Total Price ($)
Transformer	50 volts, 1 Amp.	1	6.00
Power Supply	±15 volts	1	51.00
Diodes (Rectifier)	IN4002	4	2.00
NPN Transistor (Q1)	2N, 3904	1	.50
Voltage Regulators (IC1, IC4)	μA, 78 MG	2	3.50
Precision Amplifier (IC2)	605J	1	59.00
Operational Amplifier (IC3)	741	1	1.00
JK Flip Flop (IC6)	7473	1	1.50
Relay (IC5)	W172, Dip 5	1	10.00
Switch (SW1)	10 poles Single Wafer	1	12.00
Switch (SW2)	Double Pole Single Throw	1	2.50
Switch (SW3)	Double Pole Single Throw	1	2.50
Switch (SW4)	Triple Pole Triple Throw	1	2.50
Capacitor (C1)	1000 MF, 50 V Electric	1	5.00
Capacitor (C2)	1500 MF, 50 V Electric	1	5.00
Capacitor (C3, C6)	33 pf	2	.30
Capacitor (C4, C5)	.1 MF	2	.30
Potentiometer (R1)	10k, 10 Turn	1	3.50
Resistor (R2, R3)	200Ω , 3 percent	2	4.50
Mini-Potentiometer (R4)	10kΩ	1	2.00
Resistor (R5, R10, R14)	1kΩ	3	.75
Resistors (R6, R7)	15kΩ	2	.50

TABLE F.1 (continued)

Component*	Specification or Part Number	Quantity	Price ($)
Resistor (R8)	5kΩ	1	.25
Resistor (R9)	3.5k	1	.25
Resistor (R11, R12)	200Ω	2	.50
Resistor (R13)	600Ω	1	.25
Resistor (R15)	2.1kΩ	1	.25
Resistor (R16)	8.5kΩ	1	.25
Resistor (R17)	13.5kΩ	1	.25
Resistor (R18)	36.5kΩ	1	.25
Resistor (R19)	163.5kΩ	1	.25
Bananna Plug	-	1	.25
B&C Connector	-	9	9.00
Voltmeter	7	1	150.00
Metal Box	-	1	20.00
PC Board	-	1	16.00
Probe Sockets	-	7	4.20

*The component number matching with schematic of Figure F.1 are given in parenthesis.

APPENDIX G

LCSR DATA ANALYSIS BY EXPONENTIAL STRIPPING

The first few eigenvalues of the response of a sensor to an internal step change in temperature may be obtained by graphical exponential stripping to obtain estimates of the eigenvalues. The exponential stripping technique is based on fitting the LCSR test data into an equation of the form:

$$O(t) = A_o + \sum_{i=1}^{n} A_i e^{-P_i t} + w(t) \qquad (G.1)$$

where

$P_1 < P_2 < P_3 \ . \ . \ . < P_n$; P_is = eigenvalues of LCSR test

$O(t)$ = output of the LCSR test

A_o = a constant which is zero if the test bridge is balanced at high current prior to collection of the LCSR test data. If the bridge is balanced at low current, A_o is equal to the final value of the response.

$w(t)$ = process noise level.

If A_o is specified,

$$y(t) = O(t) - A_o = \sum_{i=1}^{n} A_i e^{-P_i t} + w(t). \qquad (G.2)$$

If the eigenvalues are well separated and the noise level is not significant, the following approximation is valid

$$y_1(t) \approx A_1 e^{-P_1 t} \quad \text{for} \quad t >> \frac{1}{P_1} . \tag{G.3}$$

Thus, when the LCSR test data is plotted on semi-log paper, a straight line should be apparent when t is significantly greater than the slowest time constant. The slope of this line is equal to P_1. A second eigenvalue may be identified by subtracting the straight line from the remaining portion of the data:

$$y_2(t) = y(t) - y_1(t) = \sum_{i=2}^{n} A_i e^{-P_i t} . \tag{G.4}$$

Again, if the eigenvalues are separated one can conclude that,

$$y_2(t) = A_2 e^{-P_2 t} \qquad t << \frac{1}{P_1} . \tag{G.5}$$

The plot of Equation (G.5) on a semi-log paper is a straight line whose slope is equal to P_2. The second mode may be subtracted from the rest of the data (if any) to provide a third eigenvalue. This process may be repeated as long as the subtraction is possible. Experience indicates that identification of more than two eigenvalues by the exponential stripping technique is usually not possible. These eigenvalues are used to evaluate an approximate value of the plunge time constant. The plunge time constant is identified from the eigenvalues of the LCSR test by the following equation:

$$\tau_{plunge} = \frac{1}{P_1}\left[1 - \ln\left(1-\frac{P_1}{P_2}\right) - \ln\left(1-\frac{P_1}{P_3}\right) - \ldots \ln\left(1-\frac{P_1}{P_n}\right)\right]$$

$$P_1 < P_2 < P_3 \quad \ldots < P_n \qquad (G.6)$$

where

τ_{plunge} = the sensor time constant

$P_1, P_2, \ldots, P_n$ = the eigenvalues of the LCSR test.

Equation (G.6) is derived in Section 2.4.2.

A LCSR data set for a Rosemount 176KF RTD tested in the laboratory is given in Table G.1. The data were obtained from a teletype used to furnish the LCSR data digitized by a multichannel analyzer. The plot of this data on a semi-log paper is shown in Figure G.1. A straight line is first fitted to the final portion of the data to give the eigenvalue corresponding to the slowest time constant ($\tau_s = \frac{1}{P_1}$). The straight line is then subtracted from the rest of the data to furnish a new data set for obtaining the second eigenvalue. As shown in Figure G.1 the eigenvalues are:

$P_1 = 2.945\ \text{sec}^{-1} \rightarrow \tau_1 = .34$ sec

$P_2 = 36.125\ \text{sec}^{-1} \rightarrow \tau_2 = .028$ sec.

If P_1 and P_2 are substituted in Equation (G.1) the plunge test time constant is obtained as

$$\tau_{plunge} = \frac{1}{2.945}\left[1 - \ln\left(1-\frac{2.945}{36.125}\right)\right] = .37 \text{ sec} \quad .$$

TABLE G.1

LCSR TEST DATA FOR ROSEMOUNT 176KF*

Δt = .008 sec			
Analyzer's Channel	Sensor's Output	Analyzer's Channel	Sensor's Output
89	7586	114	2326
90	5813	115	2264
91	5092	116	2215
92	4707	117	2149
93	4450	118	2110
94	4229	119	2043
95	4068	120	2012
96	3897	121	1944
97	3781	122	1923
98	3633	123	1855
99	3541	124	1838
100	3407	125	1770
101	3330	126	1757
102	3205	127	1688
103	3141	128	1679
104	3023	129	1611
105	2970	130	1606
106	2861	131	1542
107	2813	132	1537
108	2711	133	1481
109	2662	134	1470
110	2574	135	1422
111	2519	136	1403
112	2445	137	1365
113	2387	138	1336

TABLE G.1 (continued)

Δt = .008 sec			
Analyzer's Channel	Sensor's Output	Analyzer's Channel	Sensor's Output
139	1307	153	957
140	1272	154	905
141	1252	155	916
142	1211	156	868
143	1200	157	876
144	1154	158	835
145	1149	159	837
146	1099	160	805
147	1098	161	796
148	1049	162	775
149	1050	163	758
150	1000	164	747
151	1004	165	723
152	951	166	722

* Data are obtained by balancing the bridge at high current.

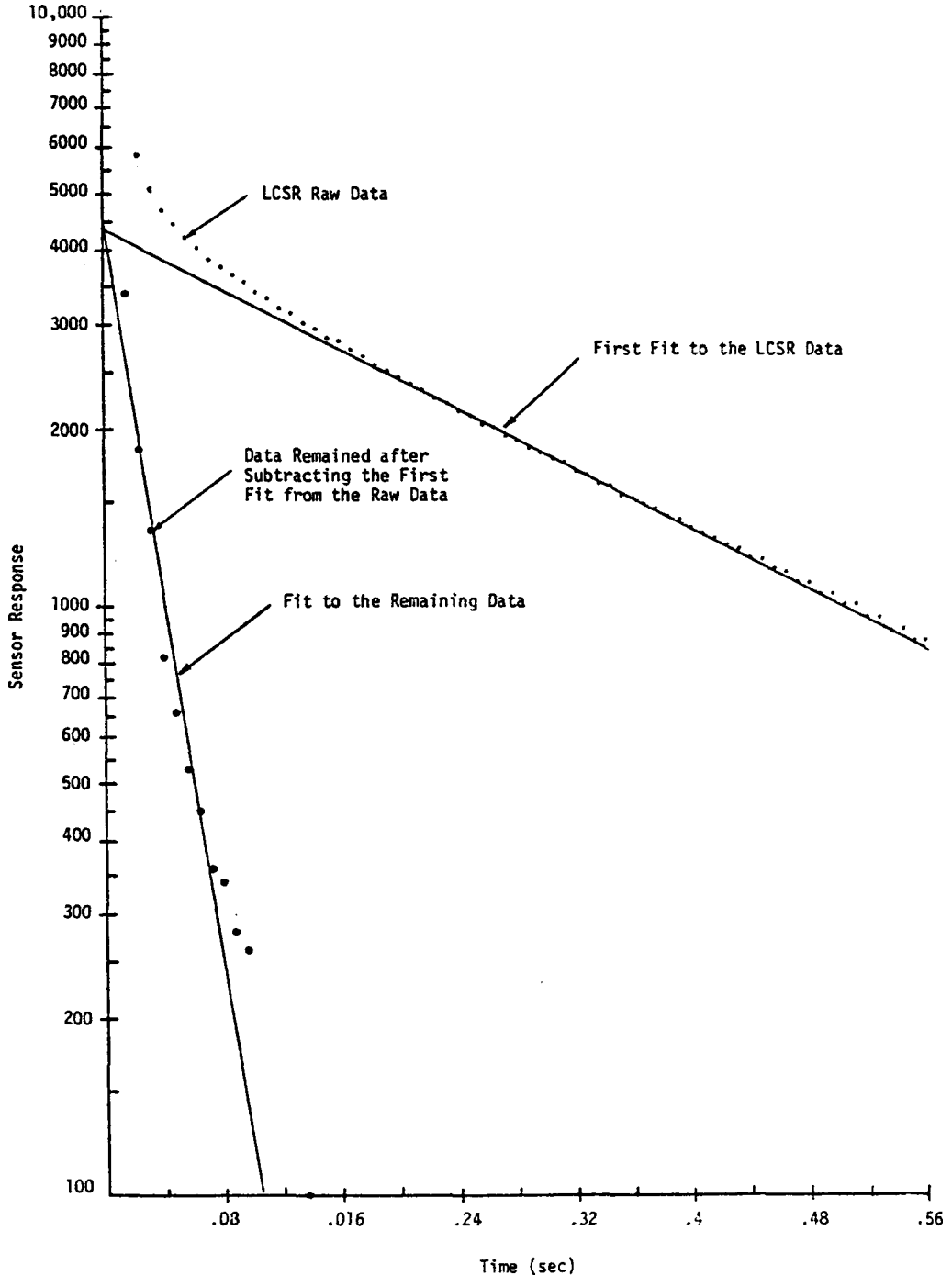

Figure G.1. Graphical Exponential Stripping for Identification of LCSR Eigenvalues (for Rosemount 176KF RTD).

This compares well with a time constant of .38 sec obtained from a plunge test performed under the same conditions as this LCSR test.

If the test bridge is balanced at a low current prior to collection of the LCSR test data, the final value of the response must be subtracted from the data before plotting on semi-log paper. A LCSR data set for which the bridge was balanced at a low current is given in Table G.2. The data were obtained from the strip chart recorder for a Rosemount 177GY RTD tested in the laboratory. The eigenvalues of the LCSR test obtained from the plot of the data in Figure G.2 are:

$$P_1 = .238 \text{ sec}^{-1}$$

$$P_2 = 1.20 \text{ sec}^{-1} \quad .$$

The plunge test time constant is:

$$\tau_{plunge} = \frac{1}{.238} \left[1 - \ln \left(1 - \frac{.238}{1.20}\right)\right] = 5.13 \text{ sec} \quad .$$

TABLE G.2

LCSR TEST DATA SET FOR ROSEMOUNT 177GY RTD*

$T_{final} = A_o = 715$

$\Delta t = .2$ sec

T (sensor's output)	$T_f^{**}-T$	T (sensor's output)	T_f-T
293	422	589	126
433	282	595	120
457	258	602	113
474	241	607	108
489	226	612	103
502	213	617	98
513	202	620	95
525	190	625	90
534	181	629	86
545	170	633	82
554	161	638	77
562	153	641	74
570	146	645	70
576	138	648	67
583	132	650	65

*Bridge was balanced at low current prior to collection of this data set.

**T_f is an abbreviation of T_{final}.

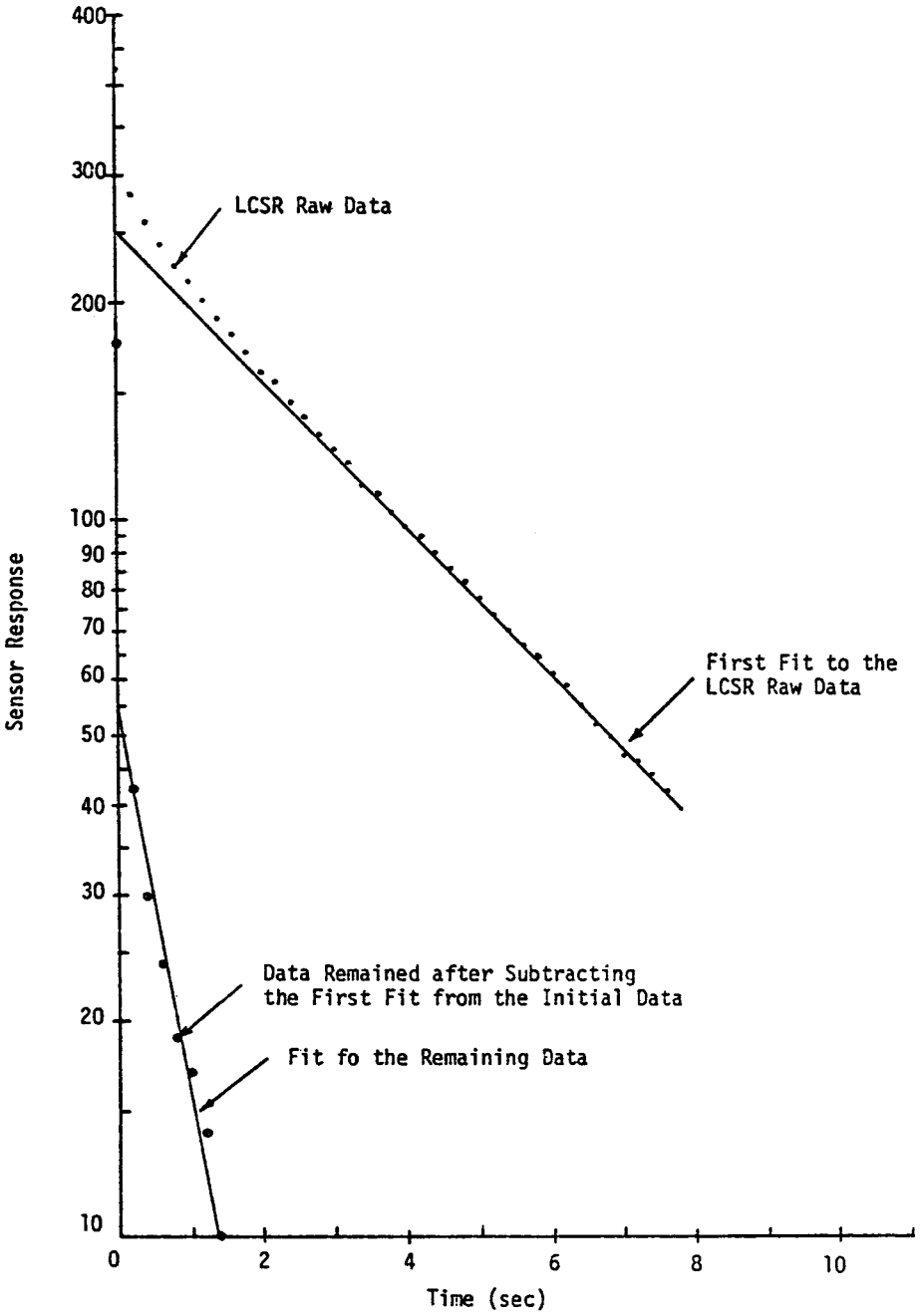

Figure G.2. Identification of LCSR Eigenvalues by Graphical Exponential Stripping Technique (for Rosemount 177GY RTD).